

**AN INTEGRATED SIMULATION-BASED
PROCESS CONTROL AND OPERATION
PLANNING SYSTEM FOR MARINE OILY
WASTEWATER MANAGEMENT**

by

©**Liang Jing**

A thesis submitted to the School of Graduate Studies
in partial fulfillment of the requirements for the
Degree of Doctor of Philosophy

**Faculty of Engineering and Applied Science
Memorial University of Newfoundland
December, 2014**

St. John's

Newfoundland and Labrador

Canada

LETTER OF TRANSMITTAL

Faculty of Engineering and Applied Science
Doctoral Thesis Examination and Oral Defense

of

Liang Jing

LETTER OF TRANSMITTAL

We, the members of the supervisory committee of the Ph.D. research of Mr. Liang Jing, have reviewed the thesis submitted by him and certify that it is prepared in accordance with the faculty guidelines for the submission. The candidate has expressed the readiness to proceed with the defense.

While every effort has been made to give the appropriate guidance to the candidate in preparing the thesis, the above statement does not necessarily imply an unqualified approval of its contents.



Dr. Bing Chen
Supervisor



Dr. Helen Zhang
Supervisor



Dr. Abdel-Zaher Kamal Abdel-Razek
Supervisory Committee



Dr. Hongxuan Peng
Supervisory Committee

ABSTRACT

The chronic discharge of oily wastewater, mainly including bilge water, offshore produced water and ballast water, has been referred to as a major contributor to marine oil pollution. Although gravity-based treatment techniques have been widely used to separate oil from wastewater, many dissolved toxic organics, particularly Polycyclic Aromatic Hydrocarbons (PAHs), are not likely to be effectively removed and may cause severe environmental problems. Further treatment has therefore become necessary for the shipping and offshore oil and gas industries, particularly in the harsh environments (e.g., the Arctic Ocean) where ecosystems are extremely vulnerable. Among many chemical and biological treatment techniques, ultraviolet (UV) irradiation and advanced oxidation techniques have been recently regarded as promising solutions to the removal of PAHs. Such advanced treatment systems, as compared to the traditional ones, are usually lack of in-depth understanding of reaction mechanisms and kinetics, process control requirements, and long-term planning strategies. More particularly, the integration of process control and operation planning has been proven in the literature to greatly reduce process cost and improve system performance. However, such integration is usually complicated by many factors such as the multi-scale nature of decisions, the lack of knowledge of process dynamics and control, and uncertainty. These deficiencies can drastically hinder the widespread application of these advanced treatment systems in the shipping and offshore industries. In response to these knowledge and technique gaps, this research proposes an integrated process control and operation planning system to aid marine oily wastewater management based on experimental study, process modeling, process control, operation planning and their coupling.

The UV induced photodegradation of a typical PAH, namely naphthalene in seawater, was chosen as an example for studying the reaction mechanism and parameter effects. The experimental results showed that the removal of naphthalene followed first order kinetics and the most influential factors were fluence rate, temperature and the interaction between temperature and initial concentration. The reaction rate constants varied from 0.0018 to 0.0428 min⁻¹. Further analysis revealed that the reaction rate constants were linearly related to the number of lamps. High salinity suppressed the performance of UV irradiation which was mainly caused by the presence of bromide (Br⁻), carbonate (CO₃²⁻) and bicarbonate (HCO₃⁻) ions in seawater. In addition, increasing temperature seemed to stimulate the removal of naphthalene in seawater by exciting the collision between photons and molecules. The effect of initial concentration was not prominent while the average reaction rate constant at high concentration was slightly lower than that at low concentration.

Based on the experimental results, a three-layer backpropagation neural network was developed to simulate the UV-induced photodegradation of naphthalene in marine oily wastewater. The photochemical process was successfully predicted by using 12 neurons in the hidden layer and the Levenberg-Marquardt backpropagation algorithm. The network was trained to provide a good overall linear fit with a slope of 0.97 and a correlation of determination (R^2) of 0.943. All input variables in this study (i.e., initial concentration, salinity, fluence rate, temperature and reaction time) had considerable effects on the photodegradation process. The results showed that the developed ANN model was capable of accurately simulating the naphthalene removal process and reproduce the experiment.

The process control module, namely the artificial neural network based dynamic mixed integer nonlinear programming (ANN-DMINP) approach, was constructed based on the experimental study of PAH degradation, the degradation simulation using ANN, and the process dynamic optimization using genetic algorithm. Naphthalene degradation by UV irradiation was used as a case study to help develop these models. The results from the case study showed that the treatment cost in a fixed 36-hour period was minimized to \$9.11 by using the ANN-DMINP approach. As a comparison, the single-stage optimization with constant variables was also applied and the treatment cost was 25.7% higher at \$11.45. A Monte Carlo simulation was also performed to conclude that if the operator randomly set the flow rate and the number of lamps as constants during the 36-hour period, then there would be a great chance that the treatment standard cannot be met. If considering time as another flexible variable, the treatment cost reached its minimum at 27 hours with \$8.71 and \$8.94 for the ANN-DMINP approach and the single-stage optimization, respectively. A sensitivity analysis showed that more optimization stages can generally reduce treatment cost, but may lead to extra manpower needs and affect system stability. It was recommended to first seek the best solution with less optimization stages, and then using the solution as an initial population for more optimization stages, if necessary.

On the other hand, the operation planning module was proposed based on the stochastic simulation-based hybrid interval fuzzy programming (SHIFP) approach and the hybrid fuzzy stochastic analytical hierarchy process (FSAHP) approach. A case study related to recovered oily water treatment during offshore oil spill cleanup operations was carried out to test the SHIFP approach. The decision makers were looking for solutions

that how to arrange different facilities and how much wastewater should be delivered to each facility. The results demonstrated that the maximum daily treatment capacity was likely to follow the normal distribution within the range from 3,000 to 3,700 tonnes. In addition, the shapes of the fuzzy decision variables, corresponding to the maximized objective function, can be categorized into seven groups with different probability such that decision makers can more confidently allocate limited resources. Another case study related to ballast water management was carried out to verify the feasibility and efficiency of the FSAHP approach. Five treatment technologies were evaluated against a number of environmental, economic, and technical criteria by nine experts from academia and government. The results revealed that UV was ranked with the highest overall score at 100% confidence level, indicating that the null assumption that it was not probabilistic optimal (versus the alternate assumption that it is) was rejected. Ozone, heat treatment, and ultrasound had the second, third, and fourth places at the confidence levels of 61.0–71.4%, 56.0–68.4%, and 78.4–84.6%, respectively. Considerable overlaps existed among these three alternatives which may be attributed to the irreducible uncertainty caused by subjective judgments or lack of knowledge. The proposed FSAHP approach can offer a number of benefits such as the capability of capturing human's appraisal of ambiguity and addressing the effects of uncertain judgment when dealing with insufficient information or biased opinions.

The coupling between process control and operation planning was innovatively realized by integrating neural networks, genetic algorithm, dynamic programming, and Monte Carlo simulation into the integrated simulation-based process control and operation planning (IS-PCOP) system. A real-world case study related to offshore

wastewater management on a FPSO was conducted to examine the efficacy of the proposed integration. The ANN-DMINP approach was used to optimize the treatment cost of removing naphthalene from bilge water using UV irradiation. Treated effluent, depending on the remaining concentration of naphthalene, was reused and could produce varying benefit. Monte Carlo simulation was applied to generate the parameters (e.g., volume, concentration and temperature) of daily bilge water and examine the net cost to obtain the distribution of optimal solutions at a series of treatment standards. The results showed that choosing the $20 \mu\text{g L}^{-1}$ treatment standard was the most economically competitive option. As compared to the traditional operation planning without process control, the integrated approach achieved more economically competitive results.

The proposed IS-PCOP system can well link process control and operation planning by simultaneously adopting different time-scales in computation. The hourly process control strategy forwarded the results to the operation planning module where long-term arrangements can be further evaluated. The use of ANN modeling also played a key role in predicting the nonlinear behaviour of the treatment process. In addition, Monte Carlo simulation yielded a better insight on uncertainties, which may arise from a number of different sources. By addressing the uncertainties and expressing the results in probability distributions, the decision makers would have more confidence in making proper decisions regarding the short-term and long-term operation of the advanced wastewater treatment systems.

ACKNOWLEDGEMENT

First and foremost, I would like to express my sincere appreciation to my advisors, Dr. Bing Chen and Dr. Baiyu Zhang for their guidance, inspiration, suggestions, criticism and financial support that they have provided throughout the course of my research and studies. Special thanks are also extended Dr. Abdel-Zaher Abdel-Razek and Dr. Hongxuan Peng for taking the time to review this dissertation and serving on the Supervisory Committee.

I also gratefully acknowledge the Faculty of Engineering and Applied Science, the Memorial University of Newfoundland (MUN), the Natural Sciences and Engineering Research Council of Canada (NSERC), the Canada Foundation for Innovation (CFI), the Development Corporation of Newfoundland and Labrador (RDC), Fisheries and Oceans Canada (DFO) and American Bureau of Shipping (ABS) for financial support.

Additional gratitude is given to my colleagues Dr. Pu Li, Hongjing Wu, Jisi Zheng, Xiao Zheng, Zelin Li, Bo Liu, He Zhang, Weiyun Lin, and Dr. Yinchun Ma for their friendship and assistance in the course of my research programme.

Finally, I would like to express my special appreciation to my parents for their love and continued support. The deepest thanks are expressed to my fiancée Jingjing Cai for her endless love, encouragement and patience.

TABLE OF CONTENTS

| | |
|---|--------------|
| ABSTRACT..... | III |
| ACKNOWLEDGEMENT | VIII |
| TABLE OF CONTENTS..... | IX |
| LIST OF FIGURES | XIV |
| LIST OF TABLES | XVIII |
| LIST OF SYMBOLS AND ABBREVIATIONS..... | XX |
| LIST OF APPENDICE..... | XXIV |
| CHAPTER 1 | 1 |
| INTRODUCTION | 1 |
| 1.1 Background and Challenges..... | 2 |
| 1.2 Research Objectives | 7 |
| 1.3 Structure of the Thesis | 8 |
| CHAPTER 2..... | 11 |
| LITERATURE REVIEW | 11 |
| 2.1 Overview of Marine Oily Wastewater | 12 |
| 2.1.1 Offshore Produced Water | 12 |
| 2.1.1.1 <i>Environmental Impacts.....</i> | <i>13</i> |
| 2.1.1.2 <i>Legislation and Management Practices</i> | <i>14</i> |
| 2.1.2 Ballast Water | 15 |
| 2.1.2.1 <i>Environmental Impacts.....</i> | <i>17</i> |
| 2.1.2.2 <i>Legislation and Management Practices</i> | <i>18</i> |
| 2.1.3 Bilge Water..... | 19 |
| 2.1.3.1 <i>Environmental Impacts.....</i> | <i>20</i> |
| 2.1.3.2 <i>Legislation and Management Practices</i> | <i>21</i> |

| | |
|---|-----------|
| 2.2 Treatment of Marine Oily Wastewater | 22 |
| 2.2.1 Gravity Separation | 23 |
| 2.2.2 Flotation | 23 |
| 2.2.3 Coagulation | 24 |
| 2.2.4 Membrane Separation | 25 |
| 2.2.5 Absorption and Adsorption | 26 |
| 2.2.6 Biological Treatment..... | 26 |
| 2.2.7 Challenges for Marine Applications | 27 |
| 2.2.8 UV Irradiation and Advanced Oxidation | 29 |
| 2.3 Treatment Process Control | 32 |
| 2.3.1 Modeling the Treatment Process..... | 33 |
| 2.3.2 Application of Artificial Neural Networks..... | 35 |
| 2.3.3 Simulation-based Process Control | 37 |
| 2.4 Treatment System Operation Planning | 40 |
| 2.5 Integration of Process Control and Operation Planning | 46 |
| 2.6 Summary | 49 |
| CHAPTER 3..... | 53 |
| NOVEL OPERATION PLANNING TOOLS FOR MARINE OILY WASTEWATER MANAGEMENT..... | 53 |
| 3.1 A Stochastic Simulation–Based Hybrid Interval Fuzzy Programming (SHIFP) Approach | 54 |
| 3.1.1 Background | 54 |
| 3.1.2 Methodology | 56 |
| 3.1.2.1 <i>Fuzzy Sets and Fuzzy Logic</i> | 56 |
| 3.1.2.2 <i>Interval Theory</i> | 58 |
| 3.1.2.3 <i>Stochastic Programming by Monte Carlo Simulation</i> | 58 |
| 3.1.2.4 <i>The SHIFP Approach</i> | 59 |
| 3.1.3 Case Study | 62 |
| 3.1.4 Results and Discussion | 68 |
| 3.2 A Hybrid Fuzzy Stochastic Analytical Hierarchy Process (FSAHP) Approach | |

| | |
|---|------------|
| | 75 |
| 3.2.1 Background | 75 |
| 3.2.2 Methodology | 77 |
| 3.2.2.1 Fuzzy Sets and Fuzzy Numbers..... | 78 |
| 3.2.2.2 Stochastic Programming by Monte Carlo Simulation..... | 78 |
| 3.2.2.3 The FSAHP Approach | 78 |
| 3.2.3 Case Study | 83 |
| 3.2.3.1 Hierarchy Structure | 84 |
| 3.2.3.2 Data Acquisition..... | 87 |
| 3.2.4 Results and Discussion | 91 |
| 3.3 Summary | 102 |
| CHAPTER 4..... | 105 |
| AN EXPERIMENTAL STUDY ON THE TREATMENT OF MARINE | |
| OILY WASTEWATER USING UV IRRADIATION | 105 |
| 4.1 Background | 106 |
| 4.2 Materials and Methods | 107 |
| 4.2.1 Reagents and Standards | 107 |
| 4.2.2 Photoreactor and Light Source..... | 108 |
| 4.2.3 UV Fluence Rate Determination..... | 108 |
| 4.2.4 Experimental Procedure | 109 |
| 4.2.5 Analytical Method..... | 110 |
| 4.2.6 Statistical Analysis | 111 |
| 4.3 Results and Discussion | 113 |
| 4.3.1 ANOVA..... | 113 |
| 4.3.2 Effect of Fluence Rate..... | 117 |
| 4.3.3 Effect of Salinity | 118 |
| 4.3.4 Effect of Temperature | 125 |
| 4.3.5 Effect of Initial Concentration | 126 |
| 4.4 Summary | 131 |

| | |
|---|------------|
| CHAPTER 5..... | 133 |
| SIMULATION OF THE TREATMENT OF MARINE OILY WASTEWATER USING UV IRRADIATION..... | 133 |
| 5.1 Background | 134 |
| 5.2 Methodology..... | 135 |
| 5.2.1 Experimental..... | 135 |
| 5.2.2 Model Inputs | 135 |
| 5.2.3 Artificial Neural Networks (ANNs)..... | 135 |
| 5.2.4 Analysis of Variance (ANOVA)..... | 139 |
| 5.2.5 Verification of the ANN Model..... | 139 |
| 5.3 Results and Discussion | 141 |
| 5.3.1 ANN Modeling..... | 141 |
| 5.3.1.1 Selection of backpropagation training algorithm | 141 |
| 5.3.1.2 Optimization of the number of hidden neurons | 141 |
| 5.3.1.3 Training, validation and testing of the model..... | 146 |
| 5.3.1.4 Sensitivity analysis..... | 146 |
| 5.3.2 ANOVA..... | 152 |
| 5.3.3 ANN Model Verification..... | 154 |
| 5.4. Summary | 162 |
| CHAPTER 6..... | 163 |
| SIMULATION-BASED DYNAMIC PROCESS CONTROL OF MARINE OILY WASTEWATER TREATMENT | 163 |
| 6.1 Background | 164 |
| 6.2 Methodology..... | 164 |
| 6.2.1 The General ANN-DMINP Approach..... | 164 |
| 6.2.2 Application of ANN-DMINP in Marine Oily Wastewater Treatment..... | 169 |
| 6.3 Case Study..... | 175 |
| 6.4 Results and Discussion | 182 |
| 6.4.1 Comparison with the Single-Stage Optimization | 182 |

| | |
|--|------------|
| 6.4.2 Minimization of Time and Cost | 189 |
| 6.4.3 Effect of the simulation time-step and the number of optimization stages..... | 190 |
| 6.5 Summary | 195 |
| CHAPTER 7 | 196 |
| AN INTEGRATED SIMULATION-BASED PROCESS CONTROL AND OPERATION PLANNING (IS-PCOP) APPROACH FOR MARINE WASTEWATER MANAGEMENT | 196 |
| 7.1 Background | 197 |
| 7.2 The IS-PCOP Approach for Marine Wastewater Management..... | 199 |
| 7.3 Case Study..... | 204 |
| 7.3.1 Bilge Water Treatment System..... | 204 |
| 7.3.2 Bilge Water Characterization | 205 |
| 7.3.3 Problem Formulation | 206 |
| 7.4 Results and Discussion | 208 |
| 7.4.1 Integrated Process Control and Operation Planning | 208 |
| 7.4.2 Comparison with Operation Planning without Process control | 210 |
| 7.5 Summary | 222 |
| CHAPTER 8..... | 223 |
| CONCLUSIONS AND RECOMMENDATIONS..... | 223 |
| 8.1 Summary | 224 |
| 8.2 Research Contributions | 231 |
| 8.3 Publications | 233 |
| 8.4 Recommendations for Future Research | 238 |
| APPENDICE | 241 |
| REFERENCES..... | 247 |

LIST OF FIGURES

| | |
|--|-----|
| Figure 3.1 Probability distributions of the lower bound, vertex point, upper bound, and defuzzified centroid of the objective function | 65 |
| Figure 3.2 Probability density estimates of the lower bound, vertex point, upper bound, and defuzzified centroid of the objective function | 66 |
| Figure 3.3 Normal probability plot of the centroid of the objective function..... | 67 |
| Figure 3.4 Probability density estimates of the lower bound, vertex point, upper bound, and defuzzified centroid of the O&M cost of incineration barge | 69 |
| Figure 3.5 Probability distributions of the lower bound, vertex point, upper bound, and defuzzified centroid of the O&M cost of incineration barge..... | 70 |
| Figure 3.6 Normal probability plot of the centroid of the O&M cost of incineration barge | 71 |
| Figure 3.7 Optimal solutions of operation hours of each treatment facility | 72 |
| Figure 3.8 Membership spread of linguistic scales..... | 85 |
| Figure 3.9 Hierarchy structure of the ballast water treatment technology selection problem | 86 |
| Figure 3.10 Probability distributions of alternative scores with regard to human risk..... | 95 |
| Figure 3.11 Probability density estimates of decision criteria weights..... | 96 |
| Figure 3.12 Probability distributions of alternative overall scores | 97 |
| Figure 3.13 Box plots of overall scores for each alternative | 98 |
| Figure 4.1 (a) Layers and (b) measuring points of UV fluence rate within the quartz sleeve | 112 |
| Figure 4.2 (a) Top layer, (b) mid layer, (c) bottom layer, and (d) 3-layer average | |

| | |
|--|-----|
| distributions of UV fluence rate with four lamps | 119 |
| Figure 4.3 Three-layer average distributions of UV fluence rate with (a) two, (b) four, (c) six, and (d) eight lamps..... | 120 |
| Figure 4.4 (a) Concentration change and (b) the first-order regression of $10 \mu\text{g L}^{-1}$ naphthalene photodegradation in 40 psu seawater (Temperature = $23 \text{ }^{\circ}\text{C}$) | 121 |
| Figure 4.5 Reaction rate constants of naphthalene photodegradation at salinity levels of 25, 32.5 and 40 psu | 123 |
| Figure 4.6 Effect of salinity on the photodegradation of naphthalene using six UV lamps (initial concentration = $10 \mu\text{g L}^{-1}$; temperature = $23 \text{ }^{\circ}\text{C}$)..... | 124 |
| Figure 4.7 Effect of temperature at (a) an initial concentration of $500 \mu\text{g L}^{-1}$ and two UV lamps, and (b) an initial concentration of $10 \mu\text{g L}^{-1}$, a salinity level of 25 psu and six UV lamps | 127 |
| Figure 4.8 Reaction rate constants at different initial concentrations (run numbers refer to Table 4.1) | 130 |
| Figure 5.1 Relationship between the number of hidden neurons and MSE_{t-t} | 144 |
| Figure 5.2 Optimized structure of the developed ANN model | 145 |
| Figure 5.3 Comparison between ANN modeled and experimentally measured values of naphthalene removal rate for the (a) training, (b) validation, (c) testing and (d) overall datasets | 147 |
| Figure 5.4 Comparison between ANN output and experimental results obtained from supplementary experimental tests (a) E-1, (b) E-2, (c) E-3 and (d) overall tests (see Table 5.1) | 157 |
| Figure 5.5 Comparison between ANN output and experimental results at different fluence | |

| | |
|---|-----|
| rates (other experimental conditions: $10 \mu\text{g L}^{-1}$, 32.5 ppt and $40 \text{ }^\circ\text{C}$) | 158 |
| Figure 5.6 Comparison between ANN output and experimental results at different temperatures (other experimental conditions: $500 \mu\text{g L}^{-1}$, 25 ppt and 2.88 mw cm^{-2})... | 159 |
| Figure 5.7 Comparison between ANN output and experimental results at different salinity levels (other experimental conditions: $500 \mu\text{g L}^{-1}$, 8.27 mw cm^{-2} and $40 \text{ }^\circ\text{C}$) | 160 |
| Figure 5.8 Comparison between ANN output and experimental results at different initial concentrations (other experimental conditions: 32.5 ppt, 2.88 mw cm^{-2} and $40 \text{ }^\circ\text{C}$)..... | 161 |
| Figure 6.1 Flow chart of the ANN-based dynamic mixed integer nonlinear programming (ANN-DMINP) approach | 170 |
| Figure 6.2 A schematic plot of the flow-through UV treatment system of the case study | 174 |
| Figure 6.3 Variations of the concentrations in the storage and reaction tanks and the treatment cost during the 36-hour UV exposure using the ANN-DMINP approach | 185 |
| Figure 6.4 Variations of the flow rate and the number of UV lamps during the 36-hour UV exposure | 186 |
| Figure 6.5 Variations of the concentrations in the storage and reaction tanks and the treatment cost during the 36-hour UV exposure using the single-stage optimization | 187 |
| Figure 6.6 Minimization of treatment time and total cost using both multi-stage (ANN-DMINP) and single-stage optimization..... | 188 |
| Figure 7.1 Flowchart of the IS-PCOP Approach for marine wastewater management .. | 202 |
| Figure 7.2 A schematic plot of the UV treatment system on the FPSO | 203 |
| Figure 7.3 Probability density estimates of the daily treatment cost and net cost of the 15 | |

| | |
|---|-----|
| $\mu\text{g L}^{-1}$ standard..... | 214 |
| Figure 7.4 Probability density estimates of the daily treatment cost and net cost of the 20 | |
| $\mu\text{g L}^{-1}$ standard..... | 215 |
| Figure 7.5 Probability density estimates of the daily treatment cost and net cost of the 10 | |
| $\mu\text{g L}^{-1}$ standard..... | 216 |
| Figure 7.6 Probability density estimates of the daily treatment cost and net cost of the 5 | |
| $\mu\text{g L}^{-1}$ standard..... | 217 |
| Figure 7.7 Probability density estimates of the daily treatment cost and net cost of the 25 | |
| $\mu\text{g L}^{-1}$ standard..... | 218 |
| Figure 7.8 Probability density estimates of the daily treatment cost and net cost of the 30 | |
| $\mu\text{g L}^{-1}$ standard..... | 219 |
| Figure 7.9 Error bar plot of daily treatment cost, reusing benefit, and net cost of each | |
| treatment standard..... | 220 |
| Figure 7.10 The cumulative treatment cost comparison over the 20-day period between | |
| operation planning with process control and without process control..... | 221 |

LIST OF TABLES

| | |
|--|-----|
| Table 3.1 Detailed description of treatment facilities of recovered oily water | 64 |
| Table 3.2 Expert assessment for ballast water treatment technologies | 89 |
| Table 3.3 Expert assessment for evaluation criteria..... | 90 |
| Table 3.4 Ranking with regard to human risk based on the COG method | 93 |
| Table 3.5 Ranking with regard to human risk based on Chen’s method..... | 94 |
| Table 3.6 Summary of the simulation results for the final ranking based on the COG method | 99 |
| Table 3.7 Summary of the simulation results for the final ranking based on Chen’s method | 100 |
| Table 4.1 Reaction rate constants of all factorial runs | 115 |
| Table 4.2 ANOVA for natural logarithmic transformed response of naphthalene photodegradation | 116 |
| Table 4. 3 Single factor ANOVA of naphthalene photodegradation at different initial concentrations | 129 |
| Table 5.1 Mixed level full factorial DOE for ANN model development..... | 137 |
| Table 5.2 Conditions of the supplementary experimental tests for ANN model verification | 140 |
| Table 5.3 Comparison of backpropagation algorithms with 10 neurons in the hidden layer | 143 |
| Table 5.4 Weights between the input and output layers (W1), weights between the hidden and output layers (W2) and biases | 149 |
| Table 5.5 Relative importance of input variables on the removal of naphthalene..... | 150 |

| | |
|--|-----|
| Table 5.6 Evaluation of possible combinations of input variables | 151 |
| Table 5.7 ANOVA for square root transformed response of naphthalene photodegradation | 153 |
| Table 6.1 The removal rates $r_{\Delta t}$, r_{out} , and r_{in} after one time step Δt at different initial concentrations (c_{r0}) in the reaction tank..... | 180 |
| Table 6.2 The comparison of minimized treatment cost based on different N_p and N_g combinations | 181 |
| Table 6.3 Statistical results of the Monte Carlo Simulation | 192 |
| Table 6.4 Sensitivity analysis of the number of optimization stages with 36 hours | 193 |
| Table 6.5 Comparison between hourly stage and two stage optimization | 194 |
| Table 7.1 Summary of the optimization results at different treatment standard | 213 |

LIST OF SYMBOLS AND ABBREVIATIONS

| | |
|-----------------|---|
| A | pre-exponential factor depending on compound |
| a | minimum value of the triangular fuzzy number |
| a_{ij} | minimum value of \tilde{x}_{ij} |
| a_i | geometric mean of the minimum value of the fuzzy elements on the i^{th} row |
| a_{sum} | sum of a_i |
| b_{ij} | most likely value of \tilde{x}_{ij} |
| b_i | geometric mean of the most likely value of the fuzzy elements on the i^{th} row |
| b_{sum} | sum of b_i |
| b | most likely value of the triangular fuzzy number |
| c_i | geometric mean of the maximum value of the fuzzy elements on the i^{th} row |
| c_{sum} | sum of c_i |
| c_{ij} | maximum value of \tilde{x}_{ij} |
| c | maximum value of the triangular fuzzy number |
| CI_F | inconsistency index |
| c_{nap} | concentration of naphthalene ($\mu\text{g L}^{-1}$) |
| c_t | instant concentration of naphthalene ($\mu\text{g L}^{-1}$) |
| c_0 | initial concentration of naphthalene ($\mu\text{g L}^{-1}$) |
| c_s | post-concentration in the storage tank ($\mu\text{g L}^{-1}$) |
| c_r | post-concentration in the reaction tank ($\mu\text{g L}^{-1}$) |
| c_{r0} | pre-concentration in the reaction tank ($\mu\text{g L}^{-1}$) |
| $c_{r\Delta t}$ | concentrations of naphthalene remains in the reaction tank at time points Δt ($\mu\text{g L}^{-1}$) |
| c_{rt} | concentrations of naphthalene remains in the reaction tank at time points t ($\mu\text{g L}^{-1}$) |
| c_{s0} | concentration of naphthalene in the storage tank ($\mu\text{g L}^{-1}$) |
| $Cost_x$ | cost coefficient associated with x |
| $Cost_y$ | cost coefficient associated with y |
| E | actual fluence rate (mW cm^{-2}) |
| E_0 | unit fluence rate (mW cm^{-2}) |

| | |
|------------------|--|
| f | nonlinear objective function |
| g | nonlinear equality constraints |
| h | nonlinear inequality constraints |
| I_j | relative significance of the j^{th} input variable on the output variable |
| k_r | reaction rate constant (min^{-1}) |
| k_0 | reaction rate constant of per mW cm^{-2} fluence rate |
| lb | lower bounds |
| $mean$ | mean value |
| min | minimum value |
| $modal$ | most probable value |
| max | maximum value |
| M_j | upper bounds of decision variables (maximum daily operation hours of each facility in hours) |
| N_i | the number of input neurons |
| N_h | the number of hidden neurons |
| N_j | total numbers of each facility |
| n_r | reaction order |
| p | the number of equality constraints |
| q | the number of inequality constraints |
| R | universal gas constant ($\text{J K}^{-1} \text{mol}^{-1}$) |
| r | reaction rate ($\mu\text{g L}^{-1} \text{min}^{-1}$) |
| r_t | removal rate at time point t |
| $r_{\Delta t}$ | naphthalene removal in percentage |
| $r_{\Delta t}^*$ | removal rates in wastewater coming from the storage tank at time points Δt |
| r_t^* | removal rates in wastewater coming from the storage tank at time points t |
| $Random$ | random numbers |
| $std_{reaction}$ | desired concentration in the reaction tank ($\mu\text{g L}^{-1}$) |
| $std_{storage}$ | desired concentration in the storage tank ($\mu\text{g L}^{-1}$) |
| $stdev$ | standard deviation |
| s_i^L | minimum value of the optimal solution |
| s_i^M | most likely value of the optimal solution |

| | |
|------------------------|---|
| s_i^U | maximum value of the optimal solution |
| t_r | reaction time (min) |
| T | temperature (K) |
| Δt | time period |
| ub | upper bounds |
| W | connection weights between layers |
| w_i^* | crisp overall scores of the i^{th} alternative |
| w_i | normalized crisp overall scores of each decision alternative |
| X | original data |
| X_{min} | minimum value of X |
| X_{max} | maximum value of X |
| x | flow rates ($L \text{ min}^{-1}$) |
| y_1 | the number of UV lamps operated in the first hour |
| y | UV intensity during each hour |
| z | random daily volume of bilge water (m^3/day) |
| α^* | shape factor |
| β | treatment standard |
| β^* | shape factor |
| σ | linguistic scale |
| $\mu_{\tilde{w}_i}(x)$ | corresponding membership functions of \tilde{w}_i |
| \bar{a}_j | fuzzy operation and maintenance costs of each facility (CAD/hr) |
| \bar{a}_{ij} | fuzzy constraint coefficients |
| \bar{a}_w | minimum bounds of \bar{w} |
| \bar{b} | fuzzy maximum daily total budget (CAD) |
| \bar{b}_i | fuzzy right-hand sides of constraints |
| \bar{c}_j | fuzzy objective function coefficients (hourly treatment capacities of each facility in tonnes/hour) |
| \bar{c}_w | maximum bounds of \bar{w} |
| \bar{d}_j | fuzzy transportation costs of each facility (CAD/tonne) |
| \bar{e}_j | fuzzy selling prices of recovered bunker oil from each facility (CAD/tonne) |
| $\bar{\min}$ | minimum bounds of \bar{a}_{ij} and \bar{c}_j |
| $\bar{\max}$ | maximum bounds of \bar{a}_{ij} and \bar{c}_j |

| | |
|------------------|--|
| V_s | volume of seawater in the storage tank (m ³) |
| V_r | volume of seawater in the reaction tank (m ³) |
| \tilde{w}_{ip} | fuzzy weights of the i^{th} alternative against the p^{th} criterion |
| \tilde{w}_p | fuzzy weights of the p^{th} criterion in terms of the goal |
| \bar{w} | fuzzy number |
| \tilde{x}_{ij} | non-diagonal fuzzy element |
| \bar{X}_j | fuzzy decision variables (daily operation hours of each facility in hours) |
| \bar{Z} | value of the fuzzy objective function (total daily treatment capacity in tonnes/day) |
| \bar{Z}^* | corresponding value of the fuzzy objective function |
| \bar{Z}^1 | current best fuzzy objective function |

LIST OF APPENDICE

| | |
|--|-----|
| Appendix A: Datasets for developing the ANN model..... | 242 |
|--|-----|

CHAPTER 1

INTRODUCTION

1.1 Background and Challenges

The rapid development of ocean industries can affect and alter the marine environment in many ways, of which contamination caused by accidental or operational release of oils draws growing concerns (Li et al., 2012). Such contamination can result in serious, long-term damage to local industries such as fishery and tourism, coastal communities, and the environment (Atlas and Hazen, 2011). Betti et al. (2011) reported that the annual amount of oil entering the global marine environment from sea-based activities was approximately 1.25 million tonnes. However, the range is wide, from a possible 470,000 tonnes to a possible 8.4 million tonnes per year. According to National Research Council (1985), marine oil pollution caused by big spills, routine maintenance, down the drain, up in smoke, offshore drilling, and natural seepage are 37, 137, 363, 92, 15, and 62 million gallons per year. A report published by National Research Council (2003) stated that oil enters the marine environment through natural seepage from seabed (46%), operational discharge from ships and offshore facilities (37%), accidental spills (12%), and extraction of oil (3%). It can be concluded that operational discharge of oily waste is the dominant source of oil pollution at sea.

The discharge of oil from oil and gas development and shipping operations is usually the result of either accidents or deliberate operational activities. Accidental discharges (oil spills) occur when vessels collide or come in distress at sea (e.g., engine breakdown, fire, and explosion) and break open, or run aground close to the shore, or when there is a blowout of an offshore oil well, or when a pipeline breaks. However, such accidents are uncommon and only account for a relatively small amount (12%) of the world's oil pollution in the oceans. Operational discharges, on the other hand, are mostly deliberate

and "routine", and can accumulate to an extraordinarily large amount over time. Typical operational oil pollution can be caused by routing activities such as loading, unloading, washing, discharge of untreated or inappropriately treated oily wastewater, and equipment failure or process interruption on offshore drilling facilities. Among them, the discharge of oily wastewater, usually including bilge water, offshore produced water and ballast water, has been referred to as "chronic oil pollution" on account of the fact that these discharges occur on a daily basis without triggering any major mitigation response. There is a growing recognition that the impacts associated with oily wastewater can be cumulative and longstanding (O'Hara and Morandin, 2010). Owing to the stringent environmental regulations imposed in recent years, a thorough treatment of these waste streams must be carried out prior to discharge.

Oil contained in oily wastewater can be classified into three fractions: dispersed free oil, oil-in-water or water-in-oil emulsions, and dissolved components (Klaassen, et al., 2005). While the first two can be mostly removed by gravity separation or hydrocyclone (requires demulsification, if necessary), residual oil droplets and dissolved organic compounds including particularly polycyclic aromatic hydrocarbons (PAHs) would, however, remain unaffected. The occurrence of PAHs is usually of the greatest concern because of their high resistance towards biodegradation, extreme toxicity to marine biota, and possible carcinogenicity and mutagenicity (Tsapakis et al., 2010; Harman et al., 2011). Therefore, a polishing treatment becomes much necessary to further remove PAHs from marine oily wastewater prior to discharge.

Removal of PAHs from oily wastewater effluent (e.g., after gravity separator and flotation) is possible via many techniques such as biofiltration, biodegradation,

adsorption, and phytoremediation (Haritash and Kaushik, 2009). However, most of these methods are not directly suitable for marine applications on offshore oil and gas production facilities due to space, efficiency, cost, and safety concerns. In recent years, ultraviolet (UV) photooxidation and other advanced oxidation techniques (e.g., UV/H₂O₂, UV/O₃) have been gaining significant attention and regarded as promising solutions because of their relatively small footprint, low cost, and high efficiency. They are attractive alternatives to the traditional non-destructive wastewater treatment processes (e.g., air stripping, adsorption, and membrane) because they can mineralize contaminants from water as opposed merely transporting them from one phase to another (Kishimoto and Nakamura, 2011). Many studies have experimentally investigated the degradation of PAHs in water and wastewater by using UV irradiation or its combination with other oxidants, such as ozone and H₂O₂ (Sanches et al., 2011). However, most of these studies have focused on freshwater systems rather than marine environments where salinity and complex matrix effects play a dominant role. Moreover, the research efforts on numerical modeling and performance optimization of these techniques have also been limited due to their multiphysics nature and the complexity of synergistic effects. Such advanced treatment systems, as compared to the traditional ones, still lack in-depth understanding of their reaction mechanisms, performance evaluation, process optimization, and operation planning, which can drastically hinder their widespread applications in shipping and offshore oil and gas industries.

Process control techniques have been receiving significant attention over the years because they can be applied to optimize control strategies and thereby reduce operating cost. Process modeling is regarded as the foundation of any effective process control

strategy as it provides the response of the process to any inputs on which control optimization is based. Artificial neural networks (ANNs), as a group of nonlinear mapping/modeling systems, can effectively recognize and reproduce cause-effect relationships for any nonlinear complex system that may not be accurately modeled by traditional chemical/physical models. Based on the modeling techniques, many researchers have engaged in the development and application of process control tools, particularly for wastewater treatment, to meet the needs for performance and sustainability (Marchitan et al., 2010; Frontistis et al., 2012; Li et al., 2012). Soft computing methods, including artificial neural networks (ANN), adaptive network-based fuzzy inference system (ANFIS), genetic algorithm (GA), and fuzzy logic (FL), have received increasing attention in this regard (Bhatti et al., 2011; Ma et al., 2011). Recently, the combined use of soft computing techniques has also attracted much interest, particularly the integration of ANN and GA (Liu et al., 2013; Soleimani et al., 2013; Ghaedi et al., 2013; Badrnezhad and Mirza, 2014). Nonetheless, only a few have taken changing conditions and dynamic system control into account. Instead of optimizing the treatment process at the beginning with constant operation conditions, the concept of dynamic control can be used to rationally make a series of decisions at different time points and to achieve better performance in terms of cost and efficacy (Yu et al., 2008).

Operation planning tools, on the other hand, have also been widely used to create a policy, change an internal procedure, design a facility, or construct a service program in terms of minimizing the cost or maximizing the profit, especially in environmental applications where decisions are commonly driven by long-term social-economic, political, and technical factors. System optimization and planning approaches are

necessary for supporting wastewater treatment processes because they can make all relevant units orderly, complete the scheduled tasks within the shortest time period to minimize costs and environmental impacts. However, these approaches are usually subject to various uncertainties and complex interactions among technical, environmental and managerial factors. On the other hand, with the increasingly stringent standards and more sophisticated treatment systems, operators have become more and more reliant on mathematical tools instead of their personal experience to optimize the control strategy and actions. The knowledge and prediction of dynamic responses to the variations of environmental conditions and operational factors are critical to ensure a sound design and optimal operation of the treatment process.

It has been recognized that, regardless their difference, the combination of process control and operation planning can ensure the meeting of the economic objectives and the timely completion of the tasks associated with the plans (Hans et al., 2007; Hüfner et al., 2009). Such a coupling can greatly reduce system cost and maximize economic and environmental benefits. Kamar (2010) argued that if appropriate process control is not implemented during a system planning procedure, there might be potential benefits lost because traditional planning tends to be more conservative and less risk-taking. However, such integration is oftentimes complicated by many factors such as the multi-scale nature of decisions, the lack of knowledge of process dynamics and control, and various types of uncertainties.

Firstly, the most commonly cited technical challenge is the multiple time and length scales, or in other words, the coupling between middle/long-term planning decisions such as capital investment, portfolio management and policy-making with a planning horizon

spanning from months to decades, and short-term decisions such as production process control and logistics that are based on day-to-day or even hour-to-hour operations. Secondly, many operation processes of wastewater treatment usually consist of a number of complex physical, chemical, and biological sub-systems and their interactions that are preferably described by nonlinear functions. Nonlinear processes are difficult to control because the process input–output relationship can have so many variations. The issue becomes more complicated if a nonlinear characteristic of the system changes with time and there is a need for an adaptive change of the nonlinear behaviour. Lastly, it can be further complicated by various uncertainties, which may arise from a number of different sources, such as the demands for materials and finished products, feedstock supplies, environmental and economic conditions, and stakeholders' preference and interest. How to more accurately couple process control with operation planning has been a major challenge for the improvement of wastewater treatment systems' performance. To date, the attempt of investigating the feasibility and efficacy of coupling process control and operation planning on marine oily wastewater treatment has not been well documented.

1.2 Research Objectives

The goal of this research, therefore, is to develop an integrated simulation-based process control and operation planning system for marine oily wastewater management. It is developed based on experimental results, process modeling, process optimization, and a coupling between short- and long-term optimization. The experimental study serves as the foundation for process modeling. Process optimization is mainly a coupling

between the process modeling method and advanced optimization tools. Then the short-term process optimization can be integrated with long-term operation optimization. The major research tasks include: 1) to investigate the UV induced degradation kinetics of a representative PAH, namely naphthalene, through photolysis experiments in a bench-scale reactor. It should be noted that UV irradiation is used as an illustrative example in this research to support the following research objectives related to modeling system development; 2) to develop an ANN simulation model for predicting the removal of naphthalene based on the experimental results; 3) to develop an ANN-based dynamic mixed integer nonlinear programming (ANN-DMINP) approach that can help better optimize the performance of marine oily wastewater treatment using a dynamic concept; 4) to develop a set of novel decision making tools for supporting marine oily wastewater management in terms of operation planning; 5) to propose an integrated optimization approach that combines process control with operation planning; and 6) to test the feasibility and effectiveness of the proposed methods via case studies.

1.3 Structure of the Thesis

Chapter 2 focuses on the comprehensive review of marine oily wastewater from the perspectives of background overview, legislative development, conventional treatment technologies, process control, operation planning and their coupling.

Chapter 3 introduces the development and application of two decision-making tools for operation planning, namely the stochastic simulation-based hybrid interval fuzzy programming (SHIFP) approach and the hybrid fuzzy stochastic analytical hierarchy process (FSAHP) approach. Case studies related to oily water treatment planning and

ballast water management are provided for each approach, respectively.

Chapter 4 examines the photodegradation process of naphthalene in marine oily wastewater through bench-scale experiments. The efficiency of UV treatment is tested under varying ambient conditions including salinity, UV fluence rate, initial concentration and temperature. A full factorial design of experiments (DOE) is employed to determine the significance of each factor being tested as well as their interactions. The results obtained in this chapter serves as an example for developing the simulation and optimization approaches in the following chapters.

Chapter 5 provides the development of a three-layer backpropagation neural network model to simulate the UV-induced photodegradation of naphthalene. The importance of each model parameter is evaluated through analysis of variance (ANOVA) and sensitivity analysis and further compared with the experimental results obtained in Chapter 4.

Chapter 6 presents a novel process control methodology, namely the ANN-based dynamic mixed integer nonlinear programming (ANN-DMINP) approach. The ANN simulation model is based on the results obtained in Chapter 5 while genetic algorithm is embedded using a dynamic concept. The proposed approach is validated through a case study with regard to the removal of naphthalene from oily wastewater using UV irradiation and a circulation system.

In Chapter 7, the coupling between process control and operation planning is innovatively realized by integrating neural networks, genetic algorithm, dynamic programming, and Monte Carlo simulation into the integrated simulation-based process control and operation planning (IS-PCOP) system. A case study focusing on the UV secondary treatment of bilge water on an offshore floating production, storage, and

offloading (FPSO) vessel is presented to demonstrate the feasibility and efficacy of this coupling system.

Chapter 8 concludes this study with summarized contribution and recommendations for future research.

CHAPTER 2

LITERATURE REVIEW

This chapter is based on and expanded from the following papers:

Jing, L., Chen, B., Zhang, B.Y., and Peng, H.X. (2012). A review of ballast water management practices and challenges in harsh and arctic environments. *Environmental Reviews*, 20, 83-108, doi: 10.1139/a2012-002

Role: Liang Jing solely worked on this study and acted as the first author of this manuscript under Dr. Bing Chen, Dr. Baiyu Zhang, and Dr. Hongxuan Peng's guidance. Most contents of this paper was written by him and further edited by the other co-authors.

2.1 Overview of Marine Oily Wastewater

Oily wastewater can be generated from a variety of different industrial processes, such as petroleum refining, oil storage and transportation, petrochemical, food, leather and metal finishing. In the marine environment, oily wastewater usually refers to the following sources:

2.1.1 Offshore Produced Water

Produced water is the general description of formation water produced to surface or recycled water from water injection during onshore or offshore oil drilling operations. A global average of 210 million barrels per day was estimated in 1999 and this number has been increasing up to 254 million barrels per day (Neff et al., 2011a and 2011b). Around 65% of the produced water generated in the US is injected back into the producing formation, 30% into deep saline formations and 5% is discharged to surface waters. As a result, water to oil ratio is around 3:1 that is to say water cut is 70%.

The volume, composition, and properties (such as salinity, density, etc.) of offshore produced water may vary significantly between fields and even within the same field depending on many factors (Ebrahimi et al., 2010; Harman et al., 2011). The volume can usually be affected by the method of well drilling, the location of well, the type of well completion, the type of water separation technology, and use of water injection/flooding for oil recovery, and underground communications (Veil, 2011). Offshore produced water usually contains organic and inorganic substances from geologic formation, including produced hydrocarbons, traces of minerals, dissolved salts, and solid particles (Fakhru'l-Razi et al., 2009). It may also come in contact with different types of treatment

and production chemicals (e.g., corrosion inhibitors, scale inhibitors, and biocides) used during drilling, stimulation, production, and oil water separation processes (Kelland, 2014).

Oil in produced water can be classified as dispersed and dissolved oil. Dispersed oil refers to the small oil droplets, which may range from sub-microns to hundreds of microns, whereas dissolved oil represents the oil in produced water in a soluble form. Both dispersed and soluble oil components in offshore produced water consist of petroleum hydrocarbons and other organic compounds such as aliphatic hydrocarbons, aromatic hydrocarbons (e.g., PAHs), organic acids, and phenols (Xu et al., 2008). The amount of dissolved oil largely depends on the type of oil, the volume of water production, artificial life technique, and the age of production. The amount of dispersed oil in produced water is determined by the density of oil, the shear history of the droplet, the amount of oil precipitation and interfacial tension between the water and oil (Stephenson, 1992).

2.1.1.1 Environmental Impacts

Substances of possible concern in offshore produced water include hydrocarbons, heavy metals, radionuclides, and production chemicals. Studies on the environmental impacts caused by produced water discharge from offshore oil and gas operations have been reported in the literature (Alley et al., 2011). The deposited oil can seriously affect the marine environment both as a result of physical smothering and toxic effects (Pivel and Freitas, 2010). Offshore produced water is typically more toxic than other marine wastewater streams as being extremely saline and containing a very broad range of

carcinogens, heavy metals and radionuclides as well as man-made chemicals (e.g., biocides) used in the drilling process. As it is a complex mixture of hundreds of components, in order to assess the associated toxicity, some studies have measured the toxicity of produced water as a whole while others have focused on each individual component (Fakhru'l-Razi et al., 2009). When a component in produced water is bioavailable, it can be taken up by marine organisms. Ekins et al. (2005) suggested that the high bioavailability of contaminant in offshore produced water could result in the accumulation within the organisms (i.e., bioaccumulation via water and food, bioconcentration via water only). These impacts on the marine environment are usually characterized by the complex interrelation between the characteristics of the components in offshore produced water and the characteristics of the receiving water body as well as the exposure period.

2.1.1.2 Legislation and Management Practices

The discharge of offshore produced water to the marine environment has been regulated by regional, national, and international guidelines. Most regulations require intensive studies on environmental impact or risk assessment prior to setting specific limits on the concentrations of oil and grease or dispersed oil in offshore produced water. For example, the current limit for total oil and grease (dispersed and dissolved oil) in treated produced water destined for disposal in offshore waters of Canada is 60 ppm daily maximum and 30 ppm monthly average (Neff et al., 2011a). This 30 ppm oil-in-water standard usually refers to the concentration of oil dissolved or emulsified in water. The same 30 ppm standard has been adopted by the Australian government. The US offshore

produced water discharge standard for oil and grease in the Gulf of Mexico is 29 ppm (Neff et al., 2011b). Recommendations by Oslo Paris Convention in 2001 stipulate that every offshore platform has to comply with the 30 ppm monthly average dispersed oil in water discharge (Igunnu and Chen, 2012). In Australia, the maximum permitted discharge of oil and grease into the oceans is 30 ppm, while this number is set as 10 ppm in China. The Convention for the Protection of the Marine Environment of the North–East Atlantic sets the annual average limit for discharge into the sea at 40 ppm (Veil et al., 2004). Most management practices for offshore produced water focus on onsite treatment and geological disposal. One of the major purposes of offshore produced water treatment is to treat “reverse emulsion” (oil droplets suspended in the continuous water phase). Treated produced water can also be re-injected to the oil production zone to help maintain reservoir pressure and to drive oil toward production well. This option may be chosen when ocean discharge is not permitted in some locations, which may lead to complete elimination of all contaminants in offshore produced water that may threaten the ocean environment (Ahmadun et al., 2009).

2.1.2 Ballast Water

Ballast water is carried by cruise ships, large tankers, and bulk cargo carriers to acquire the optimum propeller depth and to maintain manoeuvrability and stability. It is usually pumped into dedicated ballast tanks or empty cargo holds in coastal waters during the cargo unloading process and discharged at the next port when ship receives cargo (Gregg and Hallegraeff, 2007). Current statistics suggest that shipping facilitates transportation of over 80% of the world’s commodities and transports over 4 billion

metric tonnes of ballast water per year (Tsolaki and Diamadopoulos, 2010).

Over the past decades, aside from being recognized as a major media for global invasive species, ballast water has also been blamed for contributing to marine oil pollution, particularly from the traditional single hull oil tankers (Tamburri et al., 2002). These old-fashioned tankers need to carry enough ballast water in the empty cargo holds after unloading oil cargo. Before any international conventions were adopted to prevent marine oil pollution, a common practice for these tankers was to wash out the cargo holds with water, pump the mixture of oil and water into the sea, and then pump in new ballast water that would be definitely polluted by oil residues. Zakaria et al. (2001) showed that the waters and beaches of the Straits of Malacca have received a significant share (30%) of its oil pollution from the Middle East petroleum through tanker accidents and/or tanker ballasting discharges or washing. Payne et al. (2005) stated that approximately 107 L/day of ballast water which contained 8 mg oil/L has been discharged into the Port Valdez, Alaska by a ballast water treatment plant.

A total of 9,650 oil tankers, representing 1,888 million tonnes of oil, were in service in late 2008. Fortunately, the 2003 amendment to MARPOL 73/78 has accelerated phasing out of all single hull tankers and required the use of double hull tanker in oil trade. Most double hull tankers have segregated ballast tanks that can effectively prevent ballast water from being polluted by cargo oil or fuel oil. The oil pollution threats caused by oily ballast water discharge are likely to be greatly reduced. However, in the rare and exceptional event, extra ballast water may be loaded into a cargo tank to meet tanker's draft and trim requirements. And there will still be single hull tankers in operation in the next few years. Hence, the monitoring and treatment of oily ballast water should still be

given enough attention.

2.1.2.1 Environmental Impacts

Aquatic organisms carried by ballast water may survive lengthy voyages and adapt to new biogeographic regions. Introduced aquatic species have demonstrably adverse effects on local ecological systems, such as decrease in abundance, loss of biodiversity, and even extinction of native species (Tamburri et al., 2002). Invasive species mediated by ballast water are a growing threat to the world's economy, such as aquaculture, fisheries, and international trade (Jing et al., 2012a; Li et al., 2014). The first invasive species was postulated by Ostenfeld (1908) who claimed the observation of an Indo-Pacific diatom in the North Sea. Over 70 fish species native to the U.S. are threatened or endangered by non-indigenous ones (Pimentel et al., 2000). The Chinese mitten crab has invaded and established itself in 11 European countries and across North America such as San Francisco Bay and the St. Lawrence River, causing significant impacts on local biodiversity by eating fish bait (Rudnick et al., 2003; Herborg et al., 2005). Zebra mussels (e.g., *Musculista senhousia* and *Mytilus galloprovincialis*) can also cause dramatic ecological impacts when abundant, ranging from potential displacement of native clams to alternation of energy and nutrient flows in large ecosystems (Cataldo, 2001).

Various hydrocarbons contained in oily ballast water can also cause severe adverse impacts on sea mammals, fish, and other wildlife due to their acute toxicity, limit the photosynthesis of marine plants and phytoplankton, and even affect long-term population growth of the exposed organisms. Ballast water from oil tankers or ballast water

treatment facilities may also contain a considerable amount of dissolved hydrocarbons (Law, 1994). Zakaria et al. (2001) showed that the waters and beaches of the Straits of Malacca have received a significant share (30%) of its oil pollution from the Middle East petroleum through tanker accidents and/or tanker ballasting discharges or washing. Payne et al. (2005) stated that approximately 107 L/day of ballast water which contained 8 mg oil/L has been discharged into the Port Valdez, Alaska by a ballast water treatment plant. These hydrocarbons can cause severe adverse impacts on sea mammals, fish, and other wildlife due to their acute toxicity, limit the photosynthesis of marine plants and phytoplankton, and even affect long-term population growth of the exposed organisms (Kingston, 2003).

2.1.2.2 Legislation and Management Practices

Currently, ballast water exchange (BWE) by sequential exchange or flow-through dilution at designated areas has been recognized as the most commonly applied method to minimize the environmental impacts from transporting and discharging ballast water. Nonetheless, the effectiveness of BWE may be exceedingly influenced by weather conditions, voyage duration and route, vessel capacity, and structural characteristics. Many physical, chemical, and biological treatment methods and their combinations have been tested and applied through both laboratory trials and field practices to remove solids, particulates, organic compounds, and unwanted organisms from ballast water. The International Maritime Organization (IMO) convention also adopts new ballast water management strategies, such as designated exchange areas and onshore ballast water treatment, and especially requires implementation of an onboard and ship-specific ballast

water management plan setting out safe and effective procedures for ballast water management practices (Jing et al., 2012a and 2012b). In case of oil polluted ballast water (e.g., extra ballast water loaded into cargo tanks), the IMO MARPOL Annex I well states the management procedure that includes crude oil tank-washing, gravity separation of oily ballast water, discharge of water below the oil/water interface, and transfer of the remaining oily water to the slop tank for further treatment (IMO, 2011).

2.1.3 Bilge Water

Bilge water, as one of the chronic marine oil pollution sources, has been blamed to cause around 20% of the total oily water released by vessels into the oceans worldwide (Tomaszewska et al., 2005). The bilge is the lowest compartment on a ship where water drained from the deck can be temporarily stored below decks and therefore creates a safer environment for the crew and passengers, particularly in heavy weather (Körbahti and Artut, 2010). It is not uncommon on ships for oil or water to leak into the bilge from various seals, gaskets, fittings, piping, connections, and from related maintenance and activities associated with these systems (Körbahti and Artut, 2013). Depending on the size, function, and design of the ship, bilge water is the mixture of water, fuel oil sludge, lubricating waste oil, cylinder oil, cleaning fluids, and other similar wastes from a variety of different sources (e.g., engines, piping, and other mechanical and operational processes) (Cazoir et al., 2012). For safety concerns, bilge water usually needs to be pumped overboard to prevent the bilge from overflowing the tank tops.

This oily bilge water has been gaining significant attention such that it not only degrades water quality but is also toxic to human and marine life and environment, in

general (Rincón and La Motta, 2014). Oily bilge water is usually caused by petroleum hydrocarbons and contains two distinct components: a gravity separable phase which refers to free oil and an emulsified phase which represents hydrocarbons in stable suspension. The presence of detergents and surfactants in bilge water can also cause chemical emulsification of oil. The stability of emulsion depends on the surfactant concentration which forms a film and avoids the coalescence of oil droplets (Maiti et al., 2011). Emulsified oil (i.e., oil droplets smaller than 20 μm) is the hardest to treat because its neutral buoyancy makes it difficult to separate by gravity alone (Otero et al., 2014).

2.1.3.1 Environmental Impacts

At least to some level, though, most ships have the potential to create marine environment pollution through the discharge of oily bilge water due to malfunctioning oil water separator, accidents, malfunctioning bilge monitor, or a deliberate bilge water bypass (Körbahti and Artut, 2010). Oily bilge water may contain emulsified oil and grease, diesel, hydraulic oil, lube oil, and many other marine fuel oils. Generally, bilge water discharge is considered viscous and therefore has lower risk to vertical mixing (Otero et al., 2014). Nonetheless, the toxicity of numerous petroleum compounds can be significant such that even a small release or spill may result in the abundance decrease of local organisms from the cellular- to the population-level (National Research Council, 2003). National Research Council (2003) also considered the discharge of bilge water to be moderate in terms of physical losses (e.g., evaporation, dispersion), formation of tar balls, and long-distance transport potential. Additionally, possible long-term impacts due to oily bilge water discharge may include: impaired survival or reproduction, chronic

toxicity of persistent components, and habitat degradation (Peterson and Holland-Bartels, 2002).

2.1.3.2 Legislation and Management Practices

The Canadian government has set a 15 ppm oil and grease standard for offshore bilge water discharge. The Clean Water Act (33 CFR 153.305) also prohibits the use of soaps or other dispersing agents to dissipate oil on the water or in the bilge without obtaining permission from the U.S. Coastal Guard. Oily bilge water can be either retained onboard in a holding tank and discharged to an onshore facility or treated onboard. Conventional bilge water systems use an oil water separator to remove oil to meet regulatory standards (i.e., 15 ppm as an international standard set by IMO) prior to discharge. Currently other advanced treatment technologies include adsorbents, flocculants, ultrafilters, membrane, electrocoagulation, and chemical addition with temperature-enhanced centrifugal devices, and polymeric surface modified filtration (Benito et al., 2007; Asselin et al., 2008). Each treatment technology encompasses its pros and cons depending on the complexity of operations, as well as the capital and operating costs. There is no single off-the-shelf technology that can meet all requirements. The selection of the best technology will depend on, in addition to capital and operating costs, the type of ship (i.e. steam ship vs. gas turbine), the amount of loading, the degree of emulsification, the throughput and the robustness required of the unit. The evaluation of average bilge water composition and the degree of emulsification should be taken into account when choosing oily bilge water treatment equipment.

2.2 Treatment of Marine Oily Wastewater

The discharge of untreated or partially treated oily wastewater can cause severe damage to the environment and harmful consequences on public health. That is why many governmental authorities have adopted stringent regulatory standards for oily wastewater management, particularly in the marine environment. Commonly applied management practices include, but not limited to, the following options (Jing et al., 2012a):

- 1) Directly treat wastewater onboard and discharge overboard when the treated effluent meets the environmental standards;
- 2) Dispose or manage wastewater and recoverable materials in permitted locations and facilities, such as near-shore wastewater treatment plants;
- 3) Reduce the generation of wastewater by adopting the-state-of-art clean production techniques, such as using segregated ballast tanks to minimize oily ballast water;
- 4) Reuse or recycle treated oily wastewater whenever possible and practical, such as reusing treated offshore produced water for re-injection. This would save water consumption and eliminate the need for disposal;
- 5) Properly store wastewater and avoid co-mingling wastewater of different classifications, such as separating recyclable wastewater from non-recyclable wastewater.

Onboard treatment is usually the only practical management solution for ships and platforms operating in the marine environment. Several most commonly used onshore oily wastewater treatment methods are briefly summarized as follows:

2.2.1 Gravity Separation

Traditionally, many ocean-going ships and offshore platforms have used gravity separation equipment to treat oily wastewater. These separators are usually equipped with parallel plate or filter coalescing technologies to separate oil from water based on different specific gravities and their immiscibility with each other. The coalescing materials, such as polypropylene and oleophilic polymer, can retain free and dispersed oil droplets (Salu et al., 2011). The droplets continue to accumulate and eventually break free from the plate or media and rise to the surface of the oily water. A sensor can detect the existence of floating oil layer and subsequently trigger an automatic pump to transfer the collected oil to a waste oil tank. However, it should be noted that gravity separation is generally not effective at removing emulsified oil from water because buoyancy differences can be too small. In addition, it is not applicable for removing colloidal metals and soluble organic compounds. Therefore, gravity separation alone is not sufficient to meet the discharge standard and is usually used as the primary treatment unit prior to other advanced techniques.

2.2.2 Flotation

Flotation is the process by which dispersed solid or liquid particles and precipitates in an aqueous solution are floated to the solution surface by injecting and rising continuous gas bubbles. The most commonly used types include impeller flotation, dissolved air flotation, electro-flotation, and pneumatic flotation (Ksenofontov and Ivanov, 2013). Hamia et al. (2007) investigated the performance of combining dissolved air flotation with activated carbon in treating refinery wastewater and obtained high

chemical oxygen demand removal efficiency. Painmanakul et al. (2010) studied the treatment of oily wastewater containing anionic surfactant by using the modified induced air flotation process. They further claimed that the removal efficiency was related to alum dosage, pH value, and gas flow rate. Palomino Romero et al. (2013) reported the optimum conditions for biodiesel wastewater treatment using an integrated electro-flotation and electro-oxidation method. It was demonstrated that electro-flotation could effectively remove turbidity, total solids, oils, and grease. Xu et al. (2014) proposed a cyclonic-static micro bubble flotation column for oily removing oil contents from wastewater. The column was advantageous over traditional flotation techniques in terms of effective separation size, short separation time, large handling capacity, and low operating cost.

2.2.3 Coagulation

Coagulation has been widely used to remove emulsified oil and dissolved oil in recent years. However, it should be noted that due to the complex composition of oily wastewater, the selection of proper coagulant may raise some concerns that would be addressed through experiments (Ahmad et al., 2006). Zeng et al. (2007) developed a new coagulant with cationic polymer synthesized by polysilicic acid and zinc sulfate. Under the optimum conditions of coagulation/flocculation, more than 99% of oil was removed by using the new coagulant cooperated with anion polyacrylamide. Zhao et al. (2014) provided a novel and economic approach of treating oily wastewater based on the enhanced coagulation-flocculation process that integrates synthetic polymers with natural diatomite. Hoseini et al. (2013) employed aluminum sulfate, ferric chloride, and

polyaluminum chloride as coagulants to destabilize the emulsions in oily wastewater. They also integrated coagulation with mechanically induced air flotation and found the optimum operational condition for removing total petroleum hydrocarbons. Such a combination of coagulation with mechanical air flotation has been gaining significant attention in the past decade and appearing as a promising solution (El-Gohary et al., 2010; Rattanapan et al., 2011; Santo et al., 2012).

2.2.4 Membrane Separation

Membranes can selectively separate (fractionate) materials via pores and minute gaps in the molecular arrangement of a continuous structure. Depending on the pore size and the pressure that drives the process, membrane separation can be classified as micro-filtration, ultra-filtration, nano-filtration, ion-exchange, and reverse osmosis (Salahi et al., 2012). Membranes can be made of a variety of materials such as metals, polymers, ceramics, glass fibres, and even stainless steel. Due to its chemical-free nature, membrane separation has been widely applied in water and wastewater treatment. Yu et al. (2006) developed a tabular ultra-filtration module, which was equipped with polyvinylidene fluoride membranes modified by inorganic nano-sized alumina particles. The module was tested on wastewater from an oil field and the results indicated that the quality of permeation water was suitable for oilfield injection. Zhang et al. (2009) applied polysulfone to remove oil contents from wastewater with an oil retention rate over 99% and an oil concentration in the permeation as low as 0.67 ppm. Yang et al. (2011) proposed a Kaolin/MnO₂ bi-layer composite dynamic membrane in oily wastewater treatment. It was discovered that with the increase of oil concentration, the steady

permeate flux decreased while the oil retention ratio increased. Jin et al. (2012) developed a novel nano-filtration membrane incorporated with silica nano-particles by interfacial polymerization on polysulfone ultra-filtration membrane. This nano-membrane was able to not only reduce oil contents but also significantly remove salts from oily wastewater.

2.2.5 Absorption and Adsorption

For both absorption and adsorption treatment process, oily wastewater is pumped through sorption media in a reactor vessel or a contactor. Once the sorption media's capacity is exhausted, the media can be replaced or regenerated. Oil contained in wastewater can be absorbed by granular substances and absorbents or cartridge filters that have high affinity for emulsified oil droplets. Two commonly used absorption materials are organoclay and curable polymeric surfactant (Ibrahim et al., 2010). Organoclay can remove emulsified oil, greases, and large chlorinated hydrocarbons through a partitioning process. The oleophilic property of curable polymeric surfactant can be transferred into filter substrate materials and therefore enhance the attraction of organic compounds to the substrate. On the other hand, adsorption stands for the physical adherence or bonding of organic compounds onto the surface of adsorption media (Wang et al., 2012). One of the most widely used adsorption media is the granular activated carbon, which can effectively remove dissolved oil and hydrophobic organic chemicals from oily wastewater. However, it should be noted that the adsorption media usually needs to be regenerated after a certain period of using time.

2.2.6 Biological Treatment

Biological treatment, as the name indicates, refers to the use of microorganisms in converting petroleum hydrocarbons to carbon dioxide and products that of the catabolic pathways. Technologies that fall into this category include activated sludge, biofilter, which are the most often applied, trickling filter, biological contact oxidation, and anaerobic process. Biological treatment is effective at both dispersed oil droplets and emulsified oil, which can be difficult to remove by many physical/chemical methods. In addition, it can simultaneously remove many other pollutants such as glycols, solvents, detergents, jet fuel, surfactants, nitrogen, and phosphorus. Despite its high capital cost, biological treatment can be environmentally friendly as it only needs aeration, nutrients and pH adjustment without any other add-in chemicals. Shariati et al. (2011) reported a 97% removal efficiency of hydrocarbon pollutants in petroleum refinery wastewater by biodegradation within membrane sequencing batch reactors. Sharghi et al. (2013) treated high salinity synthetic oilfield produced water in a submerged membrane bioreactor with an enrichment culture consisting of a mixed halophilic bacterial species. The results suggested that the proposed system can greatly reduce oil and grease and accommodate high salinity conditions, which can be troublesome for traditional biological treatment. Peng et al. (2014) applied a biological-physicochemical pre-treatment with anaerobic digestion to enhance the treatment of oily wastewater and the production of biogas. The results indicated that the digestion process was promoted due to the inoculation by oil degrading bacteria.

2.2.7 Challenges for Marine Applications

Gravity separation, air flotation, and coagulation are currently most commonly used

in offshore industries, but they are primarily applied towards dispersed and free oil rather than the dissolved fractions. For vessels and platforms operating in the marine environment, the emission of residual oil droplets and dissolved organic compounds including particularly PAHs must be strictly controlled. This is especially true for the Arctic Ocean where zero discharge policy prevails and the release of any organic pollutants may be disastrous. PAHs are ubiquitous environmental pollutants that may originate from both natural and anthropogenic processes such as oil seeps, volcanic eruptions, burning of fossil fuel, coal tar, used lubricating oil and oil filters, and petroleum spills and discharge (Tobiszewski and Namieśnik, 2012).

According to OGP (2002) and Neff et al. (2011b), the typical concentrations of naphthalene, phenanthrene and fluorene in produced water are somewhere between 5 and 841, 9 and 111, and 4 and 67 $\mu\text{g L}^{-1}$, respectively, whereas the other 13 EPA PAHs tend to have much lower concentrations ranging from 0.1 to 15 $\mu\text{g L}^{-1}$. The total concentration of benzene, toluene, ethylbenzene and xylene (BTEX) is between 730 and 24070 $\mu\text{g L}^{-1}$, while phenols have a total concentration around 400 $\mu\text{g L}^{-1}$; however, they are generally less toxic and their natural degradation tends to be much faster than that of PAHs (Neff et al. 2011b). The occurrence of PAHs is usually of the greatest concern because of their high resistance towards biodegradation, extreme toxicity to marine biota, and possible carcinogenicity and mutagenicity (Tsapakis et al., 2010; Harman et al., 2011). The accumulated PAHs may cause many issues such as the inhibition of enzyme activities by disturbing mRNA transcription through DNA damage in the cell and. They can also induce DNA structural perturbations, which are directly correlated with mutagenesis, leading to cellular transformation (Chary et al., 2013). Lee et al. (2011) reported that the

accumulated PAHs can cause severe oxidative DNA damage and therefore lead to tumors and cancer.

Therefore, additional polishing treatment techniques are much desirable after the conventional oil-water separation. Removal of PAHs from preliminarily treated marine oily wastewater (e.g., gravity separation) is possible via many techniques. As described above, biological treatment is considered as an environmentally benign option, except that the capital cost tends to be high and the operation requirements are stringent. The use of membrane separators and adsorption materials has been proven to be viable for both dispersed and dissolved petroleum hydrocarbons, but with considerably high operating and maintenance costs as well as backwash/regeneration needs. Many other methods such as biofiltration, biodegradation, adsorption, and phytoremediation (Haritash and Kaushik, 2009) are greatly restricted by space and safety concerns, low efficiency, high operating cost, corrosion, and re-contamination problems (Yang et al., 2012).

2.2.8 UV Irradiation and Advanced Oxidation

To removal PAHs from primary treatment effluent (e.g., gravity separator, and flotation), UV irradiation and advanced oxidation processes have been gaining significant attention and regarded as promising solutions because of their relatively small footprint, low cost, and high efficiency. They are attractive alternatives to the traditional non-destructive wastewater treatment processes (e.g., air stripping, adsorption, and membrane) because they can mineralize contaminants from water as opposed merely transporting them from one phase to another (Kishimoto and Nakamura, 2011). In recent years, many previous studies have investigated the degradation of PAHs in water and

wastewater by using UV irradiation or its combination with other oxidants (Sanches et al., 2011). Woo et al. (2009) characterized the photocatalytic degradation efficiencies and pathways of five major PAHs in aqueous solution. Kwon et al. (2009) studied the degradation of lowly concentrated phenanthrene and pyrene in aspect of kinetics under UV irradiation. The results suggested an inverse relation between the reaction constants and the number of molecules due to agglomeration of hydrophobic molecules in the aqueous environment. Aliaga et al. (2009) reported the removal of organic capping agents from Platinum colloid nanoparticles using UV/ozone treatment. Wang et al. (2009) studies the decomposition of two haloacetic acids by means of UV and ozone as well as their combinations including UV/ozone, UV/H₂O₂, ozone/H₂O₂, and UV/ozone/H₂O₂. They argued that single UV or ozone did not result in perceptible decomposition of target organics.

Lucas et al. (2010) further examined the effectiveness of ozone, UV/ozone, and UV/ozone/H₂O₂ on the treatment of winery wastewater in a pilot-scale bubble column reactor. Analysis of the experimental data demonstrated that UV/ozone/H₂O₂ has the highest efficiency, followed by UV/ozone and ozone at the natural pH. Vilhunen et al. (2010) designed a re-circulated photoreactor in order to compare the UV photolysis and UV/H₂O₂ oxidation process in removing PAHs from groundwater contaminated with creosote wood preservative. Kishimoto and Nakamura (2011) investigated the effects of ozone bubble size and pH on the efficacy of UV/ozone treatment. The results indicated that increase in bubble size and the decrease in pH resulted in higher ozone utilization efficiency. They argued that this enhancement of ozone utilization was attributed to the shift of the production pathway of OH from O₃⁻ to the UV photolysis of H₂O₂.

Włodarczyk-Makula (2011) discovered a significant impact on the photolysis of PAHs when changing the exposure time from 10 to 20 s as the removal efficiencies were believed to be proportional to the length and intensity of UV exposure. Salihoglu et al. (2012) applied UV irradiation to remove PAHs from municipal sludge and obtained a removal rate up to 77% after 24 hours. The removal rate tended to increase as the temperature elevated during the UV irradiation. Tehrani-Bagha et al. (2012) applied UV-enhanced ozonation processes to the degradation of two organic surfactants and confirmed that the synergistic effects of ozone and UV were more effective than the individual processes. Malley and Kahan (2014) measured the photolysis kinetics of anthracene, pyrene, and phenanthrene in bulk ice and at ice surfaces containing organic matter. The results indicated that bulk ice and ice surfaces have special effects and the presence of organic matter can affect PAH photolysis kinetics by altering the physical environment.

However, most of these studies have focused on freshwater systems. The investigation of UV and advanced oxidation systems for marine wastewater treatment has been limited to a few studies where artificial seawater was mostly used (Kot-Wasik et al., 2004; Saeed et al., 2011; de Bruyn et al., 2012; Jing et al., 2014a and 2014b). It is still unclear how efficient they are in marine applications. In addition, the effects of different environmental and operational factors as well as their interactions on the treatment process are mainly unknown. How to wisely operate the treatment system to acquire the best performance with the least cost has been a challenge for operators. These knowledge gaps may seriously prevent their wide application in the offshore industries. Therefore,

this research will mainly focus on tackling these gaps through an example of UV photolysis of naphthalene.

2.3 Treatment Process Control

Process control is defined as an engineering discipline that deals with mechanisms and algorithms for maintaining the output of a specific engineering process within a desired range. Since wastewater treatment usually consists of a number of complex physical, chemical, and biological processes, controlling such a comprehensive subject largely depends on the quality of treatment effluent and realized through an operator's experience. With the increasingly stringent standards and more sophisticated treatment systems, operators have become more and more reliant on mathematical tools instead of their personal experience to optimize the control strategy.

Zhang and Stanley (1999) developed a neural network process control system for the coagulation, flocculation, and sedimentation processes. The model was found to consistently predict the optimum alum and power activated carbon doses for different control actions. Yu et al. (2010) studied a novel Fenton process control strategy using ANN models and oxygen reduction potential monitoring to treat synthetic textile wastewater. Chiroșcă et al. (2011) examined the fuzzy control of a wastewater treatment process in which the organic substances were removed. Numerical simulations demonstrated that fuzzy control can be used as a reliable alternative to traditional experience-based control. Song et al. (2012) introduced a robust PID controller to control the dissolved oxygen (DO) concentration in wastewater treatment process by considering the characteristics of the time-delay, inertia and time-varying of DO. Abouzlam et al.

(2013) presented a continuous-time transfer function model and an LQ controller in order to minimize the consumption of electrical power and ozone gas of a catalytic ozonation wastewater treatment reactor. Huang et al. (2013) proposed an extended Elman neural network-based energy consumption model to study the relationship between energy consumption and effluent quality in a wastewater treatment plant. Han et al. (2014) used a nonlinear multi-objective model-predictive control scheme, which consisted of self-organizing basis function neural network and multi-objective gradient-based optimization, to find the optimal control of wastewater treatment process.

The knowledge and prediction of dynamic responses to the variations of environmental conditions and operational factors are critical to ensure an optimal operation of the treatment process. A clear understanding of the process mechanism will help to qualify the direct relationships among the inputs and outputs and the indirect relationship such as the time series correlation. To help understand the mechanisms, simulate the process, predict the behaviour, and eventually wisely control the process, modeling methods have been recognized as an essential component and foundation for any successful process control strategies.

2.3.1 Modeling the Treatment Process

As compared to the research efforts on experimental investigation, the numerical modeling and performance optimization of the UV treatment technology has been a challenging area of research due to its multiphysics nature and the complexity of the synergistic effects. Crittenden et al. (1999) developed a kinetic model for the UV/H₂O₂ process in a completely mixed batch reactor. The model includes the known elementary

chemical and photochemical reactions, and literature reported photochemical parameters and chemical reaction rate constants are used in this model to predict organic contaminant destruction. Johnson and Mehrvar (2008) proposed a kinetic model to predict the removal of aqueous metronidazole using the UV/H₂O₂ process. The simulation results of three different photoreactors revealed that the optimal initial H₂O₂ dose was correlated with the reactor radius. Elyasi and Taghipour (2010) developed a computational fluid dynamics (CFD) model in order to simulate UV photoreactors in the Eulerian framework for chemical removal using a UV-based hydroxyl radical initiated oxidation process. Along with a modified planar laser-induced fluorescence technique, the authors were able to simulate and optimize the UV reactor with different geometries and operating conditions. Mohajerani et al. (2012) proposed a pseudo-kinetic model for the treatment of a distillery wastewater by the UV/H₂O₂ process in a continuous tubular photoreactor. The organic degradation rates were measured based on chemical oxygen demand and total organic carbon.

Unlike the single phase flow in regular UV or UV/H₂O₂ reactors, modeling of ozonation usually involves a more complex gas-liquid flow regime which can be further complicated when considering chemical reactions and ozone decay. Bolaños et al. (2008) evaluated the performance of ozone disinfection in fine bubble column contactors based on the principle of computational fluid dynamics and the kinetics of ozone decay. A mixture two-phase flow model and two transport equations were employed to predict the concentration profiles of ozone. Audenaert et al. (2010) simulated a full-scale drinking water plant using equations associated with ozone decomposition, organic carbon removal, disinfection and bromate formation. A scenario analysis was performed to

investigate the performance of this ozonation system at different operational conditions. Cardona et al. (2010) designed a semi-batch ozone bubble column reactor and investigated the gas-liquid mass transfer using the unstationary film theory. Talvy et al. (2011) presented a mathematical model of the momentum and mass transport phenomenon to couple the gas-liquid flow with ozone mass transfer and decay in an industrial scale drinking water treatment plant.

2.3.2 Application of Artificial Neural Networks

The complexity of marine oily wastewater, particularly the presence of inorganic ions including chloride (Cl^-), bromide (Br^-), carbonate (CO_3^{2-}), and bicarbonate (HCO_3^-), may interfere with photochemical treatment and therefore cause challenges in applying traditional chemical reaction models (Nandi et al., 2010; Pendashteh et al., 2011; Li et al., 2012). Although the chemical or physical reactions involved are generally well known in principle, the ability to describe these reactions numerically is limited. Therefore, the major challenge lies on how to establish the nonlinear relationship between inputs and outputs.

Artificial neural networks (ANNs), on the other hand, can effectively recognize and reproduce cause-effect relationships for a complex system. ANNs are inspired by the functionality of human brain where billions of neurons are interconnected to simultaneously process complex information. Since the first application in the 1940s (McCulloch and Pitts, 1943), ANNs have been widely used to simulate complex physical and chemical processes, predict future trends and solve multifaceted problems without mathematically describing the phenomena which are sometimes infeasible. In addition,

not only can the ANNs learn to respond to varying inputs, they are strongly capable of implementing nonlinear functions by allowing a uniform approximation of any continuous function. Such features are fundamental and desirable in studying environmental systems that usually exhibit complex and variable responses (Yoon et al., 2011; May and Sivakumar, 2011; Nourani et al., 2012).

On the other hand, ANNs have also been criticized for their “black box” nature such that the linearity or quadratic dependence of the transfer equations can not readily be understood. The computational burden and the proneness to overfit the training set have also been mentioned in the literature (Elmolla et al., 2010; Colbourn et al., 2011). Among many types of ANNs, two popular ones are the multilayer feed-forward neural network trained by backpropagation algorithm and the Kohonen self-organizing mapping (Aleboyeh et al., 2008; Jiao, 2010; Gazzaz et al., 2012).

Recently, the application of ANNs to simulate wastewater treatment processes, especially photodegradation has been gaining increasing attention. Aleboyeh et al. (2008) have developed a multilayer feed-forward ANN to predict the photochemical decolorization of azo dye by using UV and hydrogen peroxide. Durán et al. (2009) have established a three layers feed-forward network to describe the photodegradation of cyanides and formats in power station effluent under UV/Fe(II)/H₂O₂ process. Elmolla et al. (2010) have examined the implementation of ANNs in simulating and predicting the degradation of antibiotic in aqueous solution by Fenton process. Lin et al. (2012) have applied ANN models to generate relationships among multiple monitored parameters and the total coliform counts to monitor and control UV and UV-TiO₂ disinfections for municipal wastewater reclamation. Many other previous studies have also shown that

ANNs could effectively reproduce experimental data and predict the behaviour of photochemical wastewater treatment processes (Khataee and Kasiri, 2010; Antonopoulou et al., 2012; Frontistis et al., 2012; Pirdashti et al., 2013; Zhou et al., 2013).

2.3.3 Simulation-based Process Control

Experimental and modeling efforts are devoted to understand the behaviour of the UV and advanced oxidation treatment systems, to quantify the influence of each operational parameter, and to predict the performance. However, the lack of process optimization and optimal control of the treatment systems could drastically hinder their widespread applications in shipping and offshore oil and gas industries. Many researchers have engaged in the development and application of process control and optimization tools, particularly for wastewater treatment, to meet the needs for performance and sustainability (Marchitan et al., 2010; Frontistis et al., 2012).

Statistical experimental design methods, such as the Taguchi method and response surface method (RSM), have been widely applied for the sake of improved product yields, reduced process variability, and reduced development time in engineering optimization problems. Zhu et al. (2011) used Box–Behnken experimental design (BBD) and RSM to design and optimize the performance of Fenton and electro-Fenton oxidation processes. Salahi et al. (2012) optimized the operating conditions of nano-porous system membrane processes by using the RSM. G önder et al., (2012) applied the Taguchi method to find the optimum working conditions for the ultrafiltration process in paper mill wastewater treatment. Zirehpour et al. (2014) determined the optimum conditions for achieving higher membrane permeate flux in oily wastewater treatment by using the Taguchi robust

design method.

On the other hand, many soft computing methods, including artificial neural networks (ANN), adaptive network-based fuzzy inference system (ANFIS) (Huang et al., 2009; Elmolla et al., 2010; Turkdogan-Aydinol and Yetilmezsoy, 2010), genetic algorithm (GA), and fuzzy logic (FL), have also received increased attention in this regard (Colbourn et al., 2011; Mullai et al., 2011; Antonopoulou et al., 2012; Lin et al., 2012). Soft computing is known for the combined use of new computation techniques that can achieve higher tolerance towards imprecision, uncertainty, partial truth and approximation. It is usually defined as a methodology that synergically fuses fuzzy logic, neural networks, evolutionary algorithms, and nonlinear distributed systems (Chandwani et al., 2013). The application of these soft computing techniques has been dramatically extended to environmental systems in the past decade (Hu et al., 2012; Shokakar et al., 2012; Jing et al., 2014b; Ghaedi et al., 2014).

Recently, the combined use of the aforementioned techniques has also attracted much attention. Han and Qiao (2011) developed a dynamic structure neural network to control the dissolved oxygen in a wastewater treatment process. The results showed that the proposed approach can improve the control performance due to its adaptive strategy, particularly when the required dissolved oxygen level is changed in the control. Bhatti et al. (2011) developed a three-layer ANN model to predict the removal efficacy of copper from electrocoagulation wastewater as well as the consumption of energy. GA was also used over the ANN model to maximize removal efficiency and to minimize energy consumption. Ma et al. (2011) proposed a hybrid ANN-GA numerical technique to model and optimize the removal of chemical oxygen demand (COD) in an anoxic/oxic system.

Liu et al. (2013) combined GA with ANFIS for estimating effluent nutrient concentrations in a full-scale biological wastewater treatment plant. The results indicated that the GA-ANFIS technique outperformed the traditional ANFIS in terms of effluent prediction accuracy. Soleimani et al. (2013) applied an ANN model to simulate the permeation flux and fouling resistance in separation of oil from industrial oily wastewater. The optimum operating conditions, including trans-membrane pressure, cross-flow velocity, feed temperature and pH, were acquired by using multi-objective GA. Ghaedi et al. (2013) successfully predicted the adsorption of reactive orange 12 using a three layer principle component analysis-ANN. They further demonstrated the optimum operating variables to achieve the maximized adsorption efficiency based on GA. Badrnezhad and Mirza (2014) also integrated ANN with GA to model and optimize the operating parameters involved in the cross-flow ultrafiltration of oily wastewater. Temperature, feed pH, trans-membrane pressure, cross-flow velocity, and filtration time were used as inputs and optimized to get the optimum permeate flux as an output.

Although many studies have investigated the combined use of soft computing techniques, particularly ANN and GA in modeling and optimization of wastewater treatment systems, only a few have taken changing conditions and dynamic system control into account. Instead of optimizing the treatment process at the beginning with constant operation conditions, the algorithm of dynamic control can be used to rationally make a series of decisions at different time points and to achieve better performance in terms of cost or efficacy (Yu et al., 2008). Such a multi-stage control strategy is usually complex and well suited to nonlinear systems where traditional models have difficulty incorporating continuous decisions (Liu et al., 2010; Ferrero et al., 2012). In addition, to

date, no attempt has been reported to integrate dynamic system control with ANN and GA in order to improve the effectiveness and efficiency of marine oily wastewater treatment.

2.4 Treatment System Operation Planning

Operation planning is a complex decision making process that includes the challenge to choose among alternatives that provide, on one hand, a sufficient level of flexibility to react on unforeseen future development and, on the other hand, are economically efficient. An optimized planning can make all relevant units orderly, complete the scheduled tasks within the shortest time period to minimize costs and associated environmental impacts. Environmental decisions can be complex because of the inherent trade-offs among environmental, social, ecological, and economic factors (Kiker et al., 2005; Matott et al., 2009). To deal with this, the application of system optimization approaches for supporting environmental planning processes could be a promising solution (Krohling and Campanharo, 2011; Wandera et al., 2011). This is especially true for wastewater treatment systems as such investments are commonly built, operated, and maintained to generate social and environmental benefits while regulating the discharge of pollutants into the receiving environments (Chang et al., 2011; Zeferino et al., 2012; Lyko et al., 2012; Dong et al., 2014).

Cunha et al. (2009) tried to determine the best possible configuration for the wastewater treatment system according to economic, environmental, and technical criteria. This decision-support model can aid the designing process by covering all the issues involved in the implementation of an integrated water resources management approach. Zeferino et al. (2010) proposed a multi-objective model for regional

wastewater systems planning through the weighting method and simulated annealing algorithm. The model could simultaneously address the minimization of capital costs, the minimization of operating and maintenance costs, and the maximization of dissolved oxygen. Brand and Ostfeld (2011) applied a genetic algorithm model for the optimal design of the transmission gravitational and pumping sewer pipelines, decentralized treatment plants, and end users of reclaimed water of a regional wastewater system. Liu et al. (2011) developed a mathematical programming approach to optimize water resources management by taking into account population distribution, water use/quality and wastewater generation, as well as geographical considerations. The outputs from this model provided the location of desalination plants and wastewater treatment and water reclamation plants, as well as the water conveyance infrastructure needed. Hakanen et al. (2011) described a new interactive tool for wastewater treatment plant design by combining with a treatment process simulator. It utilized interactive multi-objective optimization approach that enabled the design process to be associated with conflicting evaluation criteria. Tsuzuki et al. (2013) quantitatively analyzed pollution discharge indicators to develop a strategy for planning and management of municipal wastewater treatment systems. However, the application of operation planning tools towards marine wastewater treatment has not been well studied in the literature.

Strategic flexibility is usually considered in the evaluation of operation planning solutions in order to accommodate planning uncertainties, which can be caused by the inaccuracies or perturbations of the parameter values, and the ambiguity or lack of information. Uncertainties can be one of the most significant difficulties in making a sound and robust wastewater system planning (Zeferino et al., 2014). Precise information

is generally difficult to obtain due to imperfect knowledge, measurement error, limited data accessibility, and the variations of parameters which are inherent to the environment. System optimization problems, therefore, are usually subject to various uncertainties and complex interactions among technical, environmental and managerial factors. As one of the traditional optimization approaches, fuzzy linear programming (FLP) has long been investigated and advanced since the early stage of fuzzy set theory which allows the representation of uncertainties due to human impreciseness in the form of membership functions (Bellman and Zadeh, 1970; Maleki et al., 2000; Zhang et al., 2003; Veeramani et al., 2011). It can be used to effectively reflect known possibilities and formulate the vagueness inherent in decision making processes in an efficient way. Many attempts have been reported in the literature to use FLP in environmental decision making (Chen et al., 2003; Xu et al., 2009; Li and Chen, 2011; Tan et al., 2011).

On the other hand, stochastic methods also have been widely used to tackle uncertainties with known probability distribution functions especially for objective and constraint coefficients. Review of the existing studies suggests that the most rigorous method of fitting a probability distribution is using the normal distribution (Kiemele et al., 1997; Dunn and Clark, 2009). However, the central limit theorem defines that a normal distribution can only be approximated with a sufficiently large sample size which is often impractical under normal circumstances (Liu et al., 2010). Many parameters and decision variables are usually unknown or replaced with interval estimates based on references or experts' opinions (Chen et al., 2005a, 2005b; Li et al., 2006; He et al., 2009; Cao et al., 2011).

Sometimes people facing situations where quantitative information or mathematical solutions are not readily available. For example, industrial stakeholders need to make a long-term decision on purchasing a suitable oily wastewater treatment system for onboard use by taking economic, environmental and technological factors into account. Decision makers, under such circumstances, usually need to reach a subjective consensus based on their personal experience, expertise as well as individual style and perspective. Many multi-criteria decision making (MCDM) approaches have been developed to facilitate decision making under such uncertainties and the lack of knowledge. Kornysheva and Salinesi (2007) classified them into categories such as outranking methods, analytic hierarchy process, multi-attribute utility theory, weighting methods, fuzzy methods, and multi-objective programming.

Among them, the analytic hierarchy process (AHP), first proposed by Saaty (1980), is one of the most widely used MCDM approaches. It structures the rational analysis of decision making by dividing a problem into hierarchies including goal, criteria, sub-criteria (if any), and decision alternatives. One of the most important features, or in other words, the strengths of the AHP revolves around the possibility of evaluating quantitative as well as qualitative criteria and alternatives on the same preference scale. Pairwise comparison judgments are given by decision makers using numerical, verbal or graphical scales and are subsequently synthesized to obtain the overall priorities. This comparison enables the AHP to capture subjective and quantitative judgment made by decision makers. Many attempts have been reported in the literature to apply the AHP in problems with high complexity and uncertainty, especially in the environmental sector (Tolga et al., 2005; Chowdhury and Husain, 2006; Jablonsky, 2007; Tiryaki and

Ahlatcioglu, 2009; Sadiq and Tesfamariam, 2009; Kaya and Kahraman, 2011). However, the AHP has been criticized for its inability to quantify the uncertainty associated with decision making (Deng, 1999). Banuelas and Antony (2004) highlighted that the basic theory of the AHP does not allow any statistical conclusion to be drawn. Rosenbloom (1996) stated that a small difference in the utilities of alternatives may not be appropriate to conclude that one alternative is superior to the other. Carlucci and Schiuma (2009) argued that the AHP is not able to address the interactions and feedback dependencies between the elements of a decision problem. In addition, in many real-world applications, the available information is imprecise, incomplete and occasionally unreliable due to the unquantifiable nature of data or lack of knowledge. Human experts tend to use linguistic terms (e.g., good, poor, excellent) to express their judgments which may not be handled effectively using crisp scales.

To overcome the aforementioned limitations, much research effort has therefore been directed towards taking uncertainties (e.g., through fuzzy sets and probability distributions) into account in the AHP. On one hand, to capture linguistic information, Yu (2002) employed an absolute term linearization technique and a fuzzy rating expression into a GP-AHP model for solving fuzzy AHP problems. Tolga et al. (2005) combined the use of fuzzy set theory with the AHP to address the uncertainty of assigning crisp concepts in decision-making topics. Tesfamariam and Sadiq (2006) incorporated uncertainty into the AHP using fuzzy arithmetic operations for environmental risk management. Chowdhury and Husain (2006) integrated fuzzy set theory, the AHP, and the concept of entropy to select the best management plan for a drinking water facility. Kaya and Kahraman (2011) proposed a hybrid fuzzy AHP-ELECTRE approach for

modeling the uncertainty of linguistic expression. On the other hand, to deal with insufficient information and opinion difference in group decision-making processes, pairwise comparison elements were suggested to be viewed as random variables and computed via Monte Carlo simulation by Rosenbloom (1996), Eskandari and Rabelo (2007) and Jing et al. (2013b and 2013c).

To date, triangular distribution is the most commonly used distribution for modeling expert judgment in the AHP (Banuelas and Antony, 2004; Hsu and Pan 2009). However, it may place too much emphasis on the most likely value at the expense of the values to either side (Phanikumar and Maitra, 2006). It is possible to overcome this disadvantage of the triangular distribution by using the beta-PERT distribution. The beta-PERT distribution has also been widely used for modeling expert judgments and providing a close fit to normal distributions with less demand for data (Coates and Rahimifard, 2009; Jing et al., 2012b). It uses the most likely, minimum, and maximum values of expert estimates to generate a distribution that more closely resembles realistic probability distribution. Jing et al. (2012b) proposed a Monte Carlo simulation aided analytic hierarchy process (MC-AHP) approach by employing the beta-PERT distribution to prioritize nonpoint source pollution mitigation strategies. Jing et al. (2013b) further integrated the uniform distribution with interval judgment to a hybrid stochastic-interval analytic hierarchy process (SIAHP) approach for group decision making on wastewater reuse.

2.5 Integration of Process Control and Operation Planning

Operation planning tools has been widely used to create policy, change an internal procedure, design a facility, or construct a service program in terms of minimizing the cost or maximizing the profit, especially in environmental applications where decisions are commonly driven by social-economic, political, and technical factors. On the other hand, process control techniques have also been receiving significant attention over the years because they can be applied to optimize control strategies and thereby reduce operating cost. With the advance of modern technology, a variety of new techniques and equipment have become available and the cost-savings by optimally controlling such processes become more economically attractive. It is not uncommon that decision makers or stakeholders would like to integrate process control techniques into their planning and strategic decision making framework.

Recently, it has been recognized that, regardless their difference, the combination of process control and operation planning can ensure the meeting of the economic objectives and timely completion of the tasks associated with the plans (Hans et al., 2007; Hüfner et al., 2009). Hüfner et al. (2009) reported that a high-quality production planning needs to reflect the uncertainties associated with the market and technical parameters and to accommodate the feasible operation scheduling. Kamar (2010) argued that if appropriate process control is not implemented during the operation planning procedure, there might be potential benefits lost because traditional planning tends to be more conservative and less risk-taking. Verl et al. (2011) stated the importance of distinguishing between “detailed scheduling and process control” and “operation planning”. Nonetheless, they also claimed that process control consists of the anticipatory consideration and the

reaction to unexpected occurrences, while long-term planning is usually a prerequisite for detailed scheduling and process control. How to take process control and scheduling into account during operation planning have become a rapidly growing area of research and a subject of interest to academicians and practitioners alike.

However, such integration is oftentimes complicated by many factors such as multi-scale nature of decisions, the lack of knowledge of process dynamics and control, and various types of uncertainties. Firstly, the most commonly cited technical challenge is the multiple time and length scales, or in other words, the coupling between long-term planning decisions such as capital investment, portfolio management and policy-making with a planning horizon spanning from months to decades, and short-term decisions such as production process control and logistics that are based on day-to-day or even hour-to-hour operations. Many advanced processes are now required to be modeled on as fine-grained a time scale as hour to hour to represent their variability accurately, whereas most traditional operation planning strategies still follow a much coarser time scale such as month-to-month or year-to-year. How to effectively merge these different time scales presents a daunting challenge.

Secondly, many operation processes usually consist of a number of complex physical, chemical, and biological sub-systems that are preferably described by nonlinear functions. Traditional process models that are developed based on classic theorems may not effectively describe these complex sub-systems because the models are usually created by applying different abstraction methods in which essential properties and key process indicators are preserved and insignificant details are left out. Therefore, how to precisely simulate the nonlinear systems and predict the outputs with high accuracy has been an

obstacle for learning the behaviour of many operation processes.

Lastly, the coupling of process control and operation planning can be further complicated by various uncertainties, which may arise from a number of different sources, such as demands for materials and finished products, feedstock supplies, environmental and economic conditions, and customers' willingness to pay. The rapid development of technologies may also bring uncertainties as most technologies are in the process of maturing and the relevant costs and yields are not likely to be certain, not to mention the policies that are highly influenced by unpredictable political factors (Engell, 2009).

Despite the above mentioned difficulties, there has been some research efforts directed towards the aforementioned needs of coupling process control and operation planning. Chakraborty and Bhattacharaya (2006) developed a process-based mathematical model to not only help the rational design of the methane production process but also enable the effective dynamic control of the production. Janak et al. (2006) implemented a continuous-time formulation for short-term scheduling (i.e., a few days) of batch processes with multiple intermediate due dates and finally led to a medium-term production planning framework. Hüfner et al. (2009) presented a new combined algorithm to solve long-term planning and short-term scheduling problems of batch production process under uncertainty. A two-stage stochastic linear integer program was employed to solve the planning problem while a priced timed automata model was designed for the scheduling problem. This two-layer concept can return a penalty back to the planning layer and re-evaluate the long-term plans if the scheduling targets are not met. Yan et al. (2009) combined short-term ship routing and long-term fleet planning models in order to maximize the total benefit of a fleet voyage problem. Verl et al. (2011)

proposed a model-based energy efficiency optimization for production system planning by using multilevel monitoring and control system. The material flow simulation of the process chain with state-based energy models of manufacturing resources were taken into account as process control modules. Powell et al. (2012) proposed a stochastic multi-scale model according to the concept of dynamic programming and can be used for both deterministic and stochastic problems. The model had a theoretic framework to derive near-optimal policies by running hourly simulations over multiple decades. Lee (2012) concluded that the control and scheduling of many engineering processes during system planning are usually influenced by the lack of knowledge and precise modeling tools due to the wide existence of nonlinearity. However, to date, there has been no such attempt made to investigate the feasibility and efficacy of coupling process control and operation planning on wastewater treatment applications, particularly for marine oily wastewater.

2.6 Summary

Marine oily wastewater has been recently criticized as a major source of oil pollution in the marine environment. Unlike catastrophic oil spills, the discharge of oily wastewater, including ballast water, offshore produced water, and bilge water, usually occurs on a daily basis without triggering any mitigation response. The accumulated effects of discharging untreated or partially treated oily wastewater can lead to significantly negative impacts on marine lives and even human health. One of the best management practices is onboard treatment. The treatment of oily wastewater can be undertaken using a number of physical, chemical, and biological methods, such as gravity separation, air

flotation, coagulation, membrane filtration, absorption, adsorption, and biological treatment. However, most of them are only used for removing dispersed/free oil (e.g., gravity separation) or even not applicable (e.g., biological treatment) for onboard treatment due to safety, space and cost concerns. The emission of residual oil droplets and dissolved organic compounds including particularly PAHs are not likely to be affected and must be stringently controlled. This is especially true for the Arctic Ocean and the North Atlantic where zero discharge policy prevails and the release of any organic pollutants may be disastrous. Therefore, additional polishing treatment technique is much desirable after the conventional oil-water separation to further remove PAHs.

Recently, UV irradiation and advanced oxidation processes have been gaining significant attention and regarded as promising solutions because of their relatively small footprint, low cost, and high efficiency. However, most of the previous studies have focused on freshwater systems rather than marine environments where salinity and complex matrix effects play a dominant role. Moreover, the research efforts on numerical modeling and performance optimization of these techniques have also been limited due to their multiphysics nature and the complexity of synergistic effects. Such advanced treatment systems, as compared to the traditional ones, are still lack of in-depth understanding of their reaction mechanisms, performance evaluation, process optimization, and operation planning, which can drastically hinder their widespread applications in shipping and offshore oil and gas industries.

A good treatment system operation usually requires both process control and operation planning to minimize treatment cost, minimize treatment time, and maximize treatment efficiency. System optimization and planning approaches are necessary for

supporting wastewater treatment processes because they can make all relevant units orderly, complete the scheduled tasks within the shortest time period to minimize costs and associated environmental impacts. However, these approaches are usually subject to various uncertainties and complex interactions among technical, environmental and managerial factors. Sometimes people facing situations where quantitative information or mathematical solutions are not readily available. Decision makers, under such circumstances, usually rely on multi-criteria decision making (MCDM) approaches to reach a subjective consensus. On the other hand, with the increasingly stringent standards and more sophisticated treatment systems, operators have become more and more reliant on mathematical tools instead of their personal experience to optimize the control strategy. A clear understanding of the process mechanism will help to qualify the direct relationships among the inputs and outputs and the indirect relationship such as the time series correlation.

Process modeling is usually regarded as the foundation of any effective process control strategy as it provides the response of the process to any inputs on which control optimization is based. Recently, the combined use of soft computing methods, including artificial neural networks (ANN), adaptive network-based fuzzy inference system (ANFIS), genetic algorithm (GA), and fuzzy logic (FL), has been of growing interest in process control. Such a combination can achieve higher tolerance towards imprecision, uncertainty, partial truth and approximation as compared to traditional methods. However, most of the literature studies have focused either on process-control or operation-planning strategies while the integration has been drastically limited, particular in the field of marine wastewater management. More research efforts should be directed to such

integration as it can provide the decision makers or operators of marine wastewater treatment systems a boarder perspective of performance optimization in terms of economic, environmental, and technical considerations.

CHAPTER 3

NOVEL OPERATION PLANNING TOOLS FOR MARINE OILY WASTEWATER MANAGEMENT

This chapter is based on and expanded from the following papers:

Jing, L., Chen, B., and Zhang, B.Y. (2013). A hybrid fuzzy stochastic analytical hierarchy process (FSAHP) approach for evaluating ballast water treatment technologies. *Environmental Systems Research*, 2:10, doi:10.1186/2193-2697-2-10.

Role: Liang Jing solely worked on this study and acted as the first author of this manuscript under Dr. Bing Chen and Dr. Baiyu Zhang's guidance. Most contents of this paper was written by him and further edited by the other co-authors.

Jing, L., Chen, B., Zhang, B.Y., and Li, P. (2012). A stochastic simulation-based hybrid interval fuzzy programming approach for optimizing the treatment of recovered oily water. *The Journal of Ocean Technology*, 7(4), 59-72.

Role: Liang Jing solely worked on this study and acted as the first author of this manuscript under Dr. Bing Chen and Dr. Baiyu Zhang's guidance. Most contents of this paper was written by him and further edited by the other co-authors.

3.1 A Stochastic Simulation–Based Hybrid Interval Fuzzy Programming (SHIFP) Approach

3.1.1 Background

An offshore oil spill is defined as the discharge or release of petroleum hydrocarbons into the ocean or coastal waters. It may be due to the collision and/or grounding of oil tankers, accidental spill or leakage from offshore platforms and drilling rigs, and natural disasters such as typhoons and earthquakes that can cause huge damage to sea-based facilities and tankers. Oil spills can constitute a direct hazard to marine ecosystems and human health through a variety of pathways, including the digestion of oil, oiling of feathers and skins, the avoidance of oil habitat, inhalation or dermal contact, and the indirect threats to seafood safety and mental health (Boehm et al., 2008). The cleanup of offshore oil spills is usually subject to many constraints such as the type of oil, oil-water volume fraction, and temperature. The most commonly used methods include booming and skimming, chemical dispersants, biodegradation, in-situ burning, and the use of sorbents. Each method has its own advantages and disadvantages while skimming is one of the most environmentally friendly oil removal techniques (Pezeshki et al., 2000; You and Leyffer, 2011). Oil skimmers can float across the top of the slick contained within the boom and suck or scoop the oils of different viscosities into storage tanks without adding chemicals. It is worth noting that most crude oils and intermediate to heavy products can emulsify and form so-called water-in-oil-emulsions when spilled at sea. Therefore, the recovered mixture usually contains not only oil but also water and needs to be further treated before discharge (Gaaseidnes and Turbeville, 1999; Maguire-Boyle and Barron, 2011).

The simplest treatment is nothing more than using a series of large holding tanks to allow water and oil to be separated under the action of gravity alone. In addition to that, centrifugal separators are known in which the oily mixture is forced to rotate at extremely high angular velocities thereby causing the separation of oil and water by density (Krebs et al., 2012). Other management options such as destruction by incineration and direct disposal to landfill have also been implemented in some areas to accommodate the limited storage or processing capacity. However, a rich body of literature documents indicated that the transportation and treatment of recovered oily water usually requires a large number of personnel and equipment (Dollhopf and Durno, 2011). This may, if not properly planned, significantly increase the cost and time of cleanup and pose a variety of technical challenges, particularly in the context of harsh environments where cold water, low temperature, dynamic/strong wave and current can significantly affect the applicability of these measures (Jing et al., 2012c). While an optimized contingency plan can make all relevant units orderly, complete the scheduled tasks within the shortest time period to minimize costs and associated environmental impacts. To deal with this, the application of system optimization approaches for supporting environmental decision making processes seems a promising solution.

Precise information is difficult to obtain due to imperfect knowledge, measurement error, limited data accessibility, and the variations of parameters which are inherent to the environment. System optimization problems, therefore, are usually subject to various uncertainties and complex interactions among technical, environmental and managerial factors. Although various types of uncertainty have been discussed in the literature, there has been no study investigating the feasibility of handling both types of fuzzy,

probabilistic and interval inputs in system optimization problems. The interval-based FLP, uniform distribution, and Monte Carlo simulation would be integrated to simultaneously communicate fuzzy, interval, and stochastic uncertainties caused by imprecise information, subjective judgment, and variable environmental conditions into the optimization process.

Therefore, in this section, a stochastic simulation–based hybrid interval fuzzy programming (SHIFP) approach is developed to aid the decision making process by solving fuzzy linear optimization problems. Fuzzy set theory, probability theory, and interval analysis are combined to provide decision makers with a better understanding of the impact of their decisions. A case study related to recovered oily water treatment during offshore oil spill cleanup operations is conducted to illustrate the feasibility of the SHIFP approach.

3.1.2 Methodology

3.1.2.1 Fuzzy Sets and Fuzzy Logic

Zadeh (1965) first introduced the concept of fuzzy logic which was oriented to the rationality of uncertainty due to imprecision or vagueness. It is an extension of the classical set theory in which elements have grades of membership ranging from 0 to 1. Unlike classical set theory, fuzzy logic is a superset of conventional (Boolean) logic that has been extended to handle the concept of partial truth- truth values between “completely true” and “completely false”. As its name suggests, it is the logic underlying modes of reasoning which are approximate rather than exact. The importance of fuzzy logic derives from the fact that most modes of human reasoning and especially common

sense reasoning are approximate in nature. The essential characteristics of fuzzy logic include the following aspects: 1) exact reasoning is viewed as a limiting case of approximate reasoning; 2) everything is a matter of degree to a certain set, or in other words, everything has elasticity and nothing is absolute; 3) any logical system can be fuzzified; 4) knowledge is interpreted as a collection of elastic or, equivalently, fuzzy constraint on a collection of variables; and 5) inference is viewed as a process of propagation of elastic constraints.

If Ω is a set, then a fuzzy subset \bar{A} is defined by its membership function $\bar{A}(x)$, which produces values in $[0, 1]$ for all x in Ω . Therefore, $\bar{A}(x)$ is a function mapping Ω into the range of $[0, 1]$. If $\bar{A}(x_0)$ equals to 1, then it can be stated that x_0 completely belongs to the fuzzy subset \bar{A} . If $\bar{A}(x_1)$ equals to 0, then it means that x_1 does not belong to \bar{A} at all. If $\bar{A}(x_2)$ equals to a fractional, say 0.5, then it can be concluded that the membership value of x_2 in \bar{A} is 0.5, indicating that the possibility of value x_2 being classified into the category of \bar{A} is 50%. Most of the fuzzy sets can be described by fuzzy numbers, most commonly triangular fuzzy numbers (TFNs). A triangular fuzzy number, with a membership function $\mu(x)$, is defined by three numbers a , b , and c where the base of the triangle is the interval $[a, c]$ and its vertex at b .

$$\mu(x) = \begin{cases} (x-a)/(b-a), & a \leq x \leq b \\ (x-c)/(b-c), & b \leq x \leq c \\ 0, & \textit{otherwise} \end{cases} \quad (3.1)$$

3.1.2.2 Interval Theory

Interval theory was developed in the 1950s as an approach to putting bounds on rounding errors and measurement errors in mathematical computation and thus developing numerical methods that yield reliable results. The main focus is on the simplest way to calculate upper and lower endpoints for the range of values of a function in one or more variables due to uncertain information or vagueness. These barriers are not necessarily the supremum or infimum, since the precise calculation of those values can be difficult or impossible. For instance, instead of roughly estimating the concentration of benzene in water using standard arithmetic as 1 ppm, interval arithmetic gives a more confident concentration range between 0.5 and 1.5 ppm. The most common use is to keep track of and handle rounding errors directly during the calculation and of uncertainties in the knowledge of the exact values of physical and technical parameters. The latter often arise from measurement errors and tolerances for components or due to limits on computational accuracy. Interval arithmetic has helped people find reliable and guaranteed solutions to equations and optimization problems.

3.1.2.3 Stochastic Programming by Monte Carlo Simulation

Monte Carlo simulation, which applies probability theory to address variable and uncertain phenomena, relies on statistical representation of available information. It has been widely applied to obtain more detailed information for systems that are too complex to be solved analytically. Monte Carlo simulation in its simplest form involves random sampling from a probability distribution. Various probability distributions (e.g., uniform, normal, beta, and lognormal) have been used in connection with Monte Carlo simulation

to model the uncertainty of environmental systems. Banuelas and Antony (2004) presented a modified analytic hierarchy process with triangular probability distribution to include uncertainty in the judgments. Li and Chen (2011) developed a fuzzy-stochastic-interval linear programming (FSILP) approach for supporting municipal solid waste management by tackling uncertainties expressed in normal probability distributions, fuzzy membership functions and discrete intervals.

3.1.2.4 The SHIFP Approach

In a decision process using the traditional FLP model, coefficients and variables may be fuzzy, instead of precisely given numbers as in crisp linear programming models. Consider the following FLP problem with fuzzy variables and fuzzy constraints (Kumar et al., 2011; Dubey et al., 2012):

$$\max_{X_j} \bar{Z} = \sum_{j=1}^n \bar{c}_j \bar{X}_j \quad (3.2)$$

subject to:

$$\sum_{j=1}^n \bar{a}_{ij} \bar{X}_j \leq \bar{b}_i \quad 1 \leq i \leq m \quad (3.3)$$

$$0 \leq \bar{X}_j \leq M_j \quad 1 \leq j \leq n \quad (3.4)$$

where \bar{Z} is the value of the objective function; \bar{c}_j are the objective function coefficients; \bar{X}_j are the decision variables; \bar{a}_{ij} are the constraint coefficients; \bar{b}_i are the right-hand sides of constraints; and M_j , which are real numbers, are the upper bounds of decision variables. A basic assumption is that \bar{c}_j , \bar{X}_j , \bar{a}_{ij} , and \bar{b}_i are all triangular fuzzy numbers. Note that \bar{b}_i

and M_j are usually given by literature data or subjective experience. On the other hand, \bar{a}_{ij} and \bar{c}_j , such as machine hours, labour force, required materials, and operating cost are usually imprecise due to incomplete information and the lack of complete understanding. Their minimum and maximum bounds can be determined based on literature review or expert survey. To account for imprecise knowledge and to model the uncertainty, triangular fuzzy numbers with regard to \bar{a}_{ij}, \bar{c}_j , and the corresponding \bar{X}_j are randomly generated using Monte Carlo simulation within given intervals such that the left spread, right spread, and vertex values are assumed to have uniform distributions. The uniform distribution is commonly used where one can specify only the minimum and maximum possible values for the input variable. Subsequently, the constraints are examined to verify if any of them has been violated. If all constraints are satisfied, \bar{X}_j are determined to be feasible and a corresponding value of the objective function \bar{Z}^* can be calculated. If \bar{Z}^1 is the current best and $\bar{Z}^* \geq \bar{Z}^1$, then \bar{Z}^1 should be replaced with \bar{Z}^* , otherwise \bar{Z}^* is discarded. Repeat the above procedure for a number of replications; the optimization results can be obtained as probability distributions (Alba et al., 2011; Li et al., 2013). The detailed algorithm can be summarized as follows:

Step 1: Assign triangular fuzzy numbers to \bar{b}_i and crisp values to M_j based on literature review or subjective opinions. It is noted that M_j are treated as real numbers because the intervals $[0, M_j]$ are used to generate random fuzzy numbers.

Step 2: Review literatures and collect expert opinions about the values of each constraint and objective function coefficient which can be either intervals or discrete numbers. Set the minimum and maximum bounds for each coefficient such that uniform distributions

can be assumed within the bounds.

Step 3: Sobol quasi-random numbers of uniform distribution are generated in sets of three (i.e., left spread, right spread, and vertex point of a triangular fuzzy number) and bounded between 0 and 1. Equation 3.5 is then applied to convert the random numbers from unit interval [0, 1] to the preset intervals of each coefficient (i.e., $\overline{a_{ij}}$ and $\overline{c_j}$). It should be satisfied that left spread \leq vertex \leq right spread to ensure the triangular shape.

$$Random = \overline{min} + urnd(\overline{max} - \overline{min}) \quad (3.5)$$

where *Random* represents the random numbers for the left, right, and vertex points of $\overline{a_{ij}}$ and $\overline{c_j}$; \overline{min} and \overline{max} are the minimum and maximum bounds determined in Step 2, respectively; and *urnd* are Sobol quasi-random numbers of uniform distribution.

Step 4: As with Step 3, for each specific set of $\overline{a_{ij}}$ and $\overline{c_j}$, random triangular fuzzy numbers are generated for $\overline{X_j}$ and bounded between 0 and M_j .

Step 5: Examine the constraints to ensure the validity of $\overline{X_j}$. Calculations are based on the α -cuts and interval arithmetic (Buckley and Lowers, 2008). If any constraint is not satisfied, then $\overline{X_j}$ need to be regenerated.

Step 6: The objective function is calculated as \overline{Z}^* using feasible $\overline{X_j}$ and further compared with the current best value \overline{Z}^1 using Chen's Method (Chen and Hwang, 1992). If $\overline{Z}^* \geq \overline{Z}^1$, then \overline{Z}^1 should be replaced with \overline{Z}^* , otherwise \overline{Z}^* is discarded.

Step 7: Repeat Steps 4 through 6 for a preset number of replications (e.g., 1,000, and 5,000) to obtain the maximum objective function as a triangular fuzzy number in terms of each set of $\overline{a_{ij}}$ and $\overline{c_j}$. The centre of gravity method is used to defuzzify the fuzzy objective

function value (i.e., triangular fuzzy number) into a crisp value (Van Broekhoven and De Baets, 2006).

$$COG(\bar{w}) = \frac{\int_{a_w}^{c_w} x\mu_w(x)dx}{\int_{a_w}^{c_w} \mu_w(x)dx} \quad (3.6)$$

where a_w and c_w are the minimum and maximum bounds of fuzzy number \bar{w} ; and μ_w is the membership function.

Step 8: Repeat Steps 3 through 7 for a preset number of replications (e.g., 1,000, and 5,000), the defuzzified maximum objective function can be obtained as a probability distribution function in order to reflect the inherent uncertainty in the optimization process.

3.1.3 Case Study

The objective of this case study is to examine the effectiveness of the proposed SHIFP approach in handling various uncertainties in the system optimization process. A hypothetical case of oil spill was assumed to occur in the North Atlantic near shore of Newfoundland and Labrador. An estimated total of 50,000 tonnes of bunker oil was accidentally spilled and needed to be cleaned up. Numerous weir skimmers and drum skimmers were employed to collect spilled oil which was more or less blended with seawater. The local authority had a number of incineration barges, vacuum trucks, centrifugal separators, and temporary storage facilities to treat the recovered oily water. However, it was unknown that how many units should be used and how much wastewater should be delivered to each facility. The objective was therefore to maximize the

treatment capacity of recovered oily water on a daily basis in order to reduce environmental risks. The main constraint was associated with the costs encountered in the treatment processes such that the total net cost should not exceed a given limit. The decision variables were chosen as the daily operation hours of each treatment facility by which decision makers could arrange the schedule for cleanup actions.

$$\max_{\overline{X}_j} \overline{Z} = \sum_{j=1}^4 \overline{c}_j \overline{X}_j \overline{N}_j \quad (3.7)$$

subject to:

$$\sum_{j=1}^4 \overline{a}_j \overline{X}_j \overline{N}_j + \sum_{j=1}^4 \overline{c}_j \overline{d}_j \overline{X}_j \overline{N}_j - \sum_{j=1}^4 \overline{c}_j \overline{e}_j \overline{X}_j \overline{N}_j \leq \overline{b} \quad (3.8)$$

$$0 \leq \overline{X}_j \leq M_j, \quad j = 1, 2, 3, 4 \quad (3.9)$$

where \overline{Z} is the total daily treatment capacity which needs to be maximized (tonnes/day); \overline{c}_j are the hourly treatment capacities of each facility; \overline{X}_j and \overline{N}_j are the daily operation hours and the total numbers of each facility, respectively; \overline{a}_j and \overline{d}_j are the operation and maintenance (O&M), and transportation costs, respectively; \overline{e}_j are the selling prices of recovered bunker oil from each facility; and \overline{b} is the maximum daily total budget (in CAD) which was set by the local authority as (110,000, 130,000, 150,000); and M_j are the maximum daily operation hours of each facility, in other words, the upper bounds of each decision variable. The corresponding lower and upper bounds of the coefficients and decision variables were arbitrarily assumed for computational simplicity (Table 3.1). It should be noted that the number of Monte Carlo iterations used here was determined as 1,000 by taking time constraints and the efficiency of convergence into account.

Table 3.1 Detailed description of treatment facilities of recovered oily water

| Facilities | Sequence | Total number | Daily hours (hr) | O&M cost (CAD/hr) | Transportation cost (CAD/tonne) | Hourly capacity (tonnes/hr) | Recovered oil price (CAD/tonne) |
|-----------------------|----------|--------------|------------------|-------------------|---------------------------------|-----------------------------|---------------------------------|
| | j | N_j | \bar{X}_j | \bar{a}_j | \bar{d}_i | \bar{c}_j | \bar{e}_j |
| Incineration barge | 1 | 6 | [0, 12] | [100, 500] | [4.5, 6] | [0.15, 0.25] | 0 |
| Vacuum truck | 2 | 20 | [0, 24] | [200, 300] | [20, 30] | [3, 5] | [26, 35] |
| Centrifugal separator | 3 | 10 | [0, 20] | [100, 250] | [20, 30] | [8, 11] | [30, 50] |
| Temporary storage | 4 | 5 | [0, 16] | [20, 60] | [33, 40] | [4, 5.5] | [18, 24] |

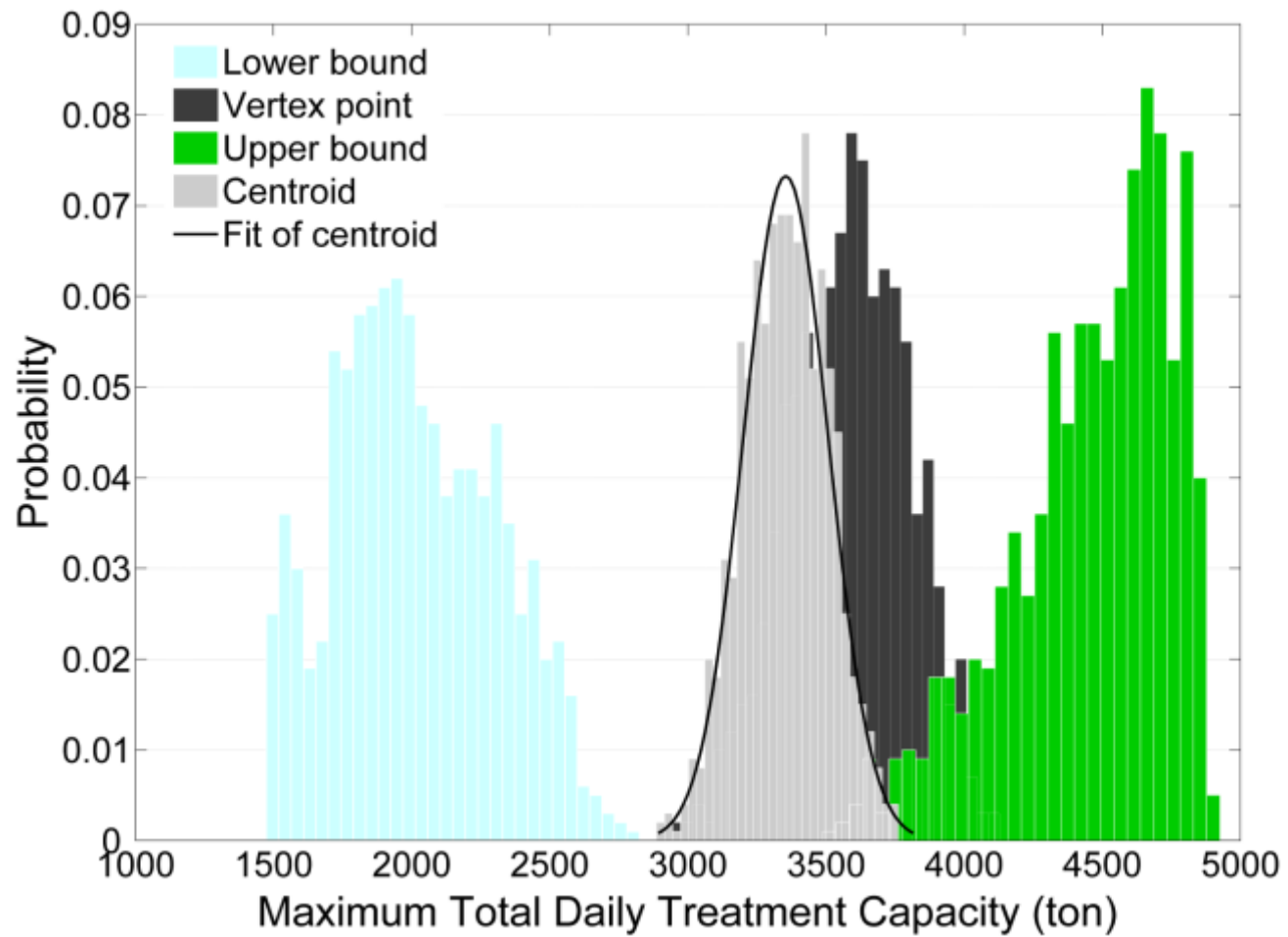


Figure 3.1 Probability distributions of the lower bound, vertex point, upper bound, and defuzzified centroid of the objective function

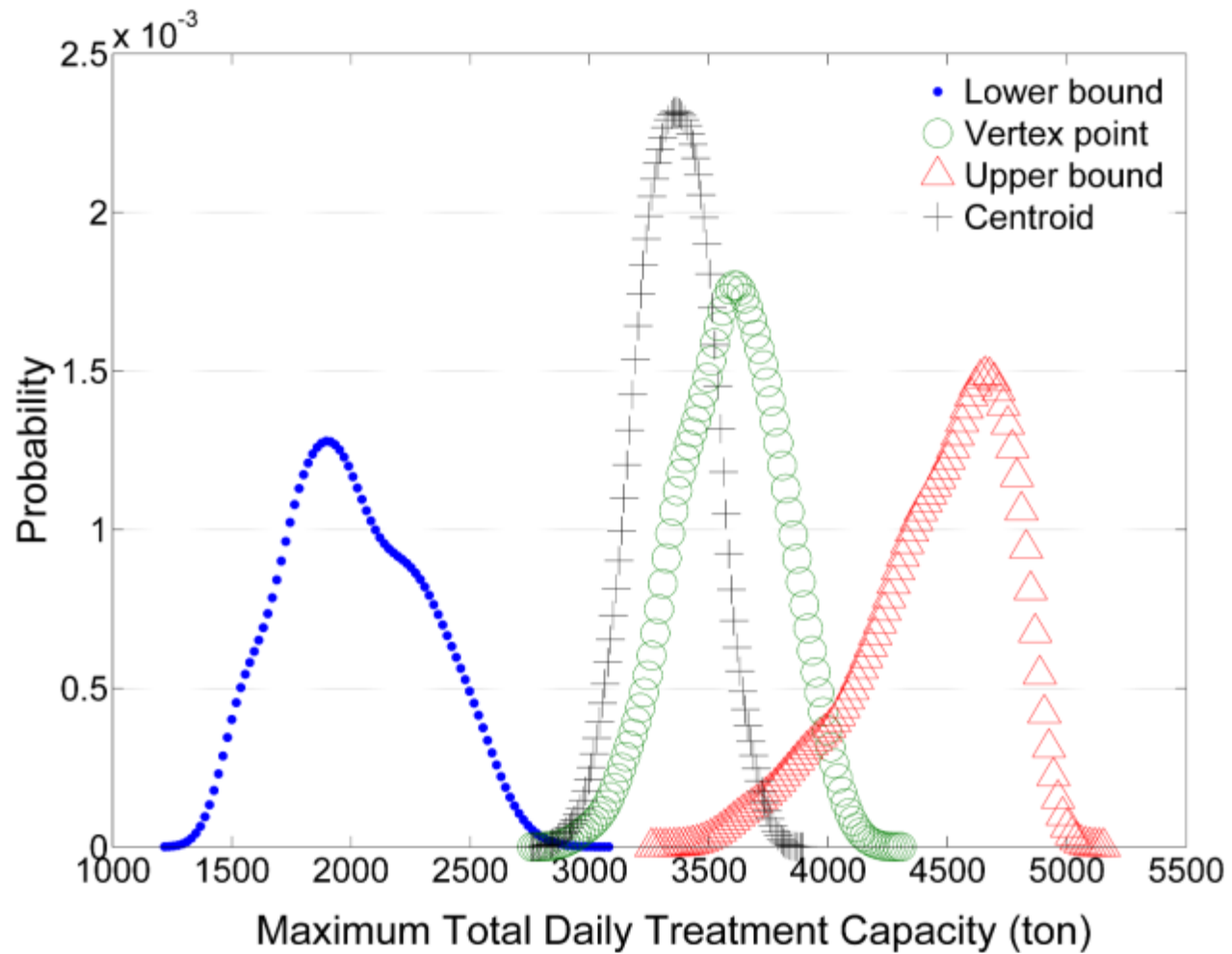


Figure 3.2 Probability density estimates of the lower bound, vertex point, upper bound, and defuzzified centroid of the objective function

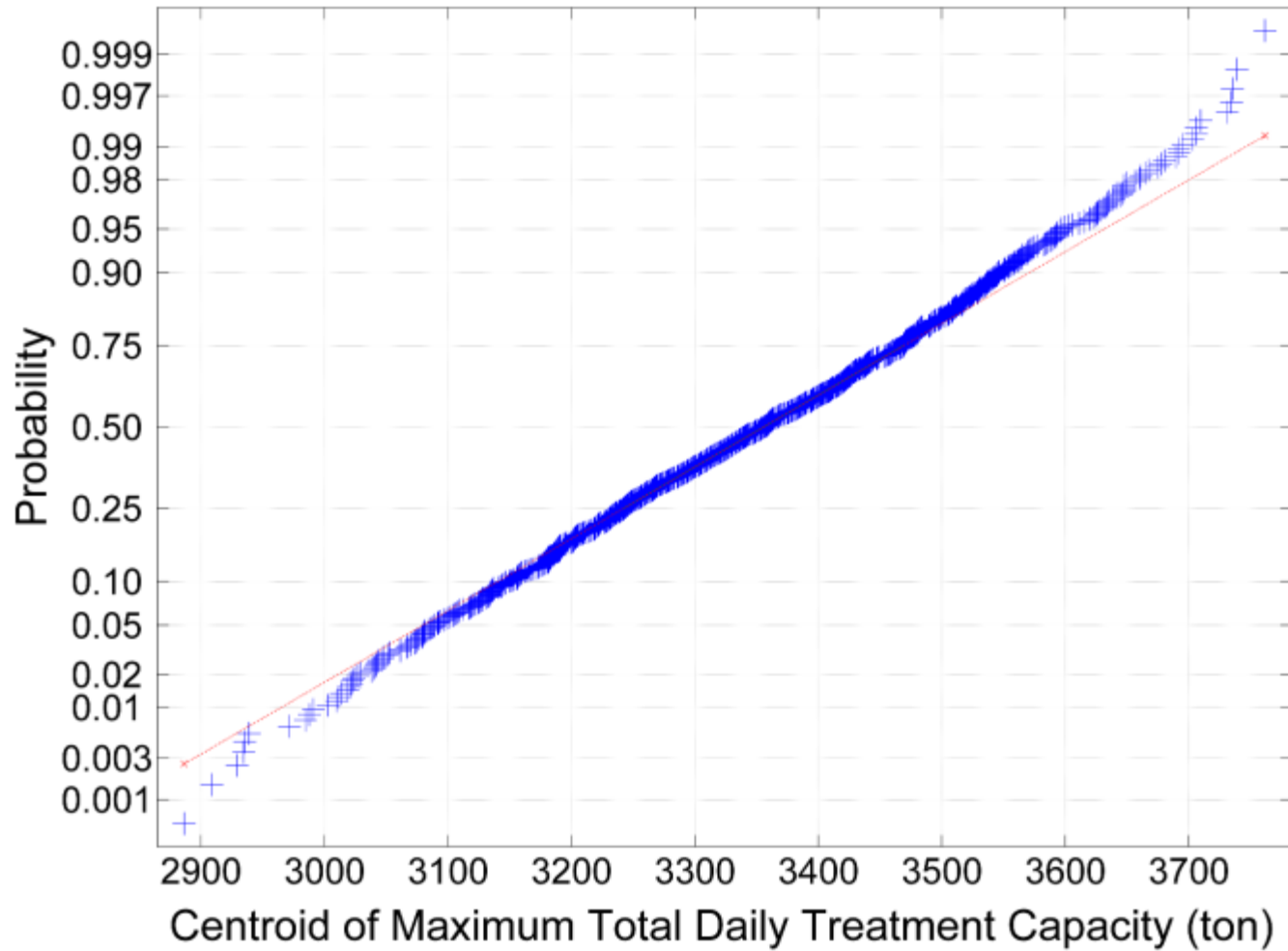


Figure 3.3 Normal probability plot of the centroid of the objective function

3.1.4 Results and Discussion

The histograms in Figure 3.1 depict that the distributions of the lower bounds, vertex points, and upper bounds of the maximized objective function were all close to normal. However, the results from the Lilliefors test, which is a two-sided goodness-of-fit test of normality, suggested that the null hypothesis of their normal distribution was rejected at a significance level of 5%. The offset of lower bounds and upper bounds towards the vertex points implies that the optimization results tended to concentrate in the range of 2,000-4,500 tonnes. These findings can be further demonstrated in Figure 3.2 by using the kernel-smoothing method to plot the probability density estimates. Another interesting finding is that the distribution of the defuzzified optimization results was well fitted by the normal distribution with a mean value of 3,352 tonnes and a standard deviation of 155.4 tonnes. The Lilliefors test cannot reject the null hypothesis that the centroid distribution was normal at a significance level of 5%. Its normality was further evaluated and confirmed by the normal probability plot as shown in Figure 3.3. In this case study, the results revealed that the maximum daily treatment capacity was likely to range from 3,000-3,700 tonnes given the budget constraint. In other words, from the technical perspective, it induces that oil skimmers are not recommended to operate if the amount of recovered oily water exceeds the treatment capacity unless other treatment or storage facilities are available.

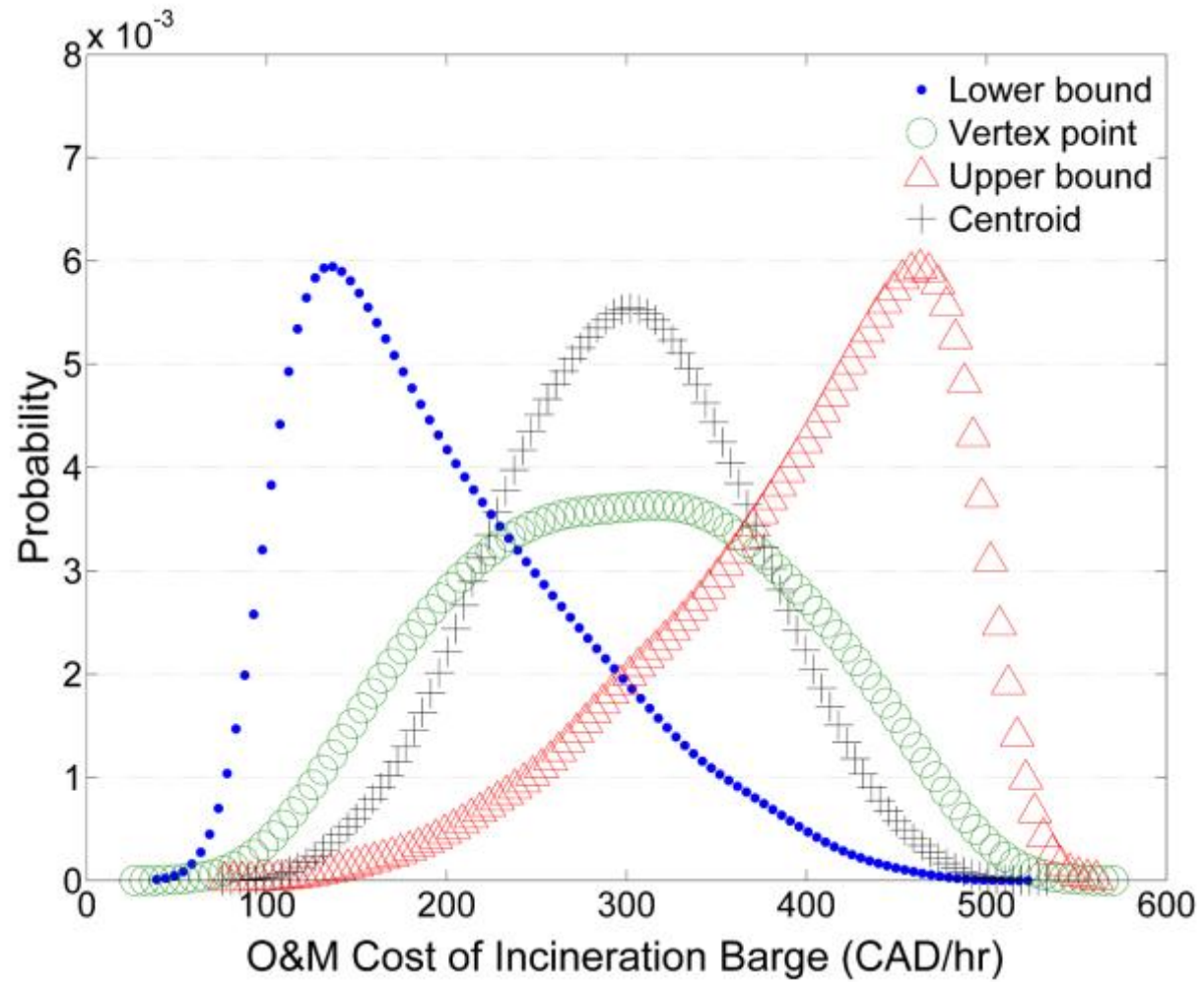


Figure 3.4 Probability density estimates of the lower bound, vertex point, upper bound, and defuzzified centroid of the O&M cost of incineration barge

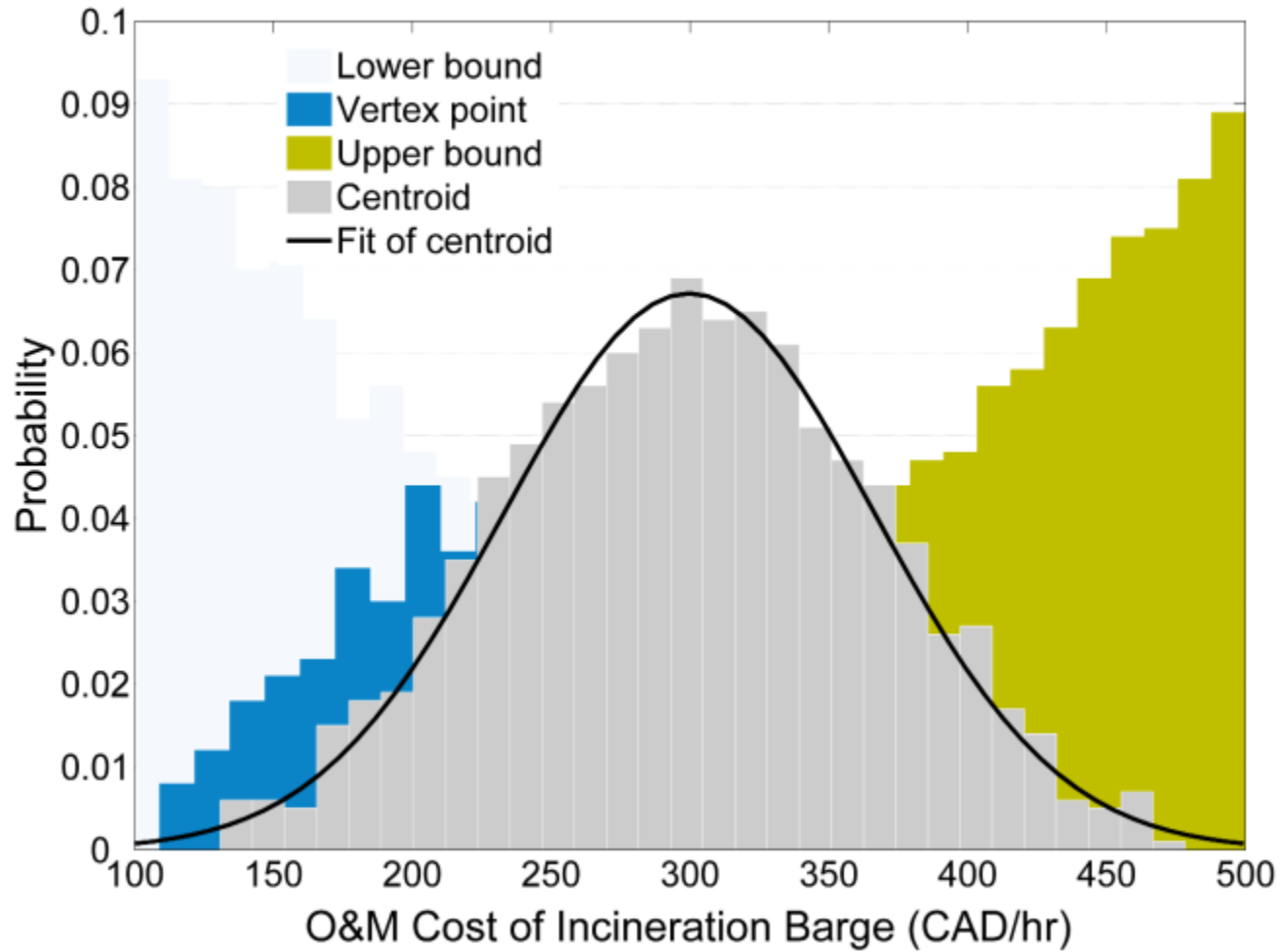


Figure 3.5 Probability distributions of the lower bound, vertex point, upper bound, and defuzzified centroid of the O&M cost of incineration barge

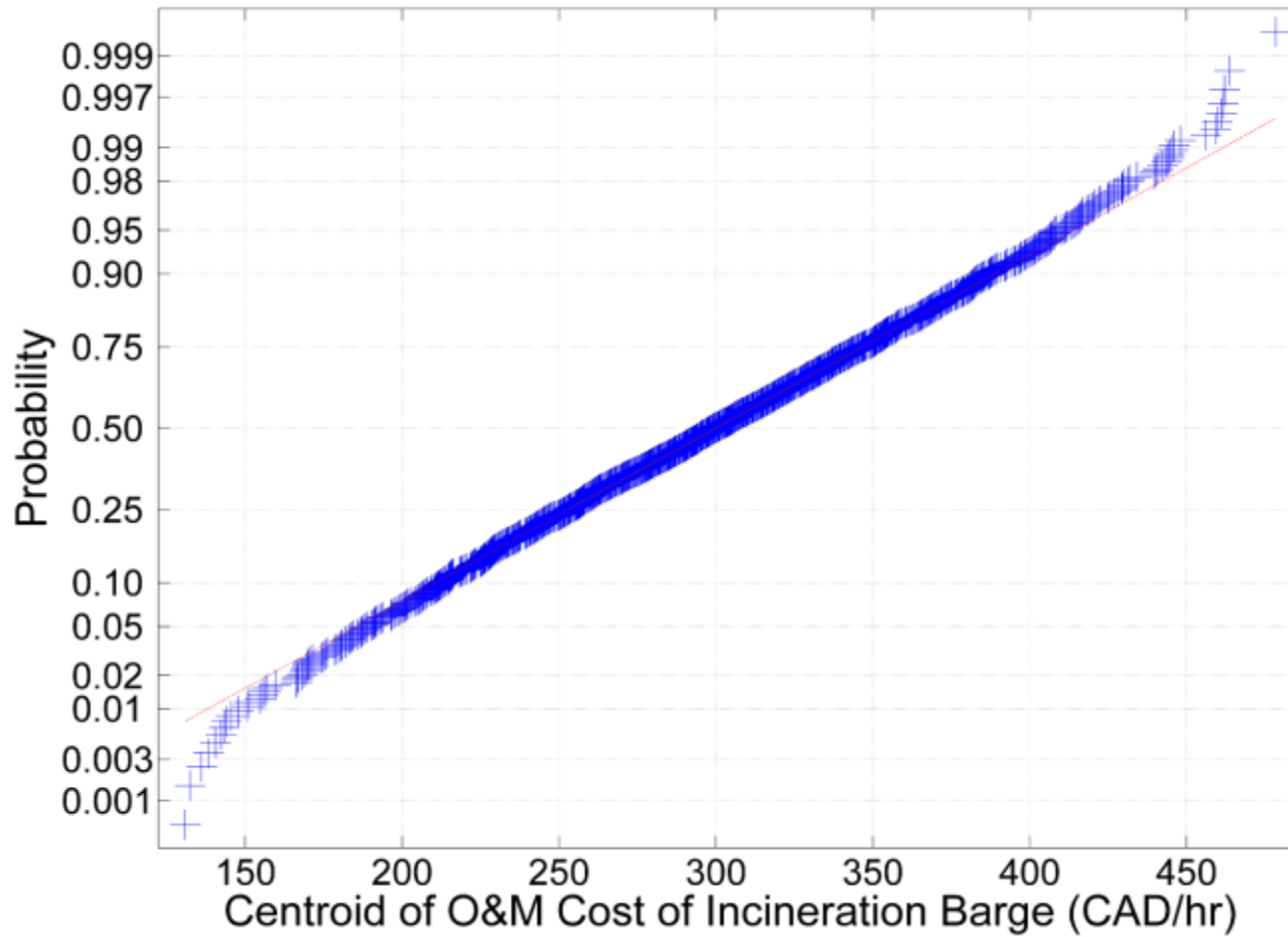


Figure 3.6 Normal probability plot of the centroid of the O&M cost of incineration barge

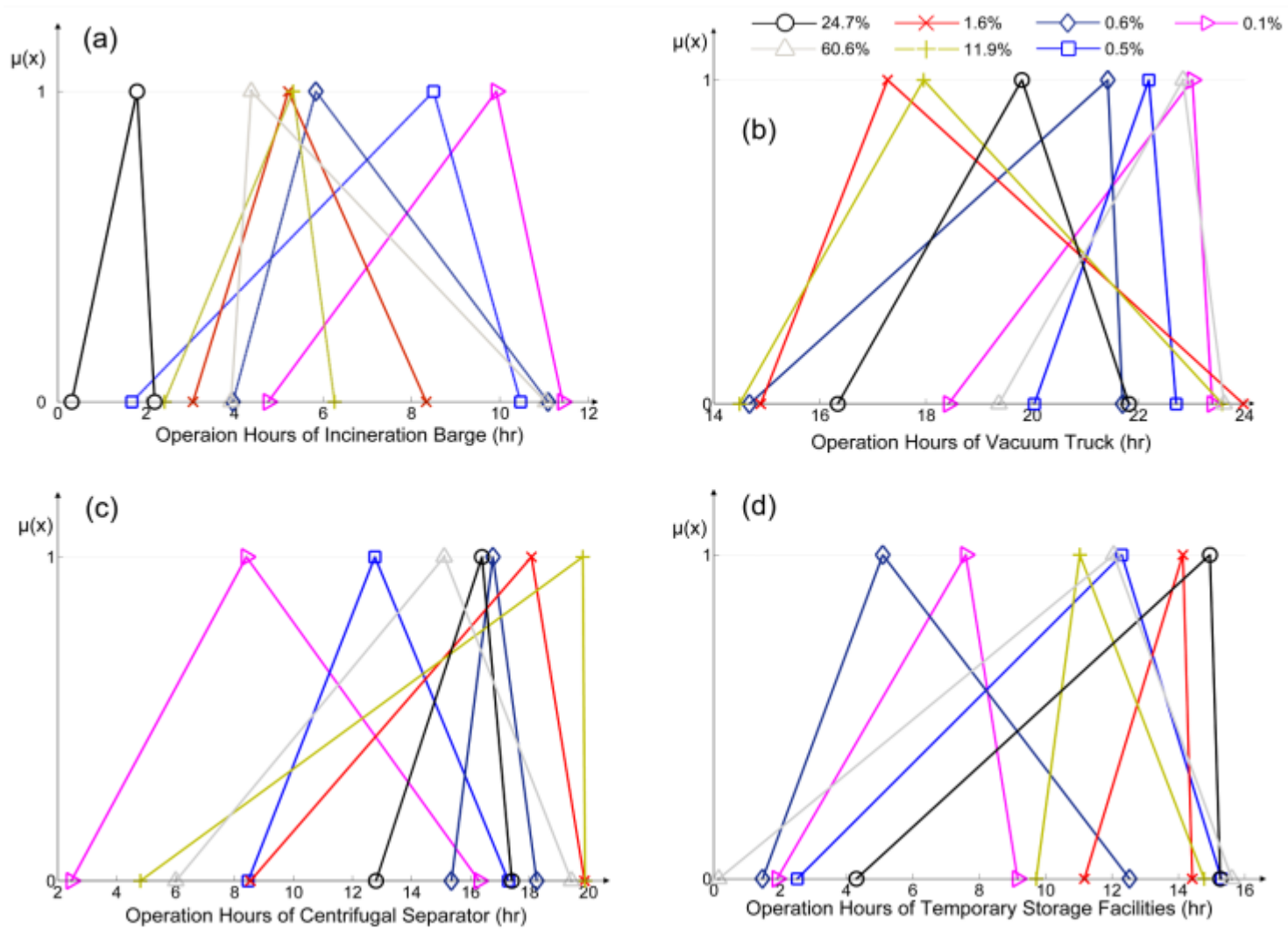


Figure 3.7 Optimal solutions of operation hours of each treatment facility

Figures 3.4 and 3.5 show the lower bounds, upper bounds, vertex points, and centroids of the stochastically generated fuzzy numbers with regard to the coefficient of O&M cost of incineration barge. The lower and upper bounds mostly appeared at the edges of the predefined interval (100, 500), indicating that the support of random fuzzy numbers tended to be wider rather than concentrating around the middle value. The Lilliefors test was used to test the null hypothesis that data come from a normally distributed population, when the null hypothesis does not specify which normal distribution. Based on the Lilliefors test at the 5% significance level, its centroid distribution well fitted the normal distribution with a mean value of 299.8 CAD/hr and a standard deviation of 89.5 CAD/hr which are also reported in the corresponding normal probability plot (Figure 3.6). This finding elucidates that producing a random sequence of triangular fuzzy numbers in a given interval is equivalent to a normal distribution when using the centroid defuzzification method. It is worth noting that, if Figure 3.2 is compared with Figure 3.4, the centroids of both the random fuzzy coefficients and the fuzzy optimal solutions follow normal distribution. The normality seems to be able to propagate throughout the optimization process, yet this interesting finding deserves more in-depth study and needs more rigorous mathematical proof to validate its applicability and feasibility.

Another interesting point to discuss is that the shapes of the fuzzy decision variables, corresponding to the maximized objective function, can be categorized into groups (Figure 3.7). For each set of the random coefficients, Monte Carlo simulation randomly generated fuzzy decision variables, validated the constraints, and found and recorded the particular group of decision variables that led to the maximum objective function. The

above procedure was repeated 1,000 times such that 1,000 groups of decision variables were obtained. It should be noted that the optimal decision variables appeared repeatedly in seven different shapes as shown in Figure 3.7. The percentages listed in the legend illustrate how many times each shape was referred to in 1,000 optimization runs. For example, in Figures 3.7, the four triangular fuzzy numbers (i.e., operation hours of the incineration barges, vacuum trucks, centrifugal separators, and temporary storage facilities) whose minimum, maximum, and vertex points are marked with triangles, were selected as the optimal variables in 60.6% of the total runs (i.e., 606 out of 1,000). This can be further interpreted that, if the operation hours can be determined within the range of the triangular fuzzy numbers marked by the triangles (e.g., (4, 11) in Figure 3.7a), the probability of achieving maximum treatment capacity would be 60.6% under the condition of uncertain coefficients. Moreover, the fuzzy outputs can help the decision makers choose other compromising points rather than the vertex points (e.g., Figure 3.7a, triangular fuzzy numbers (4, 4.2, 11), vertex point 4.2) and provide them with the corresponding possibility of getting the maximum treatment capacity (i.e., possibility of the vertex points is 1 and decreases along both sides as shown in Figure 3.7). Contrastingly, in Figures 3.7, another four triangular fuzzy numbers marked by circles denote that in 24.7% of the replications (i.e., 247 out of 1,000), the objective function was maximized by setting decision variables in these shapes. This particular setting might also be considered as viable when the primary choice (settings with 60.6% probability) cannot be applied due to safety or technical concerns.

These interesting findings are believed to have important and broader implications relating to oil spill cleanup and wastewater disposal such that decision makers can wisely

allocate limited resources with higher confidence in a short period of time. This is particularly true for harsh environments where available resources are usually in short supply and extreme weather conditions are likely to create more uncertainty in estimating the associated costs and time. In addition, from the ecological prospective, harsh environments tend to have more vulnerable ecosystems and shorter food chains than those in the low-latitude regions. Therefore, making quick and sound decisions will not only help reduce the oil spill cleanup cost but also minimize environmental risks.

3.2 A Hybrid Fuzzy Stochastic Analytical Hierarchy Process (FSAHP)

Approach

3.2.1 Background

Many multi-criteria decision making (MCDM) approaches have been developed to facilitate decision making under such uncertainties and the lack of knowledge. Among them, the analytic hierarchy process (AHP), first proposed by Saaty (1980), is one of the most widely used MCDM approaches. It structures the rational analysis of decision making by dividing a problem into hierarchies including goal, criteria, sub-criteria (if any), and decision alternatives.

However, the traditional AHP method uses 1-9 crisp values for pairwise comparisons when you compare two decision alternatives on one particular criterion. However, in many real-world applications, the available information that can be used for comparisons is usually imprecise, incomplete and occasionally unreliable due to the unquantifiable nature of data or the lack of knowledge. Therefore, decision makers would

feel more comfortable in using linguistic terms (e.g., good, poor, excellent) to describe the performance of each alternative on the criterion instead of making direct comparisons. On the other hand, stochastic uncertainty is also worth being adopted because resultant rankings from the traditional AHP are not statistically testable and the statistical difference between two alternatives is unclear if their scores are close. In addition, for a group decision making problem, biased preferences, incomplete information and judgment uncertainty may arise when not enough decision makers/experts are available. To date, triangular distribution is the most commonly used distribution for modeling expert judgment in the AHP (Banuelas and Antony, 2004; Hsu and Pan 2009). However, it may place too much emphasis on the most likely value at the expense of the values to either side (Phanikumar and Maitra, 2006). It is possible to overcome this disadvantage of the triangular distribution by using the beta-PERT distribution. The beta-PERT distribution has also been widely used for modeling expert judgments and providing a close fit to normal distributions with less demand for data (Coates and Rahimifard, 2009; Jing et al., 2012b).

In response to this, in this section, a hybrid fuzzy stochastic analytical hierarchy process (FSAHP) approach is developed by integrating the beta-PERT distribution, fuzzy set theory, pairwise comparison and Monte Carlo simulation. A real-world case study for ballast water management is presented to test the feasibility and efficiency of the proposed approach in a group decision-making environment. Ballast water is carried by ships to acquire the optimum operating depth of the propeller and to maintain manoeuvrability and stability (Endresen et al., 2004). It is recognized as the principle source of invasive species and pollutants in coastal freshwater and marine ecosystems,

causing severe effects on the environment and human health (Jing et al., 2012a). To address the associated concerns, the International Maritime Organization (IMO) has adopted many legal instruments whereby ships will be required to establish a ballast water management system between 2009 and 2016 (Gollasch et al., 2007). Many treatment technologies such as filtration, heat treatment, hydrocyclone, ultraviolet, ozonation, oxidization, electric pulse, and deoxygenation have been tested and applied to remove unwanted species and pollutants from ballast water (Jing et al., 2012a). However, Gregg and Hallegraeff (2007) argued that no treatment option had been shown fully biologically effective, environmentally friendly, safe and practical for onboard applications. In addition, the performance of most treatment processes is likely to be affected by the cold environment and unpredictable weather conditions (Endresen et al., 2004; Jing et al., 2012a). For example, when using heat treatment, low temperature would require the heating coil to be work at higher capacity in order to maintain the desired temperature in the ballast tank so that the microorganisms can be killed. UV treatment can also be affected due to the rough sea, which may increase the possibility of having a broken lamp where mercury may be released. Many other treatment facilities can also be damaged when the waves are high and the wind is strong. The evaluation of their applicability and associated risk is of paramount importance and lacks in-depth research. How to choose the best technology from a sustainability metrics perspective still exists as a challenge to the government and other public bodies with environmental responsibilities.

3.2.2 Methodology

3.2.2.1 Fuzzy Sets and Fuzzy Numbers

See Section 3.1.2.1.

3.2.2.2 Stochastic Programming by Monte Carlo Simulation

See Section 3.1.2.3.

3.2.2.3 The FSAHP Approach

The proposed FSAHP approach is capable of capturing not only a human's appraisal of ambiguity but also the uncertainty introduced by the lack of information or scattered opinions. Experts' linguistic assessments are aggregated to approximate a series of beta-PERT distributions for randomized fuzzy pairwise comparisons. Monte Carlo simulation is then used to generate random fuzzy pairwise comparison matrices (FPCMs), calculate the fuzzy weights, and produce the final scores for each decision alternative. The detailed steps are summarized as follows:

Step 1: Structure the decision problem into a hierarchy of interrelated sub-problems that can be analyzed independently. The hierarchy usually includes a main goal, criteria, and alternatives, from the top to the bottom. Each criterion may be further decomposed into a number of lower-level sub-criteria as a new level. The goal, criteria, sub-criteria (if any), and alternatives can be determined through literature reviews and collective discussions.

Step 2: Linguistic judgments on each alternative and criterion with respect to the elements on the level immediately above can be obtained from experts through questionnaires, surveys, interviews, expert panels, and direct observations. Instead of using a crisp ratio scale, seven triangular fuzzy numbers (TFNs) (Figure 3.8) are used to

represent linguistic terms with the expectation that experts will feel more comfortable using such terms in their assessment. It should be noted that such a verbal clarification becomes impractical when too many rating scales (e.g., 10-point format) are involved because the level of agreement becomes too fine to be easily expressed in words (Dawes, 2007). In addition, a seven level judgment would be easier to make than a nine level judgment so that the participating experts will be more comfortable to make decisions.

Step 3: For the assessment of each alternative and criterion, the number of TFNs should be equal to the number of experts. The minimum (a), most likely (b) and maximum (c) values of the TFNs are aggregated into three individual groups. In order to generate random TFNs, Equations 3.10–3.13 are used to approximate an independent beta-PERT distribution for each group (Coates and Rahimifard, 2009; Jing et al., 2012b).

$$mean = \frac{min + 4modal + max}{N} \quad (3.11)$$

$$stdev = \frac{max - min}{N} \quad (3.12)$$

$$\alpha = \left(\frac{mean - min}{max - min} \right) \left(\frac{(mean - min)(max - mean)}{stdev^2} - 1 \right) \quad (3.13)$$

$$\beta = \left(\frac{max - mean}{mean - min} \right) * \alpha \quad (3.14)$$

where $mean$, min , $modal$, max , $stdev$ denote the mean, smallest, most probable, largest values, and standard deviations of a , b , and c , respectively; N is the number of experts; α and β are the shape factors. Equations 3.14–3.16 are then used to generate pseudorandom numbers (i.e., $random_a$, $random_b$, $random_c$) that follow the beta-PERT distributions for a ,

b , and c , respectively in Matlab[®]. It is noteworthy that the triangular shape needs to be verified to validate these random numbers.

$$random_a = min_a + betarnd(\alpha_a, \beta_a) * (max_a - min_a) \quad (3.15)$$

$$random_b = min_b + betarnd(\alpha_b, \beta_b) * (max_b - min_b) \quad (3.16)$$

$$random_c = min_c + betarnd(\alpha_c, \beta_c) * (max_c - min_c) \quad (3.17)$$

where *betarnd* denotes standard Matlab[®] function (i.e., beta distribution) which returns a random number between 0 and 1.

Step 4: Set up fuzzy pairwise comparison matrices (FPCMs) for each hierarchy level based on fuzzy arithmetic. For example, when m alternatives ($C_1 \dots C_m$) on a given level are evaluated against each other with regard to the p^{th} criterion ($p = 1, 2, 3 \dots n$) on the preceding level, an $m \times m$ FPCM is obtained as below

$$\begin{matrix} & C_1 & C_2 & C_3 & \dots & C_m \\ C_1 & (1,1,1) & \tilde{x}_{12} & \tilde{x}_{13} & \dots & \tilde{x}_{1m} \\ C_2 & 1/\tilde{x}_{12} & (1,1,1) & \tilde{x}_{23} & \dots & \tilde{x}_{2m} \\ C_3 & 1/\tilde{x}_{13} & 1/\tilde{x}_{23} & (1,1,1) & \dots & \tilde{x}_{3m} \\ \vdots & \vdots & \vdots & \vdots & \vdots & \vdots \\ C_m & 1/\tilde{x}_{1m} & 1/\tilde{x}_{2m} & 1/\tilde{x}_{3m} & \dots & (1,1,1) \end{matrix} \quad (3.18)$$

To calculate each non-diagonal fuzzy element (e.g., \tilde{x}_{13}), the dominance of one alternative or criterion over another is determined by the division of two TFNs. For example, if the random TFNs for C_1 and C_3 are (a_1, b_1, c_1) and (a_3, b_3, c_3) , respectively, then $\tilde{x}_{13} = (a_1/c_3, b_1/b_3, c_1/a_3)$ and $1/\tilde{x}_{13} = (a_3/c_1, b_3/b_1, c_3/a_1)$.

Step 5: Calculate the fuzzy weights of each FPCM (e.g., Equation 3.17). For example, in Equation 3.18, the geometric means of each row and the corresponding fuzzy weights are obtained using Equations 3.19-3.20. The weight assessing method by geometric mean is

applied because of its simplicity and ease when dealing with fuzzy matrices (Kaya and Kahraman, 2011).

$$a_i = \left[\prod_{j=1}^m a_{ij} \right]^{1/m}; b_i = \left[\prod_{j=1}^m b_{ij} \right]^{1/m}; c_i = \left[\prod_{j=1}^m c_{ij} \right]^{1/m} \quad i, j = 1, 2, \dots, m \quad (3.19)$$

$$a_{sum} = \sum_{i=1}^m a_i; b_{sum} = \sum_{i=1}^m b_i; c_{sum} = \sum_{i=1}^m c_i \quad (3.20)$$

$$\tilde{w}_{ip} = \left(\frac{a_i}{c_{sum}}, \frac{b_i}{b_{sum}}, \frac{c_i}{a_{sum}} \right) \quad i = 1, 2, \dots, m \quad (3.21)$$

where a_{ij} , b_{ij} , and c_{ij} are the minimum, most likely, and maximum values of each non-diagonal fuzzy element \tilde{x}_{ij} , respectively; m is the size of the FPCM or the number of decision alternatives; a_i , b_i , and c_i are the geometric means of the minimum, most likely, and maximum values of the fuzzy elements on the i^{th} row, respectively; a_{sum} , b_{sum} , and c_{sum} are the sum of a_i , b_i , and c_i , respectively; and \tilde{w}_{ip} are the fuzzy weights of the i^{th} alternative against the p^{th} criterion. Repeating this step to obtain all other \tilde{w}_{ip} and \tilde{w}_p , which are the fuzzy weights of the p^{th} criterion in terms of the goal.

Step 6: As with the traditional AHP, the proposed FSAHP approach also measures the inconsistency of each FPCM. Due to the presence of fuzzy numbers, the traditional consistency algorithms are not effective in addressing such uncertainties. Hence, in this paper, a new inconsistency index (CI_F) based on the distance of the matrix to a specific consistent matrix is adopted from Ramak and Korviny (2010).

$$s_i^L = \min_i \left\{ \frac{b_i}{a_i} \right\} \cdot \frac{a_i}{b_{sum}} \quad (3.22)$$

$$s_i^M = \frac{b_i}{b_{sum}} \quad (3.23)$$

$$s_i^U = \max_i \left\{ \frac{b_i}{c_i} \right\} \cdot \frac{c_i}{b_{sum}} \quad (3.24)$$

$$CI_F = \gamma \cdot \max_{i,j} \left\{ \max \left\{ \left| \frac{s_i^L}{s_j^U} - a_{ij} \right|, \left| \frac{s_i^M}{s_j^M} - b_{ij} \right|, \left| \frac{s_i^U}{s_j^L} - c_{ij} \right| \right\} \right\} \quad (3.25)$$

$$\gamma = \frac{1}{\max \left\{ \sigma - \sigma^{(2-2m)/m}, \sigma^2 \left(\left(\frac{2}{m} \right)^{2/(m-2)} - \left(\frac{2}{m} \right)^{m/(m-2)} \right) \right\}} \quad \text{if } \sigma < \left(\frac{m}{2} \right)^{m/(m-2)}$$

$$\gamma = \frac{1}{\max \left\{ \sigma - \sigma^{(2-2m)/m}, \sigma^{(2m-2)/m} - \sigma \right\}} \quad \text{if } \sigma \geq \left(\frac{m}{2} \right)^{m/(m-2)}$$
(3.26)

where s_i^L , s_i^M , and s_i^U are the minimum, most likely, and maximum values of the optimal solution that has the minimal measure of fuzziness, respectively; σ is the linguistic scale (i.e., $[1/7, 7]$ in this study); γ is the normality constant; CI_F is the inconsistency index of a FPCM such that a value of 0.1 or less is considered to be acceptable, otherwise the FPCM should be revised.

Step 7: The overall fuzzy priorities \tilde{w}_i of the i^{th} alternative can be calculated by aggregating the weights throughout the hierarchy:

$$\tilde{w}_i = \sum_{p=1}^n \tilde{w}_{ip} \times \tilde{w}_p \quad (3.27)$$

where \tilde{w}_{ip} are the fuzzy merits of the i^{th} alternative with regard to the p^{th} criterion, respectively; \tilde{w}_p are the fuzzy weights of the p^{th} criterion against the goal; and n is the number of evaluation criteria.

Step 8: Defuzzify \tilde{w}_i by using the center of gravity (COG) method and rank the decision alternatives based on their normalized crisp overall scores w_i .

$$w_i^* = \frac{\int_a^c x \mu_{\tilde{w}_i}(x) dx}{\int_a^c \mu_{\tilde{w}_i}(x) dx} \quad (3.28)$$

$$w_i = \frac{w_i^*}{\sum_{i=1}^m w_i^*} \quad (3.29)$$

where w_i^* are the crisp overall scores of the i^{th} alternative; a and c denote the support of \tilde{w}_i ; $\mu_{\tilde{w}_i}(x)$ are the corresponding membership functions of \tilde{w}_i ; and w_i are the normalized crisp overall scores of each decision alternative and are sequenced from high to low in the order of 1 to 5. To validate this ranking scheme, or in other words, the defuzzification results, Chen's fuzzy ranking method is also employed to further compare the overall fuzzy priorities \tilde{w}_i and rank them from the highest to the lowest.

Step 9: Repeat Steps 4 to 8 for a number of iterations (e.g., 1000 and 5000), the overall scores of alternatives can be obtained and plotted as probability density functions.

3.2.3 Case Study

This case study was conducted to demonstrate the applicability and effectiveness of the proposed FSAHP approach in addressing uncertainty in the context of group decision-making. A cargo ship was assumed to be required for an onboard ballast water treatment system in order to operate in the North Atlantic. The decision alternatives and evaluation criteria were determined based on literature review and discussion with experts from governmental ministries and academic institutions. The experts were further invited to fill out the questionnaire on the basis of linguistic terms. Their opinions were analyzed and interpreted to facilitate the implementation of the FSAHP approach.

3.2.3.1 Hierarchy Structure

As depicted in Figure 3.9, the goal was to select the best onboard treatment technology in order to eliminate invasive microorganisms and to remove water soluble organics from ballast water, particularly in the harsh environments. Five treatment technologies including heat treatment, ultraviolet (UV), ozone, ultrasound, and biocide were chosen (Jing et al., 2012a).

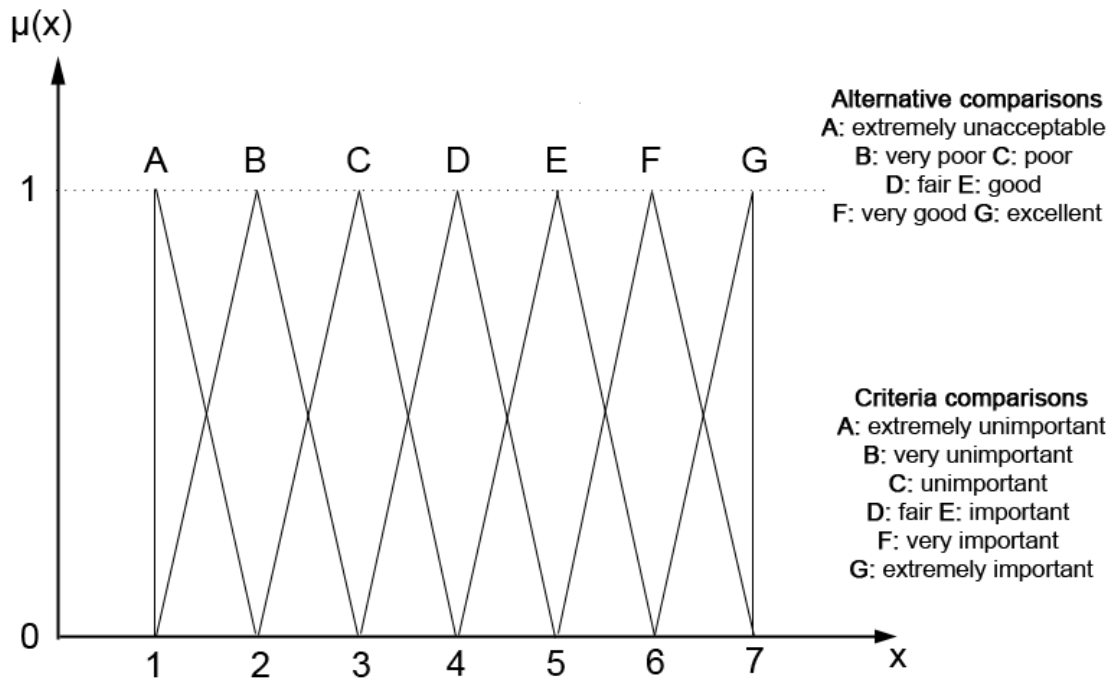


Figure 3.8 Membership spread of linguistic scales

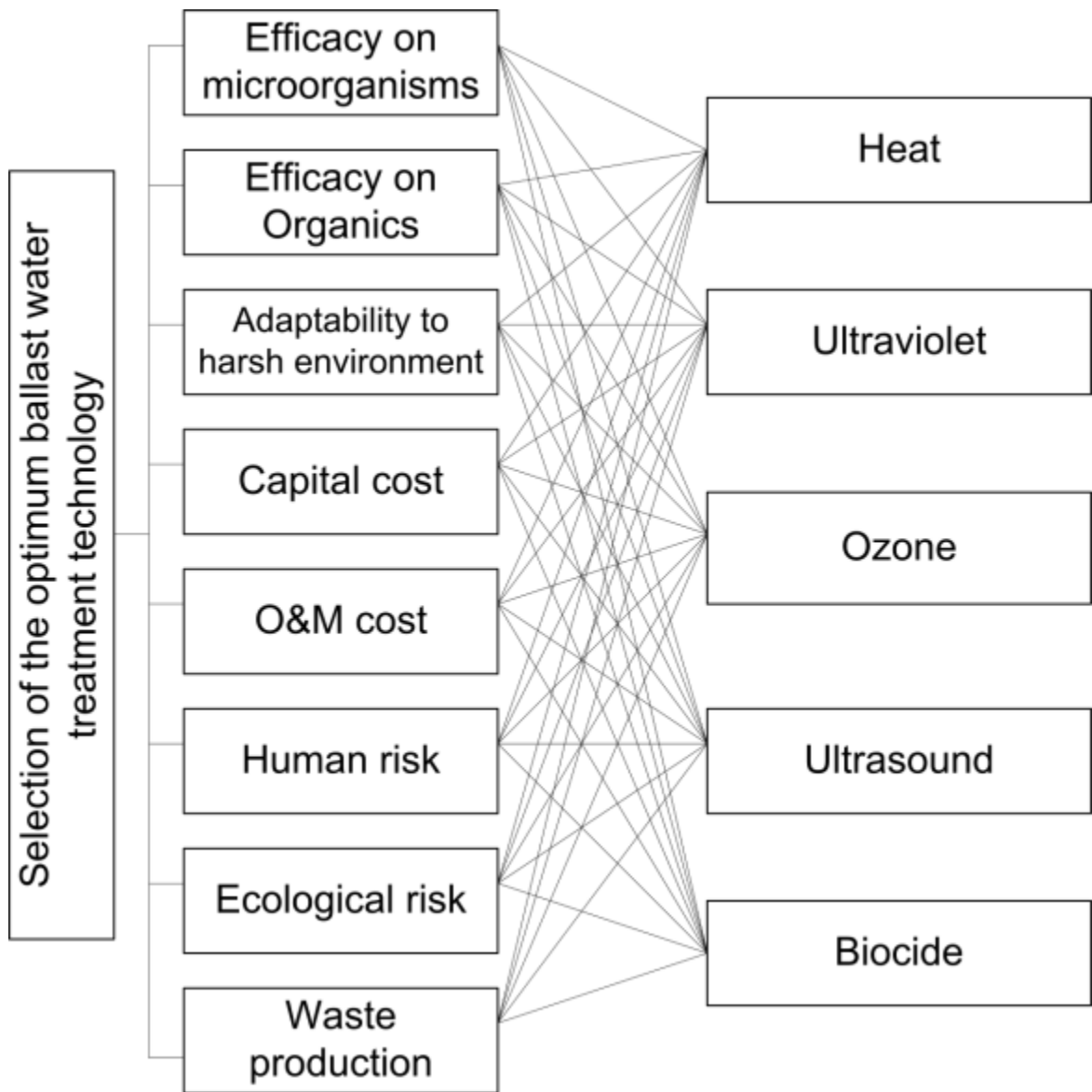


Figure 3.9 Hierarchy structure of the ballast water treatment technology selection problem

Heat treatment is capable of killing invasive species embedded in sediment that has accumulated at the bottom of the ballast tanks. It should be pointed out that discharging warm water potentially threatens biological communities and a complete treatment process may take hours or days, which is not always practicable. Despite the potential threats posed by mercury contamination and genetic mutation, UV manages to eliminate microorganisms by breaking chemical bonds in DNA and RNA molecules and cell proteins (Jing et al., 2012a). Recently, ozone has been widely employed in removing microorganisms from ballast water. The often-cited disadvantages of using ozone as a disinfectant have been reported as the possible formation of toxic by-products, low solubility, and high instability (Herwig et al., 2006). Ultrasound can induce the collapse of microscopic gas bubbles in the exposed liquid and lead to the rupture of cell membranes, yet it is less effective in killing some microorganisms such as bacteria (Holm, 2008). Many chemical biocides have been documented as possible treatment options to the problem of ballast-mediated invasive species. However, some concerns, such as risks from storage and handling, high operational and material cost, and possible discharge of toxic residues need to be taken into account (Gregg and Hallegraeff, 2007). Based on the recommendations from literature (de Lafontaine et al., 2009; Tsolaki and Diamadopoulos, 2010; Jing et al., 2012a) and expert opinions, in this study, eight evaluation criteria including efficacy on microorganisms, efficacy on organic pollutants, adaptability to harsh environments, capital cost, operation and maintenance (O&M) cost, human health risk, ecological risk, and waste production were chosen.

3.2.3.2 Data Acquisition

In the absence of quantitative data about each alternative, experts' qualitative judgments were used to measure the priorities of alternatives. The linguistic assessments for the qualitative attributes were provided by nine experts from the government of Newfoundland and Labrador and academic institutions (professors and graduate students in Faculty of Engineering and Applied Science at Memorial University). The experts are all in the environmental engineering field or closely related to it. They were asked to rate the performance of each alternative and the importance of each criterion using the linguistic scales provided in Figure 3.8. Tables 3.2 and 3.3 summarize the linguistic assessments made by each participating expert. These assessments were aggregated in groups such that the beta-PERT distributions of each group can be estimated to generate random TFNs. For example, the performance of heat, ultraviolet, ozone, ultrasound and biocide with respect to their efficacy on microorganisms was randomly generated as C (2, 3, 4), G (6, 7, 7), G (6, 7, 7), E (4, 5, 6) and F (5, 6, 7), respectively. To obtain the corresponding FPCM (i.e., Equation 3.29), elements in the first row were given by the fuzzy comparisons between the performance of heat (2, 3, 4) and all the others, respectively. The consistency of this FPCM was less than 0.1, which was acceptable, and the fuzzy weights of each alternative were able to be calculated. It should be noted that the number of Monte Carlo iterations used for this case study was determined as 1000 by taking time constraints and the efficiency of convergence into account (Hsu and Pan, 2009).

Table 3.2 Expert assessment for ballast water treatment technologies

| Criteria | Alternatives | Expert Assessment | | | | | | | | |
|------------------------------------|--------------|-------------------|---|---|---|---|---|---|---|---|
| | | 1 | 2 | 3 | 4 | 5 | 6 | 7 | 8 | 9 |
| Efficacy on microorganisms | Heat | C | D | B | B | C | C | D | C | C |
| | Ultraviolet | G | F | G | G | G | G | F | F | F |
| | Ozone | G | G | E | G | G | F | F | G | F |
| | Ultrasound | E | E | F | E | F | D | E | E | E |
| | Biocide | F | G | G | F | F | G | E | F | G |
| Efficacy on organics | Heat | B | A | A | C | C | B | C | C | B |
| | Ultraviolet | F | E | G | F | G | F | F | G | F |
| | Ozone | F | G | E | D | F | E | F | G | E |
| | Ultrasound | E | E | D | E | D | E | D | E | C |
| | Biocide | B | B | A | B | B | B | C | B | A |
| Adaptability to harsh environments | Heat | C | B | D | C | B | C | C | B | C |
| | Ultraviolet | F | E | G | F | F | E | F | E | F |
| | Ozone | F | E | E | F | G | D | E | F | G |
| | Ultrasound | E | E | F | D | E | D | E | D | D |
| | Biocide | D | D | F | E | D | E | D | C | D |
| Capital cost | Heat | F | D | E | E | F | E | F | E | E |
| | Ultraviolet | D | E | D | E | D | B | D | D | C |
| | Ozone | C | D | C | D | C | C | C | B | C |
| | Ultrasound | B | C | B | C | D | C | D | B | D |
| | Biocide | G | F | F | E | G | F | E | F | E |
| O&M cost | Heat | F | G | F | E | E | G | E | F | G |
| | Ultraviolet | D | E | E | D | D | E | D | E | E |
| | Ozone | C | C | C | D | C | E | C | D | C |
| | Ultrasound | C | B | C | C | D | D | B | C | D |
| | Biocide | D | E | D | F | F | E | D | E | F |
| Human risk | Heat | G | F | G | E | F | F | E | E | F |
| | Ultraviolet | C | C | D | C | D | C | D | C | B |
| | Ozone | C | D | B | D | E | D | E | C | D |
| | Ultrasound | B | D | D | C | D | D | E | D | C |
| | Biocide | B | B | C | C | D | C | C | D | B |
| Ecological risk | Heat | C | D | B | C | D | E | C | E | D |
| | Ultraviolet | D | F | D | E | F | G | F | D | D |
| | Ozone | F | E | D | E | E | F | F | D | E |
| | Ultrasound | E | D | E | D | E | D | E | D | D |
| | Biocide | C | B | E | D | C | C | D | C | C |
| Waste production | Heat | E | D | D | D | C | D | E | D | C |
| | Ultraviolet | F | G | F | E | F | G | G | F | E |
| | Ozone | D | E | D | D | E | E | E | F | F |
| | Ultrasound | D | C | C | C | D | D | E | D | E |
| | Biocide | C | B | C | B | D | C | E | D | B |

Table 3.3 Expert assessment for evaluation criteria

| Goal | Criteria | Expert Assessment | | | | | | | | |
|---------------------------------|------------------------------------|-------------------|---|---|---|---|---|---|---|---|
| | | 1 | 2 | 3 | 4 | 5 | 6 | 7 | 8 | 9 |
| Best treatment technology | Efficacy on microorganisms | G | F | F | E | F | E | G | E | F |
| | Efficacy on organics | E | C | D | E | F | F | D | F | D |
| | Adaptability to harsh environments | F | F | G | F | E | D | E | C | D |
| | Capital cost | F | E | B | E | C | D | F | D | C |
| | O&M cost | C | B | E | D | C | F | F | E | F |
| | Human risk | F | G | E | F | D | E | D | E | E |
| | Ecological risk | D | E | F | D | E | C | D | F | D |
| | Waste production | B | D | D | A | D | B | E | G | C |

$$\begin{array}{cccccc}
& & \textit{Heat} & \textit{Ultraviolet} & \textit{Ozone} & \textit{Ultrasound} & \textit{Biocide} \\
\textit{Heat} & & (1,1) & \frac{(2,3,4)}{(6,7,7)} & \frac{(2,3,4)}{(6,7,7)} & \frac{(2,3,4)}{(4,5,6)} & \frac{(2,3,4)}{(5,6,7)} \\
\textit{Ultraviolet} & \left[\frac{(2,3,4)}{(6,7,7)} \right]^{-1} & & (1,1) & \frac{(6,7,7)}{(6,7,7)} & \frac{(6,7,7)}{(4,5,6)} & \frac{(6,7,7)}{(5,6,7)} \\
\textit{Ozone} & \left[\frac{(2,3,4)}{(6,7,7)} \right]^{-1} & \left[\frac{(6,7,7)}{(6,7,7)} \right]^{-1} & & (1,1) & \frac{(6,7,7)}{(4,5,6)} & \frac{(6,7,7)}{(5,6,7)} \\
\textit{Ultrasound} & \left[\frac{(2,3,4)}{(4,5,6)} \right]^{-1} & \left[\frac{(6,7,7)}{(4,5,6)} \right]^{-1} & \left[\frac{(6,7,7)}{(4,5,6)} \right]^{-1} & & (1,1) & \frac{(4,5,6)}{(5,6,7)} \\
\textit{Biocide} & \left[\frac{(2,3,4)}{(5,6,7)} \right]^{-1} & \left[\frac{(6,7,7)}{(5,6,7)} \right]^{-1} & \left[\frac{(6,7,7)}{(5,6,7)} \right]^{-1} & \left[\frac{(4,5,6)}{(5,6,7)} \right]^{-1} & & (1,1)
\end{array} \tag{3.29}$$

3.2.4 Results and Discussion

The results and statistics were obtained by following the proposed FSAHP approach. Figure 3.10, for example, depicts the probability density of the scores of each alternative with respect to the criterion of human health risk after 1,000 iterations. The horizontal axis stands for the normalized scores of each alternative, while the vertical axis represents the probability of the scores. The higher the score, the better the performance. The histogram bar plot clearly demonstrates that heat treatment (0.26–0.33) appeared to be the most attractive solution in terms of the lowest health risk, followed by ozone (0.16–0.25) without any overlap. Ultrasound, biocide, and UV were seen as the least preferable option with considerable overlaps between each other, implying that the experts were not confident about ranking one over the others. The correlation coefficients between the scores of ultrasound and biocide, biocide and UV, and ultrasound and UV were -0.201, -0.476, and 0.308, respectively. A negative correlation coefficient between two variables usually implies that the increase of one variable is associated with the decrease of the other. On the other hand, a positive correlation coefficient means that two variables increase (or decrease) simultaneously in the same direction. These principles become

more prominent as the absolute value of a correlation coefficient close to 1. In this case study, negative correlation coefficients can be interpreted as larger overlaps as compared to positive correlation coefficients based on the fact that the scores were closely distributed (Figure 3.10). Tables 3.4 and 3.5 further validate these conclusions by showing the ranking of alternative priorities based on the COG and Chen's defuzzification methods, respectively. A statistical test of the null hypothesis that heat treatment was not the probabilistic optimal alternative (versus the alternate assumption that it was) was conducted to examine if the difference between it and the second best option (i.e., ozone) was statistically significant. Heat treatment was ranked first by both methods with the confidence level exceeding 95%, indicating the null assumption that it is not probabilistic optimal (versus the alternate assumption that it is) is rejected. Ultrasound took the third place in more than 75% of the iterations while UV had the least preference in over 70% of the cases. From the technical perspective, the results were reasonable because heat sources such as waste heat from the engine jacket coolers and additional auxiliary boiler are usually not accessible by most crew members. On the other hand, short-term exposure to high level ozone can temporarily influence lung function and respiratory tract; meanwhile, some by-products (e.g., bromate) produced from ozonation may also pose risks to human health. UV was ranked as the least preferable alternative because excessive human exposure to UV is positively associated with severe health problems including photoaged skin, ocular diseases, and skin cancers.

Table 3.4 Ranking with regard to human risk based on the COG method

| Treatment Technology | Rank | | | | |
|----------------------|------|------|------|------|------|
| | 1 | 2 | 3 | 4 | 5 |
| Heat | 1000 | 0 | 0 | 0 | 0 |
| UV | 0 | 3 | 6 | 260 | 731 |
| Ozone | 0 | 943 | 51 | 6 | 0 |
| Ultrasound | 0 | 50 | 798 | 150 | 2 |
| Biocide | 0 | 4 | 145 | 584 | 267 |
| Total | 1000 | 1000 | 1000 | 1000 | 1000 |

Table 3.5 Ranking with regard to human risk based on Chen's method

| Treatment Technology | Rank | | | | |
|----------------------|------|------|------|------|------|
| | 1 | 2 | 3 | 4 | 5 |
| Heat | 1000 | 0 | 0 | 0 | 0 |
| UV | 0 | 2 | 20 | 277 | 701 |
| Ozone | 0 | 929 | 57 | 11 | 3 |
| Ultrasound | 0 | 64 | 752 | 180 | 4 |
| Biocide | 0 | 5 | 171 | 532 | 292 |
| Total | 1000 | 1000 | 1000 | 1000 | 1000 |

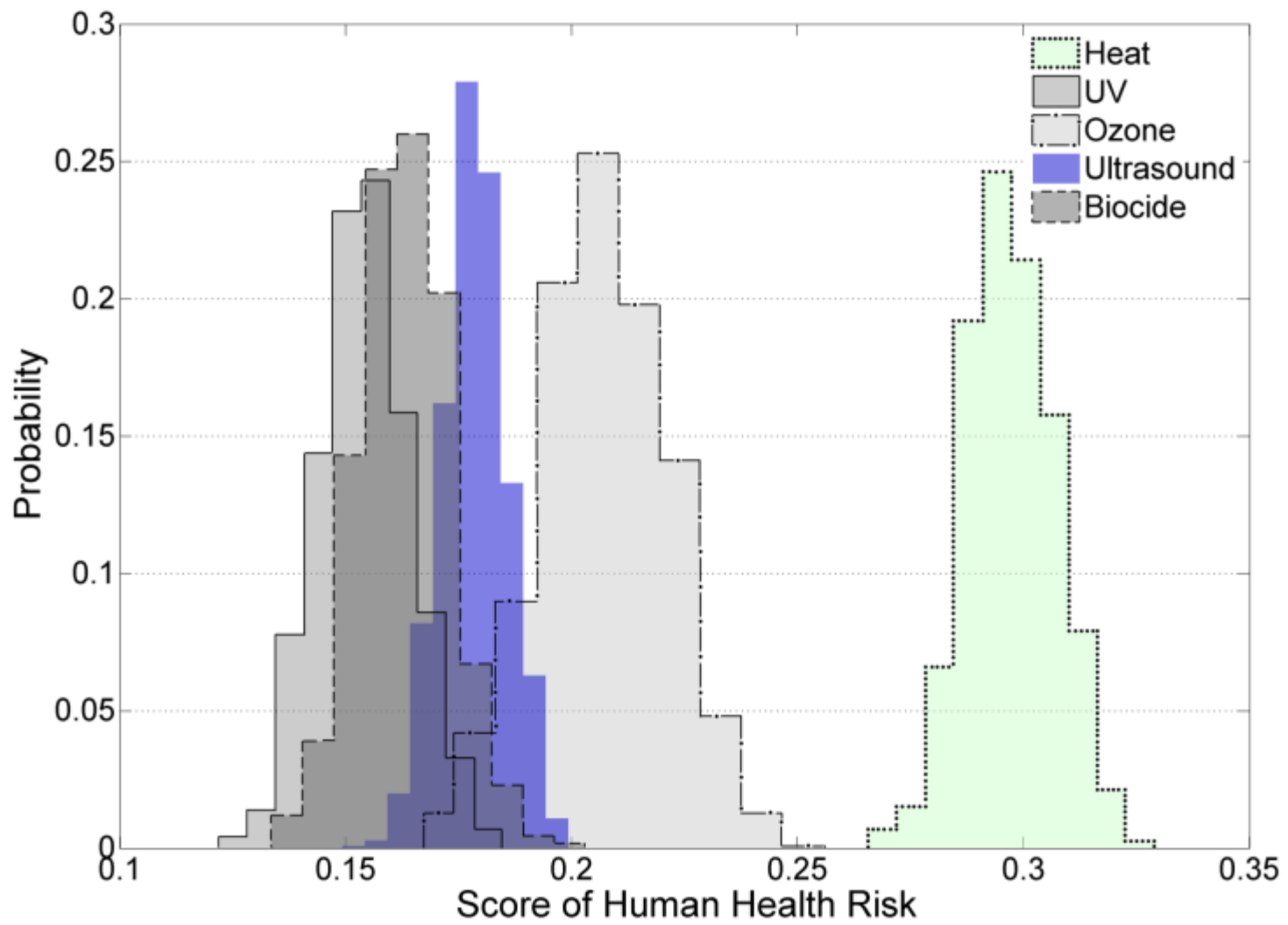


Figure 3.10 Probability distributions of alternative scores with regard to human risk

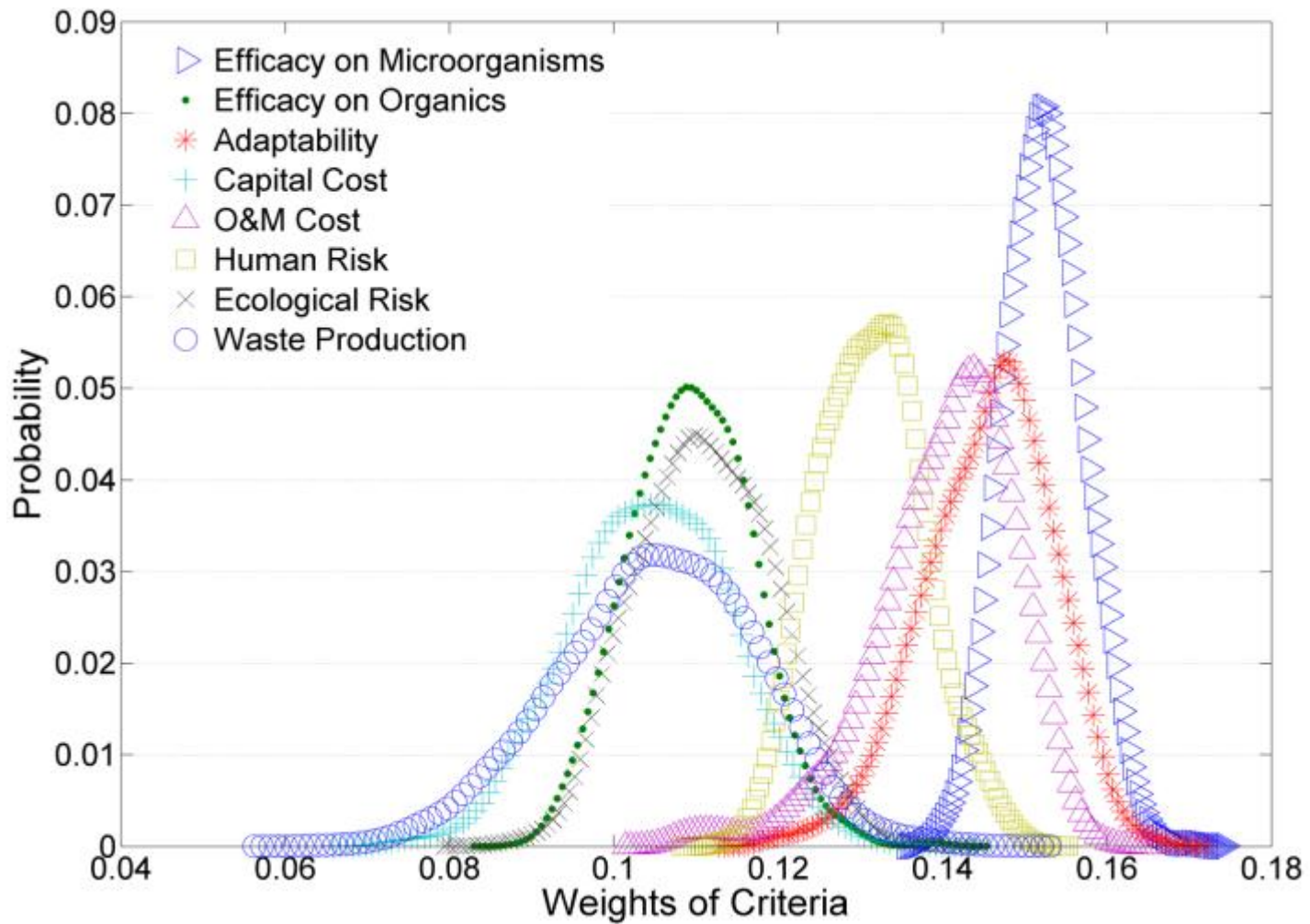


Figure 3.11 Probability density estimates of decision criteria weights

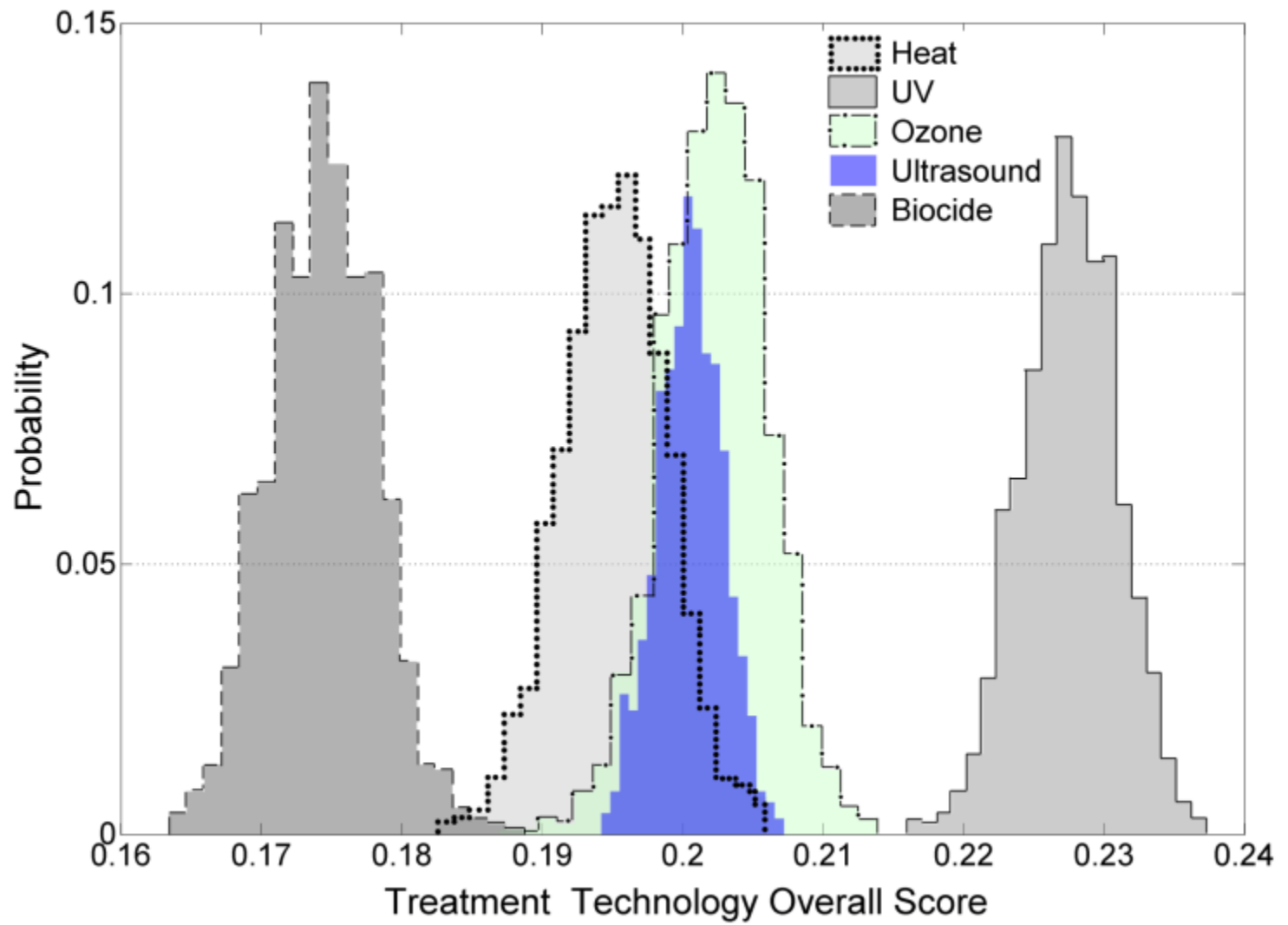


Figure 3.12 Probability distributions of alternative overall scores

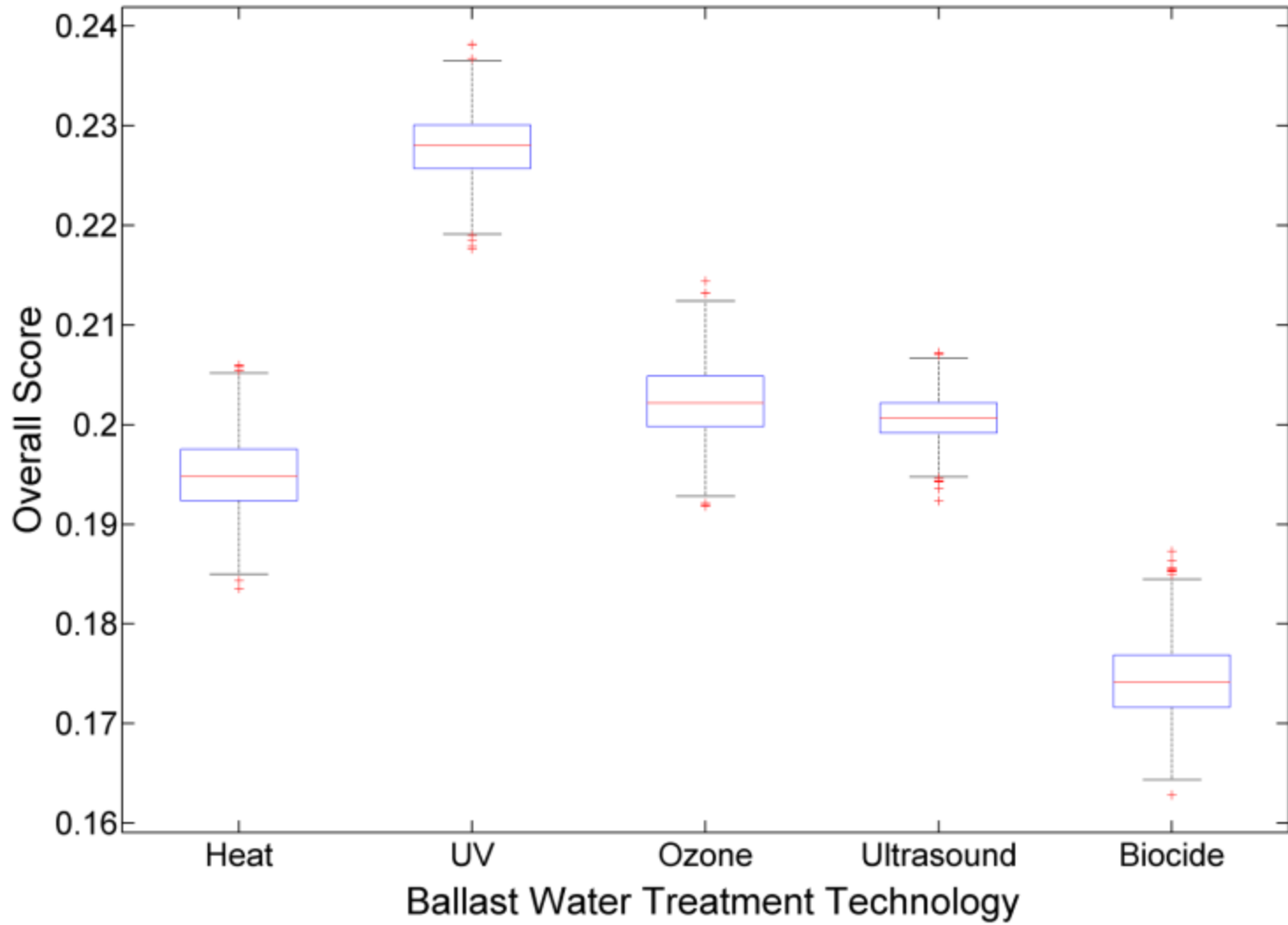


Figure 3.13 Box plots of overall scores for each alternative

Table 3.6 Summary of the simulation results for the final ranking based on the COG method

| Treatment Technology | Rank | | | | |
|----------------------|------|------|------|------|------|
| | 1 | 2 | 3 | 4 | 5 |
| Heat | 0 | 71 | 144 | 784 | 1 |
| UV | 1000 | 0 | 0 | 0 | 0 |
| Ozone | 0 | 610 | 296 | 94 | 0 |
| Ultrasound | 0 | 319 | 560 | 121 | 0 |
| Biocide | 0 | 0 | 0 | 1 | 999 |
| Total | 1000 | 1000 | 1000 | 1000 | 1000 |

Table 3.7 Summary of the simulation results for the final ranking based on Chen's method

| Treatment Technology | Rank | | | | |
|----------------------|------|------|------|------|------|
| | 1 | 2 | 3 | 4 | 5 |
| Heat | 0 | 25 | 98 | 876 | 1 |
| UV | 1000 | 0 | 0 | 0 | 0 |
| Ozone | 0 | 746 | 218 | 36 | 0 |
| Ultrasound | 0 | 229 | 684 | 87 | 0 |
| Biocide | 0 | 0 | 0 | 1 | 999 |
| Total | 1000 | 1000 | 1000 | 1000 | 1000 |

The probability density distributions of criteria weights using the kernel-smoothing method are plotted in Figure 3.11. It reveals that efficacy on microorganisms, adaptability to harsh environments, O&M cost, and human health risk were the most influential criteria that need to be prioritized in the decision making process. The overall scores of each alternative towards the goal are shown in Figure 3.12 as histograms. Another statistical test of the null hypothesis that UV was not the probabilistic optimal alternative (versus the alternate assumption that it was) was conducted. Tables 3.6 and 3.7 reveal that UV was ranked with the highest overall score at 100% confidence level, indicating that the null assumption that it is not probabilistic optimal (versus the alternate assumption that it is) is rejected. Ozone, heat treatment, and ultrasound had the second, third, and fourth places at the confidence levels of 61.0–71.4%, 56.0–68.4%, and 78.4–84.6%, respectively. Figure 3.13 further supports this ranking scheme by using box plot to graphically illustrate the minimum, lower quartiles, medians, upper quartiles, and maximum of the overall scores. It indicates that the score distribution of ozone has a remarkable overlap with that of ultrasound as their medians, lower percentiles, and upper percentiles are close to each other. Nonetheless, ozone has a wider spread of scores as compared to ultrasound, suggesting that the experts were more unanimous on the performance of ultrasound during their assessment. Another interesting point to note is that both COG and Chen's methods produced similar defuzzification results, which demonstrated their applicability in the proposed FSAHP approach. In addition, the results also depicted that the proposal approach can well address linguistic inputs in group decision making processes. The decision makers would be more comfortable and confident to give vague judgments rather than evaluating pairwise comparisons using

single numeric values. Verbal assessments were collected and compared against with each other wherein the priorities of each alternative were determined. The use of the beta-PERT distribution was also able to lessen the uncertainty caused by insufficient information or biased opinions.

3.3 Summary

Good planning can help manage the scheduled tasks within the shortest time period to minimize costs and any associated environmental impacts. The existence of different types of uncertainties due to imprecise information, subjective judgment, and variable environmental conditions may complicate the planning process to a considerable extent. A stochastic SHIFP approach was developed in this chapter to tackle uncertainties inherent in the decision making environment. As with the traditional FLP, fuzzy set theory was used to model uncertainty such that the results would provide the decision makers more flexibility for the choice of the solution. Uniform interval distribution was assumed due to the lack of precise information on both coefficients and variables. A case study related to recovered oily water treatment during offshore oil spill cleanup operations was carried out to test the proposed approach. The decision makers were looking for solutions that how to arrange different facilities and how much wastewater should be delivered to each facility. The results demonstrated that the objective function (maximum daily treatment capacity), if defuzzified by the centroid defuzzification technique, was likely to follow the normal distribution within the range from 3,000 to 3,700 tonnes. In addition, the shapes of the fuzzy decision variables, corresponding to the maximized objective function, can be categorized into seven groups with different

probability such that decision makers can more confidently allocate limited resources. This was particularly true for harsh environments where available resources were usually in short supply and extreme weather conditions were likely to create more uncertainties in estimating the cost and time. Emergency planners and administrators are expected to benefit from this study by gaining an insight into how to wisely allocate resources in responding to an offshore oil spill.

When marine oily water is collected or ready for treatment, choosing the best available technology usually becomes the first priority for decision makers. As one of the most widely exploited multi-criteria decision making (MCDM) approaches, the analytic hierarchy process (AHP) has been well documented in the literature. However, it has been criticized for its inability to quantify the uncertainty associated with decision making. A hybrid fuzzy stochastic analytical hierarchy process (FSAHP) approach was developed in order to assist decision making with more confidence by integrating fuzzy set theory, probabilistic distribution, pairwise comparison and Monte Carlo simulation. A case study related to ballast water management was carried out to verify the feasibility and efficiency of the proposed approach. Five treatment technologies were evaluated against a number of environmental, economic, and technical criteria by nine experts. The results revealed that UV was ranked with the highest overall score at 100% confidence level, indicating that the null assumption that it was not probabilistic optimal (versus the alternate assumption that it is) was rejected. Ozone, heat treatment, and ultrasound had the second, third, and fourth places at the confidence levels of 61.0–71.4%, 56.0–68.4%, and 78.4–84.6%, respectively. Considerable overlaps existed among these three alternatives which may be attributed to the irreducible uncertainty caused by subjective

judgments or lack of knowledge. The results also illustrated that both COG and Chen's defuzzification methods were able to provide the decision makers with reliable decision references. The proposed FSAHP approach can offer a number of benefits such as the capability of capturing human's appraisal of ambiguity and addressing the effects of uncertain judgment when dealing with insufficient information or biased opinions. However, this approach could be highly sensitive to expert dependence whereby any misjudgement may affect its reliability and efficiency. As a complex methodology, it requires more computational efforts in assessing composite priorities than the traditional AHP.

CHAPTER 4

AN EXPERIMENTAL STUDY ON THE TREATMENT OF MARINE OILY WASTEWATER USING UV IRRADIATION

This chapter is based on and expanded from the following paper:

Jing, L., Chen, B., Zhang, B.Y., Zheng, J.S., and Liu, B. (2014). Naphthalene degradation in seawater by UV irradiation: the effects of fluence rate, salinity, temperature and initial concentration. *Marine Pollution Bulletin*, 81, 149-156, doi: 10.1016/j.marpolbul.2014.02.003.

Role: Liang Jing solely worked on this study and acted as the first author of this manuscript. Bo Liu and Jisi Zheng participated in conducting experiments. Most contents of this paper was written by Liang and further polished by the other co-authors.

4.1 Background

A disproportionately large amount of oil pollution at sea is resulted from the operational discharge of oily wastewater (e.g., produced water, bilge water, and ballast water) from shipping and offshore oil and gas operations (Kadali et al., 2012; Jing et al., 2012a). Secondary polishing treatment techniques, right after the conventional oil-water separation, have become increasingly necessary and crucial to achieve a thorough treatment of marine oily wastewater by removing PAHs from the effluent. The occurrence of PAHs is usually of the greatest concern because of their high resistance towards biodegradation, extreme toxicity to marine biota, and possible carcinogenicity and mutagenicity. For example, according to OGP (2002) and Neff et al. (2011b), the typical concentrations of naphthalene, phenanthrene and fluorene in produced water are somewhere between 5-841, 9-111, and 4-67 $\mu\text{g L}^{-1}$, respectively, whereas the other 13 EPA PAHs tend to have much lower concentrations ranging from 0.1 to 15 $\mu\text{g L}^{-1}$. The total concentration of benzene, toluene, ethylbenzene and xylene (BTEX) is between 730 and 24070 $\mu\text{g L}^{-1}$, while phenols have a total concentration around 400 $\mu\text{g L}^{-1}$; however, they are generally less toxic and their natural degradation tends to be much faster than that of PAHs (Neff et al., 2011b). Most of the traditional PAH removal techniques, such as biofiltration, biodegradation, adsorption, and phytoremediation are not directly suitable for marine applications due to space, cost, and safety concerns (Haritash and Kaushik, 2009). UV irradiation has been named as a promising solution to fulfill this purpose as it has been widely used in freshwater applications and it can be applied in compact size with no adding chemicals (Woo et al., 2009; Włodarczyk-Makuła, 2011; Sanches et al., 2011). Because most of the previous studies have not investigated its efficiency and

applicability in dealing with marine oily wastewater, this chapter is dedicated to investigate the UV induced degradation kinetics of a typical PAH, namely naphthalene, in natural seawater through a bench-scale reactor. Naphthalene is chosen because it is a major contaminant in oily wastewater such as ballast water, bilge water and offshore produced water, and has been considered as a possible carcinogen to humans. It is relatively more soluble and less hydrophobic than other high molecular weight PAHs which raises a critical bioavailability issue due to its high concentration. Experiments also focus on examining the effects of various factors including UV fluence rate, salinity, temperature and initial concentration. This experimental study serves as an example of marine oily wastewater treatment and also the foundation of the following chapters.

4.2 Materials and Methods

4.2.1 Reagents and Standards

Naphthalene (>99%) and naphthalene D8 (>99%, internal standard) were purchased from Aldrich and used as received. Dichloromethane (Honeywell Burdick and Jackson, USA) was used for preparing stock solutions and for aqueous sample extraction. Naphthalene spiking solutions were prepared by 1:1 dilution (v/v) of the stock solutions in acetone (Honeywell Burdick and Jackson, USA). The commercial products were used as received without any further purification. Distilled water was produced on-site from a double, fused-silica distillation unit. Considering the potential interference caused by the complex matrix of offshore produced water and bilge water (e.g., other petroleum hydrocarbons, heavy metals, biocides, and solids), seawater was chosen for this preliminary investigation of the performance of UV irradiation in removing PAHs.

Natural seawater with salinity around 25 practical salinity unit (psu) was obtained from a clean coastal site in St. John's, Canada, and the site is considered free of any oil pollution. Seawater was stored and used after filtration (5 μm) to remove suspended solids that could scatter and absorb UV irradiation.

4.2.2 Photoreactor and Light Source

The photoreactor used in this study has an inner airtight quartz sleeve and an outer aluminum jacket. The inner sleeve is a clear fused quartz beaker (Technical Glass, USA) with a polycarbonate top lid sealed by a 0.64 cm thick O-ring to avoid the evaporation of naphthalene. A stainless steel stirring rod, attached to a 4.78 cm size stepper motor (4018L-01S-01, from LIN Engineering), is placed at the center of the sleeve. Two stainless steel six-bladed paddle impellers are mounted one above the other on the rod. A 50 W Eheim Jager aquarium heater (3602090, from Eheim, Germany) and a thermometer are deployed to adjust water temperature. Eight 18.4 W low-pressure UV lamps (Atlantic Ultraviolet, Canada) with emission peak at 254 nm were placed around the quartz sleeve (Figure 4.1b). The emission peak has a full width half maximum (FWHM) of 15 nm. The outer jacket has an aluminum lid that can be firmly sealed to provide heat and light insulation. Four control buttons are located on the dashboard outside of the jacket body to control lamps in any desired combinations (i.e., two, four, six, and eight lamps).

4.2.3 UV Fluence Rate Determination

Fluence rate refers to the total radiant power incident from all directions onto an infinitesimally small sphere. According to Bolton and Linden (2003), it is the appropriate

term to describe photon intensity in a UV reactor because UV can impinge on the target organic compounds from any direction. For different number of lamps, the fluence rate in the empty quartz sleeve was measured at 17 points on the top, middle, and bottom layers (Figure 4.1), respectively, by using a digital UVX Radiometer (UVP, USA). The measurements were made and summed according to the tetrahedral method described by Björn (1995) in order to account for light reflected from all directions. To determine the corresponding fluence rate when the quartz sleeve was filled with the sample water, the attenuation coefficient of UV through water (0.0264 cm^{-1}) was taken into account on the basis of Su and Yeh (1995). As most suspended solids were removed prior to the tests, a basic assumption here was that the effective attenuation length was approximated as the internal radius of the reactor (11.1 cm), implying a 25% reduction in all measurements. The adjusted measurements were then interpolated by using a Matlab[®] built-in function (i.e., `griddata`) on the top, middle, and bottom layers, respectively.

4.2.4 Experimental Procedure

To examine the effects of fluence rate, salinity, temperature, and initial concentration, a full factorial design of experiments (DOE) was employed to determine the significance of each factor being tested as well as their interactions. Two levels of UV fluence rate were obtained by switching on two and six lamps, respectively. Initial naphthalene concentrations were set as 10 and 500 $\mu\text{g L}^{-1}$ which were usually considered as the minimum and maximum values in oily seawater (OGP, 2002; Johnsen et al., 2004; Blanchard et al., 2011). Temperature was adjusted and maintained at 23 (room temperature) and 40 °C which were reported as the typical temperature range of marine

oily wastewater such as offshore produced water and bilge water (Levine and Barnes, 2010; Neff et al., 2011a; Leichsenring and Lawrence, 2011). Control experiments (without UV irradiation) were conducted at 40 °C to quantify the loss of naphthalene caused by volatilization. Salinity levels of 25, 32.5, and 40 psu were chosen on the basis of the ocean surface salinity at the coastal region of the Grand Bank in Newfoundland (Han et al., 2011) and the North Atlantic (Qu et al., 2011).

In each of the 24 experimental runs, a volume of 50 µL of naphthalene stock solution (1.2 or 60 mg ml⁻¹) was diluted in acetone (1:1, v/v) and then spiked into 6 L filtered seawater to obtain an initial naphthalene concentration of 10 or 500 µg L⁻¹, respectively. Different salinity levels were obtained by evaporating seawater and measured by a salinity meter (Thermo Scientific Orion Star A215). The mixture was vigorously stirred for 20 min to reach the thermal and volatilization equilibria. UV lamps were allowed to warm-up for 20 min before tests. Temperature was controlled by the built-in heater. The paddle impellers were driven by a stepper motor to ensure complete homogeneity during reaction. At various time intervals (e.g., 30 min) during photolysis, a 20 ml water sample was collected from the reactor using a peristaltic pump and transferred into a 20 ml amber vial.

4.2.5 Analytical Method

Ten-millilitre water sample was transferred from an amber vial into a glass centrifuge tube. A volume of 20 µL of Naphthalene D8 internal standard (5 and 250 mg L⁻¹ for an initial naphthalene concentration of 10 and 500 µg L⁻¹, respectively) was then added and subsequently mixed with 0.25 ml dichloromethane for extraction. After

shaking and centrifuging for 15 minutes in each step, 50 μL organic phase extract was transferred into a 150 μL micro vial and analyzed by a gas chromatograph (GC) (Agilent 7890A) equipped with a fused silica capillary column (30 m \times 0.25 mm \times 0.25 μm) and a mass selective detector (MS) (Agilent 5975C). Sample injection (2 μL) was performed by an auto-injector (Agilent 7693) at a temperature of 300 $^{\circ}\text{C}$. The samples were injected in the split injection mode. Oven operating parameters were set as initially 65 $^{\circ}\text{C}$ and finally 300 $^{\circ}\text{C}$ with a temperature increase rate of 60 $^{\circ}\text{C min}^{-1}$. Hydrocarbon analyses were performed in the selected ion monitoring (SIM) mode using an electron energy of 70 eV and a source temperature of 350 $^{\circ}\text{C}$.

4.2.6 Statistical Analysis

The photolysis rate constants of naphthalene in seawater were obtained for different experimental conditions. All experimental data were subjected to multi-way analysis of variance (ANOVA) to determine the significance of fluence rate, salinity, temperature and initial concentration. ANOVA tests the null hypothesis that the output means of each factor level are equal, versus them not being equal. A probability of $p < 0.05$ indicates that this factor or the interaction effects between multiple factors are significant.

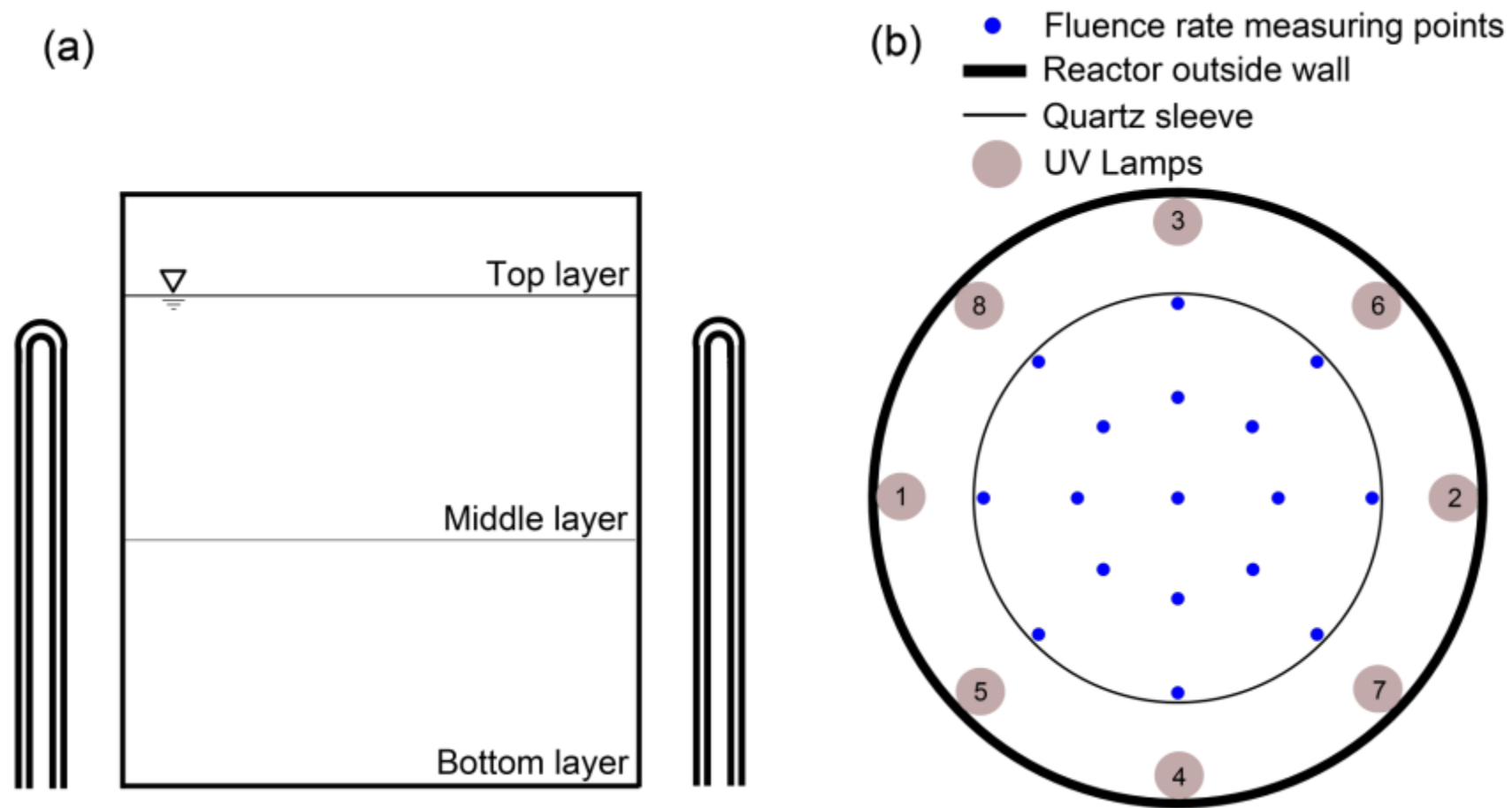


Figure 4.1 (a) Layers and (b) measuring points of UV fluence rate within the quartz sleeve

4.3 Results and Discussion

The reaction rate equation of the photodegradation of naphthalene can be expressed as follows:

$$r = \frac{dc_{nap}}{dt_r} = -k_r c_{nap}^{n_r} \quad (1)$$

where r is the reaction rate ($\mu\text{g L}^{-1} \text{min}^{-1}$); t_r is reaction time (min); c_{nap} is the concentration of naphthalene ($\mu\text{g L}^{-1}$); k_r is the reaction rate constant (min^{-1}); and n_r is the reaction order, which has been generally accepted as equal to 1 (first order kinetics) for naphthalene (Kwon et al., 2009; Kong et al., 2012). Equation 1 can be rearranged as:

$$\ln \frac{c_t}{c_0} = -kt \quad (2)$$

where c_t and c_0 are the instant and initial concentrations of naphthalene, respectively. Equation 2 can be further inferred t

$$\ln \frac{c_t}{c_0} = -k_0 \frac{E}{E_0} t \quad (3)$$

where k_0 is the reaction rate constant of per mW cm^{-2} fluence rate; E and E_0 are the actual and unit fluence rates (mW cm^{-2}), respectively. This series of k_0 can be used as a good reference to predict the removal rate of naphthalene in industrial processes where high energy UV radiation can be employed. According to Equation 2, the reaction rate constants under different experimental conditions are tabulated in Table 4.1.

4.3.1 ANOVA

The Box-Cox (B-C) plot for power transforms suggested that a natural logarithmic

transformation ($\lambda=0$) of the original outputs would better normalize the data points. The UV-induced photodegradation of naphthalene in seawater can be expressed using the following equation:

$$\ln(k) = -4.78 + 0.48X_1 - 0.11X_2 + 0.41X_3 - 0.22X_4 + 0.14X_1X_3 + 0.28X_3X_4 \quad (4)$$

where X_1 , X_2 , X_3 and X_4 are the coded inputs for fluence rate, salinity, temperature and initial concentration, respectively. Equation 4 indicates that the positive coefficients of X_1 , X_3 , X_1X_3 and X_3X_4 have a constructive effect to promote the removal of naphthalene, while the increase of X_2 and X_4 can slow down the process. Results from ANOVA on the natural logarithmic transformed response model were summarized in Table 4.2. From the Fisher's F -test, it was observed that the established model (Equation 4) was statistically significant with a F -Value of 23.32 and a probability value ($\text{Prob} > F$) of less than 0.0001. This observation was also evidenced by the adjusted and predicted R^2 values, which were 0.87 and 0.80, respectively. The predicted $R^2 = 0.80$ suggested that 80% of the sample variation could be attributed to the independent variables while the adjusted $R^2 = 0.87$ was also of statistical significance and agreed with the correlation applicability of the model.

According to Table 4.2, a factor or an interaction with a p -value less than 0.05 is defined to have significant influence on the photodegradation of naphthalene. The smaller the p -values are, the bigger the significance of the factors or their interactions. It can be observed that the effect of fluence rate was the most influential on the removal process, followed by temperature and the interaction between temperature and initial concentration. This finding was also in agreement with the fact that their model coefficients, as shown in Equation 4, were much greater than the others.

Table 4.1 Reaction rate constants of all factorial runs

| Reaction condition | | | | | k | k_0 | Regression |
|---|-------|-------------|-------------------|---------------------------------------|-----------------------|-----------------------|-------------|
| Initial Conc. ($\mu\text{g L}^{-1}$) | Run # | UV lamps | Salinity (psu) | Temperature ($^{\circ}\text{C}$) | (min^{-1}) | (min^{-1}) | coefficient |
| 10 | 1 | 6 | 25 | 23 | 0.0186 | 0.0022 | 0.992 |
| | 2 | 6 | 32.5 | 23 | 0.0160 | 0.0019 | 0.988 |
| | 3 | 6 | 40 | 23 | 0.0110 | 0.0013 | 0.982 |
| | 4 | 6 | 25 | 40 | 0.0236 | 0.0029 | 0.982 |
| | 5 | 6 | 32.5 | 40 | 0.0183 | 0.0022 | 0.955 |
| | 6 | 6 | 40 | 40 | 0.0190 | 0.0023 | 0.999 |
| | 7 | 2 | 25 | 23 | 0.0069 | 0.0024 | 0.989 |
| | 8 | 2 | 32.5 | 23 | 0.0058 | 0.0020 | 0.894 |
| | 9 | 2 | 40 | 23 | 0.0047 | 0.0016 | 0.989 |
| | 10 | 2 | 25 | 40 | 0.0073 | 0.0025 | 0.986 |
| | 11 | 2 | 32.5 | 40 | 0.0066 | 0.0023 | 0.981 |
| | 12 | 2 | 40 | 40 | 0.0062 | 0.0022 | 0.994 |
| 500 | 1 | 6 | 25 | 23 | 0.0077 | 0.0009 | 0.966 |
| | 2 | 6 | 32.5 | 23 | 0.0044 | 0.0005 | 0.727 |
| | 3 | 6 | 40 | 23 | 0.0021 | 0.0003 | 0.319 |
| | 4 | 6 | 25 | 40 | 0.0428 | 0.0052 | 0.912 |
| | 5 | 6 | 32.5 | 40 | 0.0176 | 0.0021 | 0.961 |
| | 6 | 6 | 40 | 40 | 0.0216 | 0.0026 | 0.982 |
| | 7 | 2 | 25 | 23 | 0.0031 | 0.0011 | 0.894 |
| | 8 | 2 | 32.5 | 23 | 0.0018 | 0.0006 | 0.427 |
| | 9 | 2 | 40 | 23 | 0.0034 | 0.0012 | 0.727 |
| | 10 | 2 | 25 | 40 | 0.0144 | 0.0050 | 0.921 |
| | 11 | 2 | 32.5 | 40 | 0.0051 | 0.0018 | 0.992 |
| | 12 | 2 | 40 | 40 | 0.0048 | 0.0017 | 0.850 |

Table 4.2 ANOVA for natural logarithmic transformed response of naphthalene photodegradation

| Source | Sum of squares | df | Mean squares | <i>F</i> -Value | <i>p</i> -value, Prob > <i>F</i> |
|------------------------------|----------------|----|--------------|-----------------|----------------------------------|
| Model | 2.74 | 7 | 0.39 | 23.32 | <0.0001 |
| X_1 -fluence rate | 1.05 | 1 | 1.05 | 62.42 | <0.0001 |
| X_2 -salinity | 0.24 | 2 | 0.12 | 7.25 | 0.0057 |
| X_3 -temperature | 0.78 | 1 | 0.78 | 46.43 | <0.0001 |
| X_4 -initial concentration | 0.23 | 1 | 0.23 | 13.63 | 0.0020 |
| X_1X_3 | 0.083 | 1 | 0.083 | 4.93 | 0.0411 |
| X_3X_4 | 0.36 | 1 | 0.36 | 21.35 | 0.0003 |
| Residual | 0.27 | 16 | 0.017 | | |
| Total | 3.01 | 23 | | | |

4.3.2 Effect of Fluence Rate

The fluence rate of four lamps was measured, corrected with a 25% attenuation coefficient, and interpolated on the top, middle and bottom layers, respectively (Figures 2a-2c). The spatial distributions clearly indicate that UV irradiation reaches its maxima near the lamps and gradually decreases to half its maximum value at the centre. Figure 4.2d shows a 3-layer average distribution from which the mean fluence rate inside the quartz sleeve was obtained as 5.65 mW cm^{-2} . By following the same procedure, as shown in Figure 4.3, the average fluence rates of two, six and eight lamps were obtained as 2.88, 8.27 and 10.93 mW cm^{-2} , respectively. A linear relationship between the number of lamps and the mean fluence rate was established with a regression coefficient of 0.99.

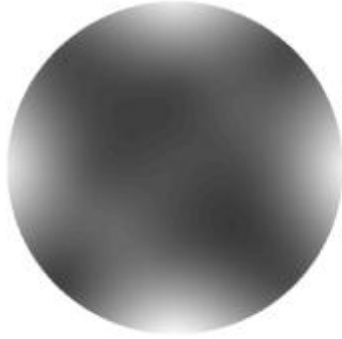
The photodegradation rates of different numbers of lamps were also noted to follow a linear pattern. For example, the average fluence rate of six lamps (8.27 mW cm^{-2}) was almost three times greater than that of two lamps (2.88 mW cm^{-2}). Under the same experimental conditions, the reaction rate constants of six lamps were approximately as much as three times higher than those of two lamps (Table 4.1). To further validate this finding, an additional series of experiments were conducted by using two, four, six, and eight lamps while keeping salinity at 40 psu, temperature at $23 \text{ }^\circ\text{C}$ and initial concentration at $10 \text{ } \mu\text{g L}^{-1}$. As shown in Figure 4a, the degradation process became much faster with the increasing number of lamps. For example, after 2 hours of irradiation, the remaining concentrations of naphthalene using two, four, six, and eight lamps were 6.1, 4.8, 2.0, and $0.9 \text{ } \mu\text{g L}^{-1}$, respectively. Semi-log plots of naphthalene concentration versus degradation time all appear to be linear with regression coefficients greater than 0.98, suggesting that the first-order kinetics is applicable regardless the intensity of UV

irradiance (Figure 4b). Further analysis revealed that the first order rate constants were 0.0047, 0.0080, 0.0110, and 0.0169 min^{-1} , respectively, which were linearly related to the number of lamps (Figure 4b). This linear pattern infers that high fluence rate can increase the collision probability between active centers and therefore generate more free radicals (e.g., OH \cdot) to promote the photodegradation process.

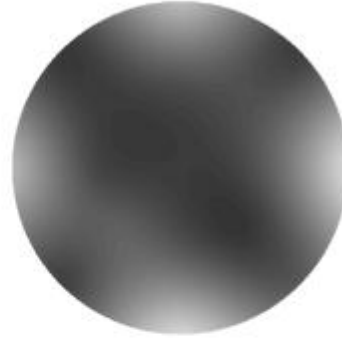
4.3.3 Effect of Salinity

The effect of salinity on the photodegradation of naphthalene is presented in Figure 4.5. A clear trend can be identified that the performance of UV irradiation was decreased at higher salinity levels. In order to further understand this inhibition effect, another two experimental runs were undertaken by using distilled water and diluting seawater with distilled water to achieve salinity series of 0 and 18 psu, respectively, under the irradiation of six lamps. Initial concentration and temperature were used as 10 $\mu\text{g L}^{-1}$ and 23 °C, respectively. As shown in Figure 4.6, naphthalene spiked in distilled water can be removed after 120 min irradiation. Contrastingly, the same amount of naphthalene in seawater would take much longer time to be fully mineralized. For example, the remaining naphthalene concentration in 40 psu seawater after 240 min exposure was 9% of the initial concentration. The reaction rate constants (k) were 0.0655, 0.0224, 0.0186, 0.0160 and 0.0110 min^{-1} for salinity levels of 0, 18, 25, 32.5 and 40 psu, respectively, implying a decreasing trend with the increase of salinity.

(a) Top Layer



(b) Mid Layer



(c) Bottom Layer



(d) 3-layer Average

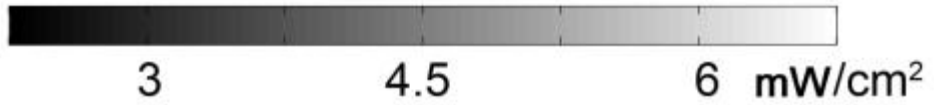
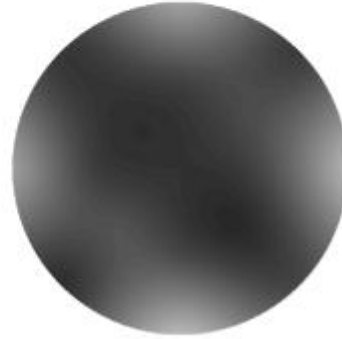
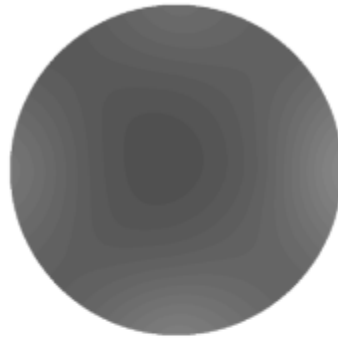
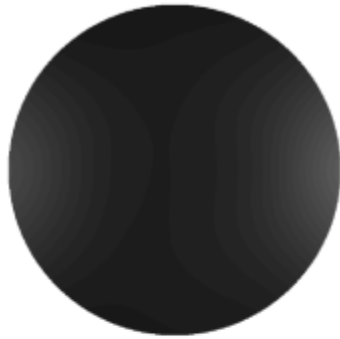


Figure 4.2 (a) Top layer, (b) mid layer, (c) bottom layer, and (d) 3-layer average distributions of UV fluence rate with four lamps

(a) Two Lamps (1-2) (b) Four Lamps (1-4)



(c) Six Lamps (1-6) (d) Eight Lamps (1-8)

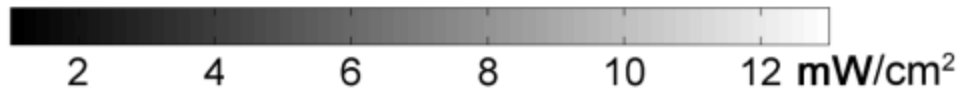
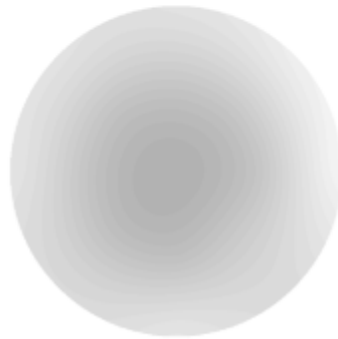
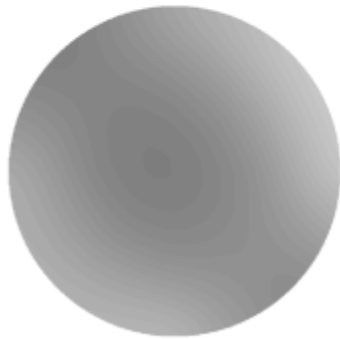


Figure 4.3 Three-layer average distributions of UV fluence rate with (a) two, (b) four, (c) six, and (d) eight lamps

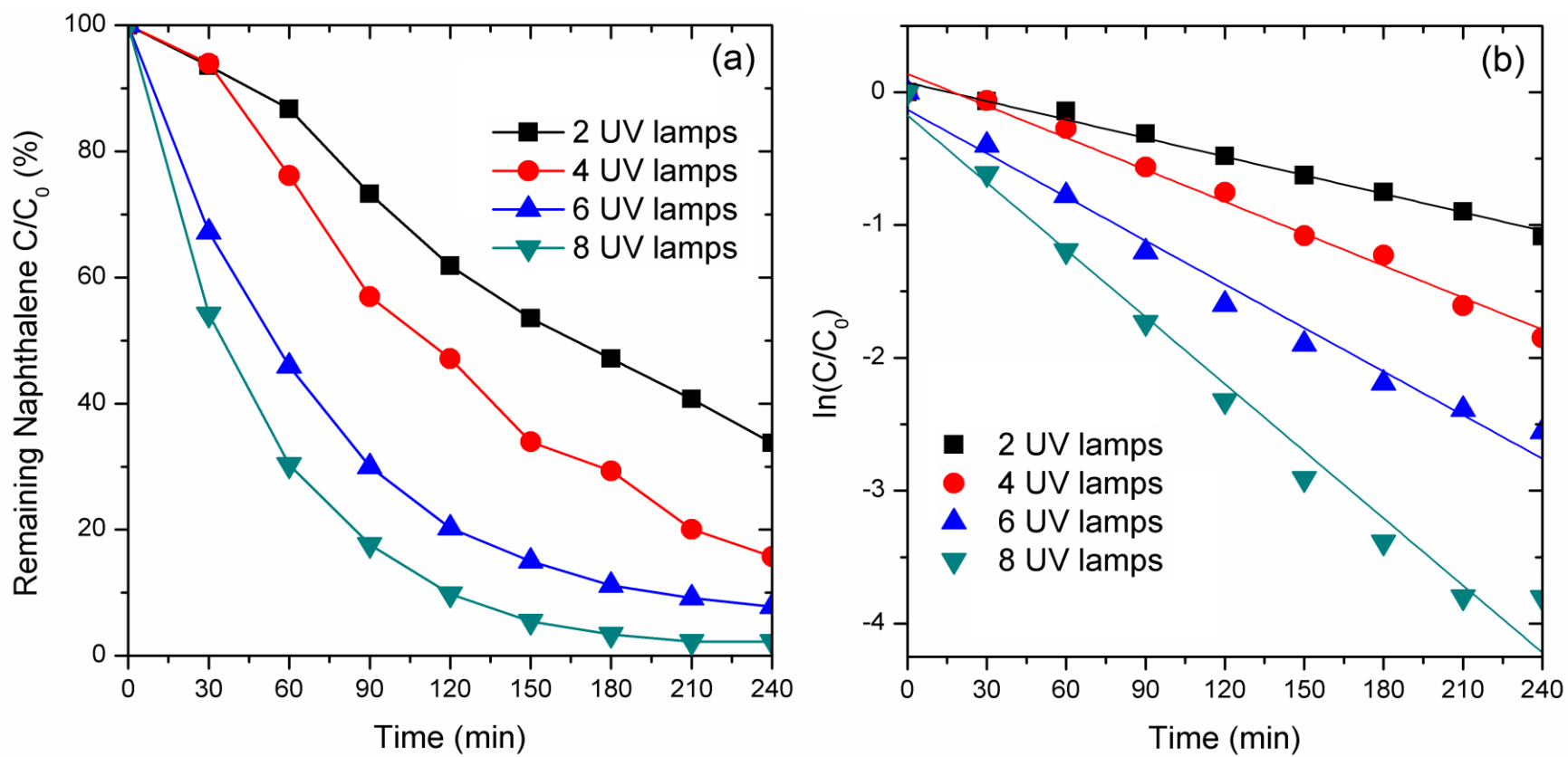


Figure 4.4 (a) Concentration change and (b) the first-order regression of $10 \mu\text{g L}^{-1}$ naphthalene photodegradation in 40 psu seawater (Temperature = 23°C)

Such effects may be caused by the presence of bromide (Br^-), carbonate (CO_3^{2-}) and bicarbonate (HCO_3^-) ions in seawater. Bromide concentration in seawater usually ranges from 65 to 80 ppm, which is approximately 0.2% of all dissolved salts. According to von Gunten (2003), $\text{OH}\cdot$ plays an important role in the oxidation of Br^- to generate the less reactive dibromide anion ($\text{Br}_2\cdot^-$). Zafiriou et al. (1987) reported that $\text{OH}\cdot$ reacts almost exclusively with Br^- as compared to CO_3^{2-} and HCO_3^- . Lair et al. (2008) argued that both CO_3^{2-} and HCO_3^- are also capable of scavenging free radicals (e.g., $\text{OH}\cdot$) excited by UV and therefore suppress the photolysis process. Measurements of sample pH revealed that an increasing salinity tended to result in higher alkalinity values (caused by CO_3^{2-} and HCO_3^-), which in turn raised the equilibrium pH of seawater (Figure 4.6). Therefore, the elevation of salinity seemingly impeded the removal of naphthalene because the concentrations of the aforementioned radical inhibitors were also expected to increase. Another possible explanation of this discrepancy may be attributed to the possible existence of some dissolved organic compounds that can absorb photons from UV irradiation. Dimou et al. (2004) found that dissolved organic matters in natural seawater could induce a decrease of Triadimefon photolysis rate due to the optical filter effect. Moreover, it is worth mentioning that the nitrate (NO_3^-) in seawater (i.e., concentration around 2–12 $\mu\text{mol L}^{-1}$ in the North Atlantic according to Steinhoff et al. (2010)) would appear to be a promising source of $\text{OH}\cdot$ during UV photolysis. However, the presence of NO_3^- can also inhibit the degradation of PAHs via an ‘inner filter’ effect (Mack and Bolton, 1999; Tedetti et al., 2007; Ji et al., 2012).

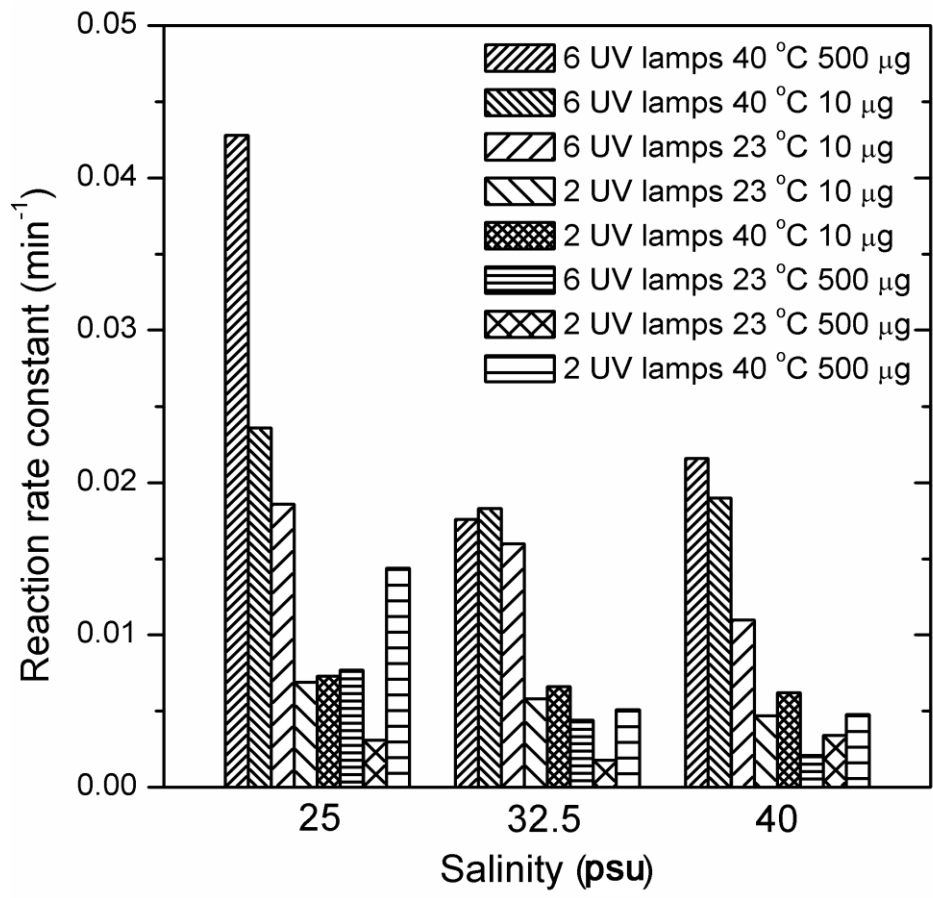


Figure 4.5 Reaction rate constants of naphthalene photodegradation at salinity levels of 25, 32.5 and 40 psu

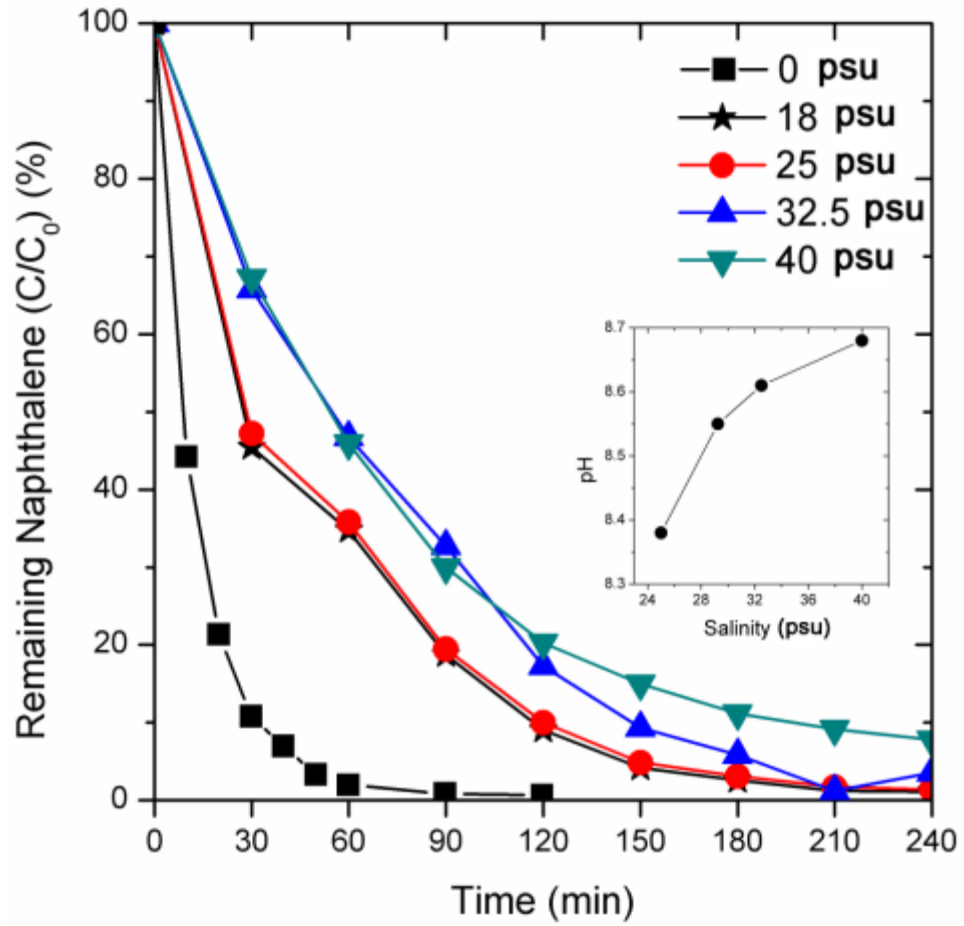


Figure 4.6 Effect of salinity on the photodegradation of naphthalene using six UV lamps (initial concentration = $10 \mu\text{g L}^{-1}$; temperature = 23°C)

4.3.4 Effect of Temperature

Given that naphthalene is volatile, control experiments (without UV irradiation) were carried out at 40 °C to measure the volatilization loss. The results demonstrated that the concentration of naphthalene remained relatively constant after a control period of 4 hours and the effect of evaporation loss was not significant. Viewed from Figure 4.7a, the elevation of temperature from 23 to 40 °C considerably accelerated the degradation of naphthalene in seawater because of the increasing collisions between photons and molecules. However, as with most photoreactions, temperature is not the major driving force to enhance UV-induced photodegradation (Nadal et al., 2006; Lee et al., 2011). The differences between reaction rate constants at 23 and 40 °C were not as remarkable as those between different fluence rates (Table 4.1). On the other hand, a temperature increase is expected to result in a decrease in oxygen solubility that lowers the generation of singlet oxygen and superoxide anion radical.

Figure 4.7b further highlights this trend by plotting the concentration of remaining naphthalene at 23 °C, 40 °C, and an additional point, 30 °C while the other conditions were kept unchanged. The reaction rate constants gradually increased by 13.9% and 11.4% from 23 to 30 °C, and 30 to 40 °C, respectively. The activation energy (E_a) of this process can also be roughly determined by plotting the reaction rate constant versus temperature. The Arrhenius law defines that k in the ln- form should be linearly related to Kelvin temperature in the form of $1/T$.

$$\ln(k) = \frac{-E_a}{R} \frac{1}{T} + \ln(A) \quad (5)$$

where R is the universal gas constant ($\text{J K}^{-1} \text{mol}^{-1}$), T is temperature (K), and A is the pre-exponential factor depending on compound. A linear trend line ($R^2 = 0.982$) revealed

that this particular E_a was $10.67 \text{ kJ mol}^{-1}$, which was about half of the value in distilled water (Lair et al., 2008). High activation energy usually corresponds to a reaction rate that is very sensitive to temperature. The higher the activation energy, the more increase in reaction rate constant when temperature goes up. This difference implied that increasing temperature would be more favourable and effective for the photodegradation of naphthalene in distilled water rather than in seawater.

4.3.5 Effect of Initial Concentration

A comparison between the results at different initial concentrations is summarized in Table 4.3. A single factor ANOVA ($p = 0.75$) rejected the hypothesis that a statistically significant difference existed between the two groups of rate constants, implying the contribution from initial concentration was not prominent. Nonetheless, the average reaction rate constant at high concentration was slightly lower than that at low concentration. It may be further interpreted as evidence that an increase in naphthalene concentration would lead to a slight decrease in reaction rate (Figure 4.8). This observation may be explained by the fact that when the initial concentration of naphthalene was low, the amount of reactive radicals generated from UV irradiation was more than enough to initiate the photoreactions. Contrastingly, when the initial concentration was 50 times higher, using the same amount of radicals may not be sufficient to sustain the reactions at the desired rate.

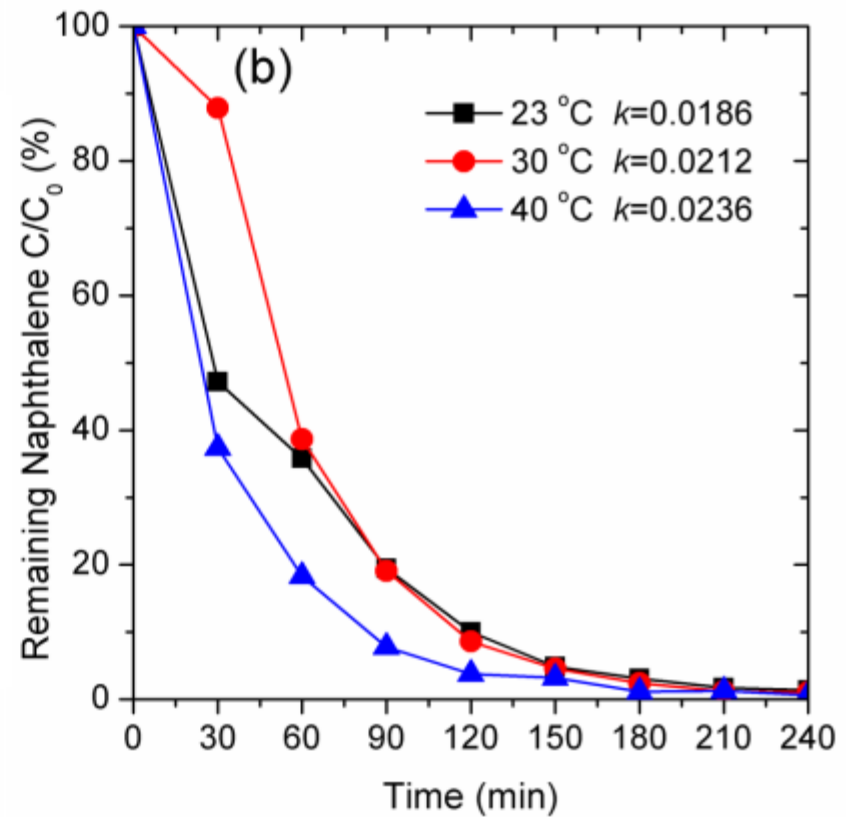
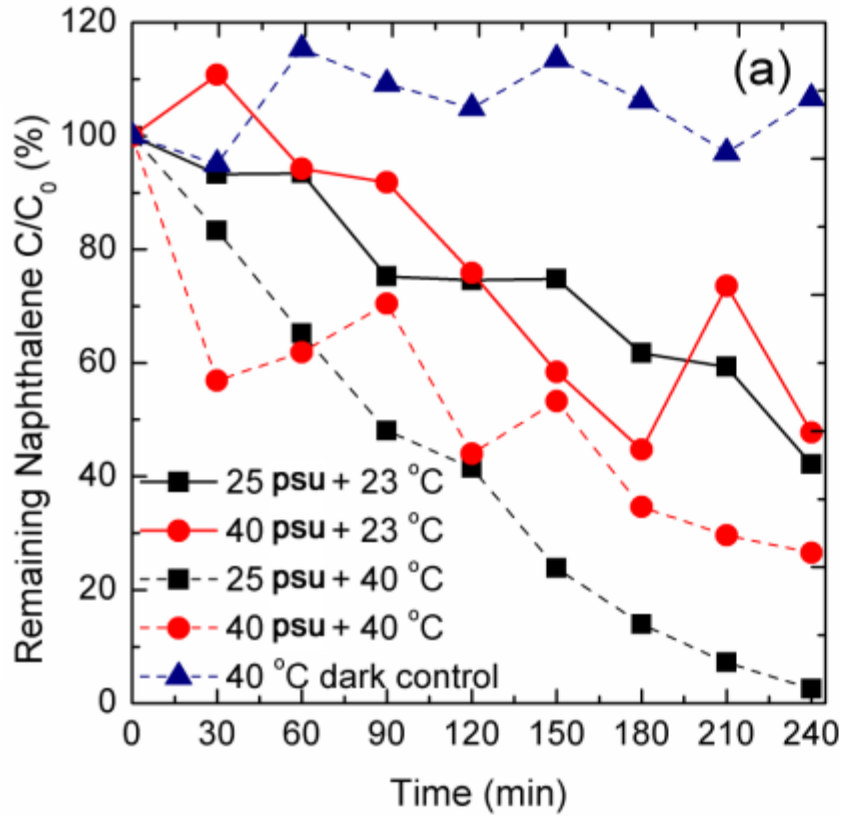


Figure 4.7 Effect of temperature at (a) an initial concentration of 500 µg L⁻¹ and two UV lamps, and (b) an initial concentration of 10 µg L⁻¹, a salinity level of 25 psu and six UV lamps

Another interesting finding was that the variance in the high concentration group was greater than that in the low concentration group. This considerable variance is mainly contributed by the interaction effect between temperature and initial concentration. As demonstrated in Figure 4.8, when the temperature of water samples was maintained at a relatively high level (i.e., 40 °C), the 4th and 10th high concentration runs had remarkably higher reaction rate constants as compared to the low concentration runs. These results suggested that temperature and initial concentration had synergistic effects on the removal of naphthalene. However, it is also noteworthy that this synergistic effect was alleviated at higher salinity levels.

It is also worth noting that, although naphthalene itself is carcinogenic and it does not act as a photosensitizer like many other PAHs (e.g., anthracene and fluoranthene), the photodegradation process is likely to produce other toxic oxygenated compounds (Barron and Ka'Aihue, 2001). According to Bernstein et al. (2001) and McConkey et al. (2002), the initial photoproducts of naphthalene, endoperoxides, are short-lived intermediates and will undergo further reactions to form several more stable photoproducts, such as 1-naphthol, 1,4-naphthoquinone and 1,4-naphthalenedione. The identification and quantification of the toxicity of these photoproducts in the marine environment has been limited in the literature and therefore deserves more research effort.

Table 4.3 Single factor ANOVA of naphthalene photodegradation at different initial concentrations

| Initial concentration ($\mu\text{g L}^{-1}$) | Average k (min^{-1}) | Variance |
|---|-----------------------------------|----------|
| 10 | 0.0120 | 4.42E-5 |
| 500 | 0.0107 | 1.45E-4 |

| Source of Variation | Sum of squares | df | Mean squares | F -value | p -value |
|---------------------|----------------|----|--------------|------------|------------|
| Between groups | 9.63E-6 | 1 | 9.63E-6 | 0.1020 | 0.7524 |
| Within groups | 2.08E-3 | 22 | 9.44E-5 | | |
| Total | 2.09E-3 | 23 | | | |

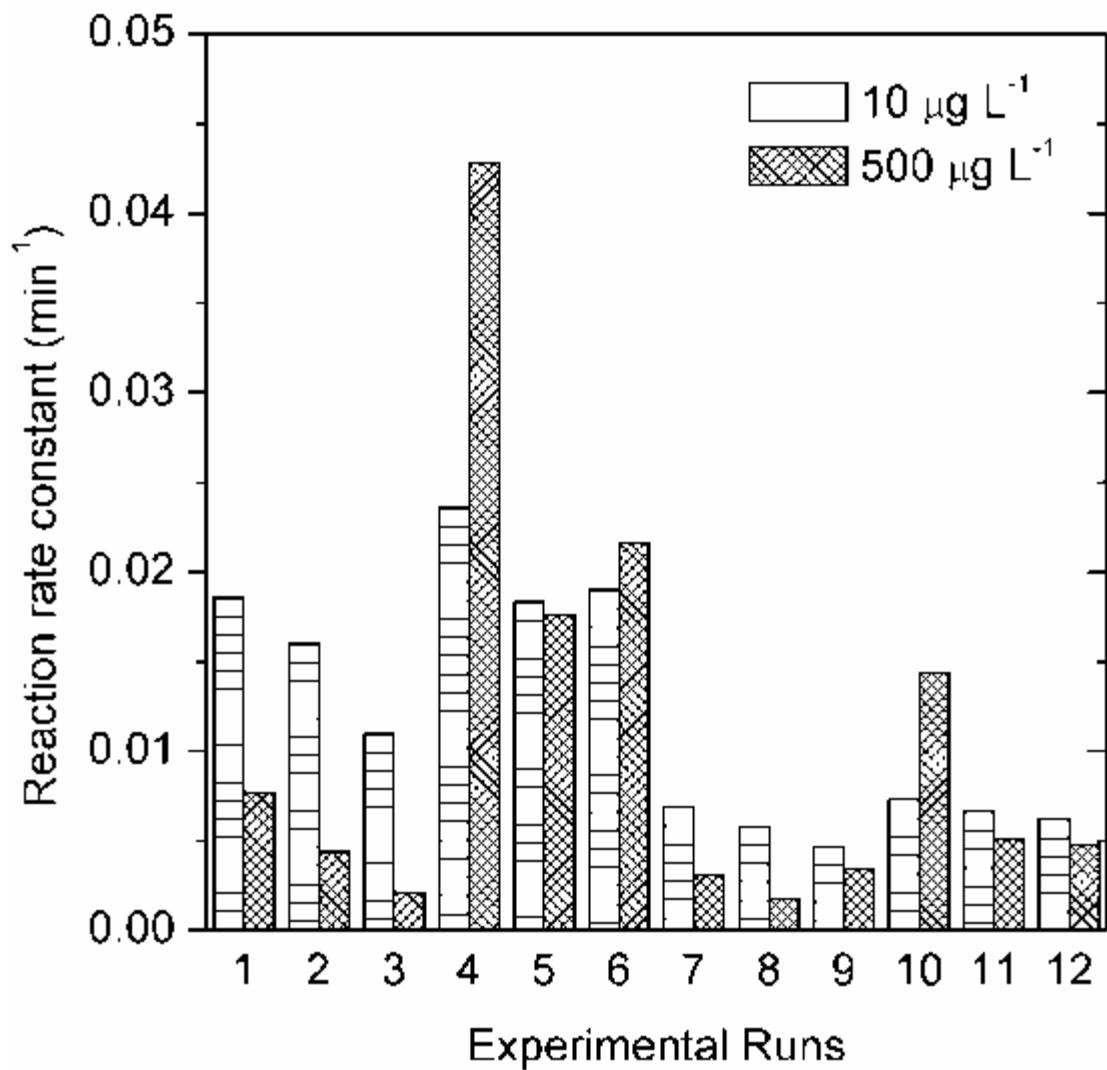


Figure 4.8 Reaction rate constants at different initial concentrations (run numbers refer to Table 4.1)

4.4 Summary

Marine oil pollution caused by operational wastewater discharges has been recognized as a challenging issue. More research efforts are demanded to develop effective treatment methods for removal of dissolved organic compounds particularly including polycyclic aromatic hydrocarbons (PAHs) and to understand the associated mechanisms. This study targeted UV irradiation of a typical PAH, namely naphthalene in seawater, and examined the degradation kinetics. The efficiency of UV treatment was tested under varying ambient conditions including salinity, UV fluence rate, initial concentration and temperature. A full factorial design of experiments (DOE) was employed to determine the significance of each factor being tested as well as their interactions.

The results showed that the removal of naphthalene followed first order kinetics in all experimental runs and the most influential factors were fluence rate, temperature and the interaction between temperature and initial concentration. A mathematical equation was obtained to describe the photodegradation process with the adjusted and predicted R^2 values of 0.87 and 0.80, respectively. A linear relationship between the number of UV lamps and the mean fluence rate was established with a R^2 value of 0.99. Further analysis revealed that the reaction rate constants were linearly related to the number of lamps. High photon flux can greatly elevate the probability of collision between active centers and photons and therefore can generate more free radicals to promote the photoreactions. High salinity suppressed the performance of UV irradiation which was mainly caused by the presence of bromide (Br^-), carbonate (CO_3^{2-}) and bicarbonate (HCO_3^-) ions in seawater. The existence of nitrate (NO_3^-) may also interfere with the photodegradation

process and thus deserves more research attention. These radical scavengers became more abundant at higher salinity levels due to increasing pH. In addition, increasing temperature from 23 to 40 °C seemed to stimulate the removal of naphthalene in seawater by exciting the collision between photons and molecules. A particular activation energy value was determined as 10.67 kJ mol⁻¹, which was about half of that in the distilled water with heterogeneous catalyst. This difference implied that, for the purpose of removing naphthalene, increasing temperature in seawater would not be as sensitive as that in distilled water. The effect of initial concentration was not prominent while the average reaction rate constant at high concentration was slightly lower than that at low concentration. In addition, the toxicity of the associated photoproducts in the marine environment may be a topic for future research.

The results from this study are expected to not only help understand the photolysis mechanism of PAHs but provide a good example to develop the integrated process control and operation planning system for marine oily wastewater management. The successful development of such a decision support system can be applied to many other wastewater treatment techniques such as ozone, photocatalysis, and membrane.

CHAPTER 5

SIMULATION OF THE TREATMENT OF MARINE OILY WASTEWATER USING UV IRRADIATION

This chapter is based on and expanded from the following paper:

Jing, L., Chen, B., and Zhang, B.Y. (2014). Modeling of UV-induced photodegradation of naphthalene in marine oily wastewater by artificial neural networks. *Water, Air, & Soil Pollution*, 225(4), 1-14, doi:10.1007/s11270-014-1906-0.

Role: Liang Jing solely worked on this study and acted as the first author of this manuscript under Dr. Bing Chen and Dr. Baiyu Zhang's guidance. Most contents of this paper was written by Liang and further polished by the other co-authors.

5.1 Background

To comply with the growingly stringent regulations on the discharge of marine oily wastewater, effective treatment must be carried out prior to discharge or disposal. Physical treatment methods (e.g., gravity separation and hydrocyclone) are commonly used in practice (Fakhru'l-Razi et al., 2009; Tony et al., 2012). While most dispersed free oil can be removed, many dissolved organic compounds, particularly polycyclic aromatic hydrocarbons (PAHs), are unlikely to be affected. UV irradiation and advanced oxidation techniques have been recently regarded as promising solutions to the removal of PAHs. As with most traditional treatment systems, the knowledge and prediction of dynamic responses to the variations of environmental conditions and operational factors are critical to ensure an optimal operation of the advanced oxidation processes. A clear understanding of the process mechanism will help to qualify the direct relationships among the inputs and outputs and the indirect relationship such as the time series correlation. However, the research efforts on numerical modeling and performance optimization have been limited due to their multiphysics nature and the complexity of synergistic effects. To help understand the mechanisms, simulate the process, predict the behaviour, and eventually wisely control the process, modeling methods have been recognized as an essential component and foundation for any successful process control strategies.

Due to the complexity of marine oily wastewater, many traditional chemical reaction models have difficulties in simulating the photochemical reactions within the marine environment (Nandi et al., 2010; Pendashteh et al., 2011). Artificial neural networks (ANNs), on the other hand, can effectively recognize and reproduce cause-effect

relationships for a complex system. Not only can the ANNs learn to respond to varying inputs, they are strongly capable of implementing nonlinear functions by allowing a uniform approximation of any continuous function. Therefore, this chapter presents a simulation model for the removal of PAHs by using ANN method. The UV experimental results obtained in Chapter 4 are used as an example for developing the ANN model.

5.2 Methodology

5.2.1 Experimental

The experiments results used in this chapter are based on Chapter 4. See Section 4.2 for details.

5.2.2 Model Inputs

As the removal rate at the beginning of the photodegradation process is always zero, the first time point (time = 0) was not included in the experimental design. This full factorial DOE (Table 5.1) was introduced in Chapter 4 and the corresponding results were used for developing the proposed ANN model.

5.2.3 Artificial Neural Networks (ANNs)

ANNs are known for their ability of simulating and predicting a complex pattern correctly by learning the relationships between inputs and outputs. The rule of thumb in successfully getting a reliable network largely relies on the selection of process variables, network structure and the available datasets for training purposes. A typical ANN is usually comprised of numerous individual processing units (i.e., neurons) that are

grouped in an input layer (independent variables), an output layer (dependent variables) and at least one hidden layer. It is worth mention that most ANNs are based on one hidden layer because the universal approximation theory suggests that one hidden layer with sufficient neurons can interpret any input-output patterns (Aleboyeh et al., 2008). Each neuron is interconnected with the ones on the preceding and succeeding layers by parallel rather than sequential mathematical transformation equations that contain adjustable weights and biases (e.g., linear, log-sigmoid and hyperbolic tangent-sigmoid).

The numbers of input and output neurons stand for the number of input variables used in prediction and output variables to be predicted, respectively, whereas the neurons contained in the hidden layer are used as feature detectors to encode the inputs. If there are fewer neurons in the hidden layer, the convergence rate of the network may be affected. On the other hand, too many neurons may result in complicated network topology, training frequency increasing, over-fitting of the model and generalization reduction. Therefore, the number of neurons in the hidden layer is one of the key factors that may significantly influence the accuracy of the network.

The weighted sum of the inputs is transferred to each hidden neuron by activation functions, and then undergoes another weighted sum transformation to get the outputs. In this study, a multilayer feed-forward ANN with one hidden layer was trained by the backpropagation algorithm to predict the photochemical removal of naphthalene from oily seawater. The transfer functions used at the hidden and output layers were log-sigmoid (logsig) and linear (purelin), respectively, given that the experimental results were described in removal efficiency, which ranges from 0 to 100% and fits well with the logsig function (Zhang et al., 2013; Abushammala et al., 2013).

Table 5.1 Mixed level full factorial DOE for ANN model development

| Variable | Levels | Unit | Values | | | | | | | |
|-----------------------|--------|----------------------|--------|------|----|-----|-----|-----|-----|-----|
| Initial Concentration | 2 | $\mu\text{g L}^{-1}$ | 10 | 500 | - | - | - | - | - | - |
| Salinity | 3 | ppt | 25 | 32.5 | 40 | - | - | - | - | - |
| Fluence rate | 2 | mw cm^{-2} | 2.88 | 8.27 | - | - | - | - | - | - |
| Temperature | 2 | $^{\circ}\text{C}$ | 23 | 40 | - | - | - | - | - | - |
| Time | 8 | min | 30 | 60 | 90 | 120 | 150 | 180 | 210 | 240 |

Neural network toolbox V6.0 of MATLAB software was used. Datasets (192 in total) were obtained from our previous study (Jing et al., 2013a) and were randomly divided into training (60%, 116 datasets), validation (20%, 38 datasets), and testing (20%, 38 datasets) subsets (see **Appendix A**). Training is the process in which the network adjusts the weights and biases to fit the input-output relation according to its error. Validation is used to measure network generalization and to halt training when generalization stops improving, whereas testing serves as an independent measure of network performance and has no influence on training. The input variables were fluence rate, salinity, temperature, initial concentration and reaction time. The output variable was naphthalene removal rate at a given time point. All input variables were normalized by rescaling their ranges of variation within the 0–1 range (Equation 5.1).

$$x_i = \frac{X_i - X_{\min}}{X_{\max} - X_{\min}} \quad (5.1)$$

where X is the original data; X_{\min} and X_{\max} are the minimum and maximum values of X , respectively; and x is the unified data of X .

The significance of each input variable concerning the model output was assessed using two sensitivity analysis techniques. The first one, proposed by Garson (1991), assesses the contributions based on the neural net weight matrix.

$$I_j = \frac{\sum_{m=1}^{N_h} \left(\left(\frac{|W_{jm}^{ih}|}{\sum_{k=1}^{N_i} |W_{km}^{ih}|} \right) \times |W_{mn}^{ho}| \right)}{\sum_{k=1}^{N_i} \left\{ \sum_{m=1}^{N_h} \left(\left(\frac{|W_{jm}^{ih}|}{\sum_{k=1}^{N_i} |W_{km}^{ih}|} \right) \times |W_{mn}^{ho}| \right) \right\}} \quad (5.2)$$

where I_j is the relative significance of the j^{th} input variable on the output variable; N_i and N_h are the number of input and hidden neurons, respectively; W are the connection

weights between layers; i , h and o refer to input, hidden and output layers, respectively; k , m and n refer to input, hidden and output neurons, respectively. The other technique is to examine the performance of all possible combinations of input variables such that the contributions from single and multiple variables can be investigated.

5.2.4 Analysis of Variance (ANOVA)

Data from the mixed level full factorial design experiments were subjected to ANOVA in order to not only evaluate the effect of each input variable as well as their interactions, but also to verify if the optimized weights can well illustrate the importance of each variable. ANOVA tests the null hypothesis that the contributions from each input variable to the output are equal, versus them not being equal. A probability of p less than 0.05 indicates that the variable has a significant effect.

5.2.5 Verification of the ANN Model

As the ANN model was trained based on the full factorial design experiments (Table 5.1), another three experimental tests (Table 5.2) were performed and compared with the prediction using the developed model. It can be seen that at least one variable had different values other than the full factorial design in order to test the generalizability of the ANN model. The supplementary experimental results were used to validate if the developed model can well predict the photolysis process with inputs values that are different from the training set. All the experimental procedures and analytical methods were the same as described in Sections 5.2 and 5.3.

Table 5.2 Conditions of the supplementary experimental tests for ANN model verification

| Tests | Initial concentration ($\mu\text{g L}^{-1}$) | Salinity (ppt) | Fluence rate (mw cm^{-2}) | Temperature ($^{\circ}\text{C}$) | Reaction time (min) |
|-------|---|-------------------|---|---------------------------------------|------------------------|
| E-1 | 10 | 25 | 5.65 | 23 | 240 |
| E-2 | 10 | 40 | 5.65 | 23 | 240 |
| E-3 | 300 | 25 | 8.27 | 23 | 240 |

5.3 Results and Discussion

5.3.1 ANN Modeling

The topology of an ANN is usually determined by the number of hidden layers, the number of neurons contained in the hidden layers and the nature of the transfer functions. In this study, one hidden layer along with the backpropagation algorithm was selected for the proposed ANN model. Therefore, the specific backpropagation algorithm and the number of hidden neurons needed to be optimized.

5.3.1.1 Selection of backpropagation training algorithm

Mean square error (MSE) measures the performance of an ANN based on the deviations between network predictions and experimental responses. The training, validation and testing subsets would have different MSE performance. In this study, the minimum value of the MSE of the training and testing subsets (MSE_{t-t}) was adopted to examine thirteen backpropagation algorithms (Yetilmezsoy and Demirel, 2008; Elmolla et al., 2010). Ten neurons were used in the hidden layer while the transfer functions were log-sigmoid (logsig) and linear (purelin) at the hidden and output layers, respectively. The maximum epoch number was set as 100. The comparison among different algorithms was summarized in Table 5.3. It was observed that the Levenberg-Marquardt backpropagation algorithm was able to produce the least MSE_{t-t} and hence was preferred over the others.

5.3.1.2 Optimization of the number of hidden neurons

The number of neurons in the hidden layer can drastically affect network convergence and prediction accuracy. If the architecture is too simple, the trained network

may not have sufficient ability to learn the process correctly; however, a complicated architecture may fail to converge properly due to the over fitted training data. The optimal number of neurons, therefore, was determined by using the trial-and-error procedure based on MSE_{t-t} . Each topology was repeated five times and averaged to avoid random correlation due to the random initialization of the weights. Figure 5.1 shows the impact of the number of neurons in the hidden layer on the network performance. It could be seen that the MSE_{t-t} reached the minimum value at 12 neurons and became stabilized thereafter. Hence, the optimized neural network structure was derived as shown in Figure 5.2.

Table 5.3 Comparison of backpropagation algorithms with 10 neurons in the hidden layer

| Backpropagation algorithm | Function | MSE _{t-t} | Epoch | Overall R^2 |
|--|----------|--------------------|-------|---------------|
| Levenberg-Marquardt | trainlm | 0.0060 | 10 | 0.910 |
| BFGS Quasi-Newton | trainbfg | 0.0089 | 6 | 0.848 |
| Scaled conjugate gradient | trainscg | 0.0118 | 12 | 0.845 |
| Random order weight/bias learning rules | trainr | 0.0936 | 100 | 0.746 |
| Rpop | trainrp | 0.0090 | 35 | 0.877 |
| Gradient descent (GD) | traingd | 0.0231 | 100 | 0.704 |
| GD with adaptive learning rate | traingda | 0.0291 | 100 | 0.673 |
| GD with momentum | traingdm | 0.0630 | 100 | 0.597 |
| GD with momentum and adaptive learning rate | traingdx | 0.0252 | 100 | 0.707 |
| One step secant | trainoss | 0.0195 | 10 | 0.780 |
| Conjugate gradient with Beale-Powell restarts | traingb | 0.0087 | 7 | 0.870 |
| Conjugate gradient with Fletcher-Reeves restarts | traingf | 0.0096 | 8 | 0.860 |
| Conjugate gradient with Polak-Ribiere restarts | traingp | 0.0080 | 6 | 0.864 |

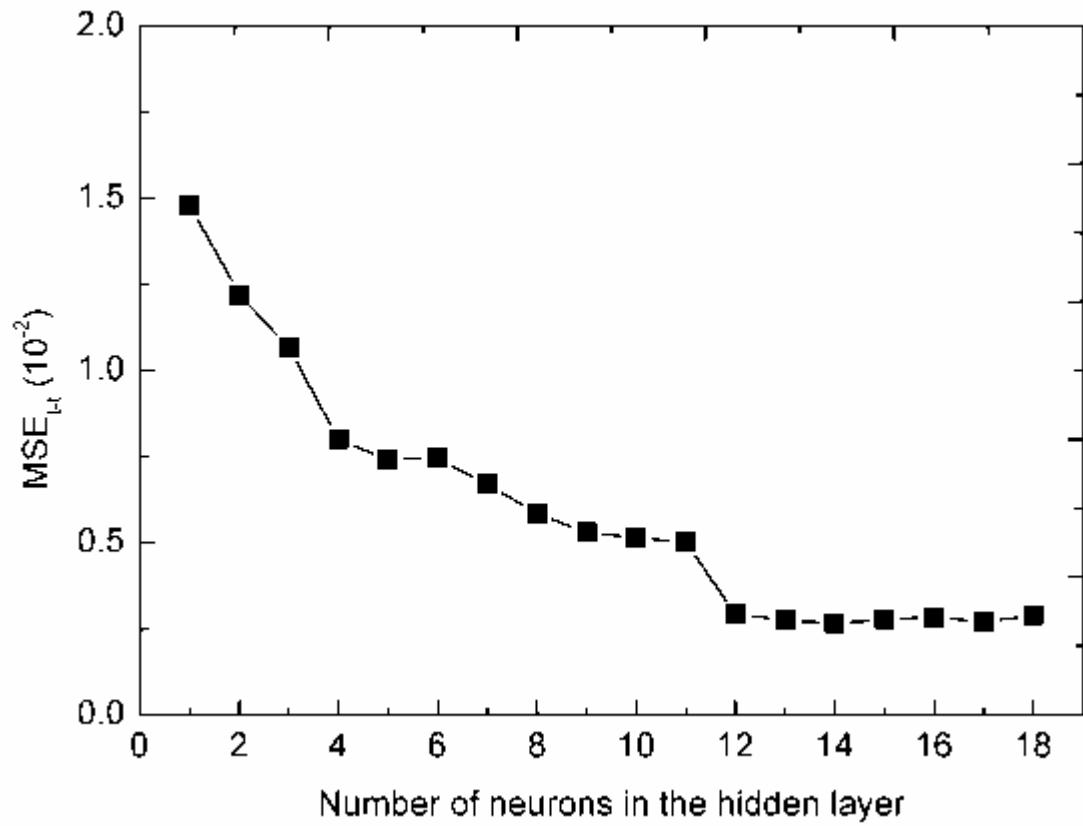


Figure 5.1 Relationship between the number of hidden neurons and MSE_{t-t}

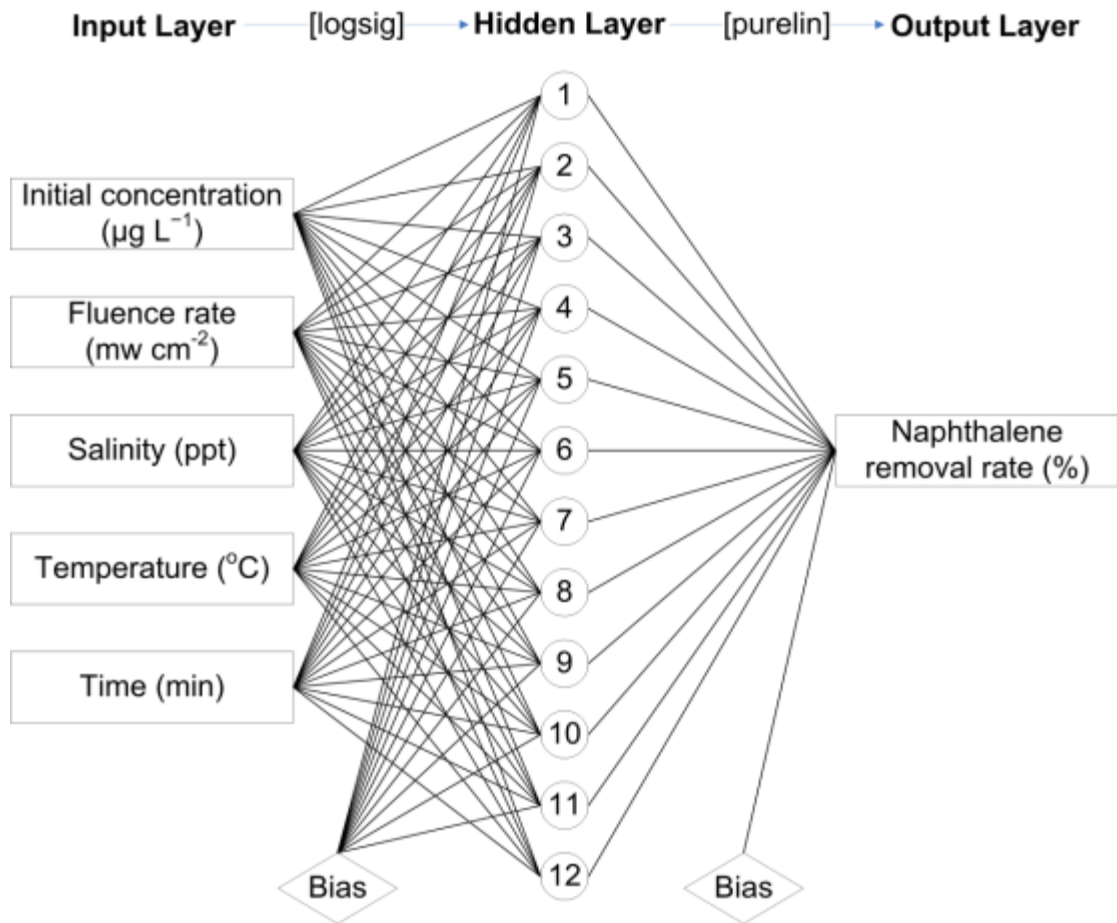


Figure 5.2 Optimized structure of the developed ANN model

5.3.1.3 Training, validation and testing of the model

The datasets were divided into three subsets including training (60%), validation (20%) and testing (20%) for model development. An inverse range scaling was performed on the modeling outputs for comparison purposes. The network was trained to provide a MSE of 0.00181 and a reasonable linear fit (correlation of determination $R^2 = 0.984$) for the training subset (Figure 5.3a). The modeled removal rates were also close to the measured ones for the validation and testing subsets (Figures 5.3b and 5.3c). The overall best linear fit equation had a slope of 0.97 (Figure 5.3d), which was remarkably close to the best linear fit (modeled = measured), an intercept of 1.3 and a R^2 of 0.943. These linear fits indicated that the developed ANN model was able to accurately simulate the naphthalene removal process and reproduce the experimental results.

5.3.1.4 Sensitivity analysis

Based on Garson equation (Equation 5.2), the detailed connection weights trained by the proposed ANN model are shown in Table 5.4. Table 5.5 shows the relative importance of the each input variable obtained by using Equation 5.2. Fluence rate was ranked with the highest contribution and therefore appeared to be the most influential variables, followed by temperature, reaction time, salinity and initial concentration. The relatively low importance of salinity indicates that the removal of naphthalene using UV irradiation is likely to be effective for a wide range of seawater salinities.

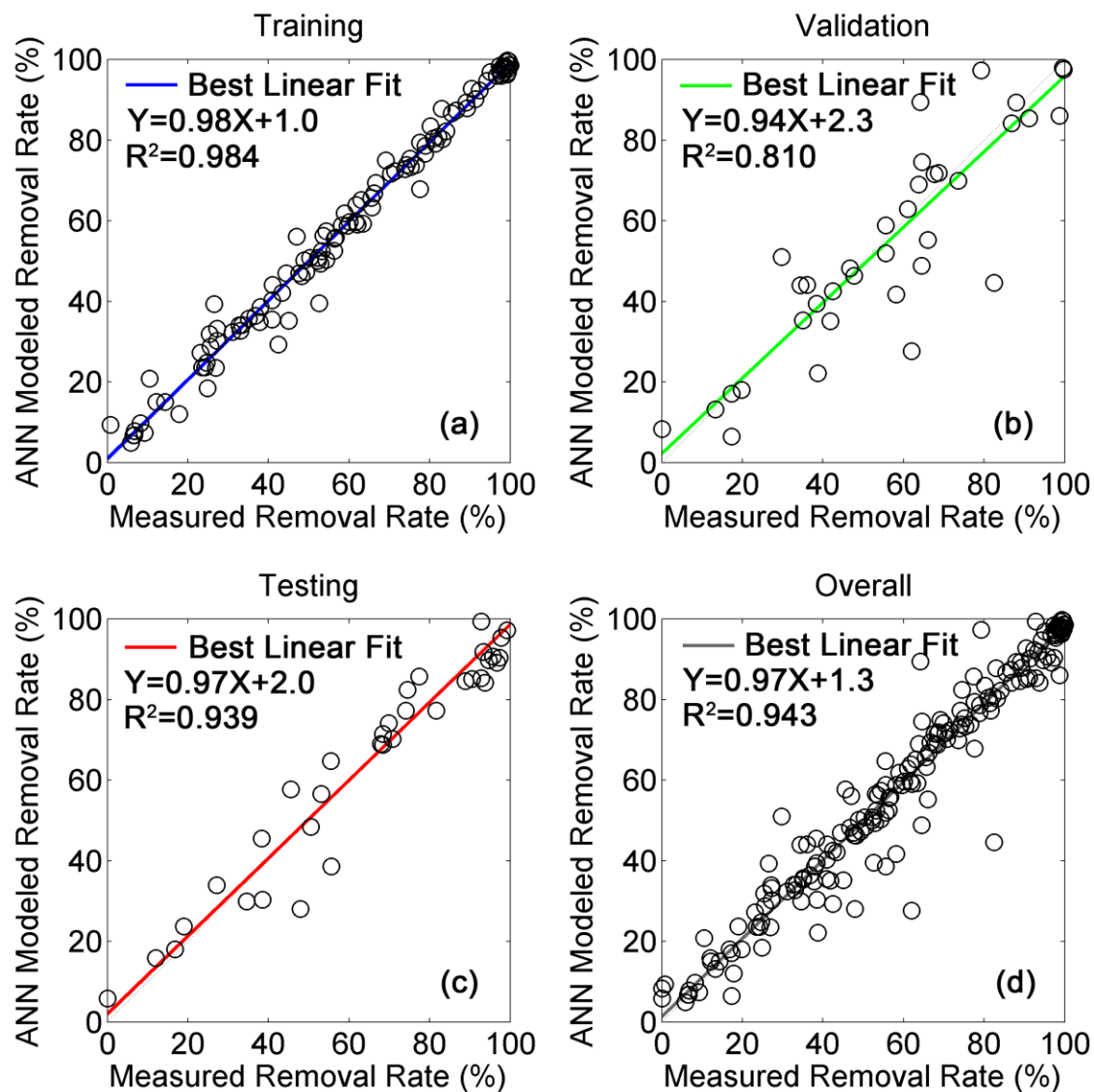


Figure 5.3 Comparison between ANN modeled and experimentally measured values of naphthalene removal rate for the (a) training, (b) validation, (c) testing and (d) overall datasets

According to the second sensitivity technique (Section 5.2.3), groups of one, two, three, four and five variables were examined by using the optimized ANN structure with 12 hidden neurons and the Levenberg-Marquardt backpropagation algorithm. MSE_{t-t} was chosen as the performance indicator such that lower values led to greater importance. As shown in Table 5.6, X_1 to X_5 stand for initial concentration, salinity, fluence rate, temperature and reaction time, respectively. In the group of one variable, fluence rate (X_3) was marked as the most contributing variable with a MSE_{t-t} of 0.0504 and an overall R^2 of 0.295. The MSE_{t-t} for two variables reached its minimum (0.0421) when both fluence rate (X_3) and temperature (X_4) were included, implying that temperature was the second most influential variable. The MSE_{t-t} continued decreasing to 0.0129, which was the minimum value of the group of three variables when reaction time (X_5) was used in combination with fluence rate (X_3) and temperature (X_4). Salinity (X_2) appeared to be the fourth important variable because its combination with fluence rate (X_3), temperature (X_4) and reaction time (X_5) had the lowest MSE_{t-t} (0.0099) in the four-variable group. When all variables including initial concentration (X_1) were used, the MSE_{t-t} decreased to 0.0025 with an overall R^2 of 0.956. Therefore, the order of variable importance (from high to low) supported by such analysis was fluence rate (X_3), temperature (X_4), reaction time (X_5), salinity (X_2) and initial concentration (X_1) which was in good agreement with the sensitivity analysis results using Garson equation (Equation 5.2).

Table 5.4 Weights between the input and output layers (W1), weights between the hidden and output layers (W2) and biases

| Neuron | W1 | | | | | | W2 | |
|--------|-----------------------|----------|--------------|-------------|---------|---------|--------------------------|---------|
| | Input variables | | | | | | Output variable | |
| | Initial Concentration | Salinity | Fluence rate | Temperature | Time | Bias | Naphthalene removal rate | Bias |
| 1 | 0.6508 | -0.7993 | 3.3177 | -1.4368 | 5.3337 | -5.6172 | -0.1511 | -1.4740 |
| 2 | -5.6207 | -3.4670 | -1.6087 | 3.7399 | -3.4642 | -3.1491 | -0.1832 | |
| 3 | 0.5361 | 0.2351 | -3.0628 | -0.3039 | 0.0621 | -4.8635 | -3.0120 | |
| 4 | 3.8022 | -1.4287 | 3.0374 | 5.2788 | -3.8535 | -0.9152 | 0.5644 | |
| 5 | 5.3680 | 2.0948 | -5.3111 | 0.7650 | -0.0967 | -1.7854 | 0.5900 | |
| 6 | -4.1609 | -1.4316 | 3.0062 | 4.1801 | 4.5628 | 0.5939 | 0.5960 | |
| 7 | 0.3029 | -1.7911 | 2.0615 | 3.3788 | 4.7574 | -1.1175 | 0.5851 | |
| 8 | 0.6302 | 0.8824 | -1.0961 | 4.8385 | -5.6007 | 1.4117 | -0.7656 | |
| 9 | -0.6757 | 5.0376 | -1.3415 | 4.4204 | 0.8125 | 5.3968 | 1.0464 | |
| 10 | -5.9498 | 4.7941 | -3.5973 | -1.8491 | -1.6449 | 1.9361 | 0.6422 | |
| 11 | 0.1282 | -5.6630 | 0.5007 | -2.5575 | -0.5933 | -3.8886 | 1.1350 | |
| 12 | -1.0131 | -0.6212 | -0.5046 | 1.3646 | -3.1814 | -5.5641 | -1.6380 | |

Table 5.5 Relative importance of input variables on the removal of naphthalene

| <u>Input Variable</u> | <u>Importance (%)</u> |
|-----------------------|-----------------------|
| Initial Concentration | 14.1 |
| Salinity | 18.0 |
| Fluence rate | 30.1 |
| Temperature | 19.7 |
| Time | 18.1 |
| Total | 100 |

Table 5.6 Evaluation of possible combinations of input variables

| Combination | MSE _{t-t} | Epoch | Overall R ² |
|--|--------------------|-------|------------------------|
| X ₁ | 0.0788 | 3 | 0.039 |
| X ₂ | 0.0849 | 3 | 0.027 |
| X ₃ * | 0.0504 | 4 | 0.295 |
| X ₄ | 0.0634 | 3 | 0.122 |
| X ₅ | 0.0565 | 3 | 0.365 |
| X ₁ +X ₂ | 0.0784 | 4 | 0.064 |
| X ₁ +X ₃ | 0.0465 | 3 | 0.330 |
| X ₁ +X ₄ | 0.0689 | 3 | 0.184 |
| X ₁ +X ₅ | 0.0549 | 9 | 0.395 |
| X ₂ +X ₃ | 0.0510 | 4 | 0.312 |
| X ₂ +X ₄ | 0.0763 | 3 | 0.148 |
| X ₂ +X ₅ | 0.0550 | 7 | 0.366 |
| X ₃ +X ₄ * | 0.0421 | 3 | 0.415 |
| X ₃ +X ₅ | 0.0493 | 8 | 0.594 |
| X ₄ +X ₅ | 0.0512 | 8 | 0.481 |
| X ₁ +X ₂ +X ₃ | 0.0464 | 5 | 0.364 |
| X ₁ +X ₂ +X ₄ | 0.0534 | 5 | 0.218 |
| X ₁ +X ₂ +X ₅ | 0.0392 | 9 | 0.367 |
| X ₁ +X ₃ +X ₄ | 0.0452 | 4 | 0.484 |
| X ₁ +X ₃ +X ₅ | 0.0228 | 9 | 0.702 |
| X ₁ +X ₄ +X ₅ | 0.0348 | 12 | 0.523 |
| X ₂ +X ₃ +X ₄ | 0.0545 | 12 | 0.407 |
| X ₂ +X ₃ +X ₅ | 0.0369 | 10 | 0.637 |
| X ₂ +X ₄ +X ₅ | 0.0344 | 14 | 0.503 |
| X ₃ +X ₄ +X ₅ * | 0.0129 | 11 | 0.776 |
| X ₁ +X ₂ +X ₃ +X ₄ | 0.0358 | 8 | 0.490 |
| X ₁ +X ₂ +X ₃ +X ₅ | 0.0155 | 16 | 0.731 |
| X ₁ +X ₂ +X ₄ +X ₅ | 0.0252 | 12 | 0.550 |
| X ₁ +X ₃ +X ₄ +X ₅ | 0.0153 | 12 | 0.869 |
| X ₂ +X ₃ +X ₄ +X ₅ * | 0.0099 | 12 | 0.821 |
| X ₁ +X ₂ +X ₃ +X ₄ +X ₅ * | 0.0025 | 12 | 0.956 |

Note: * indicates the best group performance

5.3.2 ANOVA

ANOVA was performed in this study to validate the developed ANN model by examining the importance of each input variable and their interactions. After a pre-analysis of the collected information, the Box-Cox (B-C) plot for power transforms suggested that no transformation was recommended to better normalize the data points. Results from ANOVA on the response model were summarized in Table 5.7. From the Fisher's F -test, factorial effects with p -values less than 0.05 (5% level of significance) were considered significant. Therefore, all individual input variables had significant contribution to the removal of naphthalene. The higher the F -values are, the higher the significance of the variables or their interactions. It can be seen that fluence rate seemed to dominate the removal process because its F -value was considerably higher than the others. Temperature appeared to be the second most influential variable, followed by reaction time, initial concentration and salinity, which were ranked as the third, fourth and fifth, respectively. These findings were in good accordance with the sensitivity analyses of the developed ANN model. In addition, ANOVA was able to identify some prominent interactions between different variables such as the synergetic effect between temperature and initial concentration (Jing et al., 2013a).

Table 5.7 ANOVA for square root transformed response of naphthalene photodegradation

| Source | Sum of squares | df | Mean squares | F-value | p-value, Prob > F |
|---------------------------------------|----------------|-----|--------------|---------|---------------------|
| Model | 142000 | 13 | 10919.87 | 113.26 | <0.0001 significant |
| X ₁ -initial concentration | 6200.91 | 1 | 6200.91 | 64.32 | <0.0001 |
| X ₂ -salinity | 5032.62 | 2 | 2516.31 | 26.10 | <0.0001 |
| X ₃ -fluence rate | 46871.06 | 1 | 46871.06 | 486.15 | <0.0001 |
| X ₄ -temperature | 19411.78 | 1 | 19411.78 | 201.34 | <0.0001 |
| X ₅ -time | 59020.07 | 7 | 8431.44 | 87.45 | <0.0001 |
| X ₁ X ₄ | 5421.84 | 1 | 5421.84 | 56.24 | <0.0001 |
| Residual | 17161.60 | 178 | 96.41 | | |
| Total | 159100 | 191 | | | |

5.3.3 ANN Model Verification

To better evaluate the generalizability of the developed ANN model, supplementary experimental tests were conducted by using experimental settings that were different from the ones used in the model development process (Tables 5.1 and 5.2). The detailed settings were used as input for the ANN model while the prediction outputs were compared with the experimental results. The higher the R^2 value, the better goodness of fit of the prediction, in other words, the better generalizability of the model. Figures 5.4a-5.4c show such comparison between the predicted and experimental removal rates. It can be noted that the prediction plots agree well with the experimental plots. Figure 5.4d plots the line that best fits the data of the scatter plot with a slope of 0.83, an intercept of 14.1 and a R^2 of 0.876, suggesting that the developed ANN model is capable of predicting the removal of naphthalene with acceptable accuracy.

5.3.4 Effect of Input Variables

As shown in Figure 5.5, when other experimental conditions were fixed at initial concentration $10 \mu\text{g L}^{-1}$, salinity 32.5 ppt and temperature $40 \text{ }^\circ\text{C}$, the removal process of using six lamps (8.27 mW cm^{-2}) was much quicker than using two lamps (2.88 mW cm^{-2}). This difference was equally prominent for both experimental and simulation results as they were closely related. By plotting log of experimental removal rates against degradation time, the first order reaction rate constant of six lamps (0.0183 min^{-1}) was approximately as much as three times higher than that of two lamps (0.0066 min^{-1}). These observations may be attributed to the fact that high fluence rate can increase the probability for collision between active centers and subsequently produce more highly

oxidative radicals (e.g., OH \cdot) to promote the photodegradation process.

Temperature is one of the most decisive factors in most photochemical reactions. The increase of temperature was able to considerably accelerate the removal of naphthalene. Figure 5.6 shows a comparison between the predicted and experimental values of naphthalene removal rate at 23 and 40 °C while other conditions were kept as follows: initial concentration 500 $\mu\text{g L}^{-1}$, fluence rate 2.88 mW cm^{-2} and salinity 25 ppt. After 120 min UV exposure, both simulated and experimental removal rates at 23 °C were somewhere around 30%, whereas these numbers were significantly higher at 40 °C (around 60%). After 240 min UV exposure, the removal rates at 40 °C were still drastically higher than those at 23 °C. However, sensitivity analyses of the ANN model revealed that the influence of temperature was not as strong as that of fluence rate. This finding is in accordance with literature that temperature is not the leading driving force to enhance UV-induced photodegradation (Nadal et al., 2006; Lee et al., 2011).

The increase of salinity seemed to moderately suppress the degradation of naphthalene though the tendency was not as distinct as fluence rate and temperature. Figure 5.7 compares the removal process at different salinity levels using both predicted and experimental data. It can be seen that the lines are closely spaced with numerous intersections which admits that the effect of salinity was not significant. Nonetheless, the removal process at 25 ppt was still quicker than those at 32.5 and 40 ppt. This inhibition effect may be caused by the presence of bromide (Br^-), carbonate (CO_3^{2-}) and bicarbonate (HCO_3^-) ions that are strongly capable of scavenging free radicals (e.g., OH \cdot) excited by UV.

Photodegradation was performed at different initial naphthalene concentrations, with

a constant photon flux (2.88 mW cm^{-2}), salinity (32.5 ppt) and temperature ($40 \text{ }^\circ\text{C}$). The effect of initial concentration was not prominent as the removal lines were close to each other (Figure 5.8). Nonetheless, the first order reaction rate constant at $10 \text{ } \mu\text{g L}^{-1}$ (0.0066 min^{-1}) was slightly higher than that at $500 \text{ } \mu\text{g L}^{-1}$ (0.0051 min^{-1}). This observation may be explained by the fact that when the initial concentration of naphthalene was low, the amount of reactive radicals generated from UV irradiation was more than enough to initiate the photoreactions. Contrastingly, when the initial concentration was 50 times higher, using the same amount of radicals may not be sufficient to sustain the reactions at the desired rate. Figure 5.8 demonstrates that the predicted values were in good agreement with the experimental results.

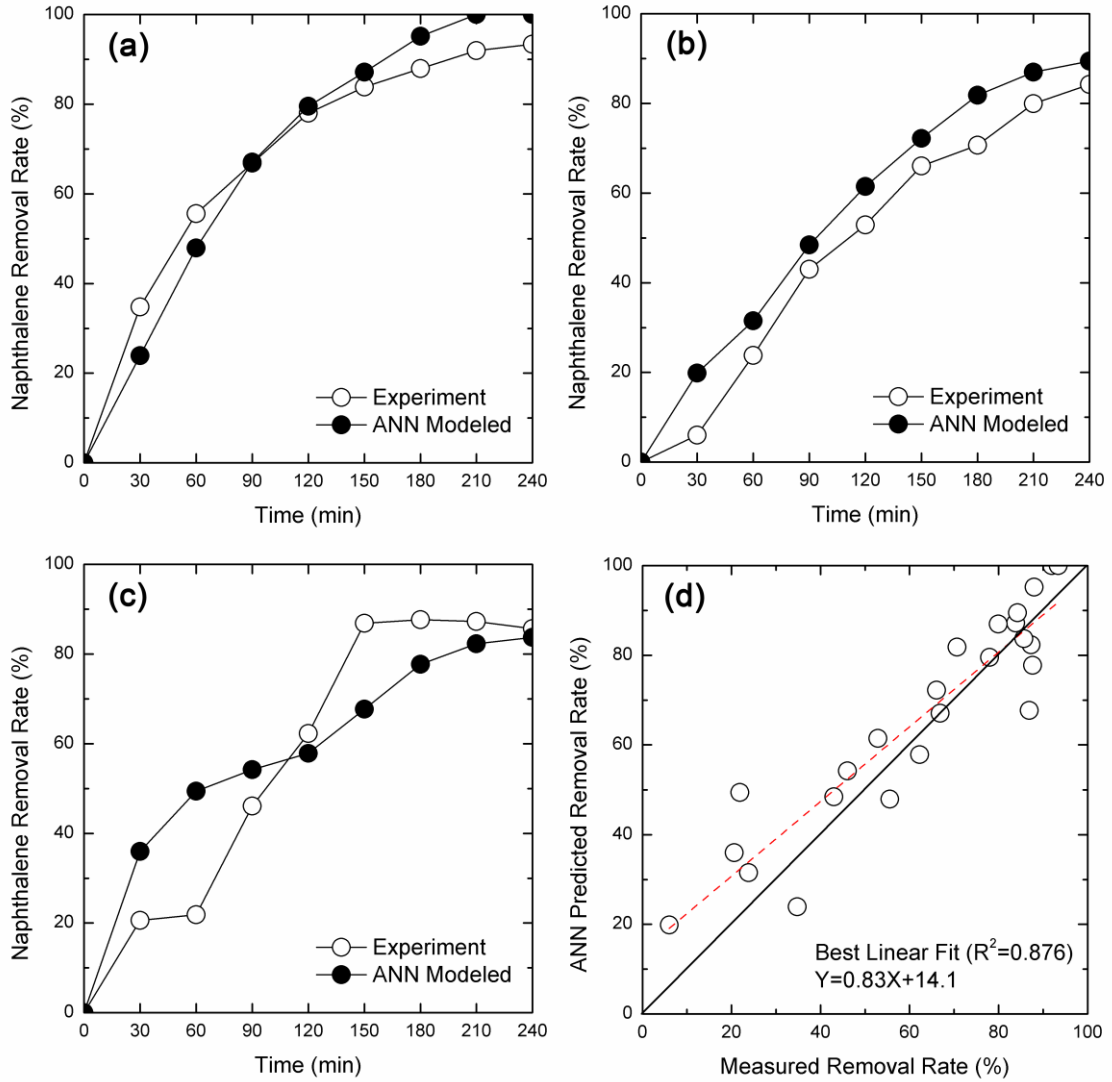


Figure 5.4 Comparison between ANN output and experimental results obtained from supplementary experimental tests (a) E-1, (b) E-2, (c) E-3 and (d) overall tests (see Table 5.1)

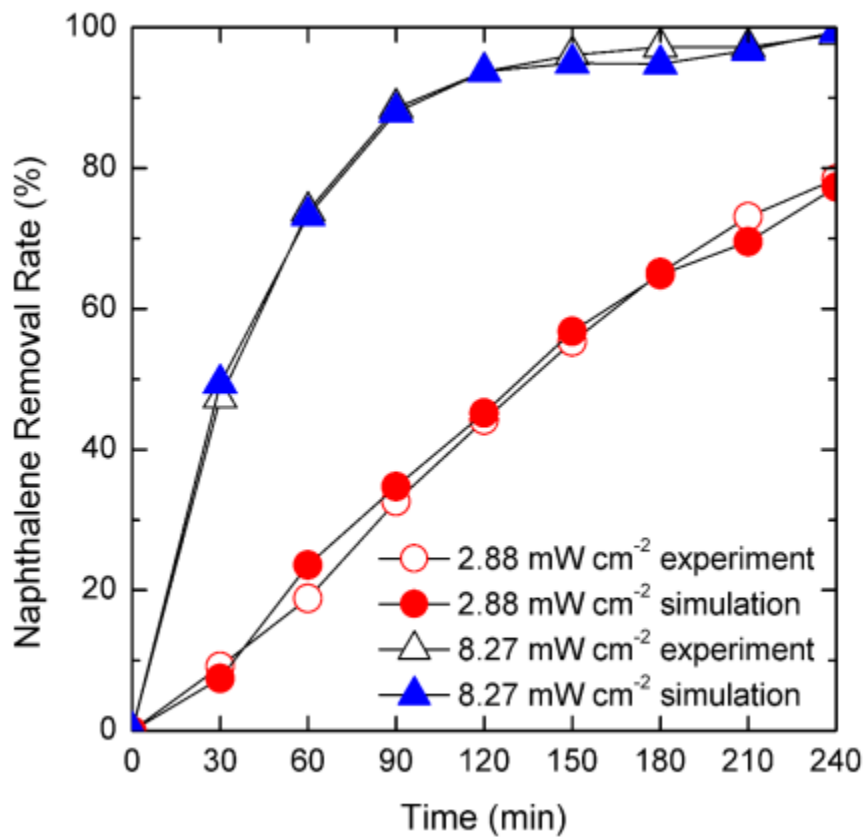


Figure 5.5 Comparison between ANN output and experimental results at different fluence rates (other experimental conditions: 10 $\mu\text{g L}^{-1}$, 32.5 ppt and 40 $^{\circ}\text{C}$)

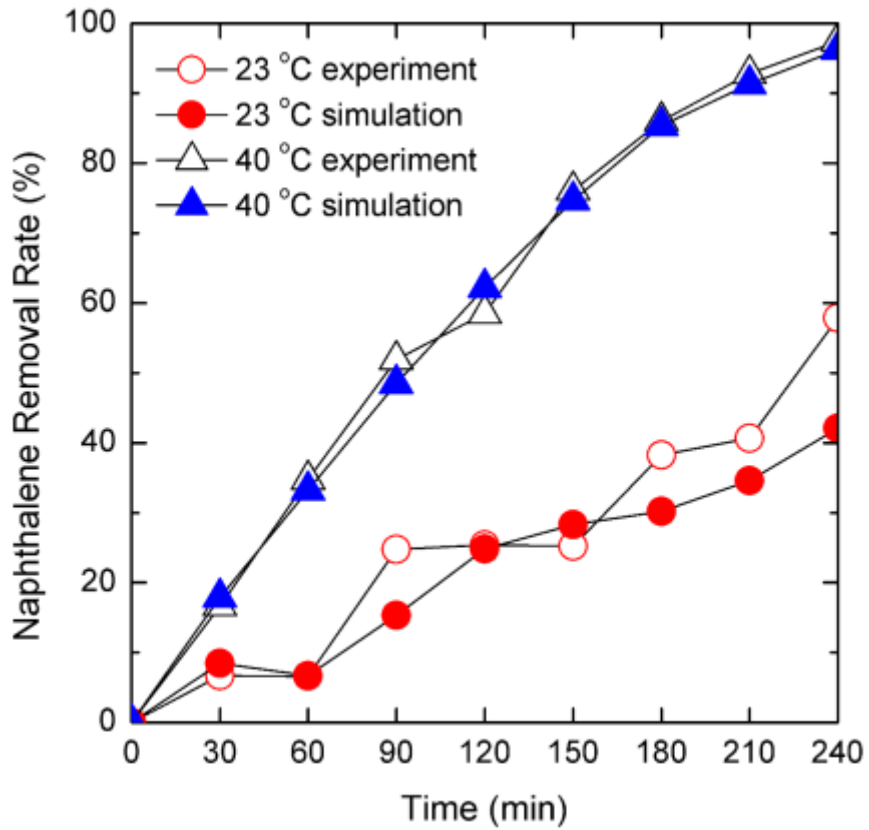


Figure 5.6 Comparison between ANN output and experimental results at different temperatures (other experimental conditions: $500 \mu\text{g L}^{-1}$, 25 ppt and 2.88 mw cm^{-2})

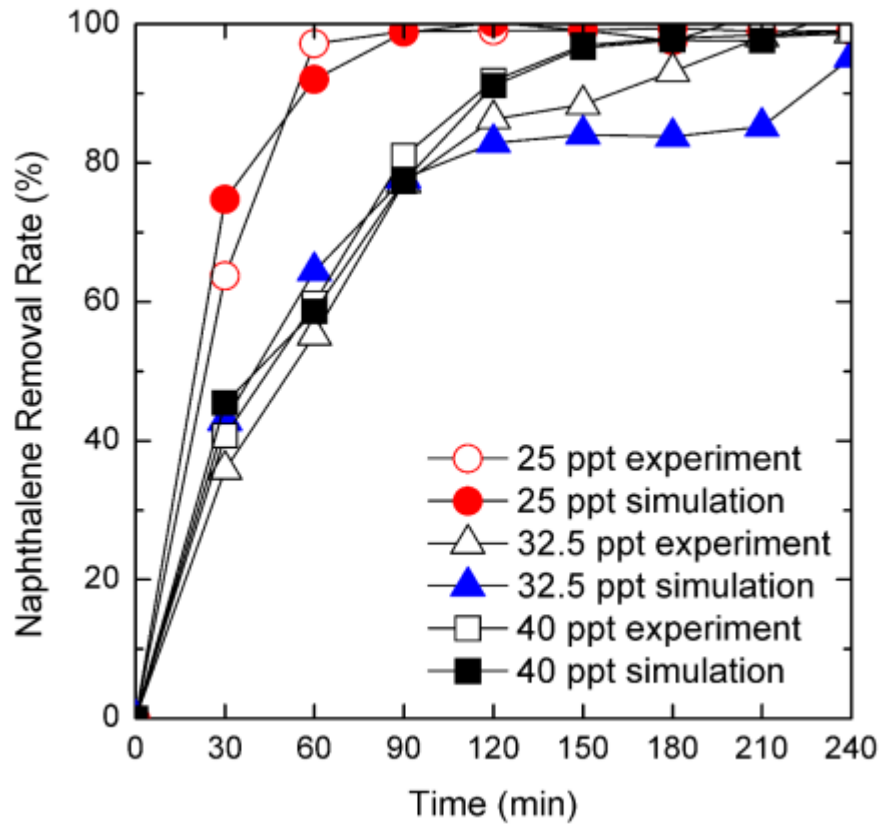


Figure 5.7 Comparison between ANN output and experimental results at different salinity levels (other experimental conditions: $500 \mu\text{g L}^{-1}$, 8.27 mw cm^{-2} and $40 \text{ }^\circ\text{C}$)

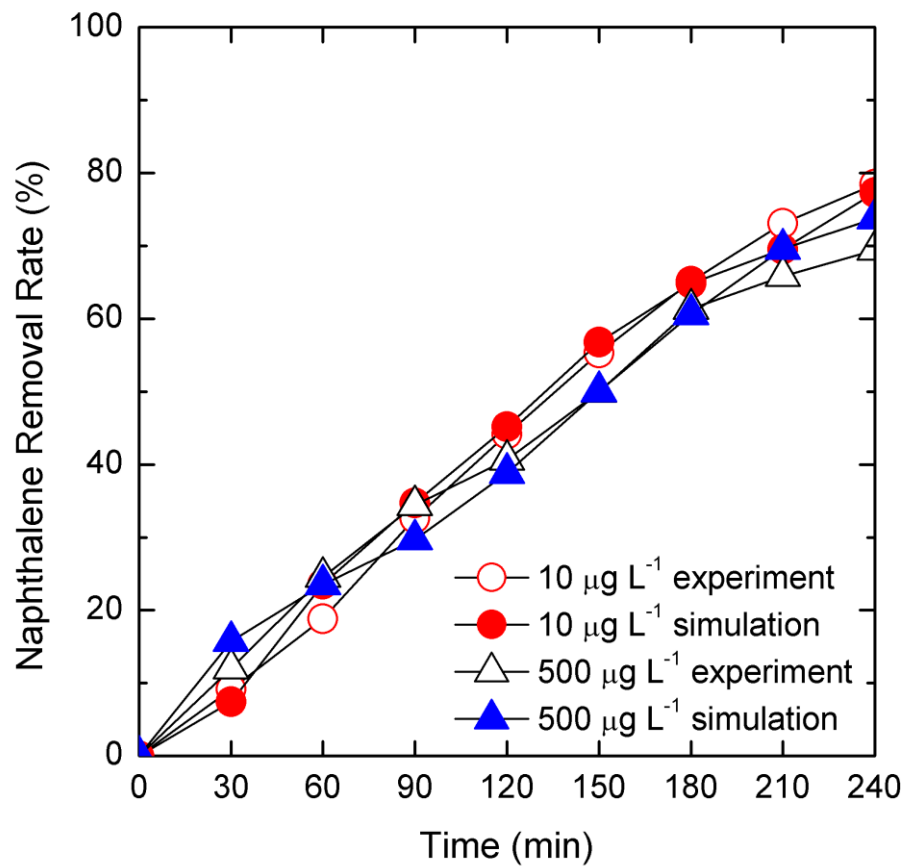


Figure 5.8 Comparison between ANN output and experimental results at different initial concentrations (other experimental conditions: 32.5 ppt, 2.88 mw cm⁻² and 40 °C)

5.4. Summary

A three-layer backpropagation neural network was developed to simulate the UV-induced photodegradation of a typical PAH, naphthalene, in marine oily wastewater. The photochemical process was successfully predicted by using 12 neurons in the hidden layer and the Levenberg-Marquardt backpropagation algorithm. The network was trained to provide a good overall linear fit with a slope of 0.97 and a correlation of determination (R^2) of 0.943. All input variables in this study (i.e., initial concentration, salinity, fluence rate, temperature and reaction time) had considerable effects on the photodegradation process. The outputs of sensitivity analysis and ANOVA revealed that fluence rate and temperature were noted as the most influential variables, which aligned with the experimental observations. The results showed that the developed ANN model was capable of accurately simulating the PAH removal process and reproduce the experiment. ANN modeling technique seemed to be a promising alternative to the traditional reaction models and regression analysis. The developed ANN model will also be coupled with optimization methods in the later chapters to optimally control the treatment process of marine oily wastewater in terms of cost and efficiency.

CHAPTER 6

SIMULATION-BASED DYNAMIC PROCESS CONTROL OF MARINE OILY WASTEWATER TREATMENT

This chapter is based on and expanded from the following paper:

Jing, L., Chen, B., Zhang, B.Y., and Li, P. (2014). Process simulation and dynamic control for marine oily wastewater treatment using UV irradiation. Water Research, under review.

Role: Liang Jing solely worked on this study and acted as the first author of this manuscript under Dr. Bing Chen and Dr. Baiyu Zhang's guidance. Most contents of this paper was written by Liang and further polished by the other co-authors.

6.1 Background

To ensure a sound design and optimal operation of offshore wastewater treatment processes in terms of costs, time and environmental standards, process control techniques are much desired. Recently, the combined use of soft computing (e.g., ANN, ANFIS, and GA) techniques has attracted much attention in optimizing the performance of many industrial processes. Nonetheless, not many studies have taken changing conditions and dynamic system control into account when applying such soft computing tools (Li et al., 2012). The algorithm of dynamic control can be used to rationally make a series of decisions at different time points and to achieve better performance in terms of cost or efficacy. To date, no attempt has been reported to integrate dynamic system control with ANN and GA in order to improve the effectiveness and efficiency of marine oily wastewater treatment. Therefore, the objective of this chapter is to develop an ANN-based dynamic mixed integer nonlinear programming (ANN-DMINP) approach that can help better optimize the performance of wastewater treatment processes by optimally adjusting treatment parameters at given time intervals (e.g., hourly or daily). The removal of naphthalene from oily seawater using UV irradiation, as described in Chapters 4 and 5, is used as a case study to demonstrate the applicability of this proposed approach.

6.2 Methodology

6.2.1 The General ANN-DMINP Approach

The proposed ANN-based dynamic mixed integer nonlinear programming

(ANN-DMINP) approach can be summarized as follows. Consider the following general nonlinear optimization problem:

$$\text{Min } f(x) \quad (6.1)$$

subject to:

$$g_j(x) = 0, \quad j = 1, 2, \dots, p \quad (6.2)$$

$$h_k(x) \leq 0, \quad k = 1, 2, \dots, q \quad (6.3)$$

$$lb \leq x \leq ub \quad (6.4)$$

where x are the decision variables; f is the nonlinear objective function that needs to be minimized; g and h are the nonlinear equality and inequality constraints, respectively; p and q are the numbers of equality and inequality constraints, respectively; and lb and ub are the lower and upper bounds of x , respectively. The bounds can be defined by consulting experts, field engineers or literatures. Traditionally, mixed integer optimization problems can be solved by mathematical programming techniques such as branch and bound (Martí and Reinelt, 2011), generalized benders' decomposition (GBD) and outer-approximation (OA) algorithms (Farkas et al., 2008; Chu and You, 2013). Particularly, when the objective function and/or constraints are coupled with simulation modules (e.g., ANN model), real-time decisions may be required to meet the control needs in terms of operating cost, control stability, and response time (Ding et al., 2006). The problem would then become a multi-stage process where the decision of the one stage would have a ripple effect on the decisions of the following stages through simulation models.

$$\text{Min } f(x_1, x_2, \dots, x_n, y_1, y_2, \dots, y_n) \quad (6.5)$$

subject to:

$$g_j(x_1, x_2, \dots, x_n, y_1, y_2, \dots, y_n) = 0 \quad j = 1, 2, \dots, p \quad (6.6)$$

$$h_k(x_1, x_2, \dots, x_n, y_1, y_2, \dots, y_n) \leq 0 \quad k = 1, 2, \dots, q \quad (6.7)$$

$$lb \leq x_i \text{ and } y_i \leq ub \quad i = 1, 2, \dots, n \quad (6.8)$$

where x_i and y_i are the decision variables of multiple stages which are usually defined by time (y_i are integers); and n stands for the number of decision stages. Such type of nonlinear problems tends to possess a dynamic nature as shown below and may not be easily solved by aforementioned traditional techniques. To remediate this situation, genetic algorithms (GAs), which are probabilistic global optimization formalisms, can be employed to solve the above multi-stage nonlinear optimization problem.

Genetic algorithms combine the “survival of the fittest” principle of natural evolution with a randomized information exchange which helps to form a stochastic search routine and produce new individuals with higher fitness (Ma et al., 2011). As compared to the traditional gradient-based optimization techniques, GAs have several distinguished features: 1) they are zero-order optimization methods that only require the scalar values of the objective function; 2) they can handle linear, nonlinear, complex and noisy objective functions; 3) their global search mechanism ensures that they are more likely to find the global optimum instead of being trapped at local optimums; 4) the stochastic solution search procedure gives them immunity to preconditions such as smoothness, differentiability, and continuity on the objective function form (Ghaedi et al., 2013; El-Fergany et al., 2014). In a typical GA procedure, the optimal solution search commences from a randomly initialized population of candidate solutions. Each solution has as many segments as the number of decision variables and is usually coded as a chromosome string of binary digits (Dong et al., 2013). Then the initial solutions are

decoded by an evaluator into the fitness function values, whose magnitude is indicative of the objective function values. For maximization and minimization problems, the fitness function value should scale up with the increasing and decreasing value of the objective function, respectively (Bhatti et al., 2011). Based on the evaluation of the fitness values of the solutions, the next generation (i.e., new population) of solutions can be produced through four GA operators, namely reproduction, crossover, and mutation, by which GA can escape from local optimal points (Badrnezhad and Mizra, 2014). The resultant population of solutions is then iteratively subject to this aforementioned procedure such that the candidate solutions are refined in a manner imitating selection and adaptation in biological evolution, until the convergence is obtained or the pre-set stopping conditions are satisfied.

Reproduction is a process in which strings with higher fitness values are copied and passed to the next generation according to their fitness values (Ma et al., 2011). The higher fitness values, the higher probability of surviving into the next generation. Reproduction can be recognized as an artificial version of natural selection through which strings with lower fitness are eliminated from the solution population (Bhatti et al., 2011). In nature, an offspring normally inherits genes from both parents and is rarely the exact same as one of them. Crossover makes this happen by randomly (with a crossover probability) exchanging parts of two parent strings to produce two child strings for the next generation (Ghaedi et al., 2013). It enables GA to extract the best genes from different individuals and inherit them into the potentially superior offspring. From the mathematical perspective, crossover offers further knowledge about the hyperplanes already represented earlier in the population and introduces representatives of new

hyperplanes into the population. Mutation, on the other hand, also plays an important role in evolution because it can bring new information into the current population. It is the random alteration of bits in parent strings such that the variability of the population in the next generation can be increased. Mutation is the key operator that helps GA to avoid local optimal points in the search space (Ma et al., 2011; El-Fergany et al., 2014).

The stepwise procedure for implementing the ANN-DMINP approach can be summarized as follows:

Step 1: Define the problem with target inputs and the number of time-stages. Set the generation count N_g to zero. Set population size N_p , iteration number N_i , reproduction probability p_r , crossover probability p_c , and mutation probability p_m .

Step 2: Create the initial population with the preset population size (e.g., $N_p = 200$) using random binary digits. Each solution string in the population has the same number of segments as the number of decision variables.

Step 3: Extract the values of each decision variable by reading and decoding certain sets of binary digits. Apply individual solutions to the predefined ANN model, run the simulation for each time stage i and obtain the simulation outputs.

Step 4: Evaluate the objective function and fitness score of each solution string. Rank the strings in the decreasing order of their fitness values. All the linear constraints and bounds should be satisfied, while the nonlinear constraints may not be all satisfied at every generation but will be met at the convergence solution.

Step 5: Create a mating pool by using a proportional selection criterion (e.g., simulated roulette) to choose solutions in the initial population. The probability of an individual solution being chosen is proportional to its fitness value.

Step 6: From the mating pool, choose parent strings to perform reproduction (P_r) and crossover (P_c) operations to obtain the offspring population.

Step 7: Perform mutation (P_m) on the offspring population.

Step 8: Update the generation count by $N_g = N_g + 1$.

Step 9: Repeat steps 3-8 to update the population pool with new generations until one of the convergence criteria is satisfied, such as the generation count N_g reaches the preset limit, or the weighted average relative change in the fitness function value over stall generations is less than function tolerance. The convergence solution is record as the final solution to the optimization problem.

6.2.2 Application of ANN-DMINP in Marine Oily Wastewater Treatment

Consider the following oily seawater treatment system to examine the effectiveness of the proposed ANN-DMINP approach and visualize the contributions of this control strategy. To accommodate with the developed ANN simulation model in Chapter 5, the treatment system here is assumed to be used for removing naphthalene from oil polluted seawater by using UV irradiation. The flow-through treatment system is assumed to consist of a storage tank and a reaction tank. The UV-induced photodegradation process is carried out within the reaction tank only where the developed ANN simulation model can be used to simulate the treatment process. Two pumps with adjustable flow rate are assumed to be used to circulate seawater through the treatment system. Seawater is assumed to be completely mixed in both tanks and no degradation occurs in the storage tank. Controlling parameters include UV intensity, pump flow rate, initial naphthalene concentration, salinity, temperature and discharge standard.

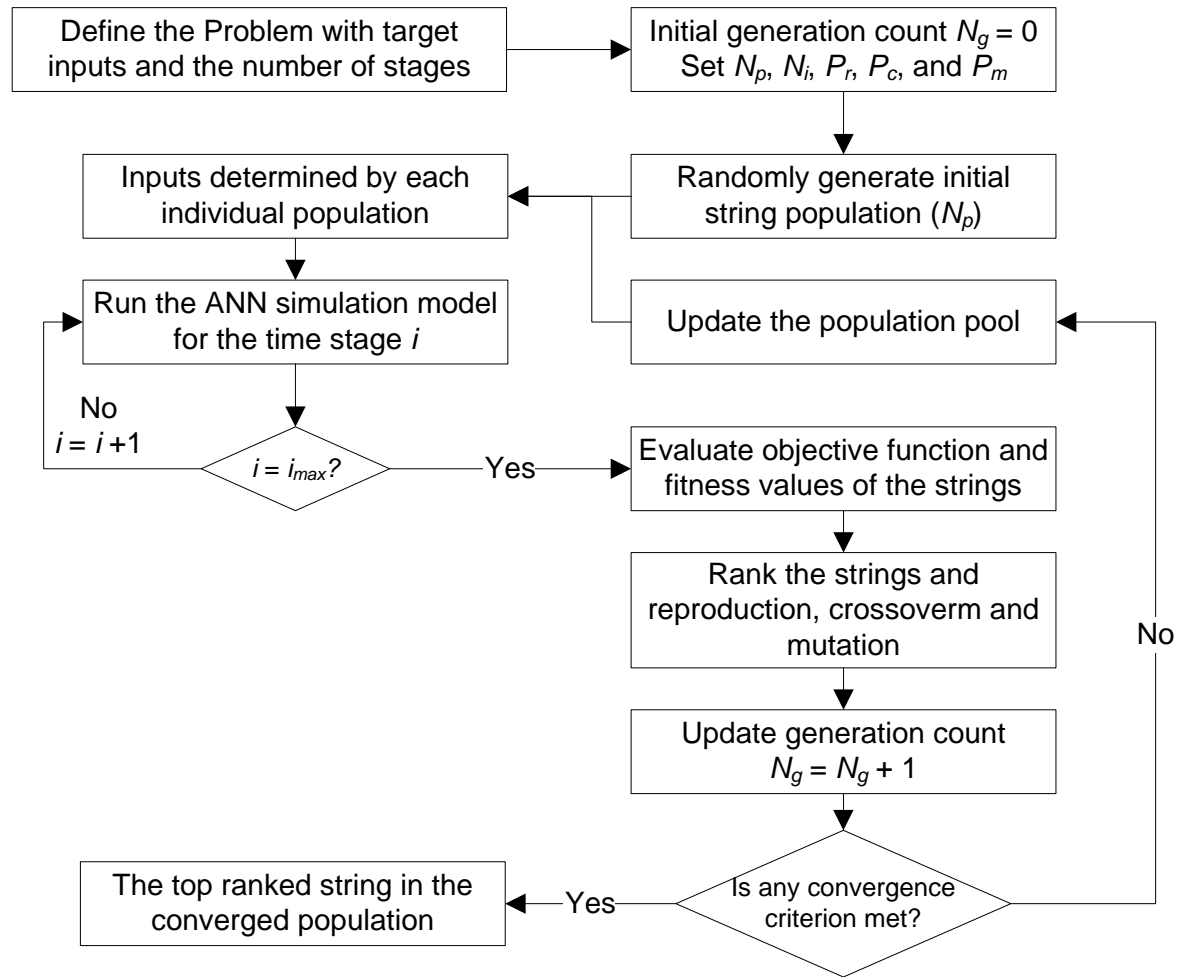


Figure 6.1 Flow chart of the ANN-based dynamic mixed integer nonlinear programming (ANN-DMINP) approach

The objective is to design an operation scheme within a certain period (e.g., 24 or 36 hours) in order to meet the discharge standard with the minimized cost. Cost is associated with the use of UV lamps and the pumps by which electricity is consumed. This problem can then be formulated as the following multi-stage mixed integer nonlinear programming problem with multiple stages.

$$\text{Min } f(x, y) = \sum_{i=1}^n (Cost_x \times x_i + Cost_y \times y_i) \quad (6.9)$$

subject to:

$$C_{storage}(x_1, x_2, \dots, x_n, y_1, y_2, \dots, y_n) \leq std_{storage} \quad (6.10)$$

$$C_{reaction}(x_1, x_2, \dots, x_n, y_1, y_2, \dots, y_n) \leq std_{reaction} \quad (6.11)$$

$$lb_x \leq x_i \leq ub_x \quad i = 1, 2, \dots, n \quad (6.12)$$

$$lb_y \leq y_i \leq ub_y \quad \text{and integer, } i = 1, 2, \dots, n \quad (6.13)$$

where x and y are the flow rates and UV intensity during each time stage, respectively; i is the number of hours; $Cost_x$ and $Cost_y$ are the cost coefficients associated with flow rate and UV intensity, respectively; n is the number of time stages; and C are the nonlinear inequity constraint associated with the final concentrations of naphthalene after treatment; $std_{storage}$ and $std_{reaction}$ are the desired concentrations in the storage and reaction tanks, respectively. The computation of the nonlinear constraints C is simplified as follows. For example, during a small time increment Δt , the initial concentrations in the storage (c_s) and reaction (c_r) tanks (assuming completely mixed conditions) can be computed as:

1) The removal rate of naphthalene in the portion of seawater that remains in the reaction tank after an exposure period of Δt can be calculated using the pre-developed ANN model as:

$$r_{\Delta t} = \text{sim}(\text{net}, [c_{r0}; \text{salinity}; y_1; \text{temperature}; \Delta t]) \quad (6.14)$$

where $r_{\Delta t}$ represents naphthalene removal in percentage; *sim* and *net* are Matlab[®] commands for ANN simulation; y_1 is the number of UV lamps operated in the first hour; c_{r0} , *salinity*, *temperature* and Δt stand for the initial concentration in the reaction tank, salinity, temperature, and time, respectively.

2) Within the time period of Δt , the volume of seawater that flows out of the reaction tank is $\Delta t \times x_1$ and its removal rate r_{out} can be integrated as shown below.

According to the first order reaction kinetics, we have

$$\ln \frac{C_{r\Delta t}}{C_{r0}} = -k\Delta t \quad (6.15)$$

$$r_{\Delta t} = 1 - \frac{C_{r\Delta t}}{C_{r0}} = 1 - e^{-k\Delta t} \quad (6.16)$$

$$r_t = 1 - \frac{C_{rt}}{C_{r0}} = 1 - e^{-kt} = 1 - e^{-\frac{\ln(1-r_{\Delta t}) \times t}{\Delta t}} \quad (6.17)$$

$$r_{out} = \int_0^{\Delta t} r_t dt / t \quad (6.18)$$

where k is the reaction rate constant; $C_{r\Delta t}$ and C_{rt} are the concentrations of naphthalene in seawater that remains in the reaction tank at time points Δt and t , respectively; and r_t is the corresponding removal rate at time point t .

3) Within the time period of Δt , the volume of seawater that flows in the reaction tank is $\Delta t \times x_1$ and its removal rate r_{in} can be integrated using the same procedure stated above.

$$r_{\Delta t}^* = \text{sim}(\text{net}, [c_{s0}; \text{salinity}; y_1; \text{temperature}; \Delta t]) \quad (6.19)$$

$$r_t^* = 1 - e^{-\frac{\ln(1-r_{\Delta t}^*) \times t}{\Delta t}} \quad (6.20)$$

$$r_{in} = \int_0^{\Delta t} r_t^* dt / t \quad (6.21)$$

where c_{s0} is the initial concentration of naphthalene in the storage tank; $r_{\Delta t}^*$ and r_t^* are the removal rates in seawater coming from the storage tank at time points Δt and t , respectively.

4) The total naphthalene removal in mass m and the concentrations in the storage tank (c_s) and reaction tank (c_r) after Δt can therefore be computed as:

$$m = (V_r - \Delta t \cdot x_1) \cdot c_{r0} \cdot r_{\Delta t} + \Delta t \cdot x_1 \cdot c_{r0} \cdot r_{out} + \Delta t \cdot x_1 \cdot c_{s0} \cdot r_{in} \quad (6.22)$$

$$c_r = \frac{(V_r - \Delta t \cdot x_1) \cdot c_{r0} \cdot (1 - r_{\Delta t}) + \Delta t \cdot x_1 \cdot c_{s0} \cdot (1 - r_{\Delta t}^*)}{V_r} \quad (6.23)$$

$$c_s = \frac{(V_s - \Delta t \cdot x_1) \cdot c_{s0} + \Delta t \cdot x_1 \cdot c_{r0} \cdot (1 - r_{\Delta t})}{V_s} \quad (6.24)$$

where V_r and V_s represent the volume of seawater in reaction and storage tanks, respectively. Repeat the above steps for the rest of the time stages to obtain the final concentrations in both tanks, which are required to be less than or equal to the discharge standard $std_{storage}$ and $std_{reaction}$, respectively. It is worth noted that choosing the value of Δt depends on the computation time constraints and the treatment system characteristics.

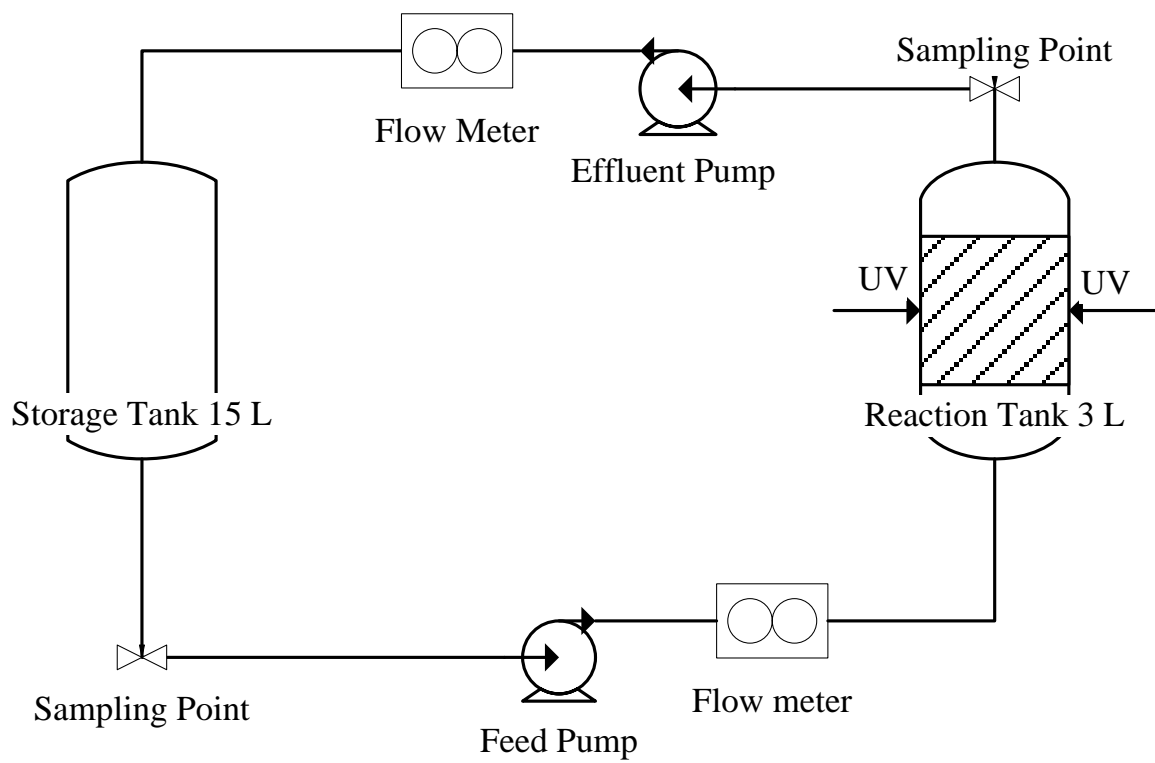


Figure 6.2 A schematic plot of the flow-through UV treatment system of the case study

6.3 Case Study

In this case study, as shown in Figure 6.2, a total volume of 15 L seawater polluted by naphthalene at a concentration of $300 \mu\text{g L}^{-1}$ needs to be treated using the above system. The treatment system consists of a storage tank, with a maximum capacity of 15 L, and a 3 L reaction tank. The ANN simulation model developed in Chapter 5 is used to simulate the removal efficiency of naphthalene within the reaction tank. The salinity is 32.5 practical salinity unit (psu) and water temperature is maintained at 25°C . According to the stringent marine water quality standard and the 15 ppm discharge standard of bilge water (CCME, 1999; McLaughlin et al., 2014), the concentration of naphthalene in both tanks are set to be lower than $10 \mu\text{g L}^{-1}$ prior to discharge. The objective of this problem is therefore to design the operation scheme for 36 hours in order to meet the discharge standard and to minimize the total treatment cost. Cost is associated with the use of UV lamps and the pumps by which electricity is consumed. Their cost coefficients are arbitrarily predefined as \$0.05 per lamp per hour and \$0.003 per liter, respectively. UV lamps can be operated in different combinations and its number has to be an integer ranging from 2 to 6. The flow rates of the pumps are equal and have to be greater than 0.1 and less than 0.5 L min^{-1} . This problem can then be formulated as the following multi-stage mixed integer nonlinear programming problem with 36 stages.

$$\text{Min } f(x, y) = \sum_{i=1}^{36} (0.003 \times 60 \times x_i + 0.05 \times y_i) \quad (6.25)$$

subject to:

$$C_{\text{storage}}(x_1, x_2, \dots, x_{36}, y_1, y_2, \dots, y_{36}) \leq 10 \quad (6.26)$$

$$C_{\text{reaction}}(x_1, x_2, \dots, x_{36}, y_1, y_2, \dots, y_{36}) \leq 10 \quad (6.27)$$

$$0.1 \leq x_i \leq 0.5 \quad i = 1, 2, \dots, 36 \quad (6.28)$$

$$2 \leq y_i \leq 6 \text{ and integer, } i = 1, 2, \dots, 36 \quad (6.29)$$

where x and y are the flow rates (L min^{-1}) and the numbers of UV lamps during each hour, respectively; i is the number of hours; and C are the nonlinear inequity constraint associated with the final concentration of naphthalene after 36-hour UV treatment ($\mu\text{g L}^{-1}$). The computation of the nonlinear constraints C is simplified as follows. For example, during a small time increment Δt in the first hour, the post-concentrations in the storage (c_s) and reaction (c_r) tanks (assuming completely mixed conditions) can be computed as:

1) The removal rate of naphthalene in the portion of seawater that remains in the reaction tank after an exposure period of Δt can be calculated using the pre-developed feedforward neural network (Jing et al., 2014b), which requires inputs of UV lamps, salinity, temperature, concentration, and reaction time

$$r_{\Delta t} = \text{sim}(\text{net}, [c_{r0}; 32.5; y_1; 25; \Delta t]) \quad (6.30)$$

where $r_{\Delta t}$ represents naphthalene removal in percentage; *sim* and *net* are Matlab commands for ANN simulation; y_1 is the number of UV lamps operated in the first hour; c_{r0} , 32.5, 25 and Δt stand for pre-concentration in the reaction tank, salinity, temperature, and time, respectively.

2) Within the time period of Δt , the volume of seawater that flows out of the reaction tank is $\Delta t \times x_1$ and its removal rate r_{out} can be integrated as shown below. According to the first order reaction kinetics, we have

$$\ln \frac{c_{r\Delta t}}{c_{r0}} = -k\Delta t \quad (6.31)$$

$$r_{\Delta t} = 1 - \frac{c_{r\Delta t}}{c_{r0}} = 1 - e^{-k\Delta t} \quad (6.32)$$

$$r_t = 1 - \frac{c_{rt}}{c_{r0}} = 1 - e^{-kt} = 1 - e^{-\frac{\ln(1-r_{\Delta t}) \times t}{\Delta t}} \quad (6.33)$$

$$r_{out} = \int_0^{\Delta t} r_t dt / t \quad (6.34)$$

where k is the reaction rate constant; $c_{r\Delta t}$ and c_{rt} are the concentrations of naphthalene in seawater that remains in the reaction tank at time points Δt and t , respectively; and r_t is the corresponding removal rate at time point t .

3) Within the time period of Δt , the volume of seawater that flows in the reaction tank is $\Delta t \times x_1$ and its removal rate r_{in} can be integrated using the same procedure stated above.

$$r_{\Delta t}^* = \text{sim}(\text{net}, [c_{s0}; 32.5; y_1; 25; \Delta t]) \quad (6.35)$$

$$r_t^* = 1 - e^{-\frac{\ln(1-r_{\Delta t}^*) \times t}{\Delta t}} \quad (6.36)$$

$$r_{in} = \int_0^{\Delta t} r_t^* dt / t \quad (6.37)$$

where c_{s0} is the initial concentration of naphthalene in the storage tank; $r_{\Delta t}^*$ and r_t^* are the removal rates in seawater coming from the storage tank at time points Δt and t , respectively.

4) The total naphthalene removal in mass m and the concentrations in the storage tank (c_s) and reaction tank (c_r) after Δt can be computed as:

$$m = (3 - \Delta t \cdot x_1) \cdot c_{r0} \cdot r_{\Delta t} + \Delta t \cdot x_1 \cdot c_{r0} \cdot r_{out} + \Delta t \cdot x_1 \cdot c_{s0} \cdot r_{in} \quad (6.38)$$

$$c_r = \frac{(3 - \Delta t \cdot x_1) \cdot c_{r0} \cdot (1 - r_{\Delta t}) + \Delta t \cdot x_1 \cdot c_{s0} \cdot (1 - r_{\Delta t}^*)}{3} \quad (6.39)$$

$$c_s = \frac{(12 - \Delta t \cdot x_1) \cdot c_{s0} + \Delta t \cdot x_1 \cdot c_{r0} \cdot (1 - r_{\Delta t})}{12} \quad (6.40)$$

Repeat the above four steps for the rest of the first hour as well as subsequent hours to obtain the final concentrations in both tanks, which are required to be less than or equal to $10 \mu\text{g L}^{-1}$. It can be seen that the length of Δt is of significance in computing the concentrations of naphthalene in both tanks, which are in turn affected by the differences among the removal rates $r_{\Delta t}$, r_{out} , and r_{in} . Ideally, Δt should be set as short as enough to approach the complete mixing assumption such that the differences among $r_{\Delta t}$, r_{out} , and r_{in} are negligible. Therefore, in this case study, Δt was tested at 0.1, 0.5, 1, 2, 3, 4, and 5 minutes, respectively, with c_{r0} varying from 300 to 100 $\mu\text{g/L}$ to determine the best compromise between computation accuracy and efficiency. As shown in Table 6.1, the concentration difference (Δc) between $r_{\Delta t}$ and r_{out}/r_{in} shows an increasing trend when Δt increases and this trend is not affected by c_{r0} . However, to simplify the computation and to avoid time-consuming iterations, a compromise on the length of Δt should be taken into account such that Δt was set as 1 min in this case study.

To solve this problem, GA optimization was performed in Matlab[®] by following the detailed procedure shown in Figure 6.1. The number of variables was 72. Population size (N_p) and maximum generation count (N_g) are usually two of the most important parameters in GA optimization. To validate if the chosen values of N_p and N_g can well achieve the desired solution, a comparative test was undertaken by examining their different combinations (Table 6.2). It can be seen that the optimization results dropped from 9.6784 to 9.1125 when N_p was hold at 30 and N_g was increased from 50 to 100. However,

a further increase of N_g from 100 to 200 did not produce any better results because the optimization process usually met the stopping criteria between 70 to 80 generations. On the other hand, higher N_p values were not associated with better performance as observed from the last three tests. It has been reported that big population size may not improve the performance of GA in meaning of speed of finding solution (El-Fergany et al., 2014). N_p was therefore set to 30 by taking computation time and resource constraints into account. Based on the test results and literature recommendations (Ma et al., 2011; Dong et al., 2013; Liu et al., 2013), the population size (N_p) and maximum generation count (N_g) were set at 30 and 100, respectively. The binary tournament selection function and doubleVector population type were used as default for mixed integer programming. The elite count for reproduction (P_r) was set at 2, while the crossover fraction (P_c) of the current population excluding the elite individuals was set at 0.8. Power mutation (P_m) was adopted by default to accommodate the integer restriction of decision variables (Deep et al., 2009).

To compare with the performance of the ANN-DMINP approach, a single-stage optimization (i.e., globally continuous problem) was conducted by using constant flow rate and constant number of lamps throughout the 36-hour period. The optimization procedure and GA settings were the same as for the multi-stage problem. In addition, a 500-iteration Monte Carlo simulation was performed to illustrate the distribution of treatment cost that might be expected from random sampling of constant flow rate and the number of lamps within their ranges. Such a random sampling can well reflect the consequence of random decision making when no optimization results are available.

Table 6.1 The removal rates $r_{\Delta t}$, r_{out} , and r_{in} after one time step Δt at different initial concentrations (c_{r0}) in the reaction tank

| Time step (min) | $c_{r0} = 300 \mu\text{g/L}$ | | | $c_{r0} = 200 \mu\text{g/L}$ | | | $c_{r0} = 100 \mu\text{g/L}$ | | |
|--------------------|------------------------------|--------------------|--------------------------------|------------------------------|--------------------|--------------------------------|------------------------------|--------------------|--------------------------------|
| | $r_{\Delta t}$ | $r_{out} = r_{in}$ | Δc ($\mu\text{g/L}$) | $r_{\Delta t}$ | $r_{out} = r_{in}$ | Δc ($\mu\text{g/L}$) | $r_{\Delta t}$ | $r_{out} = r_{in}$ | Δc ($\mu\text{g/L}$) |
| 0.1 | 0.0006 | 0.0003 | 0.09 | 0.0009 | 0.0004 | 0.09 | 0.0011 | 0.0006 | 0.06 |
| 0.5 | 0.0030 | 0.0014 | 0.45 | 0.0047 | 0.0024 | 0.48 | 0.0057 | 0.0028 | 0.28 |
| 1 | 0.0059 | 0.0030 | 0.89 | 0.0093 | 0.0047 | 0.94 | 0.0113 | 0.0057 | 0.57 |
| 2 | 0.0118 | 0.0059 | 1.77 | 0.0185 | 0.0093 | 1.86 | 0.0225 | 0.0113 | 1.13 |
| 3 | 0.0176 | 0.0088 | 2.64 | 0.0276 | 0.0138 | 2.76 | 0.0335 | 0.0168 | 1.68 |
| 4 | 0.0234 | 0.0118 | 3.53 | 0.0367 | 0.0184 | 3.68 | 0.0445 | 0.0223 | 2.23 |
| 5 | 0.0292 | 0.0147 | 4.41 | 0.0456 | 0.0230 | 4.60 | 0.0553 | 0.0278 | 2.78 |

Note: Δc stands for the difference between the concentrations of naphthalene in seawater that remains in the reaction tank and in seawater that flows out of the reaction tank. It can be calculated with $\Delta c = c_{r0} * (r_{\Delta t} - r_{out})$.

Table 6.2 The comparison of minimized treatment cost based on different N_p and N_g combinations

| Test # | N_p | N_g | Min Cost (\$) |
|--------|-------|-------|---------------|
| 1 | 30 | 50 | 9.6784 |
| 2 | 30 | 100 | 9.1125 |
| 3 | 30 | 200 | 9.1125 |
| 4 | 50 | 100 | 9.3094 |
| 5 | 100 | 100 | 9.5404 |

6.4 Results and Discussion

The results from the case study suggested that the minimum treatment cost was optimized at \$9.1125 after 36-hour UV irradiation. The final concentrations in the storage and reaction tanks were 9.97 and 7.56 $\mu\text{g L}^{-1}$, respectively, indicating that the nonlinear constraints on the discharge standards were met (Figure 6.3). The decreasing trend of both concentrations were closely linked with a correlation coefficient of 0.998, while they were reversely correlated with the treatment cost with correlation coefficients lower than -0.938. This observation infers that the decision variables were properly optimized. If the flow rate was too low, given the number of UV lamps unchanged, the concentration difference between two tanks would be much more pronounced because most treated seawater would remain in the reaction tank. If the flow rate was too high, the pollutant removal process can be somewhat accelerated but with much higher cost. On the other hand, given constant flow rate, more UV lamps may drastically promote the treatment process but also associate with higher cost, and vice versa. The flow rates and the number of UV lamps during each stage are illustrated in Figure 6.4. It is worth mentioning that the treatment system was not in its peak load condition. The number of UV lamps was kept at the minimum level (e.g., 2 lamps) in 16 hours, and the mean flow rate during the whole treatment period was just half of its top limit at 0.241 L min^{-1} . This implies that the 36-hour period may be further shortened without violating the discharge standards.

6.4.1 Comparison with the Single-Stage Optimization and Monte Carlo Simulation

The single-stage optimization yielded a constant flow rate of 0.1 L min^{-1} and 6 UV lamps during the 36-hour period. The variations of naphthalene concentrations in both

tanks with time are plotted in Figure 6.5. The degradation strictly followed the first order kinetics well with R^2 greater than 0.99 and reduced the concentrations in the storage and reaction tanks to 4.15 and 3.08 $\mu\text{g L}^{-1}$, respectively. The difference between two concentrations ranged from 1.07 to 45.92 $\mu\text{g L}^{-1}$ with a mean value of 15.75 $\mu\text{g L}^{-1}$. The mean value was larger than that of the multi-stage problem (i.e., 6.53 $\mu\text{g L}^{-1}$), indicating that the fixed parameters was not as much efficient as the variable ones in balancing the concentrations. The treatment cost was optimized to \$11.448, which was 25.7% higher than that of the multi-stage problem, suggesting the multi-stage operation plan was superior in terms of cost efficiency. This difference could be solely due to the over-exposure of UV irradiation by using 6 lamps during the treatment period as the flow rate was at its minimum level (0.1 L min^{-1}). If the number of UV lamps was adjusted to 5 while maintaining the flow rate at 0.1 L min^{-1} , the concentrations in the storage and reaction tanks would go down to 16.52 and 13.55 $\mu\text{g L}^{-1}$, respectively, which were higher than the discharge standard. The standard was not met until the flow rate was increased to 0.5 L min^{-1} with 5 lamps on, incurring a total cost of \$12.24. Therefore, using the combination of 0.1 L min^{-1} flow rate and 6 UV lamps seemed to be the best decision available for this single-stage treatment plan. Another interesting finding was that the concentrations in both tanks were lower than 10 $\mu\text{g L}^{-1}$ after only 29 hours, which means the rest of the treatment period can be readily considered as unnecessary. Therefore, as concluded from the multi-stage problem, a reduction in treatment duration could be favoured because it may also lead to lower treatment cost.

On the other hand, 83% (415 out of 500) of the Monte Carlo iterations were not able to meet the required standard (10 $\mu\text{g L}^{-1}$) due to the lack of flow rate or UV irradiation.

Only 85 iterations were recorded as feasible solution and the statistical analysis of treatment cost, flow rate, and the number of lamps is shown in Table 6.3. It can be seen that the minimum treatment cost was \$11.449, which was close to the single-stage optimization results of \$11.448. Nonetheless, the mean cost was \$12.797 with a standard deviation of \$0.728, indicating that in most Monte Carlo iterations the system performance was not at its optimal level. These results suggested that, if the operator randomly set the flow rate and the number of lamps as constants during the 36-hour period, then there would be a great chance that the treatment standard cannot be met. Even if the treatment was successful, the system can hardly reach its optimal performance due to the lack of optimization efforts.

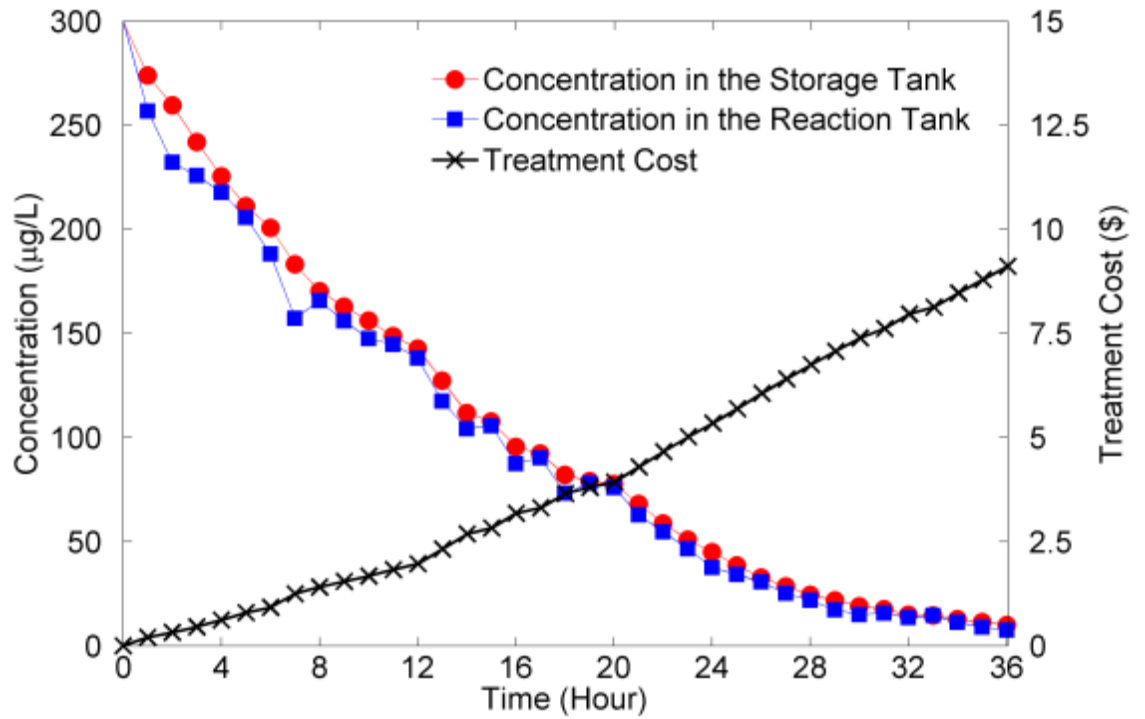


Figure 6.3 Variations of the concentrations in the storage and reaction tanks and the treatment cost during the 36-hour UV exposure using the ANN-DMINP approach

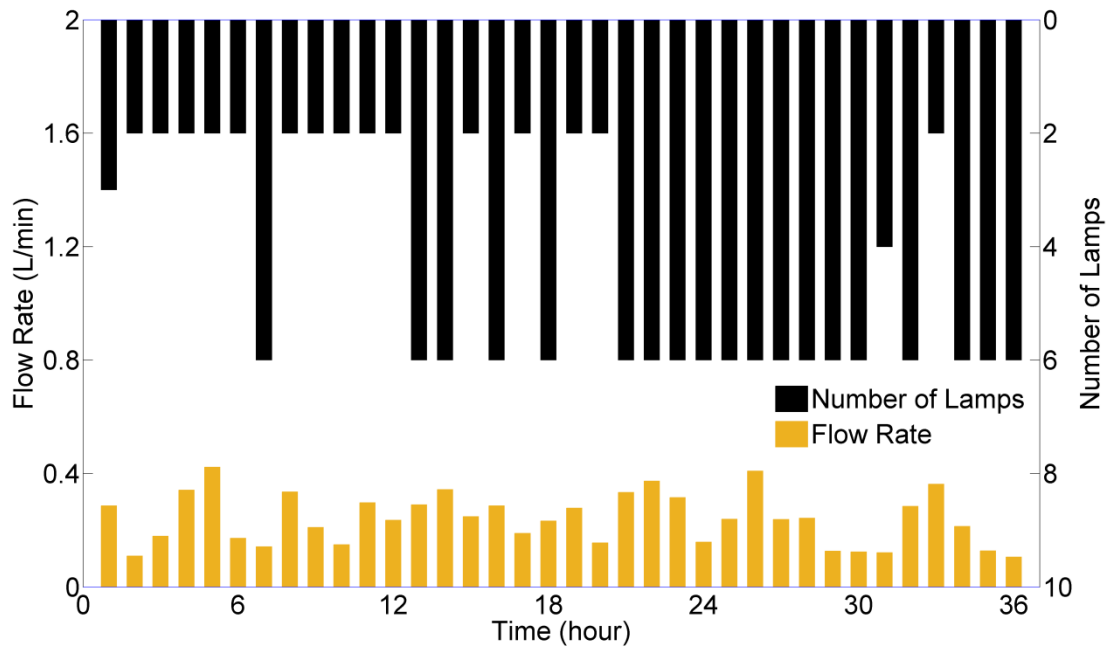


Figure 6.4 Variations of the flow rate and the number of UV lamps during the 36-hour UV exposure

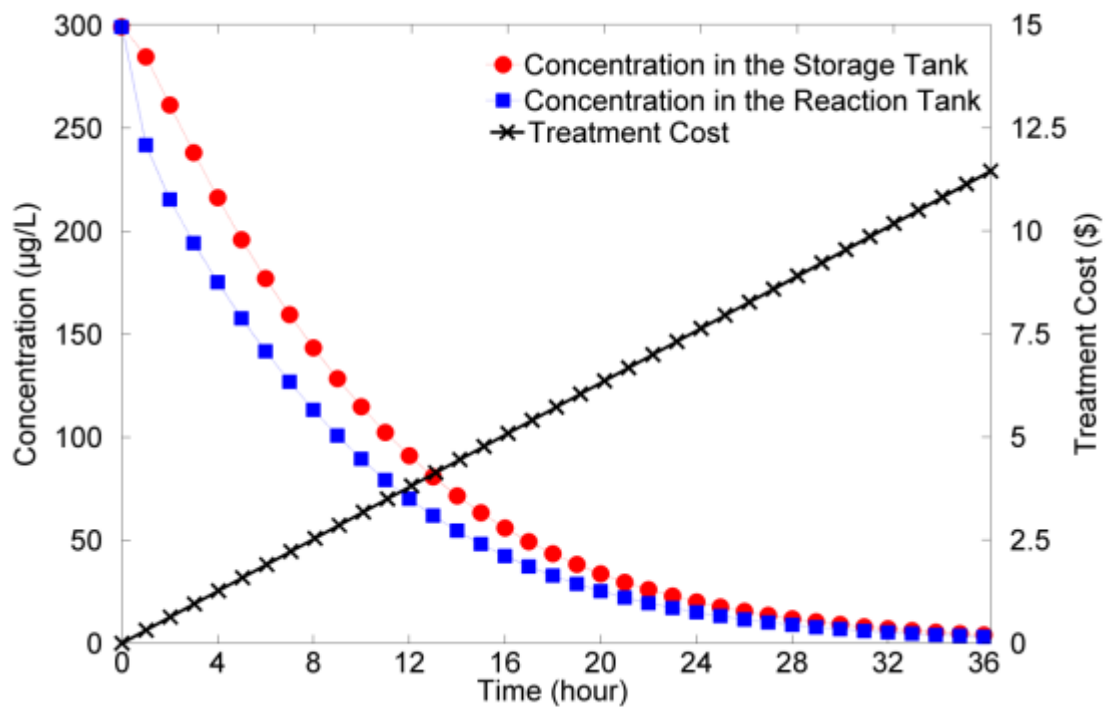


Figure 6.5 Variations of the concentrations in the storage and reaction tanks and the treatment cost during the 36-hour UV exposure using the single-stage optimization

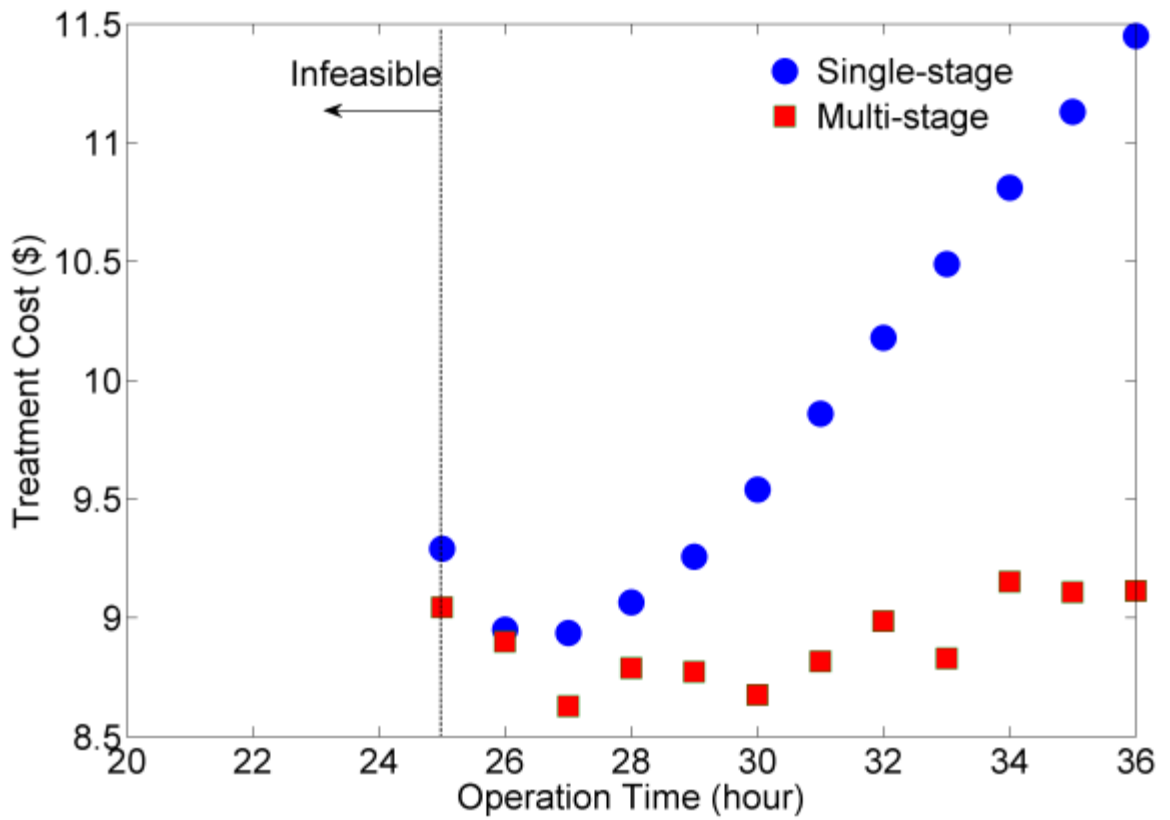


Figure 6.6 Minimization of treatment time and total cost using both multi-stage (ANN-DMINP) and single-stage optimization

6.4.2 Minimization of Time and Cost

The original problem of the case study was to minimize treatment cost given 36-hour time period. The optimization results showed that the treatment system was not operated at full capacity, indicating the operation time may be reduced. The comparative single-stage problem also revealed that a reduction in treatment duration could be necessary and cost-effective. Indeed, increasing flow rate and UV irradiation intensity may help achieve the discharge standard in a shorter operating time. To better understand the relationship between cost and operation time, the ANN-DMINP approach and the single-stage optimization were both carried out for multiple periods ranging from 25 to 36 hours by taking time constraints and the efficiency of convergence into account. The number of stages of the ANN-DMINP approach was set as the same as the number of hours (one hour per stage) for each period. The validity of constraints (final concentrations not exceeding $10 \mu\text{g L}^{-1}$) was checked such that feasible solutions in terms of cost and time were recorded. The population size (N_p), maximum generation count (N_g) and elite count for reproduction (P_r) were kept as 30, 100 and 2, respectively.

As depicted in Figure 6.6, it can be seen that the treatment costs for both multi-stage ANN-DMINP and single-stage optimization tended to decrease with decreasing time. This decreasing trend was remarkable at the beginning from 36 hours and reached a local minimum around 27 hours for both cases. The cost started to increase if the treatment time went below 27 hours and reached the threshold at 25 hours for the discharge standard to be met. The discharge standard of $10 \mu\text{g L}^{-1}$ was not able to be satisfied if the treatment time was less than 25 hours. Another interest finding is that the optimum cost of the multi-stage control scheme was lower than that of the single-stage control scheme

at an average difference of \$1.00, implying the superiority of the ANN-DMINP approach.

6.4.3 Effect of the number of optimization stages

The ANN-DMINP approach was originally proposed and implemented on an hourly basis so that each stage had one hour. However, such an hourly operation plan sometimes may not be the best option, given that changing the operation parameters too often may cause additional costs or affect the stability of the system. To understand how the number of optimization stages can influence on the optimization results, sensitivity analysis was conducted. When the total treatment period was fixed at 36 hours, it can be seen that more optimization stages generally resulted in lower total treatment cost (Table 6.4). Interestingly, when having two stages, or in other words, changing the operation parameters once after the 18th hour, the total treatment cost would reach its minimum value at \$8.3622. The flow rates and the numbers of lamps at the two stages were 0.160 and 0.199 L min⁻¹, and 2 and 6, respectively. Such an interesting observation may be explained by the nature of GA. The solution search mechanism of GA often starts from a random initial population such that the 36-stage optimization would hardly converge to the solution from the 2-stage one. With that being said, if the solution from the 2-stage case can be used as the initial population for the 36-stage case, then a better solution may be obtained. The performance of the hourly stage and 2-stage optimization was further compared at a number of other periods. As shown in Table 6.5, the results obtained from hourly stage optimization dominate those from 2-stage optimization, indicating that optimization with more stages would be more beneficial. Nonetheless, it should be taken into account that more control stages would possibly increase manpower needs and

reduce system stability. Therefore, for the sake of computation time, the operators are recommended to first seek the best solution with less optimization stages, and then use it as an initial population to seek potentially better solution with more optimization stages. Then the difference between the solutions can be evaluated to determine whether or not a more complex operation plan should be implemented.

Table 6.3 Statistical results of the Monte Carlo Simulation

| | Flow rate (L/min) | UV lamp | Cost (\$) |
|----------------|-------------------|---------|------------------|
| Min | 0.100 | 5 | 11.449 |
| Max | 0.495 | 6 | 14.000 |
| Mean | 0.315 | 5.977 | 12.797 |
| Std | 0.115 | 0.153 | 0.728 |
| 95% percentile | [0.114, 0.478] | [6, 6] | [11.538, 13.823] |

Table 6.4 Sensitivity analysis of the number of optimization stages with 36 hours

| The number of stages | Stage duration (hr) | Optimization results (\$) |
|-------------------------|------------------------|------------------------------|
| 36 | 1 | 9.1125 |
| 18 | 2 | 9.2503 |
| 12 | 3 | 8.9999 |
| 6 | 6 | 9.1148 |
| 2 | 18 | 8.3622 |
| 1 | 36 | 11.4480 |

Table 6.5 Comparison between hourly stage and two stage optimization

| Time (hr) | Optimization results (\$) | |
|-----------|---------------------------|-----------|
| | Hourly stage | Two stage |
| 32 | 8.9870 | 9.0407 |
| 30 | 8.6753 | 9.4853 |
| 28 | 8.7885 | 9.0622 |
| 27 | 8.6280 | 9.2705 |
| 26 | 9.0315 | 8.9188 |
| 25 | 9.0442 | 9.0442 |

6.5 Summary

This chapter presents an ANN-based dynamic mixed integer nonlinear programming (ANN-DMINP) approach to help optimize the performance of marine oily wastewater treatment. It is an integration of simulation (i.e., ANN), stochastic optimization (GA) and the multi-stage principle and is examined through a hypothetical case study. UV photodegradation of naphthalene, as described in Chapters 4 and 5, was chosen in the case study as an example to demonstrate the applicability of the proposed approach. The results from the case study showed that the treatment cost in a fixed 36-hour period was minimized to \$9.11 by using the ANN-DMINP approach. As a comparison, the single-stage optimization with constant variables was also applied and the treatment cost was 25.7% higher at \$11.45. A Monte Carlo simulation was also performed to conclude that if the operator randomly set the flow rate and the number of lamps as constants during the 36-hour period, then there would be a great chance that the treatment standard cannot be met. If considering time as another flexible variable, the treatment cost reached its minimum at 27 hours with \$8.71 and \$8.94 for the ANN-DMINP approach and the single-stage optimization, respectively. A sensitivity analysis for the number of stages demonstrated that, regardless the length of treatment period, more optimization stages can generally reduce treatment cost, but may lead to extra manpower needs and affect system stability. It was recommended to first seek the best solution with less optimization stages, and then using the solution as an initial population for more optimization stages, if necessary.

CHAPTER 7

AN INTEGRATED SIMULATION-BASED PROCESS CONTROL AND OPERATION PLANNING (IS-PCOP) APPROACH FOR MARINE WASTEWATER MANAGEMENT

This chapter is based on and expanded from the following paper:

Jing, L., Chen, B., and Zhang, B.Y. (2014). An integrated simulation-based process control and operation planning (IS-PCOP) approach for marine wastewater management. *Journal of Environmental Management*, to be submitted.

Role: Liang Jing solely worked on this study and acted as the first author of this manuscript under Dr. Bing Chen and Dr. Baiyu Zhang's guidance. Most contents of this paper was written by Liang and further polished by the other co-authors.

7.1 Background

In view of overall planning, the terms of “operation planning” and “process control or detailed scheduling” are quite different from each other. Operation planning, or so called system planning, usually refers to a longer period of time and is a prerequisite for process control. Based on the required product characteristics and economic and environmental constraints, the most appropriate processes, resources, and standards can be properly selected. A good operation planning tool, particularly from the long-term perspective, is an important basis and guarantee for meeting basic needs, providing high-quality service, and making the best use of available resources. This is especially true for offshore operations where resources such as power supply, available space, and man power are usually limited. Chapter 3 introduces two decision support and operation planning tools for marine oily wastewater treatment. It is worth mentioning that the optimization modules within these tools are usually complicated by many inherent nonlinear processes, such as the efficiency, cost and time requirement of different treatment technologies. The lack of understanding and knowledge has urged people to employ arbitrary opinion or empirical interpolation in order to simplify the nonlinearity. Contrastingly, process control is generally achieved by careful and accurate control and monitoring of the process parameters affecting the quality of the products. It is defined as an engineering discipline that deals with mechanisms and algorithms for maintaining the output of a specific engineering process within a desired range. With the increasingly stringent standards and more sophisticated treatment systems, operators have become more and more reliant on mathematical tools instead of their personal experience to optimize the control strategy.

An ideal combination of both process control and operation planning can greatly reduce system cost and maximize economic and environmental benefits associated with marine oily wastewater treatment. Recently, it has been recognized that, regardless their difference, the combination of process control and operation planning can ensure the meeting of the economic objectives and timely completion of the tasks associated with the plans (Hans et al., 2007; Hübner et al., 2009). Hübner et al. (2009) reported that a high-quality production planning needs to reflect the uncertainties associated with the market and technical parameters and to accommodate the feasible operation scheduling. Anuar Mohamad Kamar (2010) argued that if appropriate process control is not implemented during the system planning procedure, there might be potential benefits lost because traditional planning tends to be more conservative and less risk-taking. Verl et al. (2011) stated the importance of distinguishing between “detailed scheduling and process control” and “operation planning”. Nonetheless, they also claimed that process control consists of the anticipatory consideration and the reaction to unexpected occurrences, while long-term planning is usually a prerequisite for detailed scheduling and process control. How to take process control and scheduling into account during operation planning have become a rapidly growing area of research and a subject of interest to academicians and practitioners alike.

However, the link between process control and operation planning is most often not available due to the complexity of the integrated system, the difficulty in capturing and modeling the behaviour of the process, and the uncertainty of parameters to be considered. The first challenging aspect is the multi-scale nature of the integration, which arises as operation planning (e.g., capacity investment and design decisions) is typically made on a

much coarser (and longer) time scale than process control decisions. It is common to have benefits, investments, or capacity growth reviewed on a seasonal or yearly basis, whereas process control requires decisions and actions on a much finer time scale (e.g., hours). Secondly, wastewater treatment usually consists of a number of complex physical, chemical, and biological processes that are described by nonlinear functions. Therefore, how to precisely simulate the process and predict the outputs has been an obstacle for learning the behaviour of the treatment systems. Lastly, such coupling can be further complicated by uncertainties, which may arise from a number of different sources including wastewater characteristics, technology features and limitations, as well as environmental standards.

How to more accurately couple process control with operation planning has been a major roadblock in the development of an effective decision support system for marine oily wastewater management. To date, there has been no study reported in the literature on such integration. To fill the above knowledge gap, this chapter, therefore, aims at demonstrating the possible integration of process control with traditional operation planning by using neural networks, genetic algorithm, multistage principle, and Monte Carlo simulation. A case study of offshore wastewater management is carried out to demonstrate the efficacy of the proposed approach.

7.2 The IS-PCOP Approach for Marine Wastewater Management

Consider the following operation planning problem:

$$\text{Min } f(x) = f_1(x) + f_2(x) + \dots + f_n(x) \quad (7.1)$$

subject to:

$$g_j(x) = 0 \quad j = 1, 2, \dots, p \quad (7.2)$$

$$h_k(x) \leq 0 \quad k = 1, 2, \dots, q \quad (7.3)$$

$$lb \leq x \leq ub \quad (7.4)$$

where x are the decision variables, such as chemical dose and retention time; f is the objective function which equals to the sum of n sub-functions that are related to treatment cost or environmental risk; g and h are the equality and inequality constraints that can be associated with treatment capacity and man power restraint, respectively; p and q are the numbers of equality and inequality constraints, respectively; and lb and ub are the lower and upper bounds of x , respectively. The bounds are usually set by consulting experts or literature documents. A common situation is that, some of the sub-functions may be associated with simulation processes, while the process control tool proposed in Chapter 6 can be used to optimize these sub-functions. A prerequisite here is that the simulation process must have been well investigated, preferably supported by experimental observation data, such that an ANN simulation model can be developed (Figure 7.1). The detailed solution algorithm is summarized as follows:

Step 1: Define the operation planning objectives and constraints as introduced in Equations 7.1-7.4. Generate random numbers for the coefficients of objective functions and constraints within the corresponding upper and lower bounds. The bounds can be defined by consulting experts, field engineers or literatures.

Step 2: Generate random decision variables x within the predefined bounds lb and ub . These two steps are adopted from the SHIFP method proposed in Chapter 3.

Step 3: Define the process control problems $f_n(x)$ with inputs and the number of stages. The inputs are defined by the wastewater treatment problem (e.g., UV does and salinity)

while the number of stages are defined by the treatment period. Divide the simulation-based sub-functions $f_n(x)$ into multiple stages and obtain the corresponding minimized $f_n(x)$ using the ANN-DMINP approach (Section 6.2.1). The ANN model(s) are developed according to experimental data prior to this problem solving process.

Step 4: Evaluate the equality and inequality constraints to ensure the validity of the decision variables.

Step 5: Calculate the objective function $f(x)$ in terms of minimized $f_n(x)$ and record feasible solutions.

Step 6: Repeat Steps 2-5 for a number of iterations using Monte Carlo simulation. Note that the higher the number of iterations, the higher the chance to get a better solution distribution, and also the more computation time is required. The number of iterations should be set according to calculation accuracy and time/resources constraints. Find the minimum objective function value $f(x)$ and the value of decision variables corresponding to the random coefficients.

Step 7: Repeat Steps 1-6 using Monte Carlo simulation for a preset number of times. The objective function can be obtained as a probability distribution function in order to reflect the inherent uncertainty in the optimization process.

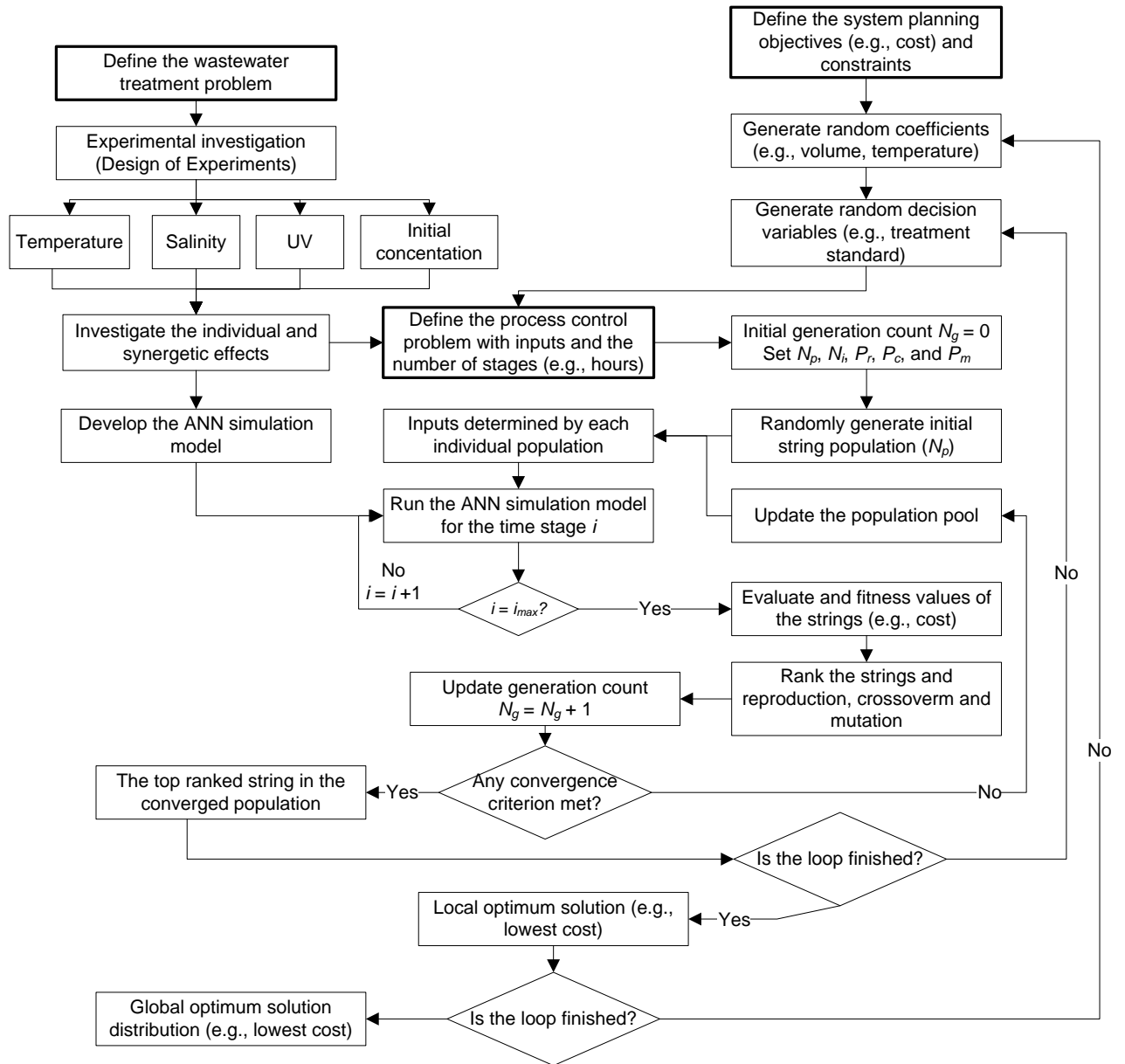


Figure 7.1 Flowchart of the IS-PCOP Approach for marine wastewater management

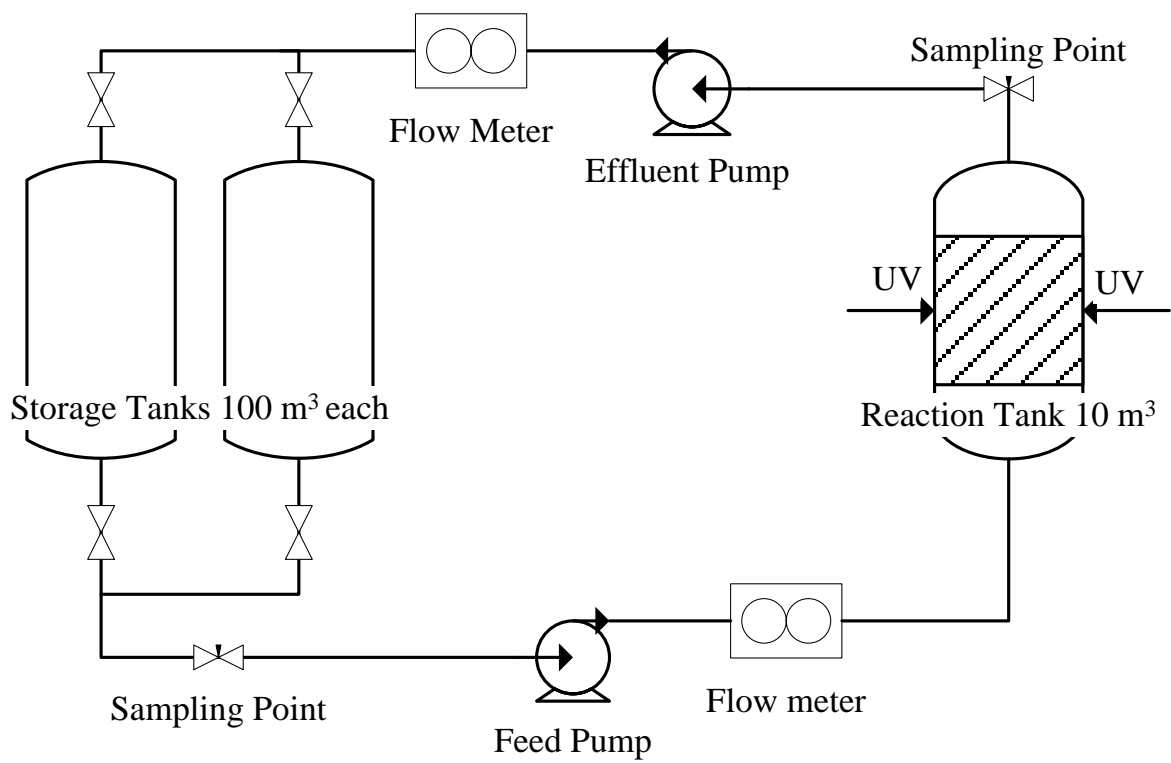


Figure 7.2 A schematic plot of the UV treatment system on the FPSO

7.3 Case Study

7.3.1 Bilge Water Treatment System

This case study is simplified based on a real-world case in the North Atlantic where a Floating Production Storage Offloading (FPSO) vessel. To protect confidentiality, all identifications have been removed. The onboard generated oily wastewater needs to be completely treated prior to discharge overboard or reuse. It should be noted that ballast water and produced water are not included in here. Produced water usually has its own separate treatment system due to the high volume. Ballast water is also not considered in this case as it is usually stored in segregated ballast tanks on new vessels and is free of any contact with oil. Therefore, in this case study, oily wastewater is mainly referred to bilge water that comes from vessel sewage leak, cooling water leak, deck drainage, machinery drainage, and the leak of jet fuel, lubricant oil, diesel oil, hydraulic oil, and crude oil.

Bilge water on the FPSO is typically directed towards the slops tank where it mixes with collected rainwater and air conditioning condensate. Mixed bilge water then undergoes oil-water separation and oil level testing to meet a discharge level at 15 ppm. Due to growing concerns and more stringent regulations (e.g., zero discharge policy in the Arctic), further treatment becomes desired to destruct dissolved organic pollutants (e.g., PAHs) left in the effluent from oil-water separator. In this case study, as described in Chapters 4, 5 and 6, UV secondary treatment system is deployed onboard to remove naphthalene, which is a typical PAH and of great environmental concern. Effluent from the oil-water separator is conveyed to storage tanks (100 m³) and then pumped to the

reaction tank for secondary treatment (i.e., UV irradiation) on a daily basis (Figure 7.2). There are two such storage tanks in order to make sure that one of them is available for storage while the other is under treatment cycle. The storage tanks are connected to an UV reaction tank (10 m³) where the average UV fluence rate can be controlled at 2.88, 4.27, 5.65, 6.96, and 8.27 mW cm⁻², respectively. This 5-level UV setting is the same as what has been used in Chapter 6, where different numbers of UV lamps (i.e., 2-6) were used to reflect different fluence rates. Water contained in storage and reaction tanks is assumed to be completely mixed. The flow rate, based on consulting local field engineers, can be adjusted from 0.05 to 0.2 m³ min⁻¹ by using two centrifugal pumps between the storage and reaction tanks. Water flow contained in the pipes between two tanks is assumed to be negligible.

7.3.2 Bilge Water Characterization

According to the corresponding monitoring program technical reports, the daily average discharge of bilge water from the FPSO is approximately 39.64 m³ day⁻¹ with a standard deviation of 5.02 m³ day⁻¹. The concentration of naphthalene in bilge water varies from 11 to 3070 µg L⁻¹, with a mean value and standard deviation of 177.47 and 17.12 µg L⁻¹, respectively (U.S. EPA, 1999; Netherlands National Water Board, 2008). Assumptions are made here that the daily discharge volume and the concentration of naphthalene both follow normal distribution determined by their mean values and standard deviations. Salinity of bilge water is assumed to follow normal distribution with a mean value and standard deviation of 22 and 2 psu, respectively. Bilge water temperature, according to relevant reports and consultation with field engineers, also

obeys normal distribution with an average value of 45 °C and a standard deviation of 2 °C.

7.3.3 Problem Formulation

For each Monte Carlo run, random bilge water volume and naphthalene concentration were generated based on their corresponding normal distributions. Then the proposed process control approach was adopted to minimize the daily treatment cost by examining 24 hours treatment periods. Effluent from the UV treatment system, depending on its quality in terms of naphthalene concentration (i.e., should be less than 30 $\mu\text{g L}^{-1}$ for safety concerns according to Kennedy (2006)), can be reused onboard and generate varying benefits. The operation planning goal was to minimize the total treatment cost over a certain period of time, subtracting the reusing benefit, in order to economically meet the discharge standard for weeks, months or years, given the wastewater characteristics would remain unchanged. The problem of this case study, therefore, can be restated as to choose the best UV treatment goal (i.e., naphthalene concentrations in both storage and reaction tanks) that can minimize the total net treatment cost over a 20-day period. Considering the available computation capacity and time constraint, the 20-day planning horizon was selected as a demonstrative example to show the effectiveness of the IS-PCOP Approach. Detailed problem formulation is summarized as follows:

Step 1: Set the UV treatment standard (β) to 30 $\mu\text{g L}^{-1}$.

Step 2: Generate random numbers for the daily volume of bilge water (z) and the concentration of naphthalene according to their pre-defined normal distributions, which are $N(39.64, 5.02)$ and $N(177.47, 17.12)$, respectively.

Step 3: Apply the ANN-DMINP approach to minimize the daily net cost f , which equals the treatment cost subtracting benefits from reusing treated water. Note that the population size (N_p) and maximum generation count (N_g) were set at 10 and 20, respectively by taking computation time into account. All other GA optimization parameters were kept the same as referring to Section 6.3.

$$\text{Min } f(x, y, z, \beta) = \sum_{i=1}^n (0.03 \times 60 \times x_i + 0.5 \times y_i) - z^{0.4} \times \text{Ln}(32 - \beta) \quad (7.5)$$

subject to:

$$h_1(x, y) \leq \beta \quad (7.6)$$

$$h_2(x, y) \leq \beta \quad (7.7)$$

$$lb \leq x, y \leq ub \quad (7.8)$$

where x and y are the flow rates ($\text{m}^3 \text{min}^{-1}$) and the intensity level of UV irradiation (i.e., 5 levels corresponding to 2.88, 4.27, 5.65, 6.96, and 8.27 mW cm^{-2}) during each hour, respectively; i is the number of hours; n in the total treatment period which could vary from 1 to 24 hours and must be integer (hour); z is the random daily volume of bilge water based on historical records (m^3); h_1 and h_2 stand for the final concentrations in the storage tank and the reaction tank, respectively; and β stands for the treatment standard. The cost coefficients in Equation 7.5 are arbitrarily predefined as \$0.5 per intensity level per hour and \$0.03 per liter, respectively. The flow rates of the pumps are equal and have to be greater than 0.05 and less than 0.2 L min^{-1} .

Step 4: Repeat Steps 2-3 for 20 iterations using Monte Carlo simulation to approximate a distribution of the daily net cost associated with the treatment standard of 30 $\mu\text{g L}^{-1}$. Note that the number of Monte Carlo iterations may be increased to obtain the output closed to

desired output. However, due to time and resource constraints, the number of iterations was set as 20 in this case study to demonstrate the feasibility of the proposed methodology. The total net cost over this 20-day period can also be obtained by summing up the daily net cost.

Step 5: Repeat Steps 1-4 for other treatment standards using Monte Carlo simulation. Ideally, the larger the number of iterations (e.g., 2000), the larger will be the computation time and the better will be the solution found. Due to concerns related to computation time, the standards are only examined at 5, 10, 15, 20 and 25 $\mu\text{g L}^{-1}$ to demonstrate the efficacy of the proposed methodology. Then a comparison can be carried out to identify the most economically advantageous strategy that should be adopted for operation planning over this 20-day period.

7.4 Results and Discussion

7.4.1 Integrated Process Control and Operation Planning

Figure 7.3 demonstrates the optimization results with the treatment standard of 15 $\mu\text{g L}^{-1}$. By generating random wastewater conditions (e.g., volume, concentration, salinity) and follow the procedure described in Section 7.3.3, the probability density estimates of the minimized daily treatment cost and net cost are plotted using the kernel-smoothing method. It can be seen that the most probable value of daily treatment cost lied between \$22 and \$32, with a mean of \$30.92. As for the net cost that takes reusing benefits into account, the most probable value ranged from \$10 to \$27 per day, with a mean of \$18.78 per day. As a comparison, the same probability density estimates of the 20 $\mu\text{g L}^{-1}$ standard seemed to shift to the lower side of costs (Figure 7.4). The most probably value

of daily treatment cost and net cost were both less than \$30 with means of \$28.94 and \$18.00, respectively. This decreasing trend indicated that, from the probability perspective, the standard of $20 \mu\text{g L}^{-1}$ can be more economically competitive over the standard of $15 \mu\text{g L}^{-1}$. Or in other words, choosing the more stringent standard (i.e., $15 \mu\text{g L}^{-1}$) resulted in an increase of treatment cost and reusing benefit. However, the increase of treatment cost overwhelmed that of benefit, leading to a higher net cost.

The same trend can be observed with the standards of 5 and $10 \mu\text{g L}^{-1}$ from Figures 7.5 and 7.6. As the tolerance of naphthalene concentration became stricter, sharp jumps in treatment cost were expected and attributable to the extended use of UV lamps and pumps. The mean treatment costs for the standards of 5 and $10 \mu\text{g L}^{-1}$ were \$55.96 and \$44.97, respectively, which were drastically higher than those of 15 and $20 \mu\text{g L}^{-1}$. On the other hand, stricter standards also offered more competitive reusing return. By reusing the treated effluent with 5 and $10 \mu\text{g L}^{-1}$ naphthalene concentrations, the average economic returns were calculated as \$14.43 and \$13.34, respectively. However, by subtracting benefits from the treatment costs, the average net costs were \$41.53 and \$31.62, respectively, which were higher than those of the 15 and $20 \mu\text{g L}^{-1}$ standards. Contrastingly, the treatment costs associated with the standards of 25 and $30 \mu\text{g L}^{-1}$ were fairly close to that of the $20 \mu\text{g L}^{-1}$ standard but slightly at the lower end (Figures 7.7 and 7.8). Their average treatment costs were \$27.64 and \$24.75, respectively; while the average net costs were \$18.70 and \$21.72, respectively (Table 7.1).

Figure 7.9 depicts the optimal daily treatment cost, net cost, and benefit at different standards, with the central points showing the average over the iterations, and the bars representing the standard deviation of the estimates. It can be seen that treatment cost and

reusing benefit both prominently went up with more stringent treatment standard. Such increases are reasonably self-explanatory because reducing the concentration of naphthalene to a lower level would certainly require more energy and therefore provide better reuse potential. Nonetheless, the increase of treatment cost was significant as the standard lowered from 15 to 5 $\mu\text{g L}^{-1}$; however, in between 20 and 30 $\mu\text{g L}^{-1}$, this trend was not prominent. As for reusing benefit, the increasing behaviour was only remarkable in between 25 and 30 $\mu\text{g L}^{-1}$. Such a difference resulted in the fact that the net cost tended to be higher at more stringent standards (Figure 7.9), implying that the increase of treatment cost dominated over the increase of benefit. A maximum and a minimum (i.e., \$41.53 per day and \$18.00 per day, respectively) were obtained at the standards of 5 and 20 $\mu\text{g L}^{-1}$, respectively, suggesting that the 20 $\mu\text{g L}^{-1}$ standard should be adopted by the decision makers as the most economically feasible option. The distance between the error bars can be further reduced if more Monte Carlo iterations can be carried out if available computation capacity becomes available. In addition, it should be noted that the calculation of reusing benefit would much dependent on the benefit function as shown in Equation 7.5. Here in this case study the reusing benefit decreased with increasing treatment standard; however, changing the benefit function may lead to totally different scenarios.

7.4.2 Comparison with Operation Planning without Process control

To validate if the coupling between process control and operation planning was advantageous over the traditional planning with no process control module, a comparison study was conducted by using the single-stage one time planning (Section 6.4.1) over the

20-day period. Traditional planning tends to be more conservative and risk-avoiding such that the single-stage planning was based on the average problem settings including daily bilge water volume (39.64 m^3), the concentration of naphthalene ($177.47 \text{ } \mu\text{g L}^{-1}$), salinity (22 psu), and temperature ($45 \text{ }^\circ\text{C}$). The UV intensity level and flow rate also remained unchanged with no process control efforts for each day within the 20-day period. Six treatment standards (i.e., 5, 10, 15, 20, 25, and $30 \text{ } \mu\text{g L}^{-1}$) were evaluated and the results are demonstrated in Figure 7.9. It can be seen that the total treatment costs (20-day period) with process control, at each treatment standard, were lower than the results from the single-stage planning. This finding indicated that integrating process control with traditional operation planning would provide more economically competitive options in operating the treatment system. Another interesting point is that, the difference between operation planning with and without process control decreased with more stringent standard. This was in accordance with the trend shown in Figure 6.5 because when the treatment needed to be completed within a short period of time or the concentration had to be lower than a strict standard, the treatment system tended to be at its full capacity and had less potential for process control tools to make a difference.

It can be seen that the combination of process control and operation planning can ensure the meeting of the economic objectives and timely completion of the tasks associated with the plans. The proposed IS-PCOP approach can well link process control and operation planning by simultaneously adopting different time-scales in computation. The hourly process control strategy forwards the results to the operation planning module where long-term arrangements can be further evaluated. The use of ANN model also plays a key role in predicting the treatment process. Many environmental processes, such

as wastewater treatment processes, tend to have a nonlinear nature that makes the prediction so complicated. Traditional process models that are developed based on classic theorems may not effectively describe these complex sub-systems because the models are usually created by applying different abstraction methods in which essential properties and key process indicators are preserved and insignificant details are left out. The use of ANN model, on the other hand, can well simulate the nonlinear processes using a black box nature which is more resistant to data uncertainty and lack of knowledge. In addition, the use of Monte Carlo simulation tackles the uncertainties, which may arise from a number of different sources, such as demands for materials and finished products, feedstock supplies, environmental and economic conditions, and customers' willingness to pay. By addressing the uncertainties and expressing the results in probability distributions, the decision makers would have more confidence in making proper decisions regarding the long-term and short-term operation of the processes.

Table 7.1 Summary of the optimization results at different treatment standard

| Standard ($\mu\text{g L}^{-1}$) | Treatment cost (\$/day) | | Net cost (\$/day) | | CR | Reusing benefit (\$/day) | |
|--------------------------------------|-------------------------|-------|-------------------|-------|-------|--------------------------|------|
| | Mean | SD | Mean | SD | | Mean | SD |
| 30 | 24.75 | 12.20 | 21.72 | 12.10 | 0.999 | 3.02 | 0.17 |
| 25 | 27.64 | 13.64 | 18.70 | 12.95 | 0.999 | 8.94 | 0.87 |
| 20 | 28.94 | 14.71 | 18.00 | 14.42 | 0.999 | 10.94 | 0.63 |
| 15 | 30.92 | 9.09 | 18.78 | 8.74 | 0.997 | 12.14 | 0.78 |
| 10 | 44.97 | 18.30 | 31.62 | 17.88 | 0.999 | 13.34 | 0.72 |
| 5 | 55.96 | 12.69 | 41.53 | 12.29 | 0.999 | 14.43 | 0.73 |

Note: CR represents the correlation coefficient between daily treatment cost and net cost; and SD stands for standard deviation.

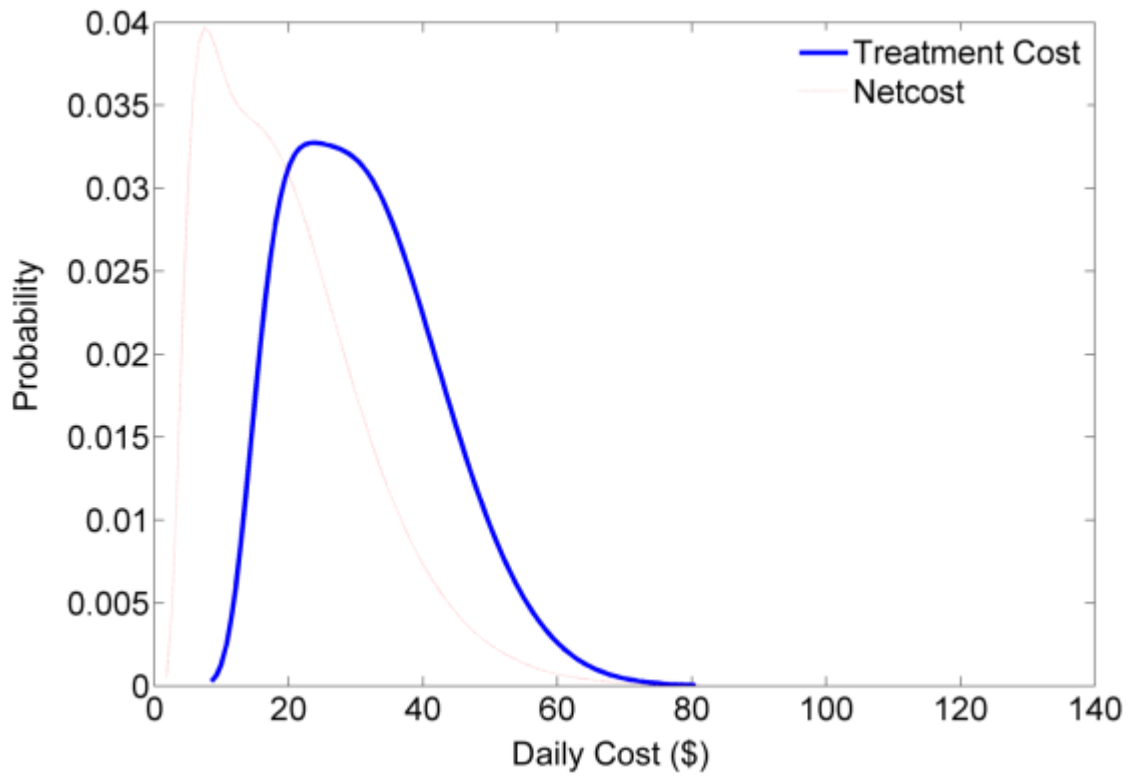


Figure 7.3 Probability density estimates of the daily treatment cost and net cost of the 15 $\mu\text{g L}^{-1}$ standard

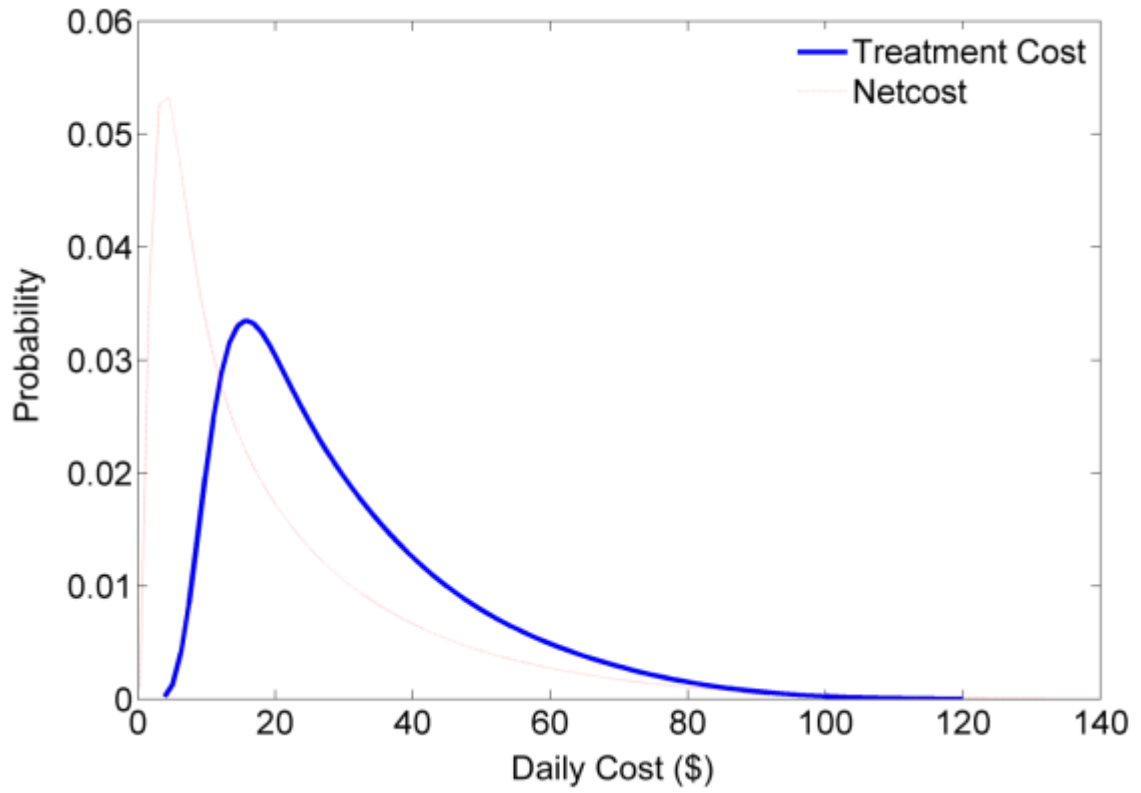


Figure 7.4 Probability density estimates of the daily treatment cost and net cost of the 20 $\mu\text{g L}^{-1}$ standard

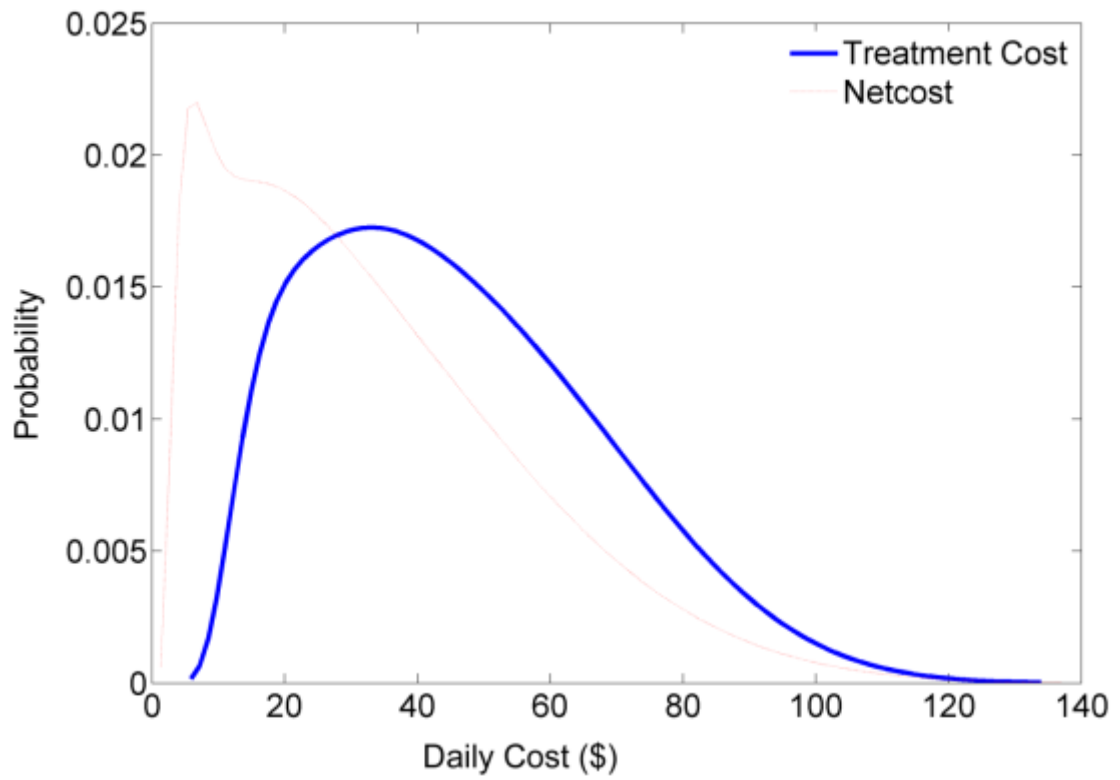


Figure 7.5 Probability density estimates of the daily treatment cost and net cost of the $10 \mu\text{g L}^{-1}$ standard

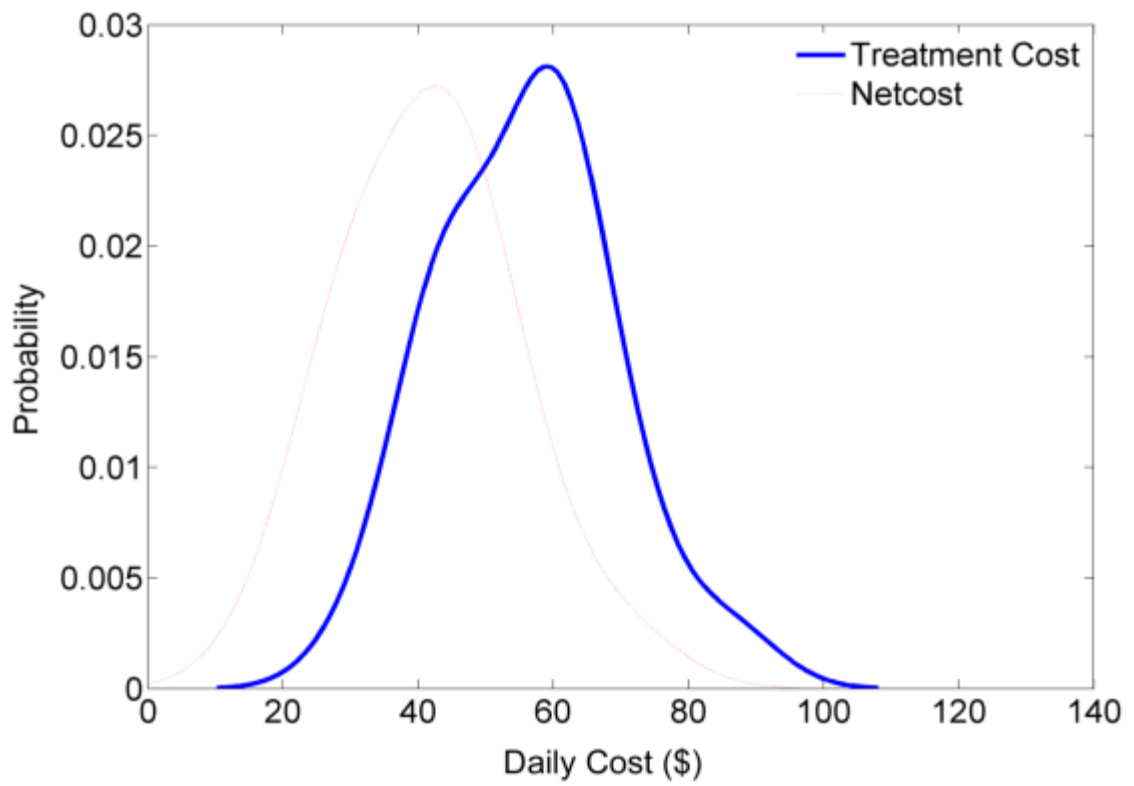


Figure 7.6 Probability density estimates of the daily treatment cost and net cost of the $5 \mu\text{g L}^{-1}$ standard

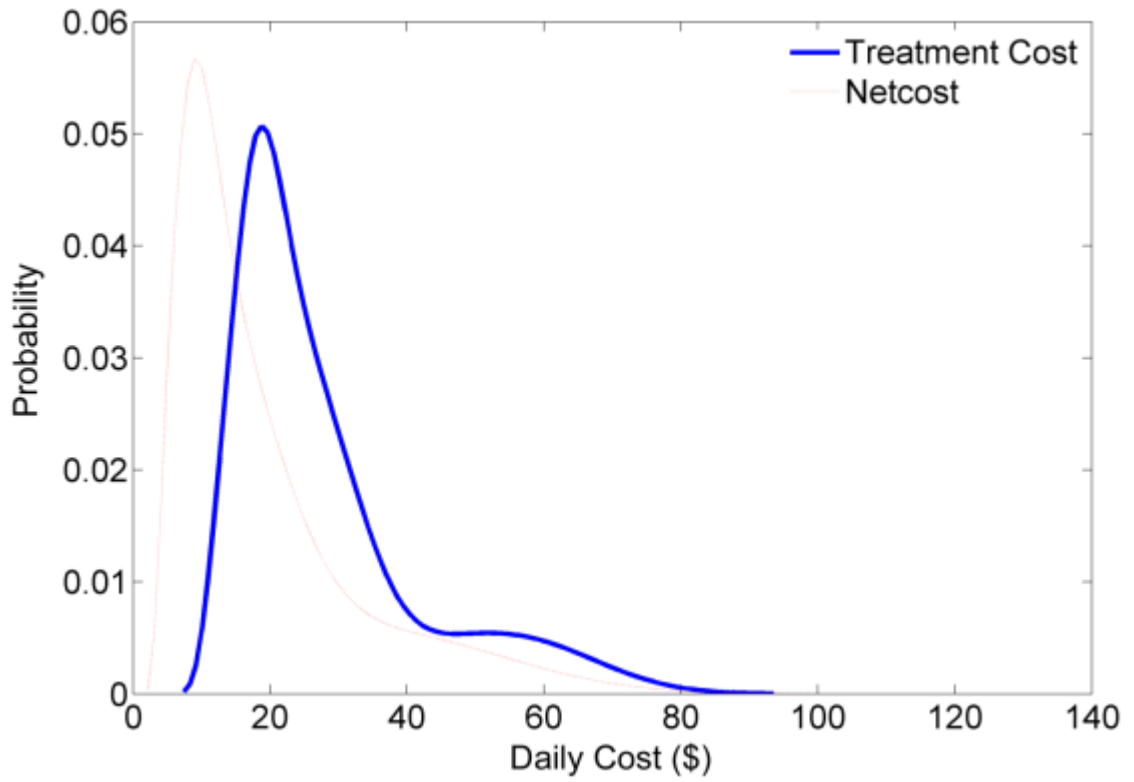


Figure 7.7 Probability density estimates of the daily treatment cost and net cost of the 25 $\mu\text{g L}^{-1}$ standard

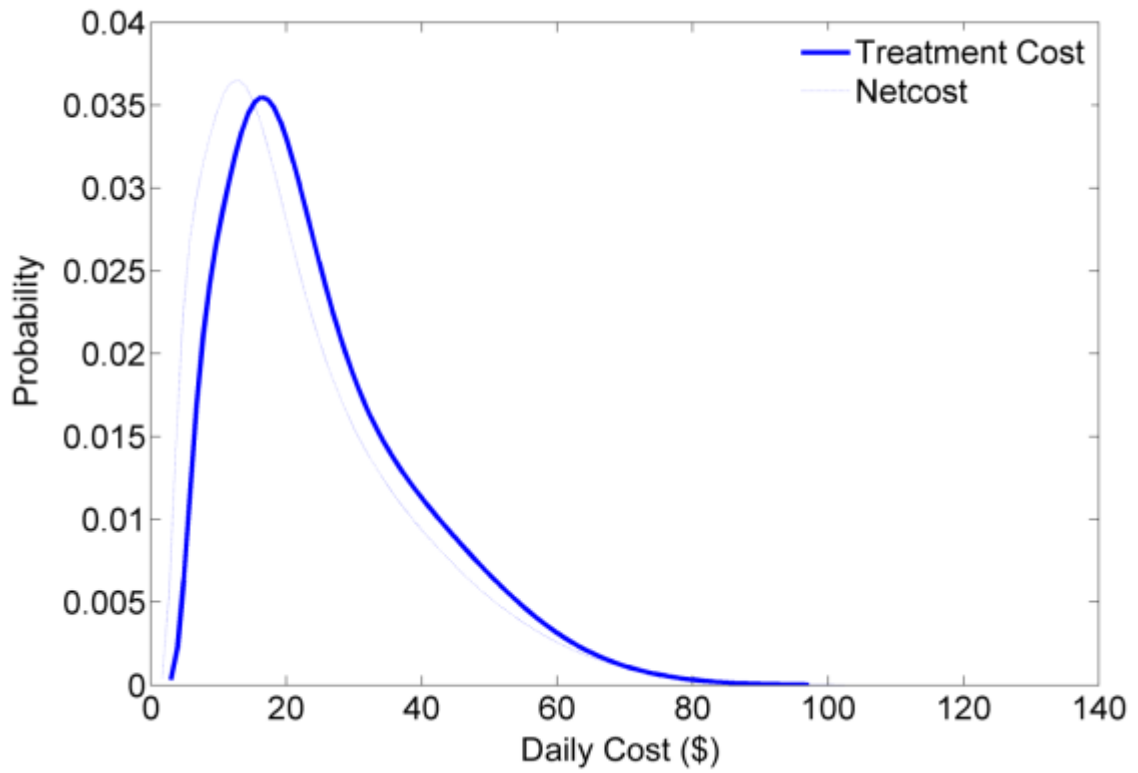


Figure 7.8 Probability density estimates of the daily treatment cost and net cost of the 30 $\mu\text{g L}^{-1}$ standard

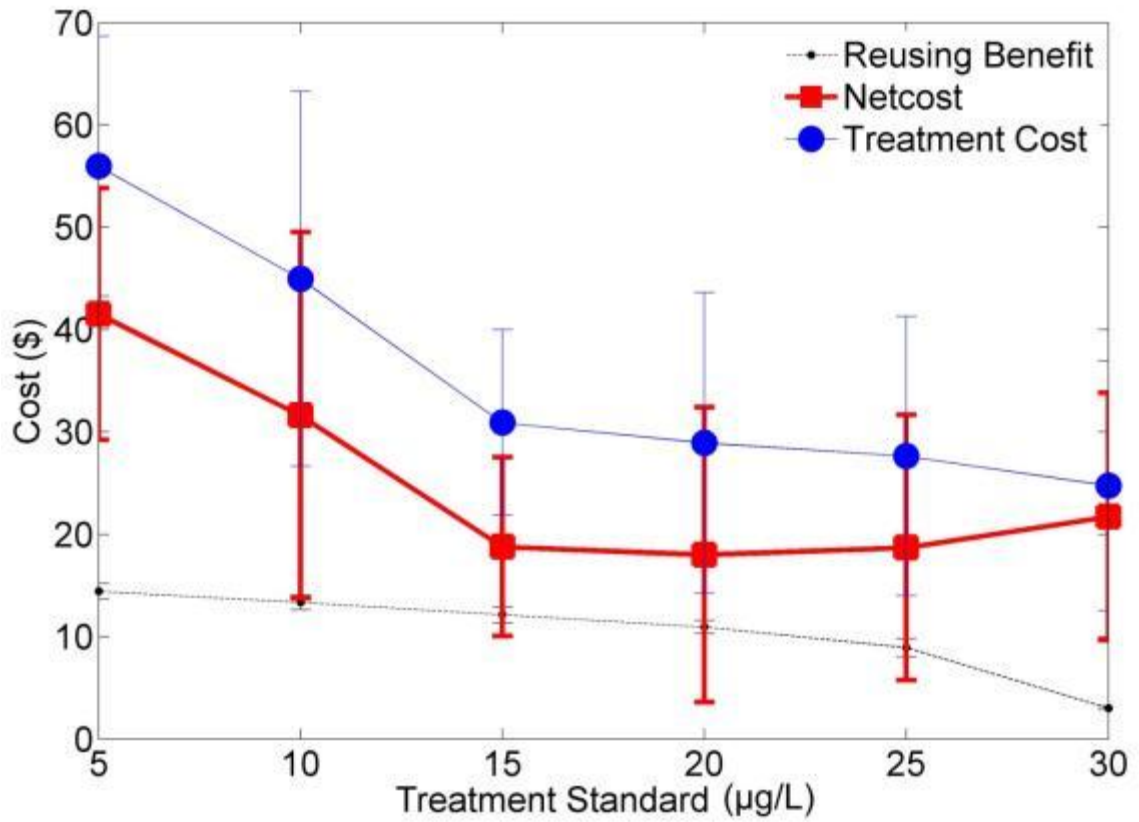


Figure 7.9 Error bar plot of daily treatment cost, reusing benefit, and net cost of each treatment standard

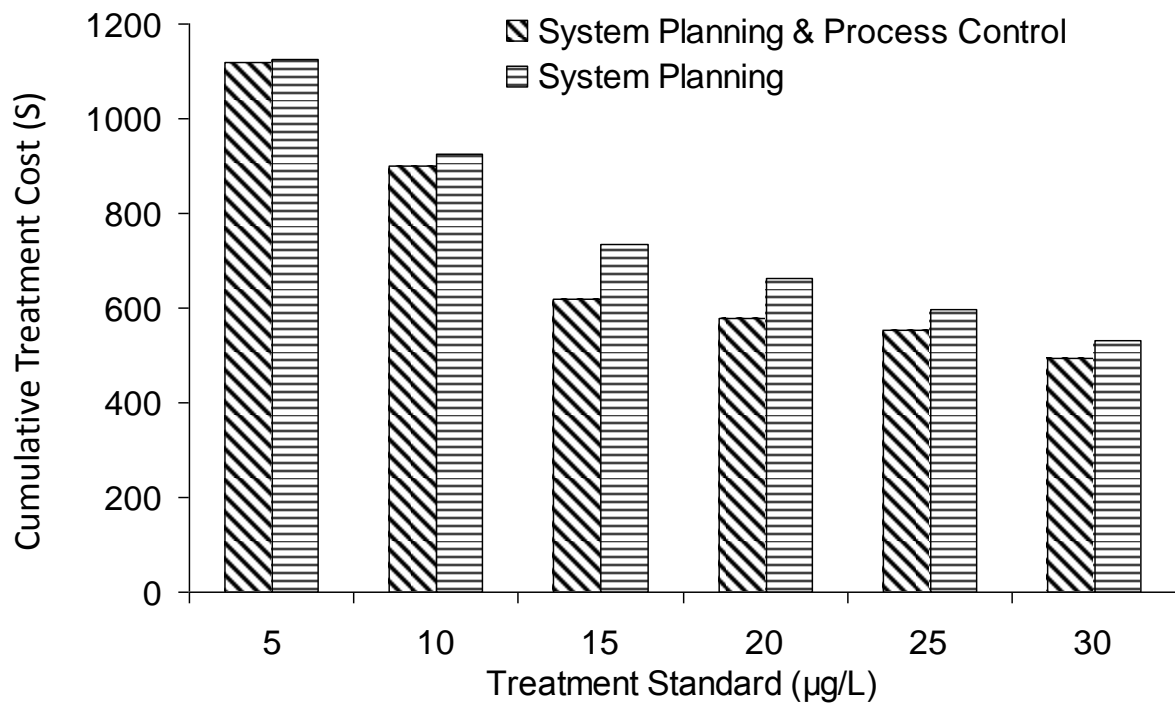


Figure 7.10 The cumulative treatment cost comparison over the 20-day period between operation planning with process control and without process control

7.5 Summary

This chapter investigates the feasibility of integrating dynamic process control with traditional operation planning as an integrated simulation-based process control and operation planning (IS-PCOP) system. A case study related to oily wastewater management on a FPSO was conducted to examine the efficacy of this proposed integration. The process control approach was used to optimize the treatment cost of removing naphthalene from bilge water using UV irradiation. Treated effluent, depending on the remaining concentration of naphthalene, was reused and could produce benefit. Monte Carlo simulation was applied to generate the parameters (e.g., volume, concentration and temperature) of bilge water and examine the net cost to obtain the distribution of optimal solutions at a series of treatment strategies. The results showed that choosing the $20 \mu\text{g L}^{-1}$ treatment standard was the most economically competitive option. As compared to the traditional operation planning without process control, the integrated approach achieved more economically competitive results. The proposed integration of dynamic process control and operation planning was successfully applied and demonstrated through this case study. Outputs from such integration can offer decision makers critical information and more confidence that is not likely to be provided by traditional techniques. Future research directions may focus on optimizing the computation procedure in order to accommodate larger number of Monte Carlo iterations, introduce fuzzy uncertainty into the proposed approach, and further validate by large-scale case studies.

CHAPTER 8

CONCLUSIONS AND RECOMMENDATIONS

8.1 Summary

Marine oily wastewater has been recently criticized as a major source of oil pollution in the marine environment. Unlike catastrophic oil spills, the discharge of oily wastewater, including ballast water, produced water, and bilge water, usually occurs on a daily basis without triggering a mitigation response. The accumulated effects of discharging untreated or partially treated oily wastewater can lead to significantly negative impacts on marine lives and even human health. While the dispersed free oil, oil-in-water or water-in-oil emulsions can be mostly removed by gravity separation or hydrocyclone, residual oil droplets and dissolved organic compounds including particularly polycyclic aromatic hydrocarbons (PAHs) would, however, remain unaffected. The occurrence of PAHs is usually of the greatest concern because of their high resistance towards biodegradation, extreme toxicity to marine biota, and possible carcinogenicity and mutagenicity. Further polishing treatment has therefore become necessary to further remove PAHs prior to discharge.

In recent years, UV photooxidation and other advanced oxidation techniques (e.g., UV/H₂O₂, UV/O₃) have been gaining significant attention. They have been regarded as promising solutions to the removal of PAHs because of their relatively small footprint, low cost, and high efficiency. However, most of the previous studies have focused on freshwater systems rather than marine environments where salinity and complex matrix effects play a dominant role. Moreover, the research efforts on numerical modeling and performance optimization of these techniques have also been limited due to their multiphysics nature and the complexity of synergistic effects. Such advanced treatment systems, as compared to the traditional ones (e.g., gravity separation and adsorption), are

still lack of in-depth understanding of their reaction mechanisms, performance evaluation, process optimization, operation planning, and particularly the coupling between process control and operation planning, which may drastically hinder their widespread applications in shipping and offshore oil and gas industries.

This research, therefore, started from proposing two novel decision making tools to guide the operation planning of marine oily wastewater management, particularly using UV or other advanced oxidation techniques. Firstly, a stochastic simulation-based hybrid interval fuzzy programming (SHIFP) approach was developed to tackle uncertainties inherent in the decision making of operation planning. As with the traditional fuzzy linear programming, fuzzy set theory was used to model uncertainty such that the results would provide the decision makers more flexibility for the choice of the solution. Uniform interval distribution was assumed due to the lack of precise information on both coefficients and variables.

A case study related to recovered oily water treatment during offshore oil spill cleanup was carried out to test the proposed approach. The local authority had a number of incineration barges, vacuum trucks, centrifugal separators, and temporary storage facilities to treat the recovered oily wastewater. However, it was unknown that how many facilities should be used and how much wastewater should be delivered to each facility. The results demonstrated that the objective function (maximum daily treatment capacity), if defuzzified by the centroid defuzzification technique, was likely to follow the normal distribution. In addition, the shapes of the fuzzy decision variables, corresponding to the maximized objective function, can be categorized into seven groups with different probability such that decision makers can more confidently allocate limited resources.

Emergency planners and administrators are expected to benefit from this study by gaining an insight into how to wisely allocate resources in responding to an offshore oil spill. Secondly, when marine oily water is collected or ready for treatment, choosing the best available technology usually becomes the first priority for decision makers.

As one of the most widely exploited multi-criteria decision making (MCDM) approaches, the analytic hierarchy process (AHP) has been well documented in the literature. However, it has been criticized for its inability to quantify the uncertainty associated with decision making. A hybrid fuzzy stochastic analytical hierarchy process (FSAHP) approach was developed in order to assist decision making with more confidence by integrating fuzzy set theory, probabilistic distribution, pairwise comparison and Monte Carlo simulation.

A case study related to ballast water management was carried out to verify the feasibility and efficiency of the proposed approach. Five treatment technologies were evaluated against a number of environmental, economic, and technical criteria. The results revealed that UV was ranked with the highest overall score at 100% confidence level, indicating that the null assumption that it was not probabilistic optimal (versus the alternate assumption that it is) was rejected. Ozone, heat treatment, and ultrasound had the second, third, and fourth places at the confidence levels of 61.0–71.4%, 56.0–68.4%, and 78.4–84.6%, respectively. Considerable overlaps existed among these three alternatives which may be attributed to the irreducible uncertainty caused by subjective judgments or lack of knowledge. The results also illustrated that both the center of gravity (COG) and Chen's defuzzification methods were able to provide the decision makers with reliable decision references. The proposed FSAHP approach can offer a number of

benefits such as the capability of capturing human's appraisal of ambiguity and addressing the effects of uncertain judgment when dealing with insufficient information or biased opinions.

The next objective of this research was to develop a process control approach that can be used to real-time control UV or other advanced oxidation treatment technologies. The foundation of any process control methods rely much on the effectiveness and accuracy of process simulation. In this study, therefore, the concept of artificial neural networks (ANNs) was adopted for simulation in order to tackle the nonlinearity inherent in these advanced treatment system. Experimental results are the prerequisite to an ANN simulation model, thus the UV induced photodegradation of a typical PAH, namely naphthalene in seawater, was chosen as an example for developing the simulation model. A full factorial design of experiments (DOE) was employed to determine the significance of each factor being tested as well as their interactions.

The experimental results showed that the removal of naphthalene followed first order kinetics in all experimental runs and the most influential factors were fluence rate, temperature and the interaction between temperature and initial concentration. Further analysis revealed that the reaction rate constants were linearly related to the number of lamps. High salinity suppressed the performance of UV irradiation which was mainly caused by the presence of bromide (Br^-), carbonate (CO_3^{2-}) and bicarbonate (HCO_3^-) ions in seawater. In addition, increasing temperature from 23 to 40 °C seemed to stimulate the removal of naphthalene in seawater by exciting the collision between photons and molecules. The effect of initial concentration was not prominent while the

average reaction rate constant at high concentration was slightly lower than that at low concentration.

Based on the experimental results, a three-layer backpropagation neural network was developed to simulate the UV-induced photodegradation of naphthalene in marine oily wastewater. The photochemical process was successfully predicted by using 12 neurons in the hidden layer and the Levenberg-Marquardt backpropagation algorithm. The network was trained to provide a good overall linear fit with a slope of 0.97 and a correlation of determination (R^2) of 0.943. All input variables in this study (i.e., initial concentration, salinity, fluence rate, temperature and reaction time) had considerable effects on the photodegradation process. The outputs of sensitivity analysis and ANOVA revealed that fluence rate and temperature were noted as the most influential variables, which aligned with the experimental observations. The results showed that the developed ANN model was capable of accurately simulating the naphthalene removal process and reproduce the experiment.

Based on the developed ANN model, an ANN-based dynamic mixed integer nonlinear programming (ANN-DMINP) approach was proposed by integrating process simulation (i.e., ANN), stochastic optimization (GA) and the multi-stage principle. This process control approach was examined through a case study simplified from a real world problem. UV photodegradation of naphthalene, as described in Chapters 4 and 5, was chosen in the case study as an example to demonstrate the applicability of the proposed approach. The results from the case study showed that the treatment cost in a fixed 36-hour period was minimized to \$9.11 by using the ANN-DMINP approach. As a comparison, the single-stage optimization with constant variables was also applied and

the treatment cost was 25.7% higher at \$11.45. A Monte Carlo simulation was also performed to conclude that if the operator randomly set the flow rate and the number of lamps as constants during the 36-hour period, then there would be a great chance that the treatment standard cannot be met. If considering time as another flexible variable, the treatment cost reached its minimum at 27 hours with \$8.71 and \$8.94 for the ANN-DMINP approach and the single-stage optimization, respectively. A sensitivity analysis for the number of stages demonstrated that, regardless the length of treatment period, more optimization stages can generally reduce treatment cost, but may lead to extra manpower needs and affect system stability. It was recommended to first seek the best solution with less optimization stages, and then using the solution as an initial population for more optimization stages, if necessary. By using UV irradiation as an example, these findings well demonstrate that the developed ANN-DMINP approach can be helpful in the context of reducing the time and cost associated with marine oily wastewater treatment, and even many other environmental processes.

The combination of process control and operation planning can ensure the meeting of the economic objectives and timely completion of the tasks associated with the plans. An integrated simulation-based process control and operation planning (IS-PCOP) system was developed in this research to fulfil that purpose. Such a combination is expected to greatly reduce system cost and to maximize economic and environmental benefits associated with marine oily wastewater treatment. The IS-PCOP system was employed to dynamically control one or more processes associated with the objective function while Monte Carlo simulation was adopted to find the optimal solution. A real-world case study related to offshore wastewater management on a FPSO was conducted to examine the

efficacy of the proposed integration. The ANN-DMINP approach was used to optimize the treatment cost of removing naphthalene from bilge water using UV irradiation. Treated effluent, depending on the remaining concentration of naphthalene, was reused and could produce varying benefit. Monte Carlo simulation was applied to generate the parameters (e.g., volume, concentration and temperature) of daily bilge water and examine the net cost to obtain the distribution of optimal solutions at a series of treatment standards. The results showed that choosing the $20 \mu\text{g L}^{-1}$ treatment standard was the most economically competitive option. As compared to the traditional operation planning without process control, the integrated approach achieved more economically competitive results.

The proposed IS-PCOP approach can well link process control and operation planning by simultaneously adopting different time-scales in computation. The hourly process control strategy forwards the results to the operation-planning module where long-term arrangements can be further evaluated. The use of ANN model also plays a key role in predicting the treatment process. Many environmental processes, such as wastewater treatment processes, tend to have a nonlinear nature that makes the prediction so complicated. Traditional process models that are developed based on classic theorems may not effectively describe these complex sub-systems because the models are usually created by applying different abstraction methods in which essential properties and key process indicators are preserved and insignificant details are left out. The use of ANN model, on the other hand, can well simulate the nonlinear processes using a black box nature which is more resistant to data uncertainty and lack of knowledge. In addition, the use of Monte Carlo simulation tackles the uncertainties, which may arise from a number

of different sources, such as demands for materials and finished products, feedstock supplies, environmental and economic conditions, and customers' willingness to pay. By addressing the uncertainties and expressing the results in probability distributions, the decision makers would have more confidence in making proper decisions regarding both long-term and short-term operations of the processes.

8.2 Research Contributions

This research can be summarized and highlighted by the following contributions:

1) Two novel operation planning tools, namely the stochastic simulation-based hybrid interval fuzzy programming (SHIFP) approach and the hybrid fuzzy stochastic analytical hierarchy process (FSAHP) approach, have been developed for marine oily wastewater treatment and management. The SHIFP approach can help operation planners and administrators in oily wastewater treatment planning while the FSAHP method has the capability of capturing human's appraisal of ambiguity and addressing the effects of uncertain judgment when dealing with insufficient information or biased opinions.

2) An experimental study has been carried out to investigate UV irradiation as an option to treat seawater that contains PAHs (e.g., naphthalene). The photolysis mechanism and kinetics of naphthalene has been tested under varying ambient conditions including salinity, UV fluence rate, initial concentration and temperature. The results from this study are expected to not only help understand the photolysis mechanism of PAHs but serve as a good example to develop the integrated process control and operation planning system for marine oily wastewater management.

3) Based on the experimental results, a neural network model has been developed to simulate the UV-induced photodegradation of naphthalene in seawater. The network has been trained to provide a good overall linear fit with a slope of 0.97 and a correlation of determination (R^2) of 0.943. The results can demonstrate the fact that the developed ANN model can accurately simulate the naphthalene removal process and reproduce the experiment. This modeling tool serves as a core part of the following integrated process control and operation planning system.

4) An ANN-based dynamic mixed integer nonlinear programming (ANN-DMINP) approach has been proposed to help optimize the performance of the UV treatment process. This approach is an integration of simulation, stochastic optimization and the multi-stage principle that has never been coupled in the literature. The results of a case study have revealed that the proposed dynamic control approach can be used to rationally make decisions at different time points and to achieve better performance in terms of cost or efficacy.

5) An innovative integration of process control with traditional operation planning has been accomplished by using neural networks, genetic algorithm, multistage principle, and Monte Carlo simulation. The proposed IS-PCOP system can well link process control and operation planning by simultaneously adopting different time-scales in computation. The use of ANN modeling plays a key role in capturing the nonlinear behaviour of the treatment process. Genetic algorithm and multistage principle can ensure the efficient stochastic search for the optimal solutions in a real-time basis. In addition, Monte Carlo simulation yields a better insight on uncertainties, which may arise from a number of different sources. By addressing the uncertainties and expressing the results in probability

distributions, the decision makers would have more confidence in making proper decisions regarding the short-term and long-term operations. It is concluded that the combination of process control and operation planning can ensure the meeting of the economic objectives and timely completion of the tasks associated with the plans. Outputs from such integration can offer decision makers critical information and more confidence that is not likely to be provided by traditional techniques. The proposed IS-PCOP system can also be used for many other engineering sectors, which involve both dynamic processes and operation planning.

8.3 Publications

Papers under preparation

1. **Jing, L.,** Chen, B., Zhang, B.Y., and Li, P. (2014). Dynamic process control of marine oily wastewater treatment using UV irradiation. *Journal of Environmental Engineering*, ASCE, to be submitted.
2. **Jing, L.,** Chen, B., and Zhang, B.Y. (2014). An integrated simulation-based process control and operation planning (IS-PCOP) approach for marine wastewater management. *Journal of Environmental Management*, to be submitted.

Refereed Journal Papers

1. **Jing, L.,** Chen, B., and Zhang, B.Y. (2014). Modeling of UV-induced photodegradation of naphthalene in marine oily wastewater by artificial neural

networks. *Water, Air, & Soil Pollution*, 225(4), 1-14, doi:10.1007/s11270-014-1906-0.

2. **Jing, L.**, Chen, B., Zhang, B.Y., Zheng, J.S., and Liu, B. (2014). Naphthalene degradation in seawater by UV irradiation: the effects of fluence rate, salinity, temperature and initial concentration. *Marine Pollution Bulletin*, 81, 149-156, doi: 10.1016/j.marpolbul.2014.02.003.
3. Li, P., Chen, B., Zhang, B.Y., **Jing, L.**, and Zheng, J.S. (2014). Monte Carlo simulation-based dynamic mixed integer nonlinear programming for supporting oil recovery and devices allocation during offshore oil spill responses. *Ocean & Coastal Management*, 89, 58-70, 10.1016/j.ocecoaman.2013.12.006.
4. **Jing, L.**, Chen, B., Zhang, B.Y., and Li, P. (2013). A hybrid stochastic-interval analytic hierarchy process (SIAHP) approach for prioritizing the strategies of reusing treated wastewater. *Mathematical Problems in Engineering*, vol. 2013, Article ID 874805, 10 pages, doi:10.1155/2013/874805.
5. **Jing, L.**, Chen, B., and Zhang, B.Y. (2013). A hybrid fuzzy stochastic analytical hierarchy process (FSAHP) approach for evaluating ballast water treatment technologies. *Environmental Systems Research*, 2:10, doi:10.1186/2193-2697-2-10.

6. **Jing, L.**, Chen, B., Zhang, B.Y., and Li, P. (2012). A stochastic simulation-based hybrid interval fuzzy programming approach for optimizing the treatment of recovered oily water. *The Journal of Ocean Technology*, 7(4), 59-72.
7. Li, P., Chen, B., Zhang, B.Y., **Jing, L.**, and Zheng, J.S. (2012). A multiple-stage simulation-based mixed integer nonlinear programming approach for supporting offshore oil spill recovery with weathering processes. *The Journal of Ocean Technology*, 7(4), 87-105.
8. **Jing, L.**, Chen, B., Zhang, B.Y., Li, P., and Zheng, J.S. (2012). A Monte Carlo simulation aided analytic hierarchy process (MC-AHP) approach for best management practices assessment in nonpoint source pollution control. *Journal of Environmental Engineering ASCE*, 139(5), 618-626, doi:10.1061/(ASCE)EE.1943-7870.0000673.
9. **Jing, L.**, Chen, B., Zhang, B.Y., and Peng, H.X. (2012). A review of ballast water management practices and challenges in harsh and arctic environments. *Environmental Reviews*, 20, 83-108, doi: 10.1139/a2012-002.
10. Chen, B., **Jing, L.**, Zhang, B.Y., and Liu, S. (2011). Wetland Monitoring, Characterization and Modeling under Changing Climate in the Canadian Subarctic. *Journal of Environmental Informatics*, 18(2), 55-64, doi:10.3808/jei.201100199.

11. **Jing, L.**, and Chen, B. (2011). Hydrological Modelling of the Deer River Watershed – a Comparison between SLURP and WATFLOOD. *Environmental Engineering Science*, 28(7), 521-533, 10.1089/ees.2010.0277.
12. **Jing, L.**, and Chen, B. (2011). Field Investigation and Hydrological Modelling of a Subarctic Wetland - the Deer River Watershed. *Journal of Environmental Informatics*, 17(1), 36-45, doi: 10.3808/jei.201100185.

Other Refereed Publications

1. **Jing, L.**, Chen, B., Zhang, B.Y., Husain, T., and Li, P. (2014). Modeling and Process Control of Marine Oily Wastewater Treatment Using UV Irradiation. Poster presented at the Arctic Oil & Gas North America Conference 2014, St. John's, Canada.
2. **Jing, L.**, Chen, B., Zhang, B.Y., Zheng, J.S. (2013). The Effects of Salinity and Temperature on the Photolysis of Naphthalene Using UVC Irradiation. *In: Proceedings of the 36th AMOP Technical Seminar on Environmental Contamination and Response*, Halifax, Canada, pp. 591-600.
3. **Jing, L.**, Chen, B., Zhang, B.Y., Li, P., and Wu, H.J. (2013). Modeling the Effects of Photon Flux, Salinity and Temperature on UVC Photolysis of Polycyclic Aromatic Hydrocarbons (PAHs) in Oily Seawater. Poster presented at the Arctic

Oil & Gas North America Conference 2013, St. John's, Canada.

4. **Jing, L.**, Chen, B., and Zhang, B.Y. (2013). A Stochastic Fuzzy Analytical Hierarchy Process for Ballast Water Management. Poster presented at the 23rd Annual International Conference on Soil, Water, Energy & Air, San Diego, U.S.
5. Zhu, Z.W., Zhang, B.Y., Chen, B., **Jing, L.**, and Lin, W.Y. (2012). Development of a 3-dimensional pilot-scale physical model for demonstration of enhanced in-situ bioremediation in Newfoundland and Labrador, Canada. *In: Proceedings of CRETE2012 - the 3rd International Conference on Industrial and Hazardous Waste Management, Chania, Greece, P49: 1-8.*
6. Li, P., Chen, B., Zhang, B.Y., and **Jing, L.** (2012). A new agro-industrial waste management model for supporting rural co-operative stewardship and sustainable development. *In: Proceedings of CRETE2012 - the 3rd International Conference on Industrial and Hazardous Waste Management, Chania, Greece, S13.3: 1-8.*
7. Li, P., Chen, B., Zhang, B.Y., **Jing, L.**, and Zheng, J.S. (2012). Development of a Multi-stage Simulation Based Mixed Integer Nonlinear Programming Approach for Supporting Offshore Oil Spill Recovery. *In: Proceedings of the 35th AMOP Technical Seminar on Environmental Contamination and Response, Vancouver, Canada, pp. 434-447.*

8. **Jing, L.**, Chen, B., Zhang, B.Y., Zheng, J.S., and Li, P. (2012). A Stochastic Analytical Hierarchy Process for Supporting Nonpoint Source Pollution Control. *In: Proceedings of the 2012 Canadian Society for Civil Engineering Annual Conference, Edmonton, Canada, pp. 1167-1176.*

9. **Jing, L.**, Chen, B., Zhang, B.Y., and Abdel-Razek, A.K. (2011). A Decision Support System for Ballast Water Management in Harsh Environments. *In: Proceedings of the 64th Canadian Water Resources Association National Conference “Our Water – Our Life – The Most Valuable Resource”, St. John's, Canada.*

8.4 Recommendations for Future Research

1) The polishing treatment of marine oily wastewater may target, aside from PAHs, many other organic pollutants that may raise environmental concerns. Such pollutants may include, but not limited to, BTEX, phenols, alkyl phenols, alkylated PAHs, and aliphatic hydrocarbons. The evaluation criteria for treatment efficiency, other than individual pollutants, may consider total petroleum hydrocarbon (TPH), total organic carbon (TOC), chemical oxygen demand (COD), and toxicity. Oily wastewater samples including offshore produced water, bilge water, and ballast water from the offshore industries are also recommended for experimental studies. In addition, the treatment options may expand to a broader perspective to include more powerful techniques, such as other advanced oxidation processes (AOPs) and nanofiltration.

2) The modeling of marine oily wastewater treatment could be further improved by

coupling ANN with fuzzy logic and stochastic uncertainty. The basic learning rule of ANN is based on the gradient method, which has been criticized for its slowness and tendency to be trapped in local minima. In addition, they tend to have difficulties in performing heuristic reasoning of the domain problem. The linguistic fuzzy-if rules can well adopt expert opinions in mapping input linguistic variables to corresponding output variables. This feature is advantageous as it allows the performance analysis within the framework of seizure prediction characteristics. On the other hand, if ANN model inputs are fixed while outputs are subject to stochastic uncertainty (i.e., known distributions of specific parameters), which can be usual in repetitive experimental investigations, the weights and biases of the ANN model may also inherit stochastic distribution to capture such uncertainty. One can also use commercial multi-physics tools COMSOL or ANSYS to simulate and optimize complex physical/chemical/biological processes with the aid of Matlab.

3) In this research, UV irradiation targeting on PAHs has been used as an example to demonstrate the applicability of the IS-PCOP system. It can also be applied to many other environmental sectors where dynamic process control and operation planning are both important. For example, to assess the impacts and optimize system configurations for a municipal solid waste collection and management system, the planning targets may include the number, sizes and locations of landfills and collection stations to minimize long-term costs while the operation parameters are subject to a finer scale such as daily truck route and hourly collection rates. Another example can be directed to a city's wastewater treatment system. Operation planning can be used to decide the location, capacity and technology of the treatment plants according to the population and water

demand of the city. Meanwhile, process control techniques are responsible for minimizing treatment costs and associated health risks. Some other potential application sectors include oil spill cleanup, soil and groundwater remediation, etc. In addition, two-stage stochastic programming and approximate dynamic programming can be further introduced into the IS-PCOP system.

APPENDICE

Appendix A: Datasets for developing the ANN model

| Initial Concentration ($\mu\text{g L}^{-1}$) | Salinity (psu) | UV Lamps | Temperature ($^{\circ}\text{C}$) | Time (min) | Removal Rate (%) |
|--|---------------------------|---------------------|--|-----------------------|-----------------------------|
| 10 | 25 | 2 | 23 | 30 | 2.52 |
| 10 | 25 | 2 | 23 | 60 | 19.70 |
| 10 | 25 | 2 | 23 | 90 | 36.58 |
| 10 | 25 | 2 | 23 | 120 | 48.56 |
| 10 | 25 | 2 | 23 | 150 | 60.66 |
| 10 | 25 | 2 | 23 | 180 | 67.99 |
| 10 | 25 | 2 | 23 | 210 | 74.09 |
| 10 | 25 | 2 | 23 | 240 | 78.78 |
| 10 | 25 | 6 | 23 | 30 | 52.81 |
| 10 | 25 | 6 | 23 | 60 | 64.18 |
| 10 | 25 | 6 | 23 | 90 | 80.54 |
| 10 | 25 | 6 | 23 | 120 | 90.00 |
| 10 | 25 | 6 | 23 | 150 | 95.15 |
| 10 | 25 | 6 | 23 | 180 | 96.93 |
| 10 | 25 | 6 | 23 | 210 | 98.30 |
| 10 | 25 | 6 | 23 | 240 | 98.63 |
| 10 | 32.5 | 2 | 23 | 30 | 0.00 |
| 10 | 32.5 | 2 | 23 | 60 | 17.25 |
| 10 | 32.5 | 2 | 23 | 90 | 38.51 |
| 10 | 32.5 | 2 | 23 | 120 | 37.80 |
| 10 | 32.5 | 2 | 23 | 150 | 50.26 |
| 10 | 32.5 | 2 | 23 | 180 | 53.99 |
| 10 | 32.5 | 2 | 23 | 210 | 77.17 |
| 10 | 32.5 | 2 | 23 | 240 | 68.72 |
| 10 | 32.5 | 6 | 23 | 30 | 34.23 |
| 10 | 32.5 | 6 | 23 | 60 | 53.30 |
| 10 | 32.5 | 6 | 23 | 90 | 67.29 |
| 10 | 32.5 | 6 | 23 | 120 | 82.71 |
| 10 | 32.5 | 6 | 23 | 150 | 90.65 |
| 10 | 32.5 | 6 | 23 | 180 | 94.16 |
| 10 | 32.5 | 6 | 23 | 210 | 98.78 |
| 10 | 32.5 | 6 | 23 | 240 | 96.45 |
| 10 | 40 | 2 | 23 | 30 | 6.42 |
| 10 | 40 | 2 | 23 | 60 | 13.25 |
| 10 | 40 | 2 | 23 | 90 | 26.73 |
| 10 | 40 | 2 | 23 | 120 | 38.14 |
| 10 | 40 | 2 | 23 | 150 | 46.46 |
| 10 | 40 | 2 | 23 | 180 | 52.86 |
| 10 | 40 | 2 | 23 | 210 | 59.27 |
| 10 | 40 | 2 | 23 | 240 | 66.26 |
| 10 | 40 | 6 | 23 | 30 | 32.82 |
| 10 | 40 | 6 | 23 | 60 | 54.06 |

| | | | | | |
|----|------|---|----|-----|-------|
| 10 | 40 | 6 | 23 | 90 | 69.99 |
| 10 | 40 | 6 | 23 | 120 | 79.74 |
| 10 | 40 | 6 | 23 | 150 | 85.00 |
| 10 | 40 | 6 | 23 | 180 | 88.81 |
| 10 | 40 | 6 | 23 | 210 | 90.82 |
| 10 | 40 | 6 | 23 | 240 | 92.24 |
| 10 | 25 | 2 | 40 | 30 | 23.42 |
| 10 | 25 | 2 | 40 | 60 | 34.91 |
| 10 | 25 | 2 | 40 | 90 | 56.36 |
| 10 | 25 | 2 | 40 | 120 | 63.35 |
| 10 | 25 | 2 | 40 | 150 | 70.94 |
| 10 | 25 | 2 | 40 | 180 | 74.91 |
| 10 | 25 | 2 | 40 | 210 | 78.43 |
| 10 | 25 | 2 | 40 | 240 | 82.45 |
| 10 | 25 | 6 | 40 | 30 | 62.66 |
| 10 | 25 | 6 | 40 | 60 | 81.70 |
| 10 | 25 | 6 | 40 | 90 | 92.25 |
| 10 | 25 | 6 | 40 | 120 | 96.20 |
| 10 | 25 | 6 | 40 | 150 | 96.78 |
| 10 | 25 | 6 | 40 | 180 | 98.84 |
| 10 | 25 | 6 | 40 | 210 | 98.73 |
| 10 | 25 | 6 | 40 | 240 | 99.39 |
| 10 | 32.5 | 2 | 40 | 30 | 9.17 |
| 10 | 32.5 | 2 | 40 | 60 | 18.83 |
| 10 | 32.5 | 2 | 40 | 90 | 32.58 |
| 10 | 32.5 | 2 | 40 | 120 | 44.19 |
| 10 | 32.5 | 2 | 40 | 150 | 55.30 |
| 10 | 32.5 | 2 | 40 | 180 | 65.16 |
| 10 | 32.5 | 2 | 40 | 210 | 73.12 |
| 10 | 32.5 | 2 | 40 | 240 | 78.44 |
| 10 | 32.5 | 6 | 40 | 30 | 47.32 |
| 10 | 32.5 | 6 | 40 | 60 | 73.88 |
| 10 | 32.5 | 6 | 40 | 90 | 88.59 |
| 10 | 32.5 | 6 | 40 | 120 | 93.74 |
| 10 | 32.5 | 6 | 40 | 150 | 96.10 |
| 10 | 32.5 | 6 | 40 | 180 | 97.20 |
| 10 | 32.5 | 6 | 40 | 210 | 97.21 |
| 10 | 32.5 | 6 | 40 | 240 | 99.00 |
| 10 | 40 | 2 | 40 | 30 | 14.28 |
| 10 | 40 | 2 | 40 | 60 | 33.24 |
| 10 | 40 | 2 | 40 | 90 | 47.94 |
| 10 | 40 | 2 | 40 | 120 | 55.24 |
| 10 | 40 | 2 | 40 | 150 | 61.77 |
| 10 | 40 | 2 | 40 | 180 | 68.27 |
| 10 | 40 | 2 | 40 | 210 | 73.70 |
| 10 | 40 | 2 | 40 | 240 | 76.99 |

| | | | | | |
|-----|------|---|----|-----|-------|
| 10 | 40 | 6 | 40 | 30 | 42.17 |
| 10 | 40 | 6 | 40 | 60 | 68.03 |
| 10 | 40 | 6 | 40 | 90 | 83.60 |
| 10 | 40 | 6 | 40 | 120 | 89.92 |
| 10 | 40 | 6 | 40 | 150 | 94.54 |
| 10 | 40 | 6 | 40 | 180 | 96.77 |
| 10 | 40 | 6 | 40 | 210 | 98.10 |
| 10 | 40 | 6 | 40 | 240 | 99.00 |
| 500 | 25 | 2 | 23 | 30 | 6.71 |
| 500 | 25 | 2 | 23 | 60 | 6.63 |
| 500 | 25 | 2 | 23 | 90 | 24.76 |
| 500 | 25 | 2 | 23 | 120 | 25.41 |
| 500 | 25 | 2 | 23 | 150 | 25.23 |
| 500 | 25 | 2 | 23 | 180 | 38.28 |
| 500 | 25 | 2 | 23 | 210 | 40.67 |
| 500 | 25 | 2 | 23 | 240 | 57.87 |
| 500 | 25 | 6 | 23 | 30 | 30.94 |
| 500 | 25 | 6 | 23 | 60 | 47.40 |
| 500 | 25 | 6 | 23 | 90 | 63.05 |
| 500 | 25 | 6 | 23 | 120 | 61.47 |
| 500 | 25 | 6 | 23 | 150 | 67.50 |
| 500 | 25 | 6 | 23 | 180 | 74.69 |
| 500 | 25 | 6 | 23 | 210 | 81.13 |
| 500 | 25 | 6 | 23 | 240 | 87.45 |
| 500 | 32.5 | 2 | 23 | 30 | 17.69 |
| 500 | 32.5 | 2 | 23 | 60 | 0.81 |
| 500 | 32.5 | 2 | 23 | 90 | 17.26 |
| 500 | 32.5 | 2 | 23 | 120 | 27.06 |
| 500 | 32.5 | 2 | 23 | 150 | 44.72 |
| 500 | 32.5 | 2 | 23 | 180 | 37.55 |
| 500 | 32.5 | 2 | 23 | 210 | 27.11 |
| 500 | 32.5 | 2 | 23 | 240 | 26.96 |
| 500 | 32.5 | 6 | 23 | 30 | 0.00 |
| 500 | 32.5 | 6 | 23 | 60 | 12.11 |
| 500 | 32.5 | 6 | 23 | 90 | 22.99 |
| 500 | 32.5 | 6 | 23 | 120 | 42.19 |
| 500 | 32.5 | 6 | 23 | 150 | 10.43 |
| 500 | 32.5 | 6 | 23 | 180 | 47.67 |
| 500 | 32.5 | 6 | 23 | 210 | 61.68 |
| 500 | 32.5 | 6 | 23 | 240 | 82.03 |
| 500 | 40 | 2 | 23 | 30 | 0.00 |
| 500 | 40 | 2 | 23 | 60 | 5.78 |
| 500 | 40 | 2 | 23 | 90 | 8.15 |
| 500 | 40 | 2 | 23 | 120 | 24.10 |
| 500 | 40 | 2 | 23 | 150 | 41.58 |
| 500 | 40 | 2 | 23 | 180 | 55.27 |

| | | | | | |
|-----|------|---|----|-----|-------|
| 500 | 40 | 2 | 23 | 210 | 26.42 |
| 500 | 40 | 2 | 23 | 240 | 52.26 |
| 500 | 40 | 6 | 23 | 30 | 52.62 |
| 500 | 40 | 6 | 23 | 60 | 51.95 |
| 500 | 40 | 6 | 23 | 90 | 57.85 |
| 500 | 40 | 6 | 23 | 120 | 45.33 |
| 500 | 40 | 6 | 23 | 150 | 65.65 |
| 500 | 40 | 6 | 23 | 180 | 64.10 |
| 500 | 40 | 6 | 23 | 210 | 49.05 |
| 500 | 40 | 6 | 23 | 240 | 56.10 |
| 500 | 25 | 2 | 40 | 30 | 16.69 |
| 500 | 25 | 2 | 40 | 60 | 34.77 |
| 500 | 25 | 2 | 40 | 90 | 51.92 |
| 500 | 25 | 2 | 40 | 120 | 58.51 |
| 500 | 25 | 2 | 40 | 150 | 76.16 |
| 500 | 25 | 2 | 40 | 180 | 86.07 |
| 500 | 25 | 2 | 40 | 210 | 92.80 |
| 500 | 25 | 2 | 40 | 240 | 97.47 |
| 500 | 25 | 6 | 40 | 30 | 63.75 |
| 500 | 25 | 6 | 40 | 60 | 97.18 |
| 500 | 25 | 6 | 40 | 90 | 98.93 |
| 500 | 25 | 6 | 40 | 120 | 99.06 |
| 500 | 25 | 6 | 40 | 150 | 99.11 |
| 500 | 25 | 6 | 40 | 180 | 99.41 |
| 500 | 25 | 6 | 40 | 210 | 98.94 |
| 500 | 25 | 6 | 40 | 240 | 99.01 |
| 500 | 32.5 | 2 | 40 | 30 | 12.01 |
| 500 | 32.5 | 2 | 40 | 60 | 24.56 |
| 500 | 32.5 | 2 | 40 | 90 | 34.42 |
| 500 | 32.5 | 2 | 40 | 120 | 40.66 |
| 500 | 32.5 | 2 | 40 | 150 | 49.97 |
| 500 | 32.5 | 2 | 40 | 180 | 61.35 |
| 500 | 32.5 | 2 | 40 | 210 | 65.84 |
| 500 | 32.5 | 2 | 40 | 240 | 69.44 |
| 500 | 32.5 | 6 | 40 | 30 | 35.82 |
| 500 | 32.5 | 6 | 40 | 60 | 55.17 |
| 500 | 32.5 | 6 | 40 | 90 | 77.14 |
| 500 | 32.5 | 6 | 40 | 120 | 86.33 |
| 500 | 32.5 | 6 | 40 | 150 | 88.41 |
| 500 | 32.5 | 6 | 40 | 180 | 93.14 |
| 500 | 32.5 | 6 | 40 | 210 | 98.16 |
| 500 | 32.5 | 6 | 40 | 240 | 98.69 |
| 500 | 40 | 2 | 40 | 30 | 43.12 |
| 500 | 40 | 2 | 40 | 60 | 38.11 |
| 500 | 40 | 2 | 40 | 90 | 29.55 |
| 500 | 40 | 2 | 40 | 120 | 55.99 |

| | | | | | |
|-----|----|---|----|-----|-------|
| 500 | 40 | 2 | 40 | 150 | 46.73 |
| 500 | 40 | 2 | 40 | 180 | 65.37 |
| 500 | 40 | 2 | 40 | 210 | 70.39 |
| 500 | 40 | 2 | 40 | 240 | 73.44 |
| 500 | 40 | 6 | 40 | 30 | 40.72 |
| 500 | 40 | 6 | 40 | 60 | 59.83 |
| 500 | 40 | 6 | 40 | 90 | 80.99 |
| 500 | 40 | 6 | 40 | 120 | 91.85 |
| 500 | 40 | 6 | 40 | 150 | 96.91 |
| 500 | 40 | 6 | 40 | 180 | 97.98 |
| 500 | 40 | 6 | 40 | 210 | 98.41 |
| 500 | 40 | 6 | 40 | 240 | 99.00 |

REFERENCES

- Abushammala, M.F.M., Basri, N.E.A., Elfithri, R., Younes, M.K., and Irwan, D. (2013). Modeling of CH₄ oxidation in landfill covers soil using an Artificial Neural Network. *Journal of the Air & Waste Management Association*, DOI:10.1080/10962247.2013.842510.
- Abouzlam, M., Ouvrard, R., Mehdi, D., Pontlevoy, F., Gombert, B., Karpel Vel Leitner, N., and Boukari, S. (2013). An optimal control of a wastewater treatment reactor by catalytic ozonation. *Control Engineering Practice*, 21(1), 105-112.
- Ahmad, A.L., Sumathi, S., and Hameed, B.H. (2006). Coagulation of residue oil and suspended solid in palm oil mill effluent by chitosan, alum and PAC. *Chemical Engineering Journal*, 118(1-2), 99-105.
- Ahmadun, F., Pendashteh, A., Abdullah, L.C., Biak, D.R.A., Madaeni, S.S., and Abidin, Z.Z. (2009). Review of technologies for oil and gas produced water treatment. *Journal of Hazardous Materials*, 170, 530-551.
- Alba, E., Angelova, D., Angelova, M., Artemchuk, S., Atanassov, E., Atanassov, K., and Ullrich, M. (2012). *Monte Carlo Methods and Applications: Proceedings of the 8th IMACS Seminar on Monte Carlo Methods, August 29–September 2, 2011, Borovets, Bulgaria*. Walter de Gruyter.
- Aleboye, A., Kasiri, M.B., Olya, M.E., and Aleboye, H. (2008). Prediction of azo dye decolorization by UV/H₂O₂ using artificial neural networks. *Dyes and Pigments*, 77, 288–294.
- Aliaga, C., Park, J.Y., Yamada, Y., Lee, H.S., Tsung, C-K., Yang, P., and Somorjai, A. (2009). Sum Frequency Generation and Catalytic Reaction Studies of the Removal

- of Organic Capping Agents from Pt Nanoparticles by UV-Ozone Treatment. *The Journal of Physical Chemistry C*, 113, 6150-6155.
- Alley, B., Beebe, A., Rodgers, J., and Castle, J.W. (2011). Chemical and physical characterization of producedwaters from conventional and unconventional fossil fuel resources. *Chemosphere*, 85(1), 74-82.
- Antonopoulou, M., Papadopoulos, V., and Konstantinou, I. (2012). Photocatalytic oxidation of treated municipal wastewaters for the removal of phenolic compounds: optimization and modeling using response surface methodology (RSM) and artificial neural networks (ANNs). *Journal of Chemical Technology and Biotechnology*, 87(10), 1385–1395.
- Anuar Mohamad Kamar, K., Khairolden Ghani, M., Egbu, C., and Arif, M. (2010). Collaboration initiative on green construction and sustainability through Industrialized Buildings Systems (IBS) in the Malaysian construction industry. *International Journal of Sustainable Construction Engineering & Technology*, 1(1), 119-127.
- Asselin, M., Drogui, P., Brar, S.K., Benmoussa, H., and Blais, J-F. (2008). Organics removal in oily bilgewater by electrocoagulation process. *Journal of Hazardous Materials*, 151, 446-455.
- Atlas, R.M., and Hazen, T.C. (2011). Oil biodegradation and bioremediation: a tale of the two worst spills in U.S. history. *Environmental Science and Technology*, 45(16), 6709–6715.

- Audenaert, W.T.M., Callewaert, M., Nopens, I., Cromphout, J., Vanhoucke, R., Dumoulin, A., Dejans, P., and Van Hulle, S.W.H. (2010). Full-scale modelling of an ozone reactor for drinking water treatment. *Chemical Engineering Journal*, 157, 551-557.
- Badrnezhad, R., and Mizra, B. (2014). Modeling and optimization of cross-flow ultrafiltration using hybrid neural network-genetic algorithm approach. *Journal of Industrial and Engineering Chemistry*, 20(2), 528-543.
- Banuelas, R., and Antony, J. (2004). Modified analytic hierarchy process to incorporate uncertainty and managerial aspects. *International Journal of Production Research*, 42(18), 3851-3872.
- Bellman, R.E. and Zadeh, L.A. (1970). Decision Making in a Fuzzy Environment. *Management Science*, Vol. 17, pp. 141-164.
- Benito, J.M., Sánchez, M.J., Pena, P., and Rodríguez, M.A. (2007). Development of a new high porosity ceramic membrane for the treatment of bilge water. *Desalination*, 214, 91-101.
- Bernstein, M.P., Dworkin, J.P., Sandford, S.A., and Allamandola, L.J. (2001). Ultraviolet irradiation of naphthalene in H₂O ice: Implications for meteorites and biogenesis. *Meteoritics & Planetary Science*, 36, 351–358.
- Betti, M., Boisson, F., Eriksson, M., Tolosa, I., and Vasileva, E. (2011). Isotope analysis for marine environmental studies. *International Journal of Mass Spectrometry*, 307, 192–199.
- Bhatti, M.S., Kapoor, D., Kalia, R.K., Reddy, A.S., and Thukral, A.K. (2011). RSM and ANN modeling for electrocoagulation of copper from simulated wastewater: Multi

- objective optimization using genetic algorithm approach. *Desalination*, 274(1-3), 74-80.
- Björn, L.O. (1995). Estimation of fluence rate from irradiance measurements with a cosine-corrected sensor. *Journal of Photochemistry and Photobiology B: Biology*, 29, 179–183.
- Blanchard, A.L., Feder, H.M., and Shaw, D.G. (2011). Associations between macrofauna and sediment hydrocarbons from treated ballast water effluent at a marine oil terminal in Port Valdez, Alaska. *Environmental Monitoring and Assessment*, 178(1–4), 461–476.
- Boehm, P.D., Page, D.S., Brown, J.S., Neff, J.M., Bragg, J.R., and Atlas, R.M. (2008). Distribution and Weathering of Crude Oil Residues on Shorelines 18 Years after the Exxon Valdez Spill. *Environmental Science and Technology*, Vol. 42, pp. 9210-9216.
- Bolaños, E.Q., Ocampo, J.T., and Rodríguez, L.C. (2008). Applicability of computational fluid dynamics to simulate ozonation processes. *Ingeniería & Desarrollo. Universidad del Norte*, 24, 107-126.
- Bolton, J.R., and Linden, K.G. (2003). Standardization of methods for fluence (UV Dose) determination in bench-scale UV experiments. *Journal of Environmental Engineering ASCE*, 129, 209–215.
- Brand, N., and Ostfeld, A. (2011). Optimal Design of Regional Wastewater Pipelines and Treatment Plant Systems. *Water Environment Research*, 83(1), 53-64.
- Buckley, J.J., and Lowers, L.J. (2008). *Monte Carlo Methods in Fuzzy Optimization: Studies in Fuzziness and Soft Computing*. Springer, Berlin.

- Cao, M.F., Huang, G.H., and He, L. (2011). An approach to interval programming problems with left-hand-side stochastic coefficients: An application to environmental decisions analysis. *Expert Systems with Application*, Vol. 38, No. 9, pp. 11538-11546.
- Cardona, S.C., López, F., Abad, A., and Navarro-Laboulais, J. (2010). ON Bubble Column Reactor Design for the Determination of Kinetic Rate Constants in Gas-Liquid Systems. *Canadian Journal of Chemical Engineering*, 88, 491-502.
- Carlucci, D., and Schiuma, G. (2009). Applying the analytic network process to disclose knowledge assets value creation dynamics. *Expert Systems with Applications*, 36(4), 7687-7694.
- Cataldo, R. (2001). Musseling in on the Ninth District Economy. *Fedgazette*. 13(1): 15-17.
- Cazoir, D., Fine, L., Ferronato, C., and Chovelon, J. M. (2012). Hydrocarbon removal from bilgewater by a combination of air-stripping and photocatalysis. *Journal of hazardous materials*, 235, 159-168.
- CCME (Canadian Council of Ministers of the Environment). (1999). *Canadian Water Quality Guidelines for the Protection of Aquatic Life: Polycyclic aromatic hydrocarbons (PAHs)*. In: *Canadian Environmental Quality Guidelines*, Canadian Council of Ministers of the Environment, Winnipeg, Canada.
- Chary, P., Stone, M. P., and Lloyd, R. S. (2013). Sequence context modulation of polycyclic aromatic hydrocarbon - induced mutagenesis. *Environmental and molecular mutagenesis*, 54(8), 652-658.

- Chakraborty, A., and Bhattacharaya, D. K. (2006). A process-based mathematical model on methane production with emission indices for control. *Bulletin of Mathematical Biology*, 68(6), 1293-1314.
- Chiroșcă, A., Dumitrașcu, G., Barbu, M., and Caraman, S. (2011). Fuzzy control of a wastewater treatment process. In *Intelligent Decision Technologies* (pp. 155-163). Springer Berlin Heidelberg.
- Chandwani, V., Agrawal, V., and Nagar, R. (2013). Applications of Soft Computing in Civil Engineering: A Review. *International Journal of Computer Applications*, 81.
- Chang, N. B., Yeh, S. C., and Chang, C. H. (2011). Optimal expansion of a coastal wastewater treatment and ocean outfall system under uncertainty (II): optimisation analysis. *Civil Engineering and Environmental Systems*, 28(1), 39-59.
- Chen, S.J., and Hwang, C.L. (1992). *Fuzzy multiple attribute decision making*. Springer, Heidelberg.
- Chen, B., Huang, G.H., and Li, Y.F. (2005a). Pesticide-loss simulation and risk assessment during flooding season – a study in the Auglaize-Blanchard Watershed. *Water International*, Vol. 30, No. 1, pp. 88-98.
- Chen, B., Guo, H.C., Huang, G.H., Maqsood, I., Zhang, N., Wu, S.M., and Zhang, Z.X. (2005b). ASRWM: an arid/semiarid region water management model. *Engineering Optimization*, Vol. 37, No. 6, pp. 609-631.
- Chen, Z., Huang, G. H., and Chakma, A. (2003). Hybrid fuzzy-stochastic modeling approach for assessing environmental risks at contaminated groundwater system. *Journal of Environmental Engineering-ASCE*, Vol. 129, No. 1, pp. 79-88.

- Chowdhury, S., and Husain, T. (2006). Evaluation of drinking water treatment technology: an entropy-based fuzzy application. *Journal of Environmental Engineering*, 132(10), 1264-1271.
- Chu, Y., and You, F. (2013). Integration of production scheduling and dynamic optimization for multi-product CSTRs: Generalized Benders decomposition coupled with global mixed-integer fractional programming. *Computers & Chemical Engineering*, 58, 315-333.
- Coates, G., and Rahimifard, S. (2009). Modelling of post-fragmentation waste stream processing within UK shredder facilities. *Waste management*, 29(1), 44-53.
- Colbourn, E.A., Roskilly, S.J., Rowe, R.C., and York, P. (2011). Modelling formulations using gene expression programming – A comparative analysis with artificial neural networks. *European Journal of Pharmaceutical Sciences*, 44(3), 366–374.
- Cunha, M. C., Pinheiro, L., Zeferino, J., Antunes, A., and Afonso, P. (2009). Optimization model for integrated regional wastewater systems planning. *Journal of water resources planning and management*, 135(1), 23-33.
- Dawes, J. (2008). Do data characteristics change according to the number of scale points used. *International Journal of Market Research*, 50(1), 61-77.
- Deng, H. (1999). Multicriteria analysis with fuzzy pairwise comparison. *International Journal of Approximate Reasoning*, 21(3), 215-231.
- de Bruyn, W.J., Clark, C.D., Ottelle, K., and Aiona, P. (2012). Photochemical degradation of phenanthrene as a function of natural water variables modeling freshwater to marine environments. *Marine Pollution Bulletin*, 64(3), 532–538.

- Dimou, A.D., Sakkas, V.A., and Albanis, T.A. (2004). Trifluralin photolysis in natural waters and under the presence of isolated organic matter and nitrate ions: kinetics and photoproduct analysis. *Journal of Photochemistry and Photobiology A: Chemistry*, 163(3), 473–480.
- Ding, H., Benyoucef, L., and Xie, X. (2006). A simulation-based multi-objective genetic algorithm approach for networked enterprises optimization. *Engineering Applications of Artificial Intelligence*, 19(6), 609-623.
- Dollhopf, R. and Durno, M. (2011). Kalamazoo River\Enbridge Pipeline Spill 2010. *Proceedings of the 2011 International Oil Spill Conference, Portland, OR, U.S.A.*, pp. 422-428.
- Dong, H. L., Huang, J. J., Cai, Z. H., and Wu, Q. F. (2013). Research on Predicted Model of Least Squares Support Vector Machine Based on Genetic Algorithm. *Advanced Materials Research*, 753, 2875-2881.
- Dong, C., Huang, G.H., Tan, Q., and Cai, Y.P. (2014). Coupled planning of water resources and agricultural landuse based on an inexact-stochastic programming model. *Frontiers of Earth Science*, 8(1), 70-80.
- Dubey, D., Chandra, S., and Mehra, A. (2012). Fuzzy linear programming under interval uncertainty based on IFS representation. *Fuzzy Sets and Systems*, 188(1), 68-87.
- Dunn, O. J. and Clark, V. A. (2009). The Normal Distribution, in *Basic Statistics: A Primer for the Biomedical Sciences*. John Wiley & Sons, Inc., Hoboken, NJ, U.S.A.
- Durán, A., Monteagudo, J.M., San Martín, I., and Sánchez-Romero, R. (2009). Photocatalytic treatment of IGCC power station effluents in a UV-pilot plant. *Journal of Hazardous Materials*, 167(1–3), 885–891.

- Ebrahimi, M., Willershausen, D., Ashaghi, K. S., Engel, L., Placido, L., Mund, P., and Czermak, P. (2010). Investigations on the use of different ceramic membranes for efficient oil-field produced water treatment. *Desalination*, 250(3), 991-996.
- Ekins, P., Vanner, R., and Firebrace, J. (2005). *Management of Produced Water On Offshore Oil Installations: A Comparative Assessment using Flow Analysis*, 2005. Final report prepared for the Policy Studies Institute.
- El-Fergany, A. A., Othman, A. M., and El-Arini, M. M., (2014). Synergy of a genetic algorithm and simulated annealing to maximize real power loss reductions in transmission networks. *International Journal of Electrical Power & Energy Systems*, 56, 307-315.
- El-Gohary, F., Tawfik, A., and Mahmoud, U. (2010). Comparative study between chemical coagulation/precipitation (C/P) versus coagulation/dissolved air flotation (C/DAF) for pre-treatment of personal care products (PCPs) wastewater. *Desalination*, 252(1), 106-112.
- Elmolla, E.S., Chaudhuri, M., and Eltoukhy, M.M. (2010). The use of artificial neural network (ANN) for modeling of COD removal from antibiotic aqueous solution by the Fenton process. *Journal of Hazardous Materials*, 179, 127–134.
- Elyasi, S., and Taghipour, F. (2010). Simulation of UV Photoreactor for Degradation of Chemical Contaminants: Model Development and Evaluation. *Environmental Science & Technology*, 44, 2056-2063.
- Endresen, Ø., Lee Behrens, H., Brynstad, S., Bjørn Andersen, A., and Skjong, R. (2004). Challenges in global ballast water management. *Marine Pollution Bulletin*, 48(7), 615-623.

- Engell, S. (2009). Uncertainty, decomposition and feedback in batch production scheduling. *Computer Aided Chemical Engineering*, 26, 43-62.
- Eskandari, H., and Rabelo, L. (2007). Handling uncertainty in the analytic hierarchy process: A stochastic approach. *International Journal of Information Technology & Decision Making*, 6(01), 177-189.
- Fakhru'l-Razi, A., Pendashteh, A., Abdullah, L.C., Biak, D.R.A., Madaeni, S.S., and Abidin, Z.Z. (2009). Review of technologies for oil and gas produced water treatment. *Journal of Hazardous Materials*, 170(2-3), 530-551.
- Farkas, T., Czuczai, B., Rev, E., and Lelkes, Z. (2008). New MINLP model and modified outer approximation algorithm for distillation column synthesis. *Industrial & Engineering Chemistry Research*, 47(9), 3088-3103.
- Ferreira, F., Matos, J., Galvão, A., and Cardoso, M. A. (2011). Assessing the environmental performance of urban wastewater systems using the INSA model: Application to the Algés-Alcântara wastewater system, in Portugal. *Journal of environmental management*, 92(11), 2944-2952.
- Ferrero, G., Rodríguez-Roda, I., and Comas, J. (2012). Automatic control systems for submerged membrane bioreactors: A state-of-the-art review. *Water Research*, 46(11), 3421-3433.
- Frontistis, Z., Daskalaki, V.M., Hapeshi, E., Drosou, C., Fatta-Kassinos, D., Xekoukoulotakis, N.P., and Mantzavinos, D. (2012). Photocatalytic (UV-A/TiO₂) degradation of 17 α -ethynylestradiol in environmental matrices: Experimental studies and artificial neural network modeling. *Journal of Photochemistry and Photobiology A: Chemistry*, 240, 33-41.

- Gaaseidnes, K. and Turbeville, J. (1999). Separation of Oil and Water in Oil Spill Recovery Operations. *Pure and Applied Chemistry*, Vol. 71, No. 1, pp. 95-101.
- Garson, G.D. (1991). Interpreting neural-network connection weights. *AI Expert*, 6(7), 47–51.
- Gazzaz, N.M., Yusoff, M.K., Aris, A.Z., Juahir, H., and Ramli, M.F. (2012). Artificial neural network modeling of the water quality index for Kinta River (Malaysia) using water quality variables as predictors. *Marine Pollution Bulletin*, 64(11), 2409–2420.
- Ghaedi, M., Ghaedi, A.M., Abdi, F., Roosta, M., Sahraei, R., and Daneshfar, A. (2013). Principal component analysis-artificial neural network and genetic algorithm optimization for removal of reactive orange 12 by copper sulfide nanoparticles-activated carbon. *Journal of Industrial and Engineering Chemistry*, In Press, DOI: 10.1016/j.jiec.2013.06.008.
- Ghaedi, M., Zeinali, N., Ghaedi, A.M., Teimuori, M., and Tashkhourian, J. (2014). Artificial neural network-genetic algorithm based optimization for the adsorption of methylene blue and brilliant green from aqueous solution by graphite oxide nanoparticle. *Spectrochimica Acta Part A: Molecular and Biomolecular Spectroscopy*, 125, 264-277.
- Gollasch, S., David, M., Voigt, M., Dragsund, E., Hewitt, C., and Fukuyo, Y. (2007). Critical review of the IMO international convention on the management of ships' ballast water and sediments. *Harmful algae*, 6(4), 585-600.

- Gönder Z.B., Arayici, S., and Barlas, H. (2012). Treatment of Pulp and Paper Mill Wastewater Using Ultrafiltration Process: Optimization of the Fouling and Rejections. *Industrial & Engineering Chemical Research*, 51(17), 6184-6195.
- Gregg, M.D., and Hallegraeff, G.M. (2007). Efficacy of three commercially available ballast water biocides against vegetative microalgae, dinoflagellate cysts and bacteria. *Harmful Algae*, 6, 567-584.
- Hakanen, J., Miettinen, K., and Sahlstedt, K. (2011). Wastewater treatment: new insight provided by interactive multiobjective optimization. *Decision Support Systems*, 51(2), 328-337.
- Hamia, M.L., Al-Hashimi, M.A., and Al-Doori, M.M. (2007). Effect of activated carbon on BOD and COD removal in dissolved air flotation unit treating refinery wastewater. *Desalination*, 216, 116–122.
- Han, H.G., and Qiao, J.F. (2011). Adaptive dissolved oxygen control based on dynamic structure neural network. *Applied Soft Computing*, 11(4), 3812-3820.
- Han, G.Q., Ma, Z.M., deYoung, B., Foreman, M., and Chen, N. (2011). Simulation of three-dimensional circulation and hydrography over the Grand Banks of Newfoundland. *Ocean Modelling*, 40, 199–210.
- Han, H. G., Qian, H. H., and Qiao, J. F. (2014). Nonlinear multiobjective model-predictive control scheme for wastewater treatment process. *Journal of Process Control*, 24(3), 47-59.
- Hans, E. W., Herroelen, W., Leus, R., and Wullink, G. (2007). A hierarchical approach to multi-project planning under uncertainty. *Omega*, 35(5), 563-577.

- Haritash, A.K., and Kaushik, C.P. (2009). Biodegradation aspects of polycyclic aromatic hydrocarbons (PAHs): a review. *Journal of Hazardous Materials*, 169, 1–15.
- Harman, C., Brooks, S., Sundt, R.C., Meier, S., and Grung, M. (2011). Field comparison of passive sampling and biological approaches for measuring exposure to PAH and alkylphenols from offshore produced water discharges. *Marine Pollution Bulletin*, 63(5–12), 141–148.
- He, L., Huang, G.H., Zeng, G.M., and Lu, H.W. (2009). An interval mixed-integer semi-infinite programming method for municipal solid waste management. *Journal of the Air & Waste Management Association*, Vol. 59, No. 2, pp. 236-246.
- Herborg, L-M., Rushton, S.P., Clare, A.S., and Bentley, M.G. (2005). The invasion of the Chinese mitten crab (*Eriocheir sinensis*) in the United Kingdom and its comparison to continental Europe. *Biological Invasions*. 7: 959-968.
- Herwig, R. P., Cordell, J. R., Perrins, J. C., Dinnel, P. A., Gensemer, R. W., Stubblefield, W. A., and Cooper, W. J. (2006). Ozone treatment of ballast water on the oil tanker S/T Tonsina: chemistry, biology and toxicity. *Marine Ecology Progress Series*, 324, 37-55.
- Holm, E. R., Stamper, D. M., Brizzolara, R. A., Barnes, L., Deamer, N., and Burkholder, J. M. (2008). Sonication of bacteria, phytoplankton and zooplankton: Application to treatment of ballast water. *Marine pollution bulletin*, 56(6), 1201-1208.
- Hoseini, S. M., Salarirad, M. M., and Alavi Moghaddam, M. R. (2013). TPH removal from oily wastewater by combined coagulation pretreatment and mechanically induced air flotation. *Desalination and Water Treatment*, doi: 10.1080/19443994.2013.846522.

- Hsu, T. H., and Pan, F. F. (2009). Application of Monte Carlo AHP in ranking dental quality attributes. *Expert Systems with Applications*, 36(2), 2310-2316.
- Hu, K., Wan, J.Q., Ma, Y.W., Wang, Y., and Huang, M.Z. (2012). A fuzzy neural network model for monitoring A²/O process using on-line monitoring parameters. *Journal of Environmental Science and Health, Part A: Toxic/Hazardous Substances and Environmental Engineering*, 47(5), 744-754.
- Huang, M.Z., Wan, J.Q., Ma, Y.W., Wan, Y., Li, W.J., and Sun, X.F. (2009). Control rules of aeration in a submerged biofilm wastewater treatment process using fuzzy neural networks. *Expert Systems with Applications*, 36, 10428-10437.
- Huang, J., Bo, Y., and Wang, H. (2011). Electromechanical equipment state forecasting based on genetic algorithm–support vector regression. *Expert Systems with Applications*, 38(7), 8399-8402.
- Huang, X., Han, H., and Qiao, J. (2013). Energy consumption model for wastewater treatment process control. *Water Science & Technology*, 67(3).
- Hüfner, M., Tometzki, T., and Engell, S. (2009). Two-layer planning and scheduling of batch production processes under uncertainty. *Computer Aided Chemical Engineering*, 27, 1197-1202.
- Ibrahim, S., Wang, S., and Ang, H. M. (2010). Removal of emulsified oil from oily wastewater using agricultural waste barley straw. *Biochemical Engineering Journal*, 49(1), 78-83.
- Igunnu, E.T., and Chen, G.Z. (2012). Produced water treatment technologies. *International Journal of Low-Carbon Technologies*, doi:10.1093/ijlct/cts049.

- International Maritime Organization (IMO). (2011). Manual on Oil Pollution Section I – Prevention. IMO Publishing, London, UK.
- Jablonsky, J. (2007). Measuring the efficiency of production units by AHP models. *Mathematical and Computer Modeling*, 46(7), 1091-1098.
- Janak, S. L., Floudas, C. A., Kallrath, J., and Vormbrock, N. (2006). Production scheduling of a large-scale industrial batch plant. I. Short-term and medium-term scheduling. *Industrial & engineering chemistry research*, 45(25), 8234-8252.
- Ji, Y.F., Zeng, C., Ferronato, C., Chovelon, J.M., and Yang, X. (2012). Nitrate-induced photodegradation of atenolol in aqueous solution: Kinetics, toxicity and degradation pathways. *Chemosphere*, 88(5), 644–649.
- Jiao, L. (2010). QSPR studies on soot–water partition coefficients of persistent organic pollutants by using artificial neural network. *Chemosphere*, 80(6), 671–675.
- Jin, L.M., Yu, S.L., Shi, W.X., Yi, X.S., Sun, N., Ge, Y.L., and Ma, C. (2012). Synthesis of a novel composite nanofiltration membrane incorporated SiO₂ nanoparticles for oily wastewater desalination. *Polymer*, 53(23), 5295-5303.
- Jing, L., Chen, B., Zhang, B.Y., and Peng, H.X. (2012a). A review of ballast water management practices and challenges in harsh and Arctic environments. *Environmental Reviews*, 20, 83–108.
- Jing, L., Chen, B., Zhang, B.Y., and Li, P. (2012b). A stochastic simulation-based hybrid interval fuzzy programming approach for optimizing the treatment of recovered oily water. *The Journal of Ocean Technology*, 7(4), 59–72.
- Jing, L., Chen, B., Zhang, B.Y., Li, P., and Zheng, J.S. (2012c). A Monte Carlo simulation aided analytic hierarchy process (MC–AHP) approach for best management

- practices assessment in nonpoint source pollution control. *Journal of Environmental Engineering ASCE*, 139(5), 618-626
- Jing, L., Chen, B., Zhang, B.Y., and Zheng, J.S. (2013a). The effects of salinity and temperature on the photolysis of naphthalene using UVC irradiation. In: *Proceedings of the 36th AMOP Technical Seminar on Environmental Contamination and Response*, Halifax, Canada. p. 591–600.
- Jing, L., Chen, B., Zhang, B.Y., and Li, P. (2013b). A hybrid stochastic-interval analytic hierarchy process (SIAHP) approach for prioritizing the strategies of reusing treated wastewater. *Mathematical Problems in Engineering*, vol. 2013, Article ID 874805, 10 pages, doi:10.1155/2013/874805.
- Jing, L., Chen, B., and Zhang, B.Y. (2013c). A hybrid fuzzy stochastic analytical hierarchy process (FSAHP) approach for evaluating ballast water treatment technologies. *Environmental Systems Research*, 2:10, doi:10.1186/2193-2697-2-10.
- Jing, L., Chen, B., and Zhang, B.Y. (2014a). Modeling of UV-induced photodegradation of naphthalene in marine oily wastewater by artificial neural networks. *Water, Air, & Soil Pollution*, 225(4), 1-14.
- Jing, L., Chen, B., Zhang, B.Y., Zheng, J.S., and Liu, B. (2014b). Naphthalene degradation in seawater by UV irradiation: the effects of fluence rate, salinity, temperature and initial concentration. *Marine Pollution Bulletin*, 81, 149-156.
- Johnsen, S., Utvik, T.I.R., Garland, E., de Vals, B., and Campbell, J., (2004). Environmental fate and effect of contaminants in produced water. Presented at the Seventh SPE International Conference on Health, Safety and Environment in Oil and Gas Exploration and Production, Calgary, AB, 29–31 March, SPE 86708, 2004.

- Kadali, K.K., Simons, K.L., Sheppard, P.J., Ball, and A.S. (2012). Mineralisation of weathered crude oil by a hydrocarbonoclastic Consortia in marine Mesocosms. *Water, Air, & Soil Pollution*, 223(7), 4283–4295.
- Kaya, T., and Kahraman, C. (2011). An integrated fuzzy AHP–ELECTRE methodology for environmental impact assessment. *Expert Systems with Applications*, 38(7), 8553-8562.
- Kelland, M. A. (2014). *Production chemicals for the oil and gas industry*. CRC press.
- Kennedy, C.J. (2006). Report on Toxicological assessment of naphthalene, benzene, ethylbenzene, toluene, and m-xylene to embryo-larval stages of fish (*Oncorhynchus mykiss*), amphibians (*Rana pipiens*) and freshwater invertebrates (*Daphnia magna*). Submitted to: BC Ministry of Environment, Water Protection Section. Victoria, BC.
- Khataee, A.R., and Kasiri, M.B. (2010). Artificial neural networks modeling of contaminated water treatment processes by homogeneous and heterogeneous nanocatalysis. *Journal of Molecular Catalysis A: Chemical*, 331(1–2), 86–100.
- Kiemele, M., Schmidt, S., and Berdine, R. (1997). *Basic Statistics: Tools for Continuous Improvement*. Springs: Air Academic Press, Colorado, U.S.A.
- Kiker, G. A., Bridges, T. S., Varghese, A., Seager, T. P., and Linkov, I. (2005). Application of multicriteria decision analysis in environmental decision making. *Integrated environmental assessment and management*, 1(2), 95-108.
- Kishimoto, N., and Nakamura, E. (2011). Effects of Ozone-Gas Bubble Size and pH on Ozone/UV Treatment. *Ozone: Science & Engineering: The Journal of the International Ozone Association*, 33(5), 396-402.

- Kingston, P.F. (2003). Long-term environmental impacts of oil spills. *Spill Science and Technology Bulletin*, 7(2): 53-61.
- Klaassen, R., Feron, P.H.M., and Jansen, A.E. (2005). Membrane contactors in industrial applications. *Chemical Engineering Research and Design*, 83(A3), 234–246.
- Kornysheva, E., and Salinesi, C. (2007). MCDM techniques selection approaches: State of the art. In *Computational Intelligence in Multicriteria Decision Making*, IEEE Symposium on (pp. 22-29). IEEE.
- Kong, C., Yoon, Y., Choi, Y.D., Lee, S.J., Oh, J., Han, J., and Her, N. (2012). Sonocatalytic degradation of naphthalene and phenol in the presence of inert glass beads and single-walled carbon nanotubes. *Journal of Nanoelectronics and Optoelectronics*, 7(5), 522–529.
- Kot-Wasik, A., Dąbrowska, D., and Namieśnik, J., 2004. Photodegradation and biodegradation study of benzo(a)pyrene in different liquid media. *Journal of Photochemistry and Photobiology A: Chemistry*, 168(1–2), 109–115.
- Körbahti, B.K., and Artut, K. (2010). Electrochemical oil/water demulsification and purification of bilge water using Pt/Ir electrodes. *Desalination*, 258, 219-228.
- Körbahti, B. K., and Artut, K. (2013). Bilge water treatment in an upflow electrochemical reactor using Pt anode. *Separation Science and Technology*, 48(14), 2204-2216.
- Krebs, T., Schroën, C.G.P.H., and Boom, R.M. (2012). Separation kinetics of an oil-in-water emulsion under enhanced gravity. *Chemical Engineering Science*, Vol. 71, pp. 118-125.

- Krohling, R.A. and Campanharo, V.C. (2011). Fuzzy TOPSIS for Group Decision Making: A Case Study for Accidents with Oil Spill in the Sea. *Expert Systems with Applications*, Vol. 38, No. 4, pp. 4190-4197.
- Ksenofontov, B.S., and Ivanov, M.V. (2013). A novel multistage kinetic modeling of flotation for wastewater treatment. *Water Science & Technology*, 68(4), 807-812.
- Kumar, A., Kaur, J., and Singh, P. (2011). A new method for solving fully fuzzy linear programming problems. *Applied Mathematical Modelling*, 35(2), 817-823.
- Kwon, S.H., Kim, J.H., and Cho, D. (2009). An analysis method for degradation kinetics of lowly concentrated PAH solutions under UV Light and ultrasonication. *Journal of Industrial and Engineering Chemistry*, 15, 157–162.
- Lair, A., Ferronato, C., Chovelon, J.-M., and Herrmann, J.-M. (2008). Naphthalene degradation in water by heterogeneous photocatalysis: an investigation of the influence of inorganic anions. *Journal of Photochemistry and Photobiology A: Chemistry*, 193, 193–203.
- Law, A. T. (1994). Oil pollution in the Malaysian seas. *Fishmail*. 6: 5-23.
- Lee, J., Chun, S.W., Kang, H.J., and Talke, F.E. (2011). Photo oxidative degradation of perfluoropolyether lubricant for data storage. *Macromolecular Research*, 19(6), 582–588.
- Lee, J., Chun, S.W., Kang, H.J., Talke, F.E., 2011. Photo oxidative degradation of perfluoropolyether lubricant for data storage. *Macromolecular Research*, 19(6), 582–588.
- Lee, J. H. (2012). Energy Supply Chain Optimization: A Challenge for Control Engineers? In Eighth IFAC international symposium on advanced control of chemical processes,

- International Federation of Automatic Control, Furama Riverfront, Singapore (pp. 361-370).
- Leichsenring, J., and Lawrence, J. (2011). Effect of mid-oceanic ballast water exchange on virus-like particle abundance during two trans-Pacific voyages. *Marine Pollution Bulletin*, 62(5), 1103–1108.
- Levine, J., and Barnes, F.S. (2010). Energy variability and produced water: two challenges, one synergistic management approach using pumped hydroelectric energy storage. *Journal of Energy Engineering ASCE*, 136(1), 6–10.
- Li, Y.P., Huang, G.H., Nie, S.L., Nie, X.H., and Maqsood, I. (2006). An interval-parameter two-stage stochastic integer programming model for environmental systems planning under uncertainty. *Engineering Optimization*, Vol. 38, No. 4, pp. 461-483.
- Li, P. and Chen, B. (2011). FSILP: Fuzzy-stochastic-interval linear programming for supporting municipal solid waste management. *Journal of Environmental Management*, Vol. 92, pp. 1198-1209.
- Li, P., Chen, B., Zhang, B.Y., Jing, L., and Zheng, J.S. (2012). A multiple-stage simulation-based mixed integer nonlinear programming approach for supporting offshore oil spill recovery with weathering processes. *Journal of Ocean Technology*, 7(4), 87–105.
- Li, P., Wu, H. J., and Chen, B. (2013). RSW-MCFP: A resource-oriented solid waste management system for a mixed rural-urban area through monte carlo simulation-based fuzzy programming. *Mathematical Problems in Engineering*, 2013.

- Li, P., Chen, B., Zhang, B.Y., Jing, L., and Zheng, J.S. (2014). Monte Carlo simulation-based dynamic mixed integer nonlinear programming for supporting oil recovery and devices allocation during offshore oil spill responses. *Ocean & Coastal Management*, 89, 58-70.
- Liao, G. C. (2011). A novel evolutionary algorithm for dynamic economic dispatch with energy saving and emission reduction in power system integrated wind power. *Energy*, 36(2), 1018-1029.
- Lin, C.H., Yu, R.F., Cheng, W.P., and Liu, C.R. (2012). Monitoring and control of UV and UV-TiO₂ disinfections for municipal wastewater reclamation using artificial neural networks. *Journal of Hazardous Materials*, 209–210, 348–354.
- Liu, X., Cardiff, M.A., and Kitanidis, P.K. (2010). Parameter Estimation in Nonlinear Environmental Problems. *Stochastic Environmental Research and Risk Assessment*, Vol. 24, No. 7, pp. 1003-1022.
- Liu, S., Papageorgiou, L. G., and Gikas, P. (2011). Management of desalinated seawater, wastewater and reclaimed water in insular and geographically isolated areas using optimisation techniques. *Desalination and Water Treatment*, 33(1-3), 3-13.
- Liu, H.B., Huang, M.Z., and Yoo, C.K. (2013). A fuzzy neural network-based soft sensor for modeling nutrient removal mechanism in a full-scale wastewater treatment system. *Desalination and Water Treatment*, 51(31-33), 6184-6193.
- Lucas, M.S., Peres, J.A., and Puma, G.L. (2010). Treatment of winery wastewater by ozone-based advanced oxidation processes (O₃, O₃/UV and O₃/UV/H₂O₂) in a pilot-scale bubble column reactor and process economics. *Separation and Purification Technology*, 72, 235-241.

- Lyko, S., Teichgräber, B., and Kraft, A. (2012). Bulking control by low-dose ozonation of returned activated sludge in a full-scale wastewater treatment plant. *Water Science & Technology*, 65(9).
- Ma, Y.W., Huang, M.Z., Wan, J.Q., Hu, K., Wang, Y., and Zhang, H.P. (2011). Hybrid artificial neural network genetic algorithm technique for modeling chemical oxygen demand removal in anoxic/oxic process. *Journal of Environmental Science and Health Part A*, 46, 574-580.
- Mack, J., and Bolton, J.R. (1999). Photochemistry of nitrite and nitrate in aqueous solution: a review. *Journal of Photochemistry and Photobiology A: Chemistry*, 128(1-3), 1-13.
- Maguire-Boyle, S.J. and Barron, A.R. (2011). A New Functionalization Strategy for Oil/Water Separation Membranes. *Journal of Membrane Science*, Vol. 382, No. 1-2, pp. 107-115.
- Maleki, H.R., Tata, M., and Mashinchi, M. (2000). Linear Programming with Fuzzy Variables. *Fuzzy Sets and Systems*, Vol. 109, pp. 21-33.
- Malley, P. P., and Kahan, T. F. (2014). Nonchromophoric Organic Matter Suppresses Polycyclic Aromatic Hydrocarbon Photolysis in Ice and at Ice Surfaces. *The Journal of Physical Chemistry A*, 118(9), 1638-1643.
- Marchitan, N., Cojocaru, C., Mereuta, A., Duca, G., Cretescu, I., and Gonta, M. (2010). Modeling and optimization of tartaric acid reactive extraction from aqueous solutions: A comparison between response surface methodology and artificial neural network. *Separation and Purification Technology*, 75(3), 273-285.

- Martín R., and Reinelt, G. (2011). Branch-and-bound. In *The Linear Ordering Problem* (pp. 85-94). Springer Berlin Heidelberg.
- Matott, L. S., Babendreier, J. E., and Purucker, S. T. (2009). Evaluating uncertainty in integrated environmental models: a review of concepts and tools. *Water Resources Research*, 45(6).
- Maiti, S., Mishra, I.M., Bhattacharya, S.D., Joshi, J.K. (2011). Removal of oil from oil-in-water emulsion using a packed bed of commercial resin. *Colloids and Surfaces A*, 389, 291.
- May, D.B., and Sivakumar, M. (2011). Prediction of urban stormwater quality using artificial neural networks. *Environmental Modeling and Software*, 24(2), 296–302.
- McLaughlin, C., Falatko, D., Danesi, R., and Albert, R. (2014). Characterizing shipboard bilgewater effluent before and after treatment. *Environmental Science and Pollution Research*, 21(8), 5637-5652.
- McConkey, B.J., Hewitt, L.M., Dixon, D.G., and Greenberg, B.M. (2002). Natural Sunlight Induced Photooxidation of Naphthalene in Aqueous Solution. *Water, Air, and Soil Pollution*, 136, 347–359.
- McCulloch, W.W., and Pitts, W. (1943). A logical calculus of ideas imminent in nervous activity. *Bulletin of Mathematical Biophysics*, 5, 115–133.
- Maeda, K., Fukano, Y., Yamamichi, S., Nitta, D., and Kurata, H. (2011). An integrative and practical evolutionary optimization for a complex, dynamic model of biological networks. *Bioprocess and biosystems engineering*, 34(4), 433-446.

- Mohajerani, M., Mehrvar, M., and Ein-Mozaffari, F. (2012). Photoreactor design and CFD modeling of a UV/H₂O₂ process for distillery wastewater treatment. *The Canadian Journal of Chemical Engineering*, 90, 719-729.
- Mullai, P., Arulselvi, S., Ngo, H.H., and Sabarathinam, P.L. (2011). Experiments and ANFIS modeling for the biodegradation of penicillin-G wastewater using anaerobic hybrid reactor. *Bioresource Technology*, 102, 5492-5497.
- Nadal, M., Wargent, J.J., Jones, K.C., Paul, N.D., Schuhmacher, M., and Domingo, J.L. (2006). Influence of UV-B radiation and temperature on photodegradation of PAHs: preliminary results. *Journal of Atmospheric Chemistry*, 55, 241–252.
- Nandi, B.K., Moparthy, A., Uppaluri, R., and Purkait, M.K. (2010). Treatment of oily wastewater using low cost ceramic membrane: Comparative assessment of pore blocking and artificial neural network models. *Chemical Engineering Research and Design*, 88(7), 881–92.
- National Research Council. (1985). *Oil in the sea*. National Academy Press, Washington D.C.
- National Research Council (NRC). (2003). *Committee on Oil in the Sea: Inputs, Fates, and Effects. Oil in the Sea III: Inputs, Fates, and Effects*. Washington, DC: National Academy Press.
- Neff, J., Lee, K., and DeBlois, E.M. (2011a). Produced water: overview of composition, fates, and effects. In: Lee K, Neff J, editors. *Produced Water: Environmental Risks and Advances in Mitigation Technologies*. New York, Springer. p. 3–54.
- Neff, J., Sauer, T.C., & Hart, A.D. (2011b). Bioaccumulation of Hydrocarbons from Produced Water Discharged to Offshore Waters of the US Gulf of Mexico. In: Lee

- K, Neff J, editors. Produced Water: Environmental Risks and Advances in Mitigation Technologies. New York, Springer. p. 441–477.
- Netherlands National Water Board. (2008). Discharge of bilge water by inland navigation. www.emissieregistratie.nl (accessed March 2014).
- Nourani, V., Baghanam, A.H., and Gebremichael, M. (2012). Investigating the ability of Artificial Neural Network (ANN) models to estimate missing rain-gauge data. *Journal of Environmental Informatics*, 19(1), 38–50.
- O’Hara, P.D., and Morandin, L.A. (2010). Effects of sheens associated with offshore oil and gas development on the feather microstructure of pelagic seabirds. *Marine Pollution Bulletin*, 60(5), 672–678.
- OGP (International Association of Oil and Gas Producers). (2002). Aromatics in produced water: occurrence, fate & effects and treatment. OGP Report no. 1.20/324. London, England, 30 pp.
- OGP (International Association of Oil and Gas Producers). (2002). Aromatics in produced water: occurrence, fate & effects and treatment. OGP Report no. 1.20/324. London, England, 30 pp
- Ostenfeld, C.H. (1908). On the immigration of *Biddulphia sinensis* Grev. and its occurrence in the North Sea during 1903-1907. *Meddelelser Fra Kommissionen for Havunder-søgelse*. Series: Plankton, Kobenhavn. 1: 1-44.
- Otero, P., Ruiz-Villarreal, M., Allen-Perkins, S., Vila, B., and Cabanas, J. M. (2014). Coastal exposure to oil spill impacts from the Finisterre Traffic Separation Scheme. *Marine pollution bulletin*, 85(1), 67-77.

- Painmanakul, P., Sastaravet, P., Lersjintanakarn, S., and Khaodhiar, S. (2010). Effect of bubble hydrodynamic and chemical dosage on treatment of oily wastewater by Induced Air Flotation (IAF) process. *Chemical Engineering Research and Design*, 88(5-6), 693-702.\
- Palomino Romero, J. A., Cardoso Junior, F. S. S., Figueiredo, R. T., Silva, D. P., & Cavalcanti, E. B. (2013). Treatment of Biodiesel Wastewater by Combined Electroflotation and Electrooxidation Processes. *Separation Science and Technology*, 48(13), 2073-2079.
- Payne, J.R., Driskell, W.B., Braddock, J.F., Bailey, J., Short, J.W., Ka'aihue, L., and Kuckertz, T.H. (2005). From tankers to tissues – tracking the degradation and fate of oil discharges in Port Valdez, Alaska. In: *Proceedings of Arctic Marine Oil Spill Conference*, Calgary, Alberta, Canada.
- Pendashteh, A.R., Fakhru'l-Razi, A., Chaibakhsh, N., Abdullah, L.C., Madaeni, S.S., and Abidin, Z.Z. (2011). Modeling of membrane bioreactor treating hypersaline oily wastewater by artificial neural network. *Journal of Hazardous Materials*, 192(2), 568–575.
- Peng, L.Y., Bao, M.D., Wang, Q.F., Wang, F.C., and Su, H.J. (2014). The anaerobic digestion of biologically and physicochemically pretreated oily wastewater. *Bioresource Technology*, 151, 236-243.
- Peterson, C.H., and Holland-Bartels, L. (2002). Nearshore vertebrate predators: constraints to recovery from oil pollution. *Marine Ecology Progress Series*, 241, 235-236.

- Petro-Canada. (2010). Terra Nova 2008 Environmental Effects Monitoring Program. Prepared by Jacques Whitford Environment Limited for Petro-Canada, St. John's, NL. 173 pp.
- Pezeshki, S.R., Hester, M.W., Lin, Q., and Nyman, J.A. (2000). The Effects of Oil Spill and Clean-up on Dominant US Gulf Coast Marsh Macrophytes: A Review. *Environmental Pollution*, Vol. 108, No. 2, pp. 129-139.
- Phanikumar, C. V., and Maitra, B. (2006). Valuing urban bus attributes: an experience in Kolkata. *Journal of Public Transportation*, 9(2), 69.
- Pimentel, D., Lach, L., Zuniga, R., and Morrison, D. (2000). Environmental and economic costs of nonindigenous species in the United States. *BioScience*. 50(1): 53-65.
- Pirdashti, M., Curteanu, S., Kamangar, M.H., Hassim, M.H., and Khatami, M.A. (2013). Artificial neural networks: applications in chemical engineering. *Reviews in Chemical Engineering*, 29(4), 205–239.
- Pivel, M.A.G., and Freitas, C.M.D.S. (2010). Evaluation of modeling as a tool to determine the potential impacts related to drilling wastes in the Brazilian offshore. *Environmental Monitoring and Assessment*, 167(1-4), 17-32.
- Powell, W. B., George, A., Sim ão, H., Scott, W., Lamont, A., and Stewart, J. (2012). Smart: a stochastic multiscale model for the analysis of energy resources, technology, and policy. *INFORMS Journal on Computing*, 24(4), 665-682.
- Qu, T.D., Gao, S., and Fukumori, I. (2011). What governs the North Atlantic salinity maximum in a global GCM? *Geophysical Research Letters*, 38:L07602, doi:10.1029/2011GL046757.

- Ramík, J., and Korviny, P. (2010). Inconsistency of pair-wise comparison matrix with fuzzy elements based on geometric mean. *Fuzzy Sets and Systems*, 161(11), 1604-1613.
- Rattanapan, C., Sawain, A., Suksaroj, T., and Suksaroj, C. (2011). Enhanced efficiency of dissolved air flotation for biodiesel wastewater treatment by acidification and coagulation processes. *Desalination*, 280(1), 370-377.
- Rincón, G. J., and La Motta, E. J. (2014). Simultaneous removal of oil and grease, and heavy metals from artificial bilge water using electro-coagulation/flotation. *Journal of Environmental Management*, 144, 42-50.
- Rosenbloom, E. S. (1997). A probabilistic interpretation of the final rankings in AHP. *European Journal of Operational Research*, 96(2), 371-378.
- Rudnick, D.A., Hieb, K., Grimmer, K.F., and Resh, V.H. (2003). Patterns and processes of biological invasion: the Chinese mitten crab in San Francisco Bay. *Basic and Applied Ecology*. 4: 249-262.
- Sadiq, R., and Tesfamariam, S. (2009). Environmental decision-making under uncertainty using intuitionistic fuzzy analytic hierarchy process (IF-AHP). *Stochastic Environmental Research and Risk Assessment*, 23(1), 75-91.
- Saeed, T., Ali, L.N., Al-Bloushi, A., Al-Hashash, H., Al-Bahloul, M., Al-Khabbaz, A., and Al-Khayat, A. (2011). Effect of environmental factors on photodegradation of polycyclic aromatic hydrocarbons (PAHs) in the water-soluble fraction of Kuwait crude oil in seawater. *Marine Environmental Research*, 72(3), 143–150.

- Salahi, A., Mohammadi, T., Nikbakht, M., Golshenas, M., and Noshadi, I. (2012). Purification of biologically treated Tehran refinery oily wastewater using reverse osmosis. *Desalination and Water Treatment*, 48(1-3), 27-37.
- Salihoglu, N.K., Karaca, G., Salihoglu, G., and Tasdemir, Y. (2012). Removal of polycyclic aromatic hydrocarbons from municipal sludge using UV light. *Desalination and Water Treatment*, 44(1-3), 324-333.
- Salu, O. A., Adams, M., Robertson, P. K., Wong, L. S., and McCullagh, C. (2011). Remediation of oily wastewater from an interceptor tank using a novel photocatalytic drum reactor. *Desalination and Water Treatment*, 26(1-3), 87-91.
- Sanches, S., Leitão, C., Penetra, A., Cardoso, V.V., Ferreira, E., Benoliel, M.J., Crespo, M.T.B., and Pereira, V.J. (2011). Direct photolysis of polycyclic aromatic hydrocarbons in drinking water sources. *Journal of Hazardous Materials*, 192(3), 1458-1465.
- Santo, C. E., Vilar, V. J., Botelho, C., Bhatnagar, A., Kumar, E., and Boaventura, R. A. (2012). Optimization of coagulation-flocculation and flotation parameters for the treatment of a petroleum refinery effluent from a Portuguese plant. *Chemical Engineering Journal*, 183, 117-123.
- Saaty, T.L. (1980). *The Analytic Hierarchy Process: Planning, Priority Setting and Resource Allocation*, McGraw-Hill, New York, NY, USA.
- Sharghi, E. A., Bonakdarpour, B., Roustazade, P., Amoozegar, M. A., and Rabbani, A. R. (2013). The biological treatment of high salinity synthetic oilfield produced water in a submerged membrane bioreactor using a halophilic bacterial consortium. *Journal of Chemical Technology and Biotechnology*, 88(11), 2016-2026.

- Shariati, S. R. P., Bonakdarpour, B., Zare, N., and Ashtiani, F. Z. (2011). The effect of hydraulic retention time on the performance and fouling characteristics of membrane sequencing batch reactors used for the treatment of synthetic petroleum refinery wastewater. *Bioresource technology*, 102(17), 7692-7699.
- Shokakar, H., Salahi, A., Kasiri, N., and Mohammadi, T. (2012). Prediction of permeation flux decline during MF of oily wastewater using genetic programming. *Chemical Engineering Research and Design*, 90(6), 846-853.
- Soleimani, R., Shoushtari, N.A., Mirza, B., and Salahi, A. (2013). Experimental investigation, modeling and optimization of membrane separation using artificial neural network and multi-objective optimization using genetic algorithm. *Chemical Engineering Research and Design*, 91(5), 883-903.
- Song, X. L., Zhao, Y. B., Song, Z. Y., and Liu, C. Y. (2012). Dissolved oxygen control in wastewater treatment based on robust PID controller. *International Journal of Modelling, Identification and Control*, 15(4), 297-303.
- Steinhoff, T., Friedrich, T., Hartman, S.E., Oschlies, A., Wallace, D.W.R., and Körtzinger, A. (2010). Estimating mixed layer nitrate in the North Atlantic Ocean. *Biogeosciences*, 7, 795–807.
- Stephenson, M.T. (1992). A survey of produced water studies. Ray, J.P., and Engelhardt, F.R. (Eds.), *Produced Water: Technological/Environmental Issues and Solutions*, Plenum Publishing Corp., New York, pp. 1–12
- Su, C.S., and Yeh, S.M. (1995). UV attenuation coefficient in water determined by thermoluminescence detector. *Radiation Measurement*, 26(1), 83–86.

- Talvy, S., Debaste, F., Martinelli, L., Chauveheid, E., and Haut, B. (2011). Development of a tool, using CFD, for the assessment of the disinfection process by ozonation in industrial scale drinking water treatment plants. *Chemical Engineering Science*, 66, 3185-3194.
- Tamburri, M.N., Wasson, K., and Matsuda, M. (2002). Ballast water deoxygenation can prevent aquatic introductions while reducing ship corrosion. *Biological Conservation*, 103, 331-341.
- Tan, Q., Huang, G.H., Wu, C.Z., and Cai, Y.P. (2011). IF-EM: An interval-parameter fuzzy linear programming model for environment-oriented evacuation planning under uncertainty. *Journal of Advanced Transportation*, Vol. 45, No. 4, pp. 286-303.
- Tedetti, M., Kawamura, K., Narukawa, M., Joux, F., Charri èrea, B., and Semp éré R. (2007). Hydroxyl radical-induced photochemical formation of dicarboxylic acids from unsaturated fatty acid (oleic acid) in aqueous solution. *Journal of Photochemistry and Photobiology A: Chemistry*, 188(1), 135–139.
- Tehrani-Bagha, A.R., Nikkar, H., Menger, F.M., and Holmberg, K. (2012). Degradation of Two Persistent Surfactants by UV-Enhanced Ozonation. *Journal of Surfactant and Detergent*, 15, 59-66.
- Tesfamariam, S., and Sadiq, R. (2006). Risk-based environmental decision-making using fuzzy analytic hierarchy process (F-AHP). *Stochastic Environmental Research and Risk Assessment*, 21(1), 35-50.
- Tiryaki, F., and Ahlatcioglu, B. (2009). Fuzzy portfolio selection using fuzzy analytic hierarchy process. *Information Sciences*, 179(1), 53-69.

- Tobiszewski, M., and Namieśnik, J. (2012). PAH diagnostic ratios for the identification of pollution emission sources. *Environmental Pollution*, 162, 110-119.
- Tolga, E., Demircan, M. L., and Kahraman, C. (2005). Operating system selection using fuzzy replacement analysis and analytic hierarchy process. *International Journal of Production Economics*, 97(1), 89-117.
- Tomaszewska, M., Orecki, A., and Karakulski, K. (2005). Treatment of bilgewater using a combination of ultrafiltration and reverse osmosis. *Desalination*, 185:203–212
- Tony, M.A., Purcell, P.J., and Zhao, Y.Q. (2012). Oil refinery wastewater treatment using physicochemical, Fenton and Photo-Fenton oxidation processes. *Journal of Environmental Science and Health, Part A. Toxic/Hazardous Substances and Environmental Engineering*, 47(3), 435–440.
- Tsapakis, M., Dakanali, E., Stephanou, E.G., and Karakassis, I. (2010). PAHs and n-alkanes in Mediterranean coastal marine sediments: aquaculture as a significant point source. *Journal of Environmental Monitoring*, 12, 958–963.
- Tsolaki, E., and Diamadopoulos, E. (2010). Technologies for ballast water treatment: a review. *Journal of Chemical Technology & Biotechnology*, 85, 19-32.
- Tsuzuki, Y., Koottatep, T., Sinsupan, T., Jiawkok, S., Wongburana, C., Wattanachira, S., and Sarathai, Y. (2013). A concept for planning and management of on-site and centralised municipal wastewater treatment systems, a case study in Bangkok, Thailand. I: Pollutant discharge indicators and pollutant removal efficiency functions. *Water Science & Technology*, 67(9).
- Turkdogan-Aydinol, F.I., and Yetilmezsoy, K. (2010). A fuzzy-logic-based model to predict biogas and methane production rates in a pilot-scale mesophilic UASB

- reactor treating molasses wastewater. *Journal of Hazardous Materials*, 182(1-3), 460-471.
- U.S. EPA. (1999). Phase I Final Rule and Technical Development Document of Uniform National Discharge Standards (UNDS). Document no: EPA-842-R-99-001.
- Van Broekhoven, E., and De Baets, B. (2006). Fast and accurate center of gravity defuzzification of fuzzy system outputs defined on trapezoidal fuzzy partitions. *Fuzzy Sets and Systems*, Vol. 157, No. 7, pp. 904-918.
- Veeramani, C., Duraisamy, C., and Nagoorgani, A. (2011). Solving Fuzzy Multi-objective Linear Programming Problems with Linear Membership Functions. *Australian Journal of Basic and Applied Sciences*, Vol. 5, No. 8, pp. 1163-1171.
- Veil, J. A., Puder, M. G., Elcock, D., and Redweik Jr, R. J. (2004). A white paper describing produced water from production of crude oil, natural gas, and coal bed methane. ANL Report under DOE (NETL) Contract W-31-109-Eng-38.
- Verl, A., Westkämper, E., Abele, E., Dietmair, A., Schlechtendahl, J., Friedrich, J., and Schrems, S. (2011). Architecture for multilevel monitoring and control of energy consumption. In *Glocalized Solutions for Sustainability in Manufacturing* (pp. 347-352). Springer Berlin Heidelberg.
- Veil, J. A. (2011). Produced water management options and technologies. In *Produced Water* (pp. 537-571). Springer New York.
- Vilhunen, S., Vilve, M., Vepsäläinen, M., and Sillanpää M. (2010). Removal of organic matter from a variety of water matrices by UV photolysis and UV/H₂O₂ method. *Journal of Hazardous Materials*, 179(1-3), 776-782.

- von Gunten, U. (2003). Ozonation of drinking water: Part II. Disinfection and by-product formation in presence of bromide, iodide or chlorine. *Water Research*, 37, 1469–1487.
- Wandera, D., Wickramasinghe, S.R., and Husson, S.M. (2011). Modification and Characterization of Ultrafiltration Membranes for Treatment of Produced Water. *Journal of Membrane Science*, Vol. 373, pp. 178-188.
- Wang, K., Guo, J., Yang, M., Junji, H., and Deng, R. (2009). Decomposition of two haloacetic acids in water using UV radiation, ozone and advanced oxidation processes. *Journal of Hazardous Materials*, 162, 1243-1248.
- Wang, D., McLaughlin, E., Pfeffer, R., and Lin, Y. S. (2012). Adsorption of oils from pure liquid and oil–water emulsion on hydrophobic silica aerogels. *Separation and Purification Technology*, 99, 28-35.
- Weirich, S. R., Silverstein, J., and Rajagopalan, B. (2011). Effect of average flow and capacity utilization on effluent water quality from US municipal wastewater treatment facilities. *Water research*, 45(14), 4279-4286.
- Włodarczyk-Makuła, M., 2011. Application of UV-rays in removal of polycyclic aromatic hydrocarbons from treated wastewater. *Journal of Environmental Science and Health, Part A: Toxic/Hazardous Substances and Environmental Engineering*, 46(3), 248–257.
- Woo, O.T., Chung, W.K., Wong, K.H., Chow, A.T., and Wong, P.K., 2009. Photocatalytic oxidation of polycyclic aromatic hydrocarbons: intermediates identification and toxicity testing. *Journal of Hazardous Materials*, 168, 1192–1199.

- Xu, P., Drewes, J.E., Heil, D., and Wang, G. (2008). Treatment of brackish produced water using carbon aerogel-based capacitive deionization technology. *Water Research*, 42(10-11), 2605-2617.
- Xu, H. X., Liu, J. T., Gao, L. H., Wang, Y. T., Deng, X. W., and Li, X. B. (2014). Study of Oil Removal Kinetics Using Cyclone-Static Microbubble Flotation Column. *Separation Science and Technology*, doi: 10.1080/01496395.2014.881879
- Xu, Y., Huang, G.H., Qin, X.S., and Huang, Y. (2009). SRFILP: A Stochastic Robust Fuzzy Interval Linear Programming Model for Municipal Solid Waste Management under Uncertainty. *Journal of Environmental Informatics*, Vol. 14, No. 2, pp. 72-82.
- Yan, Q.P., Xie, X.L., and Huo, W.W. (2009). Research and application of ship routing and fleet planning model. In *Intelligent Computation Technology and Automation, 2009. ICICTA'09. Second International Conference on* (Vol. 3, pp. 685-688). IEEE.
- Yang, T., Ma, Z.F., and Yang, Q.Y. (2011). Formation and performance of Kaolin/MnO₂ bi-layer composite dynamic membrane for oily wastewater treatment: Effect of solution conditions. *Desalination*, 270(1-3), 50-56.
- Yang, Y., Wang, H., Li, J., He, B., Wang, T., and Liao, S. (2012). Novel functionalized nano-TiO₂ loading electrocatalytic membrane for oily wastewater treatment. *Environmental science & technology*, 46(12), 6815-6821.
- Yetilmezsoy, K., and Demirel, S. (2008). Artificial neural networks approach for modeling of Pb(II) adsorption from aqueous solution by Antep pistachio (*Pistacia Vera L.*) shells. *Journal of Hazardous Materials*, 153, 1288–1300.

- Yoon, H., Jun, S-C., Hyun, Y., Bae, G-O., and Lee, K-K. (2011). A comparative study of artificial neural networks and support vector machines for predicting groundwater levels in a coastal aquifer. *Journal of Hydrology*, 396(1–2), 128–138.
- You, F. and Leyffer, S. (2011). Mixed-Integer Dynamic Optimization for Oil-Spill Response Planning with Integration of a Dynamic Oil Weathering Model. *AIChE Journal*, Vol. 57, No. 12, pp. 3555-3564.
- Yu, C. S. (2002). A GP-AHP method for solving group decision-making fuzzy AHP problems. *Computers & Operations Research*, 29(14), 1969-2001.
- Yu, S.L., Lu, Y., Chai, B.X., and Liu, J.H. (2006). Treatment of oily wastewater by organic–inorganic composite tubular ultrafiltration (UF) membranes. *Desalination*, 196(1-3), 76-83.
- Yu, R.F., Chen, H.W., Cheng, W.P., and Shen, Y.C. (2008). Dynamic control of disinfection for wastewater reuse applying ORP/pH monitoring and artificial neural networks. *Resources, Conservation, and Recycling*, 52(8-9), 1015-1021.
- Yu, R. F., Chen, H. W., Liu, K. Y., Cheng, W. P., and Hsieh, P. H. (2010). Control of the fenton process for textile wastewater treatment using artificial neural networks. *Journal of chemical technology and biotechnology*, 85(2), 267-278.
- Zadeh, L.A. (1965). Fuzzy Sets. *Information Control*, 8, 338–353.
- Zafiriou, O.C., True, M.B. and Hayon, E. (1987). Consequence of OH radical reaction in seawater: formation and decay of Br₂⁻ ion radical. In *Photochemistry of Environmental Aquatic Systems*; Zika, R.G., Cooper, W.J., Eds. American Chemical Society: Washington, DC, pp 89–105.

- Zakaria, M.P., Okuda, T., and Takada, H. (2001). Polycyclic aromatic hydrocarbons (PAH) and hopanes in stranded tar-balls on the coasts of peninsular Malaysia: applications of biomarkers for identifying sources of oil pollution. *Marine Pollution Bulletin*, 42(12), 1357-1366.
- Zeng, Y., Yang, C., Zhang, J., and Pu, W. (2007). Feasibility investigation of oily wastewater treatment by combination of zinc and PAM in coagulation/flocculation. *Journal of Hazardous Materials*, 147(3), 991-996.
- Zeferino, J. A., Antunes, A. P., and Cunha, M. C. (2010). Multi-objective model for regional wastewater systems planning. *Civil Engineering and Environmental Systems*, 27(2), 95-106.
- Zeferino, J. A., Cunha, M. C., and Antunes, A. P. (2012). Robust optimization approach to regional wastewater system planning. *Journal of environmental management*, 109, 113-122.
- Zeferino, J.A., Antunes, A.P., and Cunha, M.C. (2014). Regional Wastewater System Planning under Population Dynamics Uncertainty. *Journal of Water Resources Planning and Management-ASCE*, 140, 322-331.
- Zhang, X., Jiang, H.L., and Zhang, Y.Z. (2013). The hybrid method to predict biochemical oxygen demand of Haihe River in China. *Advanced Materials Research*, 610–613, 1066–1069.
- Zhang, Y., Cui, P., Du, T., Shan, L., and Wang, Y. (2009). Development of a sulfated Y-doped nonstoichiometric zirconia/polysulfone composite membrane for treatment of wastewater containing oil. *Separation and Purification Technology*, 70(2), 153-159.

- Zhang, Q., and Stanley, S.J. (1999). Real-time water treatment process control with artificial neural networks. *Journal of Environmental Engineering-ASCE*, 125, 153-160.
- Zhao, S., Huang, G., Fu, H., and Wang, Y. (2014). Enhanced Coagulation/Flocculation by Combining Diatomite with Synthetic Polymers for Oily Wastewater Treatment. *Separation Science and Technology*, doi: 10.1080/01496395.2013.877035.
- Zhou, J.W., Xu, Z.H., and Chen, S.W. (2013). Simulation and prediction of the thuringiensin abiotic degradation processes in aqueous solution by a radius basis function neural network model. *Chemosphere*, 91(4), 442–447.
- Zhu, X.B., Tian, J.P., Liu, R., and Chen, L.J. (2011). Optimization of Fenton and electro-Fenton oxidation of biologically treated coking wastewater using response surface methodology. *Separation and Purification Technology*, 81(3), 444-450.
- Zirehpour, A., Rahimpour, A., Jahanshahi, M., and Peyravi, M. (2014). Mixed matrix membrane application for olive oil wastewater treatment: Process optimization based on Taguchi design method. *Journal of Environmental Management*, 132, 113-120.